Carbon Turnover in Subsoil Hotspots: Are Biopores more than Voids?

Dissertation
to attain the doctoral degree (Dr. rer. nat.)
of the Faculty of Agricultural Sciences
Georg-August-Universität Göttingen

Submitted by
Callum Colin Banfield
born on the 27th July 1987 in Karlsruhe

Göttingen, September 2018

1. Referee: Prof. Dr. Michaela Anna Dippold
2. Referee: Prof. Dr. Stefan Scheu

Date of oral examination: 8th November 2018

I. Table of Contents

1 Extended Summary 1

1.1 Introduction 1

1.1.1 The relevance of subsoils for C sequestration and nutrient acquisition 1

1.1.2 Biopores facilitate access to the subsoils 2

1.1.3 Biopores and crop rotations 3

1.1.4 Biopores are the most relevant locations of C turnover in the subsoil 4

1.1.5 Objectives of this thesis 6

1.2 Experiments and Methods 7

1.2.1 Field experiment: Study site and biopore treatments 7

1.2.2 Lab experiment 1: A proof-of-concept tool for biopore re-use 10

1.2.3 Lab experiment 2: Two-year crop rotation under controlled conditions 11

1.3 Results and Discussion 13

1.3.1 Biogeochemistry of root and earthworm biopores 14

1.3.2 The relevance of root biopores in crop rotations 24

1.4 Conclusions 31

1.4.1 The relevance of biopores in organic geochemistry 31

1.4.2 The relevance of biopores in agricultural soil science 33

1.5 References 35

1.6 Contributions to the included manuscripts and publications 43

2 Publications and Manuscripts 47

2.1 Study 1: Biopores as carbon highways into the subsoil: Organic matter origin and differentiation in microbial hotspots 47

2.1.1 Introduction 49

2.1.2 Material and Methods 50

2.1.3 Results 55

2.1.4 Discussion 66

2.1.5 Conclusions 72

2.1.6 References 74

2.1.7 Supplementary Material 78

2.2 Study 2: Microbial processing of plant residues in the subsoil – The role of biopores 85

2.2.1 Introduction 87

2.2.2 Material and methods 89

2.2.3 Results 93

2.2.4 Discussion 98

2.2.5 Conclusions 104

2.2.6 References 105

2.2.7 Supplementary Material 112

2.3 Study 3: Biopore history determines the microbial community composition in subsoil hotspots 115

2.3.1 Introduction 117

2.3.2 Material and methods 119

2.3.3 Results 125

2.3.4 Discussion 131

2.3.5 Conclusions 138

2.3.6 References 140

2.3.7 Supplementary Material 147

2.4 Study 4: Six months of *L. terrestris* L. activity in root-formed biopores increases nutrient availability, microbial biomass and enzyme activity 151

2.4.1 Introduction 153

2.4.2 Material and Methods 154

2.4.3 Results 159

2.4.4 Discussion 163

2.4.5 Conclusions 166

2.4.6 References 167

2.4.7 Supplementary Material 172

2.5 Study 5: Labelling plants in the Chernobyl way: A new ^{137}Cs and ^{14}C foliar application approach to investigate rhizodeposition and biopore reuse 175

2.5.1 Introduction 177

2.5.2 Material and methods 179
2.5.3 Results 185
2.5.4 Discussion 189
2.5.5 Conclusions 194
2.5.6 References 196
2.5.7 Supplementary Material 199

2.6 Study 6: Subsoil exploitation: The re-use of root biopore hotspots in crop rotations 203

2.6.1 Introduction 205
2.6.2 Material and Methods 207
2.6.3 Results 211
2.6.4 Discussion 214
2.6.5 Conclusions 217
2.6.6 References 219
2.6.7 Supplementary Material 223

2.7 Study 7: The fate of pre-crop nitrogen: Biopores as hotspots for interannual nitrogen transfer in crop rotations? 227

2.7.1 Introduction 229
2.7.2 Material and Methods 230
2.7.3 Results 233
2.7.4 Discussion 236
2.7.5 Conclusions 238
2.7.6 References 240
2.7.7 Supplementary Material 243

2.8 Additional peer-reviewed publications 245

3 Acknowledgements / Danksagung A1

4 Curriculum vitae A3

5 Declarations / Erklärungen A4

II. List of Figures

Extended Summary:

Fig. 1 Examples of biopores formed by roots (left) and earthworms (right). Photos courtesy of Silke Hafner and Marcel Lüsebrink. 2

Fig. 2 Collage illustrating the biopore formation in the field. From top left to bottom right: a) Mapping chicory roots on plastic films in 45 cm depth, b) *L. terrestris* featuring an elastomer tag, c) refilling the topsoil and creation of a continuous biopore from the subsoil to topsoil (wooden stick), d) tagged earthworm incubation from the original soil surface. 7

Fig. 3 Timeline of the field experiment. Root biopores are three-year-old chicory roots followed by two years decay. Earthworm-incubated biopores are equivalent to the root biopores but for the last six months of decay earthworms (*L. terrestris*) were incubated into chicory root biopores). Earthworm biopores represent the native earthworm population of the field site.. 8

Fig. 4 Illustration of the earthworm and root effects, i.e. the changes of the mean biomarker content or turnover proxy relative to bulk soil. In case of the turnover proxies*, the change from the undecomposed source biomasses (shown as vertical red lines) during biopore formation is the microbial processing of OM (blue and red arrows)... 10

Fig. 5 Illustration of the ^{137}Cs labelling and imaging feasibility study (Banfield et al., 2017b). Three steps (from left to right): Labelling with $^{14}CO_2$ in an airtight chamber and ^{137}CsCl leaf feeding at the same time to simulate biopore re-use, i.e. ^{137}Cs and ^{14}C in the same rhizosphere. Cutting the soil core in 5 cm depth and two-step phosphor imaging (with and without shielding of weaker ^{14}C). Image processing, i.e. separating activities by subtraction of the attenuation-corrected ^{137}Cs image from the unshielded image, i.e. ^{14}C+^{137}Cs. Finally, checking for overlap of activities. 11

Fig. 6 Second lab experiment ‘Crop rotation’: Two different pre-crops (*C. intybus, P. tanacetifolia*) were cultivated on soil cores. After seven weeks all plants were labelled by ^{137}Cs leaf feeding, and half of the plants were labelled by ^{15}N leaf feeding. On the other half of plants, the same amount of ^{15}N was applied to the soil surface as fertiliser. After 12 weeks, the pre-crops were cut and killed, soil cores were stored at 7 °C for root biopore formation for 11 months (last two months at 20 °C). Wheat (*T. aestivum*) was grown for 12 weeks and labelled six times with 3 MBq $^{14}CO_2$. Soil cores were cut three times and biopore re-use, biopore statistics and ^{15}N uptake were determined................................ 12

Fig. 7 Two PCAs of turnover proxies (left) and the SOM fingerprints (~160 compounds; right). The left PCA describing OM turnover separated the bulk soil and root biopores better than the PCA of the SOM fingerprints, and explained a higher proportion of the total variance. OM turnover, which includes the interaction of the biota with the soil, characterises biopores better than the composition of SOM. In both cases, earthworm-influenced biopores featured much smaller within-group variance than bulk soil or root biopores, and the x-axis separated samples with frequent C inputs from those with infrequent C inputs... 18

Fig. 8 Ratio of microbial-derived galactose and mannose to plant-derived arabinose and xylose (GM/AX; grey bars) and as white bars, the ratio of mannose + fucose + ribose to arabinose and xylose (MRF/AX), both are markers for the turnover of hemicelluloses. 20

Fig. 9 The ratios of the acidic phenol to the aldehyde phenol for lignin-derived subunits (grey bars Ac:Alv for the vanillyl phenols; white bars for Ac:Als for the syringyl phenols) are proxies for the oxidation state of the lignin molecule.. ...20
Fig. 10 Microbial biomass g SOC^{-1} (grey bars) as determined by its proxy ∑ PLFAs, and the ratio of Gram-positive/Gram-negative PLFAs (red dots)....................21
Fig. 11 Enzyme activities of β-glucosidase, xylanase and cellobiohydrolase (nmol g^{-1} MUF h^{-1} or nmol g^{-1} AMC h^{-1}) at two soil depths (45–75 and 75–105 cm) in three biopores types (abbreviated BP) and bulk soil.. 23
Fig. 12 Imaging processing from Study 5. Two examples are shown for chicory and alfalfa, respectively, shown are the main root locations. The first row shows the total activity of ^{137}Cs and ^{14}C, while the second row shows just the ^{137}Cs activity. The last row shows the calculated ^{14}C activity as explained in the text. 26
Fig. 13 Phosphor imaging of a soil core in 25 cm depth after one year of root decomposition (Study 6). ^{14}C was shielded off by 320 µm of polypropylene plastic films. Red patches refer to ^{137}Cs activity which was supplied to the preceding crop about one year before. Consequently, red patches are ^{137}Cs-labelled biopores. 26
Fig. 14 Differentiation of biopores and roots growing inside or outside biopores; determination of biopore reuse. From left to right: Count of biopores across depths; wheat roots in bulk soil; wheat roots in biopores and biopore re-use (%). Red lines and black (dotted) lines represent chicory and phacelia pre-crops, respectively...27
Fig. 15 Selected biopore properties: volume, wall volume, radius and cut surface for the biopores of the two pre-crops chicory (dotted, black) and phacelia (red solid lines) down to 60 cm soil depth. 28
Fig. 16 C/N ratio, TOC and TN contents inside (dotted lines) and outside (solid lines) the biopore walls of chicory (red) and phacelia (black lines, squares). Letters indicate significant differences in one soil layer 29
Fig. 17 Fate of ^{15}N applied during the pre-crop phase (top) and plant productivity of wheat, both depending on the pre-crop species and mode of ^{15}N application(bottom). Letters indicate significant differences. 30
Fig. 18 The relevance of biopores comprises nutritional benefits, increased C input into subsoils and physical benefits, in total governed by biopore re-use. 32

Publications and Manuscripts:

Study 1

Fig. 1 Principal components analysis (PCA) based on correlation of the entire biomarker dataset. Triangles represent samples from 45–75 cm, while circles present samples form 75–105 cm. Principal component (PC) 1 (x-axis) explained 39% of the inertia, while PC 2 explained further 15%. 56
Fig. 2 Mean VSC-lignin contents ± SEM (two left bars of each treatment; µg g^{-1} soil) and their contributions to SOC ± SEM (two right bars; mg g^{-1} SOC) of the three biopore types and bulk soil in two subsoil depths (45–75 cm, 75–105 cm). 58
Fig. 3 Mean hemicellulose and hexuronic acids contents ± SEM (two left bars of each treatment; µg g^{-1} soil) and their contributions to SOC ± SEM (two right bars; mg g^{-1} SOC) of the three biopore types and bulk soil in two subsoil depths (45–75 cm, 75–105 cm)...59
Fig. 4 Mean microbial hexoses contents ± SEM (two left bars of each treatment; µg g^{-1} soil) and biomarker contributions to SOC ± SEM (two right bars; mg g^{-1} SOC)

of the three biopore types and bulk soil in two subsoil depths (45–75 cm, 75–105 cm).. 60

Fig. 5 Mean amino sugars contents ± SEM (two left bars of each treatment; µg g^{-1} soil) and their contributions to SOC ± SEM (two right bars; mg g^{-1} SOC) of the three biopore types and bulk soil in two subsoil depths (45–75 cm, 75–105 cm). 61

Fig. 6 Mean free lipids contents ± SEM (two left bars of each treatment; µg g^{-1} soil) and their contributions to SOC ± SEM (two right bars; mg g^{-1} SOC) of the three biopore types and bulk soil in two subsoil depths (45–75 cm, 75–105 cm)..... 62

Fig. 7 Mean cutin/suberin contents ± SEM (two left bars of each treatment; µg g^{-1} soil) and their contributions to SOC ± SEM (two right bars; mg g^{-1} SOC) of the three biopore types and bulk soil in two subsoil depths (45–75 cm, 75–105 cm). 63

Fig. 8 LDA biplot showing the discrimination scores as an XY scatterplot (triangles: samples from 45–75 cm, circles: samples from 75–105 cm) and the four variables with the highest discriminatory power (because of visibility)............ 65

Study 2

Fig. 1 **Left:** Principal component analysis of seven proxies describing the degree of processing: GM/AX, Ac/Al for S and V subunits, S/V and Ci/V ratios; free/bound ω-hydroxy alkanoic acids or alkanoic acids ratios, as well as the n-alkene / n-alkanes ratio. **Right:** Correlation circle describing the correlation between biomarker ratios and the two PC... 94

Fig. 2 Proxies for hemicelluloses: the GM/AX ratio ∑ (galactose + mannose) / ∑ (arabinose + xylose) as grey bars and the source-adapted MRF/AX ratio as white bars ∑ (mannose + ribose + fucose) / ∑ (arabinose + xylose). Shown are means ± standard errors of all four treatments.. 95

Fig. 3 Oxidation state of the lignin side chains. Ratios of vanillic acid/vanillin (Ac/Al)v as grey bars and syringic acid/syringaldehyde (Ac/Al)s as white bars. Shown are means ± standard errors of all four treatments.. 96

Fig. 4 Lipid-based proxies: free/bound ω-hydroxy alkanoic acids (HO-AA) as black bars on the left y-axis; free/bound alkanoic acids (AA) as white bars and ∑ n-alkenes / ∑ n-alkanes as grey bars, both on the right y-axis.. 97

Study 3

Fig. 1 Timeline of the experiment. Chicory was grown for three consecutive years (2009-2012), followed by two years during which the three biopore types differentiated 119

Fig. 2 Distribution of Σ PLFAs per unit soil organic C in each biopore type (root pores, earthworm-incubated pores, native earthworm pores) and the bulk soil in two subsoil depths (4 samples x 4 treatments x 2 depths) and ratios of Gram-negative PLFAs to Gram-positive PLFAs (top: 45 – 75 cm, bottom: 75 – 105 cm). Bars show Σ PLFAs (left vertical axis), while red circles show the ratios of Σ Gram-positive / Σ Gram-negative PLFAs (right vertical axis, note the logarithmic scale). Mean values (± SEM) are given.................................... 126

Fig. 3 Microbial communities in the three biopore types and bulk soil from two subsoil depths (4 samples x 4 treatments x 2 depths): Note the truncated y-axis. Mean values of percentage of Σ PLFAs (± SEM) are given. I................................ 127

Fig. 4 Constrained redundancy analysis on the PLFA fingerprints from Fig. 3. Response scores were calculated as weighted average scores.................. 128

Fig. 5 Contribution of the factors depth, pore type and their interactions to the total variance of microbial community composition. 129

Fig. 6 Amino sugars ratios of a) glucosamine to muramic acid, and b) galactosamine to muramic acid. Data from 4 samples x 4 treatments x 2 depths. Mean values (± SEM) are given. 130

Study 4

Fig. 1 Microbial biomass (C_{mic}) related to organic carbon content and microbial metabolic quotient (qCO_2). Error bars indicate standard deviation. RPB: root biopores, EBP: earthworm-modified biopores. 161

Fig. 2 a) Microbial biomass (total PLFA), b) ratio of biomarkers for gram-positive and gram-negative bacteria (a15:0, i15:0, i17:0, a17:0 and 16:1 ω 5c, 16:1ω7c, 18:1ω7c, Cy17:0), c) biomarkers for fungi (18:2ω6,9) and protozoa (20:4ω6) and d) biomarkers for actinobacteria (10Me16, 10Me18). Different uppercase and lowercase letters indicate significant differences between depth levels and soil compartments (ANOVA with Tukey-HSD, $p < 0.05$). Error bars indicate standard deviation. RPB: root biopores, EBP: earthworm-modified biopores. 162

Fig. 3 a) Principal-component scores for bulk soil (open circles), root biopores (gray circles) and earthworm-modified biopores (black circles) in 45–75 cm soil depth and b) selected factor loadings of the first two principal components extracted from the dataset. 163

Study 5

Fig. 1 Concept of the experiment: 1) Labelling the same plants with first ^{137}Cs and then with ^{14}C, 2) imaging with and without shielding and 3) subtracting the signals and image processing 179

Fig. 2 Imaging of ^{137}Cs and ^{14}C (top) and ^{137}Cs only (middle) activities in the soil at a depth of 5 cm for alfalfa (left) and chicory (right). Below the imagings are rotated photos of the respective soil cuts. The images presented quantum level data (QL, i.e. the pixel-wise grey values stored in 16-bit images) which was initially captured during imaging. The red colour corresponds to the higher activities. 186

Fig. 3 Procedure of image processing after conversion to PSL units and successful subtraction of ^{137}Cs activity (middle) of total activity (top) to yield the pure ^{14}C activity (bottom), shown for two examples of the largest, i.e. main roots, to which a colour map was applied 187

Fig. 4 Standardisation of ^{137}Cs and ^{14}C activities and their PSL (**p**hoto-**s**timulated **l**uminescence) values by linear regression 188

Fig. 5 Radial profiles of ^{137}Cs (left) and ^{14}C (right) activities as a function of distance from the rhizodermis for five alfalfa replicates (top) and four chicory replicates (bottom). Data averaged in radial direction around (360 °) the largest root of each plant. Error bars show the variance of the activities (as standard errors) in the respective distance from the rhizodermis 188

Fig. 6 Total ^{137}Cs and ^{14}C activities in the rhizosphere of alfalfa and chicory obtained from Eq. 4, normalised by total activities taken up by each plant and the root perimeter. The data are averaged among replicates and error bars show standard errors 189

Study 6

Fig. 1 Overview of the experimental design including tracer application during pre-crop and main crop phase, biopore formation and imaging. ^{137}Cs was applied to all pre-crop plants (fibrous *Phacelia tanacetifolia* Benth. vs tap-rooted *Cichorium intybus* L., grown for three months) to label above- and belowground biomass and, after root decay, the biopores. After 11 months of biopore formation, *T. aestivum* L. was grown for three months during which 6 pulses of $^{14}CO_2$ were applied. Spatial overlap of ^{14}C and ^{137}Cs spots was determined on soil cuts in 10, 25 and 50 cm soil depth. 207

Fig. 2 The three-step image processing calculates the spatial representation of ^{14}C by subtracting an attenuation corrected ^{137}Cs-only image from the ^{137}Cs+^{14}C image. Shown are the three consecutive steps (from top to bottom) for chicory in 25 cm soil depth (20 cm diameter). 211

Fig. 3 Physical biopore properties (means ± SE) volume, wall volume, radius and cut surface) of biopores induced by *Phacelia tanacetifolia* Benth. (dotted lines, squares) and *Cichorium intybus* L. (red, solid lines, triangles) from 0–50 cm depth. 212

Fig. 4 Biopore size distributions [%] in 10 cm (top), 25 cm (middle) and 50 cm (below) soil depth created by *Phacelia tanacetifolia* Benth. (black lines) or *Cichorium intybus* L. (red lines)... 212

Fig. 5 Physical rhizosphere properties (means ± SE) volume, wall volume, radius and cut surface) of biopores induced by *Phacelia tanacetifolia* Benth. (dotted lines, squares) and *Cichorium intybus* L. (red lines, triangles) from 0–50 cm depth.. 213

Fig. 6 Distributions of biopores and wheat roots depending on soil depth and pre-crop species (*Phacelia tanacetifolia* Benth., dotted lines; *Cichorium intybus* L., red, solid lines).. 214

Study 7

Fig. 1 A crop rotation experiment: after the pre-crop phase of either a fibrous root system crop (*P. tanacetifolia*) or tap-rooted chicory (*C. intybus*; top), the root biomass had one year to decay and enrich biopores with ^{15}N from leaf labelling. $K^{15}NO_3$ was applied either through the leaves (to label the pre-crop root biomass and therefore biopores) or onto the soil surface (to simulate fertiliser application). After the decay, wheat (*T. aestivum*) was grown (below) and ^{15}N was quantified in the wheat biomass to determine the uptake and remobilisation of ^{15}N from either biopores or bulk soil. The percent data indicates the ^{15}N partitioning between above and belowground allocation of ^{15}N ± SEM.. 232

Fig. 2 C:N ratio (top), TOC (middle) and TN contents (below) ± standard errors from 0–70 cm soil depth at the end of the experiment in biopores (dotted lines) and bulk soil (solid lines for the soil columns planted with either chicory (red) or phacelia (black with cubes as symbols, six replicates each). 234

Fig. 3 Plant productivity (dry mass of wheat shoots, white bars) and TN contents of wheat shoots (red bars); ^{15}N recovery from biopores and bulk soil (relative to applied tracer)... 235

Fig. 4 Recovery of the pre-crop applied ^{15}N in wheat (main crop; green bars, left), or in soil (black stacked bars: biopores, white stacked bars: bulk soil) – depending on pre-crop species and application mode... 236

III. List of Tables

Extended Summary

Table 1 Overview of the biomarker approaches used to characterise OM sources, turnover and microbial communities. 9

Table 2 Overview of the studies of this dissertation 13

Table 3 Basic soil and microbiological parameters of the field experiment at Klein-Altendorf: Means ± SEM of TOC, TN, MBC, C/N, $\delta^{13}C$, ∑ PLFA g^{-1} soil, ∑ PLFA g^{-1} SOC. Letters/asterisks indicate significant differences between treatments and between soil depth. Modified after Banfield et al. (2017). 15

Table 4 Biomarker contents [g^{-1} soil] and contributions to SOC [g^{-1} SOC]. Shown are means ± SEM. Letters indicate significant differences (one-way ANOVA, large: 45–75 cm, small 75–105 cm). Asterisks given in 75–105 cm show significant differences between both soil depth. 17

Publications and Manuscripts:

Study 1

Table 1 Means ± SEM of total organic carbon (TOC), total nitrogen (TN), microbial biomass (MBC, taken from Hoang et al. (2016)), count of identified compounds, matches/overlaps with the source biomass fingerprints, root/shoot biomass ratio, microbial/shoot biomass ratio and microbial/root biomass ratio; for two soil depths (45-75 cm (top) and 75-105 cm (below). 57

Table 2 ANOSIM results based on 9999 permutations (p 0.0001). Shown are pairwise Bonferroni-corrected p-values in a matrix describing the similarity of biopore types and bulk soil. Significant p-values denote significantly different treatments. 57

Table 3 Dimension reduction by partial least squares (PLS) classification (left) and linear discriminant analysis (LDA). The ten variables with the highest VIP from the PLS analysis were used to calculate linear discriminant functions, their factor structure and classification functions. 65

Study 2

Table 1 Overview of the biomarker proxies used to evaluate the microbial processing and degradation of plant inputs in biopores 92

Table 2 General soil properties and information regarding the biopores. Shown are mean values ± standard errors of TOC and TN contents, C/N ratios and $\delta^{13}C$ for root biopores, EW-incubated biopores, native earthworm biopores and bulk soil. 98

Study 3

Table 1 Summary of the PLFA data, including complimentary data: Mean values (± SEM) are given. 125

Table 2 ANOSIM results: Values reported are Bonferroni-corrected sequential p values based on 9999 permutations on the Bray-Curtis similarity matrix of the lipid fingerprint. 129

Table 3 Summary of the amino sugar data: Mean values (± SEM) are given. Different letters indicate statistically significant differences. 131

Study 4

Table 1 Total nutrient contents and P fractions in bulk soil and the walls of different pore types. Different uppercase and lowercase letters indicate significant differences between depth levels and soil compartments respectively. 160

Table 2 Enzyme activities (Vmax) in bulk soil and the walls of different pore types. Different uppercase and lowercase letters indicate significant differences between depth levels and soil compartments, respectively. 162

Study 5

Table 1 ^{137}Cs and ^{14}C budget. Shown are means of five replicates ± standard errors of the mean........ 186

Study 6

Table 1 Selected properties of the Haplic Luvisol, after Vetterlein (2013) including soil organic carbon (SOC) and total nitrogen (TN) of bulk soil, and, total organic carbon (TOC) contents ± SE in bulk soil and biopores of the soil core of the experiment. 208

Study 7

Table 1 Selected properties of the Haplic Luvisol at Klein-Altendorf (modified after Vetterlein (2013) including TN contents in bulk soil and biopores of the soil core of the experiment (own data)........ 231

IV. Abbreviations

ANOVA	Analysis of Variance
ANOSIM	Analysis of Similarity
C	Carbon
DOC	Dissolved organic carbon
EA	Elemental analyser
FAME	Fatty acid methyl ester
GC	Gas chromatography
GC-C-IRMS	Gas chromatography-combustion-isotope ratio mass spectrometer
(Tukey's) HSD	Honestly significant difference (test)
IRMS	Isotope ratio mass spectrometer
IS	Internal standard
LDA	Linear discriminant analysis
LMWOS	Low molecular weight organic substances
MBC	Microbial biomass carbon
MS	Mass spectrometer
N	Nitrogen
PLFA	Phospholipid fatty acid
PCA	Principal component analysis
OM	Organic matter
RDA	Redundancy analysis
SEM	Standard error of the mean
SIM	Selected ion mode
SOC	Soil organic carbon
SOM	Soil organic matter
SPE	Solid phase extraction
TFA	Trifluoroacetic acid
TLE	Total lipid extract
TOC	Total organic carbon
TN	Total nitrogen

V. Summary

The soil below the ploughed horizon of cropland, i.e. the subsoil, could be a large sink for carbon (C) and a valuable source of mineral-bound nutrients. C dynamics in subsoils need to be thoroughly understood to enable successful C sequestration in C-unsaturated subsoils. C turnover in the subsoil predominantly occurs in hotspots such as biopores, i.e. macropores induced by anecic earthworms or deep-rooting tap-roots. The OM in biopore walls induces preferred habitats for microorganisms as they become enriched in root detritus and earthworm faeces. Microbial action can mobilise these nutrients for future plant nutrition. This thesis consists of seven studies addressing the roles of different biopore types for C turnover and their relevance for nutrient cycling. Wall material of earthworm biopores (*Lumbricus terrestris* L.), root biopores of *Cichorium intybus* L. and their combination (‘earthworm-incubated biopores’) was sampled from 45–105 cm depth of a Haplic Luvisol and analysed for nutrient contents, microbial biomass, enzyme activities, microbial community composition and the composition of the organic matter and its decomposition state.

The fate of the **root biomass** was evident two years after root death: C contents were 2.5 times higher in root biopores than in bulk soil and concomitantly increased were microbial biomass and enzyme activities of C and N cycle. The contributions of most plant biomarkers to the soil organic carbon (SOC) pool were equal to the bulk soil, except for lignin and suberin suggesting a late decomposition stage. The narrow C/N ratio, increased $\delta^{13}C$ (relative to earthworm biopores) and turnover proxies like the lignin side-chain oxidation confirmed this. The microbial community composition reflected the ‘old’ root organic matter (OM): more phospholipid-derived fatty acids (PLFAs) of Gram-positive bacteria and actinobacteria, i.e. decomposers of residual C, were found than in the earthworm biopores. The microbial community fingerprint in root biopores was different from the earthworm-influenced biopores. Combining two C sources by **incubating earthworms into root biopores** made the largest impact on C contents and OM composition. Earthworms imported large amounts of weakly degraded OM and increased C contents by 200% and MBC (~ 30 times) relative to bulk soil. Weakly processed OM input by earthworms increased substrate richness by 30% relative to bulk soil. Among the biopores, earthworms induced the strongest increase in enzyme activities and nutrient cycling. Biopore formation generally had a low impact on the SOC composition — except for the large combined root and shoot-C input by root detritus and earthworms, which genuinely modified the SOC composition in the earthworm-incubated biopores. After six months of earthworm activities in former root biopores, the biomarker signature was overridden. More readily available OM was preferentially degraded as lignin underwent

less turnover than hemicelluloses in both earthworm-influenced biopore types. The microbial community reflected the higher C availability and the gut effects of *L. terrestris*: more PLFAs indicating fast-growing decomposers of readily available C (Gram-negative bacteria) were found than in root biopores. The microbial community in the earthworm-incubated biopores was not distinguishable from the native earthworm biopores after six months. The **native earthworm biopores** received repeated inputs of fresh OM for at least 2.5 years. This long-term activity of earthworms increased C contents by 200% relative to the bulk soil, i.e. slightly less than the combination of root detritus and earthworms. Like in the earthworm-incubated biopores, this boosted microbial biomass and increased enzyme activities. The OM in native earthworm biopores underwent the least turnover of all biopores — despite high microbial biomass and activity. This fact suggests regular C inputs and a microbial community adapted to frequently supplied, readily available OM. As a result of OM inputs, biopore walls were at least 100% enriched in nutrients like N, available P and S relative to bulk soil. Increased enzyme activities in all biopore walls suggest that these nutrients are available to crops. Therefore, from an agricultural point of view, biopores provide plant-available nutrients and improved access to subsoil resources.

Crops may only benefit from these nutrients by rooting in biopores. However, biopore re-use — the master variable governing their potential agricultural relevance — has never been quantified up to now due to a lack of methods. For the first time in soil science, ^{137}Cs was used as a tracer for hotspot formation, making use of its strong sorption to the soil matrix and β^- decay allowing visualisation of biopores. A new dual radionuclide (^{137}Cs+ ^{14}C) labelling and two-step imaging approach (with selective shielding of ^{14}C to separate the signals) allows identification of biopores (^{137}Cs), roots (^{14}C) and biopore re-use (^{137}Cs + ^{14}C). ^{137}Cs labelling was combined with ^{15}N labelling to introduce pre-crop ^{15}N simultaneously. Two pre-crops (tap-rooted *C. intybus* and fibrous *P. tanacetifolia*) induced similar biopores regarding their physical properties within one season of cover cropping. Subsequently, rhizosphere properties of the main crop wheat (*T. aestivum* L.) were not altered by the pre-crops. Pre-crop biopores were re-used by 200% more wheat roots than stochastically expected. Pre-cops allocated N down to 60 cm soil depth. Biopore re-use was positively correlated with the TN content of the wheat shoots, but wheat did not preferentially take up pre-crop ^{15}N. Positive effects of pre-crops are 1) presumably based on several nutrients and N is not the key nutrient and 2) are very likely long-term effects from a long-term nutrient reservoir established in the biopores.

In conclusion, biopores —irrespective of their formation — were not only shown to be often-used pathways for C into the subsoil but also medium-term nutrient pools. Agricultural practices that promote biopore formation in subsoils are therefore highly relevant for C allocation into the subsoils and nutrient turnover.

VI. Zusammenfassung

Der Boden unterhalb der Pflugsohle in Agrarökosystemen (Unterboden) stellt eine potentiell sehr bedeutsame, aber wenig gezielt genutzte Kohlenstoffsenke und Nährstoffquelle dar. Bevor Kohlenstoff (C) gezielt im Unterboden sequestriert werden kann, muss der C-Umsatz in diesem Teil des Bodens grundlegend verstanden werden. Mutmaßlich findet der größte Teil des mikrobiellen C-Umsatzes in eng begrenzten Volumina (‚Hotspots') wie Bioporen statt. Das sind Makroporen geformt durch anözische Regenwürmer oder Pfahlwurzeln. Deren Porenwände sind stark angereichert an organischer Substanz (OS) von Wurzeldetritus oder Regenwurmkot, und sind damit bevorzugte Habitate für Mikroorganismen im Unterboden, sowie Nährstoffreservoirs. Weiterhin erlauben Bioporen eine schnellere Durchwurzelung in den Unterboden und Zugang zu Unterbodenressourcen wie Nährstoffe und Wasser.

Bioporenwände von Regenwurmgängen von *Lumbricus terrestris* L. (nativ oder nach sechs Monaten Aktivität) und Wurzelporen von der Gemeinen Wegwarte (*Cichorium intybus* L.) unterhalb der Pflugsohle (45–105 cm Tiefe) einer Normparabraunende auf Löss wurden auf ihre bislang wenig bekannte biochemische Zusammensetzung untersucht: Biomarkergehalte für mikrobielle Biomasse, Aktivität, funktionale Zusammensetzung der mikrobiellen Gemeinschaft in Zusammenschau mit der Charakterisierung der OS und ihrem Abbaugrad. Mutmaßlich steuert die Bioporenart (Wurzel-bürtig, Regenwurm-bürtig, gemischte Genese) diese biochemischen Parameter und damit den C-Umsatz in den Bioporen.

Zwei Jahre nach dem Absterben von Wegwarte-Wurzeln war der C-Gehalt in den **Wurzelporen** 2.5-fach höher als im Bulk-Boden und damit die mikrobielle Biomasse 7-fach erhöht. Die Biomarkergehalte normiert auf den organischen Bodenkohlenstoffgehalt waren in Wurzelporen nur in wenigen Fällen (z.B. Lignin-Phenole, Suberin-bürtige Lipide) höher als im Bulk-Boden. Enzymaktivitiäten, die den Abbau komplexerer Substrate katalysieren, waren ebenfalls deutlich erhöht. Ein engeres C/N-Verhältnis, ein höherer δ^{13}C-Wert (beide relativ zu Regenwurmporen) und Umsatzmarker (z.B. Lignin-Oxidationsgrad), die ähnlich hoch wie im Bulk-Boden waren, legten einen fortgeschrittenen Abbau des Wurzeldetritus nahe. Die mikrobielle Gemeinschaft spiegelte die ‚alte' OS wider: mehr Biomarker für Gram-positive Bakterien und Aktinobakterien als in den Regenwurm-beeinflussten Poren wurden bestimmt. Der molekulare Fingerabdruck der mikrobiellen Gemeinschaft der Wurzelporen unterschied sich deutlich von den Fingerabdrücken der Regenwurm-Bioporen, aber nicht vom Bulk-Boden. Die Inkubation von **Regenwürmern in Wurzelporen** für sechs Monate führte zur höchsten OS-Akkumulation unter den drei Bioporen-Typen. Regenwürmer überprägten die Biomarker-Signatur des Wurzeldetritus

innerhalb von sechs Monaten. Relativ zum Bulk-Boden erhöhten die großen Mengen wenig degradierter Streu den C-Gehalt um 200%, die mikrobielle Biomasse (MBC) 30-fach und induzierten die höchsten Enzymaktivitäten. Fast alle Biomarker-Gehalte waren gegenüber dem Bulk-Boden erhöht, und nur die Kombination aus C-reichem Wurzeldetritus und Regenwurmaktivität führte zu einer deutlich unterschiedlichen Zusammensetzung des OS-Pools relativ zum Bulk-Boden (Biomarkergehalte normiert auf Bodenkohlenstoffgehalt). Durch häufigen Streueintrag und mutmaßlich den Einfluss von *L. terrestris* baute die mikrobielle Gemeinschaft vor allem die eher bioverfügbaren Bestandteile der OS ab, z.B. wurde Lignin weniger stark umgesetzt als Hemizellulosen, sodass weniger verfügbare Bestandteile der Streu (Lignin, Suberin) relativ akkumulierten. Die mikrobielle Gemeinschaft wurde von der hohen Kohlenstoffverfügbarkeit, u.a. im Regenwurmdarm, stark beeinflusst, da mehr Marker für schnell wachsende Destruenten einfacherer OS gefunden wurden (Gram-negative Bakterien) als im Bulk-Boden. Die mikrobielle Gemeinschaft war nach sechs Monaten Regenwurmaktivität nicht von den nativen Regenwurmporen (> 2.5 Jahre Aktivität) zu unterscheiden. Das Hauptmerkmal der **nativen Regenwurmporen** war der regelmäßige Streueintrag über mehrere Jahre. Diese Langzeit-Aktivität führte zu 200% höheren C-Gehalten, was die mikrobielle Biomasse und Enzymaktivitäten in ähnlicher Weise wie in den inkubierten Regenwurmporen ansteigen ließ. Die OS in den nativen Regenwurmporen war am wenigsten stark degradiert unter den Bioporen — bei hoher mikrobieller Aktivität und Biomasse. Demzufolge war die mikrobielle Gemeinschaft an die regelmäßige Zufuhr einfacher abzubauender Substrate angepasst.

Insgesamt führte die Bioporengenese und OS-Akkumulation dazu, dass die Substratdiversität in den Bioporen um 30% erhöht wurde. Der molekulare Fingerabdruck der OS (auf Basis aller identifizierten Substanzen) unterschied sich nicht zwischen den Bioporen, aber zwischen den Bioporen und dem Bulk-Boden. Bioporen sind somit Habitate mit stark erhöhten Nährstoffmengen und Umsatzraten im Vergleich zum restlichen Unterboden. Die N, P und S-Gehalte waren in Bioporenwänden mindestens 100% erhöht gegenüber dem Bulk-Boden.

Aus der Sicht der Agrarwissenschaften stellen Bioporen mutmaßlich pflanzenverfügbare Nährstoffreservoirs dar, die weiterhin den Zugang zu Unterbodenressourcen sicherstellen. Folglich sollten Feldfrüchte von einer Durchwurzelung der Bioporen profitieren. Die Bioporennutzung konnte bislang nicht porenspezifisch bestimmt werden — trotz der potenziellen Relevanz der Bioporen für die Pflanzenernährung und den C-Eintrag in den Unterboden. Zur Bestimmung der Bioporennutzung wurde zum ersten Mal in der bodenkundlichen Forschung eine ^{137}Cs-Blattmarkierung eingesetzt. Nach ^{137}Cs-Gabe wird der unterirdisch verlagerte Teil der Aktivität beim Absterben der Wurzeln freigesetzt und markiert aufgrund der starken

Sorption an die Bodenmatrix die entstehende Biopore. Mittels ^{137}Cs/^{14}C-Doppelmarkierung und selektiver Abschirmung des ^{14}C bei der Bildgebung konnten Vorfrucht-Bioporen (^{137}Cs) nach einem Jahr Verrottung von Hauptfrucht-Wurzeln (^{14}C) unterschieden, sowie die Bioporennutzung (^{137}Cs + ^{14}C) bestimmt werden. Die ^{137}Cs-Blattgabe wurde zeitgleich kombiniert mit einer ^{15}N-Blattgabe, um die Wiederfindung von ^{15}N im Weizenspross zu ermitteln und damit den Vorfrucht-Effekt auf Weizen.

Weizen (*Triticum aestivum* L.) durchwurzelte in einer Fruchtfolge bis zu 75% der Vorfrucht-Bioporen von *Cichorium intybus* L. und *Phacelia tanacetifolia* Benth., das heißt 3-fach mehr als stochastisch erwartet. Der Vorfrucht-Stickstoff wurde bis in 60 cm Tiefe verlagert. Nach Phacelia war die Sprossbiomasse signifikant erhöht, aber nicht der N-Gehalt. Damit wirken Bioporen positiv auf Folgefrüchte. Beide Vorfrüchte erzeugten Bioporen mit gleichen geometrischen Eigenschaften nach 12 Wochen Anbau, was ebenso identische Wurzelsystem-Eigenschaften von Weizen bewirkte. Obwohl Weizen zu einem Großteil in Bioporen wurzelte, nahm er nicht bevorzugt den isotopisch markierten Vorfrucht-Stickstoff auf. Die Bioporen-Nutzung war aber positiv mit dem Stickstoffgehalt von Weizen korreliert. Sehr wahrscheinlich basiert die positive, direkte Wirkung der Bioporen hinsichtlich der Pflanzenernährung auf verschiedenen Nährstoffen, das heißt. nicht auf Vorfrucht-Stickstoff, sondern auf der Langzeitakkumulation von Nährelementen in der Bioporenwand wie etwa K und P.

Bioporen sind nicht nur Pfade für große Mengen wenig abgebauter Streu in den Unterboden zwecks Kohlenstoffsequestration, sondern auch direkte Nährstoffreservoirs, die die Pflanzenernährung unterstützen können. Der Anbau von pfahlwurzelnden Zwischenfrüchten und ein Regenwurm-freundliches Management (zum Beispiel reduzierte Bodenbearbeitung) erschließen den Unterboden in Fruchtfolgen und unterstützen die Pflanzenernährung.

1 Extended Summary

1.1 Introduction

1.1.1 The relevance of subsoils for C sequestration and nutrient acquisition

Soils are the third largest pool in the global carbon (C) cycle (Schimel, 1995) and subsoils store approximately half of the terrestrial C (Rumpel et al., 2012). Total C contents are considerable due to high bulk densities and larger volumes, although actual C contents are frequently low and decrease with depth (Rumpel et al., 2002). C stored in the subsoil may be characterised as mainly of microbial and root origin, slow cycling, enriched in ^{13}C, and of high radiocarbon age (Miltner et al., 2012; Paul et al., 1997; Rumpel et al., 2002; Rumpel and Kögel-Knabner, 2011). Subsoils are assumed to be unsaturated in C and may act as additional C sinks (Kell, 2012; Lorenz and Lal, 2007; Rumpel and Kögel-Knabner, 2011), e.g. by physical stabilisation on unsaturated mineral surfaces (Lorenz et al., 2011). Deep rooting crops have been suggested to increase C allocation into cropland subsoils (Kell, 2012), i.e. the soil below the ploughed horizon (Kautz et al., 2013). In this way, cropland, which is one of the largest global land uses, could actively contribute to C sequestration (FAOSTAT, 2017; Lambin and Meyfroidt, 2011).

However, subsoils are not just C sinks, but also contain valuable resources including large contents of mineral-bound nutrients such as nitrogen (N), phosphorus (P), potassium (K) (Andrist-Rangel et al., 2006; Kautz et al., 2013; Schwertmann and Huith, 1975), and soil water (Gaiser et al., 2012). Usually in agriculture, mostly the topsoil is taken into account for nutrient uptake (Kautz et al., 2013). Subsoil resources may become crucial in case topsoils become nutrient-depleted (e.g. in low input systems or organic agriculture) or dry due to more frequent droughts in future (Kuhlmann and Baumgärtel, 1991). Organic agriculture aims at increasing the nutrient acquisition from mineral phases in the subsoil and closing nutrient cycles. Smart subsoil management may generally support plant productivity, and especially in times of changing environmental conditions.

Both subsoil functions (C storage and provision of subsoil resources) are exciting examples of biogeochemical cycling. Subsoils can be considered from the points of view of organic geochemistry or agricultural research. From the *organic geochemistry perspective*, C can only be stored in the subsoil through improved management practices or crop selection, if C cycling in the low-dynamics subsoil is better understood (Dungait et al., 2012). In particular, it needs to be clear where and in which form organic matter (OM) is long-term stabilised and how microorganisms and communities interact with OM inputs. C dynamics are assumed to be different in the subsoil compared to the topsoil — partly due to colder, but generally less fluctuating environmental conditions (Zhou et al., 2002) and higher spatial heterogeneity (Salome et al., 2010). From an *agricultural* point of view, subsoil nutrients bear great potential for plant nutrition. Deep-reaching roots acquire mineral-bound nutrients from the subsoil by exudation of enzymes and organic acids (Jones et al., 2009). Rhizodeposition boosts the microbial biomass, provides energy for the microbial release of mineral-bound nutrients and priming C for the turnover of soil organic matter (SOM)-bound nutrients (Bird et al., 2011; Kuzyakov, 2010).

Both subsoil functions are intertwined: nutrient acquisition from the subsoil might increase the total C input into the subsoils. The time scales at play vary considerably: while in agriculture, crop rotation effects matter (e.g. nutrient status after a pre-crop), organic geochemistry takes a long-term view of C dynamics (e.g. stabilisation of SOM).

1.1.2 Biopores facilitate access to the subsoils

While subsoil use appears promising, root-C allocation into the subsoil may be hampered by its unfavourable environmental conditions for roots, e.g. high bulk density, compaction and penetration resistance (Dungait et al., 2012). On the other hand, for nutrient acquisition, the subsoil resources are not readily accessible, e.g. due to adverse soil structure or lack of oxygen (Kautz et al., 2013). However, macropores created by biological activity like earthworms or roots provide easier access to the subsoils (McCallum et al., 2004; Stirzaker et al., 1996). Biological macropores (biopores) are quantitatively formed by

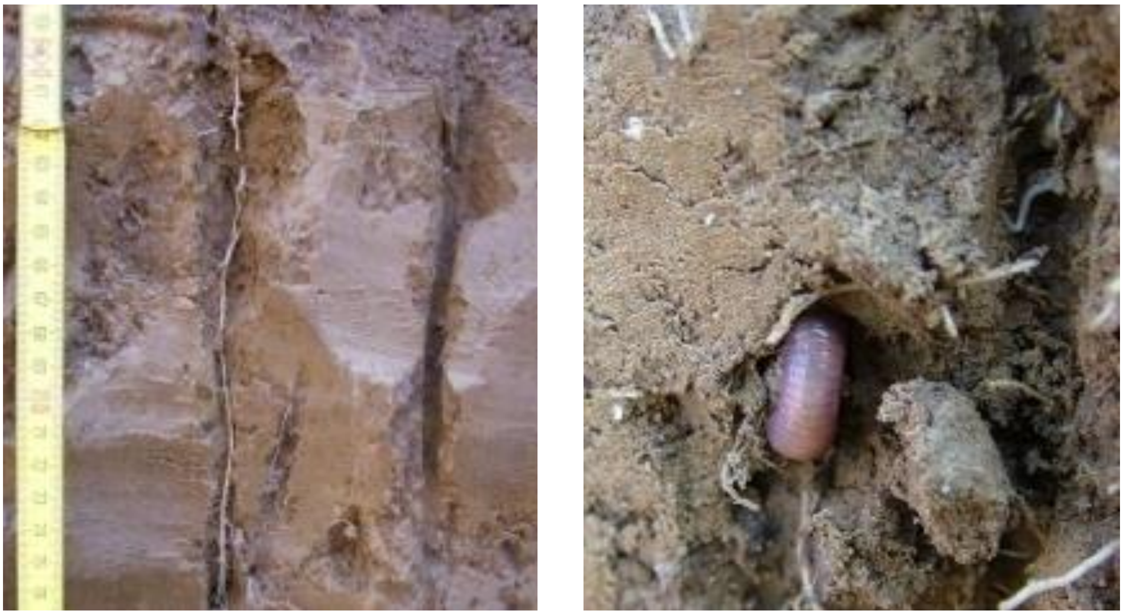

Fig. 1 *Examples of biopores formed by roots (left) and earthworms (right). Photos courtesy of Silke Hafner and Marcel Lüsebrink.*

the decomposition of tap-roots of, e.g. chicory (*Cichorium intybus* L.) or the burrowing activity of anecic earthworms like *Lumbricus terrestris* L. (Fig. 1).

Physical characteristics of biopores include inner diameters up to about 12 millimetres (Edwards and Bohlen, 1996), low tortuosity, more or less vertical alignment, and a high continuity (Hirth et al., 2005) down to 2–5 m in the soil (Cresswell and Kirkegaard, 1995). They can persist for decades (Hagedorn and Bundt, 2002), but only in the subsoil or under no-till management. Tillage removes the food sources for anecic earthworms and destroys root and earthworm biopores in the topsoil (Curry et al., 2002; Wuest, 2001). Only tap-root and earthworm biopores may be large and stable enough to reach down into the subsoil. On the larger field scale, they improve the subsoil macroporosity and soil aeration (Cresswell and Kirkegaard, 1995; Devliegher and Verstraete, 1997; McCallum et al., 2004). These properties have earned them the nickname 'highways of root growth' (Passioura, 2002) since they allow fast, unimpeded root growth into the subsoil. Consequently, biopores are an important pathway of C into the subsoil, where it may be sequestrated. Biopores contribute to subsoil C in three ways: by improving rooting in subsoils, macropore flow and particulate matter transport by anecic earthworms (Rumpel et al., 2012). Living roots release readily available C into the surrounding soil and, once they die, leave behind copious amounts of root necromass (Jones et al., 2009). Similarly, anecic earthworms import large amounts of plant litter from the soil surface, which is re-distributed during repeated ingestion, digestion and excretion (Brown, 1995; Curry and Schmidt, 2007).

Furthermore, biopores are important habitats for microbial life because of the nutrient-rich OM accumulation in their walls, which induces microbial hotspots, i.e. locations with much higher microbial activity than in bulk soil (Kuzyakov and Blagodatskaya, 2015; Nakamoto, 2000). Microbial cycling, e.g. depolymerisation, respiration and transformations of SOM, releases nutrients and supports plant nutrition (Han et al., 2017; Jastrow et al., 2007). Even though biopores only occupy 1% of the soil volume, they are likely the largest hotspots of C turnover in the subsoil as their process rates are thought to be much higher than in bulk soil (Kuzyakov and Blagodatskaya, 2015). Thus, biopores support nutrient acquisition *indirectly* by increasing the rooting activity in the subsoil, and *directly*, by providing biopore wall nutrients (Kautz et al., 2013; van Groenigen et al., 2014). Throughout this thesis, the bulk soil shall be defined as the soil which does not contain hotspots.

1.1.3 Biopores and crop rotations

Through biopore-promoting management subsoil resources could be more efficiently exploited, e.g. by including tap-rooted catch crops in crop rotations to 1) improve root access for the next cropping cycle, and 2) to accumulate nutrients in the biopore walls. The relevance of biopores for agricultural production depends on whether they actually provide nutrients and subsoil access to subsequent plants in crop rotations. Biopores are generally believed to have mostly positive effects on crops (Kautz et al., 2013). Since crop roots reportedly use biopores preferentially in compacted soils, biopores may increase yields (Jakobsen and Dexter, 1988; Logsdon and Linden, 1992).

Further findings hint at the importance of biopores for plant nutrition. Plants appear to have developed strategies to acquire biopore wall nutrients such as growing in a spiralling manner along the wall, or formation of root hairs to ‘reach out’ to the biopore wall (Athmann et al., 2013). Also, subsoil roots growing in biopores were found to be growing in contact with the biopore wall in 85% of the cases (Athmann et al., 2013). The root system architecture of barley responded on the preceding crop’s root system (fibrous *vs* tap-rooted, (Han et al., 2016). So, it seems plausible that plants use biopores and, therefore, benefit from them.

On the contrary, this may not always hold true. Roots may be trapped in biopores in hard-setting soils or in case biopore walls become too strong (Hirth et al., 2005). Root-soil contact may not always be sufficient for nutrient uptake, also possibly due to hydrophobic biopore walls (Carminati, 2013; Stirzaker et al., 1996; White and Kirkegaard, 2010). However, up to now, no quantitative information is available on the re-use of specific pre-crop-induced biopores. Furthermore, there is a knowledge gap regarding the uptake of biopore nutrients by subsequent crops. It may be possible that, despite obvious rooting strategies, biopore wall / pre-crop nutrients are not decisively beneficial to crops.

Therefore, first, quantitative data on biopore re-use is direly needed as it the principal factor for the *potential* relevance of biopores. Second, the biopore nutrient pool need to be characterised and linked to the intensity of microbial nutrient cycling to assess the availability of the nutrients. Third, the re-use and nutrient pools should be coupled with meaningful measures of plant performance to assess the implications of biopores for plant nutrition — ideally with tracer studies.

1.1.4 Biopores are the most relevant locations of C turnover in the subsoil

C turnover in the subsoil is thought to occur predominantly in hotspots. Biopores are arguably the largest hotspots by volume in the subsoil (Kuzyakov and Blagodatskaya, 2015), and therefore the most relevant locations for C turnover in subsoils. It may be hypothesised that different biopore types (earthworm *vs* root biopores) feature varying biogeochemical cycling, namely process rates and stabilisation of some parts of OM (Marschner et al., 2012; Stromberger et al., 2012). Conceptually, such differences stem from several phenomena. The OM input quality varies considerably among biopore types: the root-C in root biopores may be stabilised more than shoot-C (Abiven et al., 2005; Mendez-Millan et al., 2010; Rasse et al., 2005), which is consumed by earthworms (Curry and Schmidt, 2007). Earthworms show a species-dependent food preference, but seem to prefer litter with a high soluble C content (Curry and Schmidt, 2007), which likely affects C mineralisation. Earthworms grind and mix the litter they feed on with mucus and soil during the gut passage (Marhan and Scheu, 2005), thereby not only boosting microbial biomass but also bringing in contact OM functional groups (e.g. hydroxyl groups) with mineral surfaces. The incorporation of OM in aggregates may be a strong physical stabilisation process, albeit there are some doubts about their relevance for long-term stabilisation (Brown, 1995; Collins et al., 2000; Don et al., 2008). On the other hand, earthworms may also reduce fungal biomass (Brown, 1995; Lorenz and Lal, 2007), which in turns may lower C sequestration (Jastrow et al., 2007). Microbial community composition and spatial distribution are strongly altered by earthworms (Bonkowski and Scheu, 2004), which in turn induces interactions between soil biota (Partsch et al., 2006). Apparently, the microbial community composition does affect C cycling through varying metabolism, C use efficiency, enzyme production or residue accumulation (Sanaullah et al., 2016). Microbial residues likely play a key role in the SOM formation (Liang and Balser, 2008; Miltner et al., 2012).

As a consequence of the phenomena mentioned above, the biochemical environment of different biopore types should reflect the biopore-specific OM input, its decomposition state and microbial community composition — interactively relevant for C stabilisation. However, a comprehensive characterisation of biopore OM and the microbial community has not yet been reported despite their apparent importance to understand C turnover in subsoils better. The biopore and soil OM can be characterised by spectroscopic methods such as Fourier transformation infrared spectroscopy (Ellerbrock and Gerke, 2004), or nuclear magnetic resonance spectroscopy (Deshmukh et al., 2005). However, to characterise the OM more comprehensively, multiple biomarker analyses need to be combined. Biomarkers are organic compounds which indicate presence or past presence of its producers (Amelung et al., 2008) like phospholipid-derived fatty acids for living microorganisms (Frostegård et al., 2011) or the pentoses arabinose and xylose, which are indicative of plant hemicelluloses (Kögel-Knabner, 2002; Oades, 1984). Hence, biomarkers enable the so far unknown compound-specific characterisation of OM, its turnover and the microbial community composition in bulk soil and biopores.

1.1.5 Objectives of this thesis

Biopores functions are relevant for at least two key scientific fields: firstly, from the perspective of organic geochemistry, biopores may be the most significant locations for C turnover and support C sequestration in the subsoil. Secondly, for agriculture, biopores support nutrient acquisition from the subsoil. The time scales of interest differ in both fields: while nutrient dynamics are of interest in time scales of crop rotations, i.e. two or more growing seasons, subsoil C dynamics from the perspective of organic geochemistry represent long-term processes. Different sets of methods and different scales are therefore necessary to study the corresponding effects. The primary objective of this thesis was to assess the relevance of biopores as locations of C turnover in agricultural subsoils. As nutrient-rich OM provides valuable nutrients to crops, the second objective was to assess the importance of biopores for plant nutrition depending on biopore re-use.

The specific objectives were:

- Biogeochemical assessment of biopore hotspots of different genesis
    - Characterisation of the OM of three subsoil biopore types (derived from earthworms, tap-roots or both), linking biopore OM to the source biomasses and comparison to the bulk SOM.
    - Assessment of biopore-specific C turnover.
    - Characterisation of the microbial community composition and activity to assess the intensity of C and nutrient cycling.

- Assessment of benefits of root biopores based on their re-use in crop rotations
    - Development of a technique to determine root biopore re-use in crop rotations.
    - Quantification of biopore re-use depending on the preceding crop’s root system in crop rotations.
    - Assessment of biopores as nutrient storage in crop rotations.
    - Coupling biopore re-use to plant nutritional benefits of main crops, i.e. assessing interannual N transfer in crop rotations.

1.2 Experiments and Methods

1.2.1 Field experiment: Study site and biopore treatments

The field site near Bonn, Germany, features a maritime climate with temperate humid conditions (9.6 °C mean annual temperature, 625 mm annual precipitation). The soil type is a Haplic Luvisol (Hypereutric, Siltic; full details Table 1 on page 231) with a loamy texture and a high silt content (IUSS Working Group WRB, 2008; Vetterlein et al., 2013). Bulk TOC contents were 0.41 ± 0.02% and 0.35 ± 0.05% for the 45–75 cm and the 75–105 cm layer, respectively. Only biopores and bulk soil material below the ploughing depth were sampled. For the experiment, common chicory (*Cichorium intybus* L., var. Puna) was grown for three consecutive years to form roots of a specific age and diameter in the subsoil. In 2012, the soil down to 45 cm depth was removed. Three biopore types were induced and matured under the same environmental conditions (Fig. 3): root biopores, earthworm-incubated root biopores and native earthworm biopores, in a completely randomised block design. A comprehensive explanation of the treatments can be found in Study 3. In short, 'root biopores' represent three-year-old chicory roots, which were left to decay for two years — forming voids filled with root detritus. 'Earthworm-incubated root biopores' are 1.5-year-old

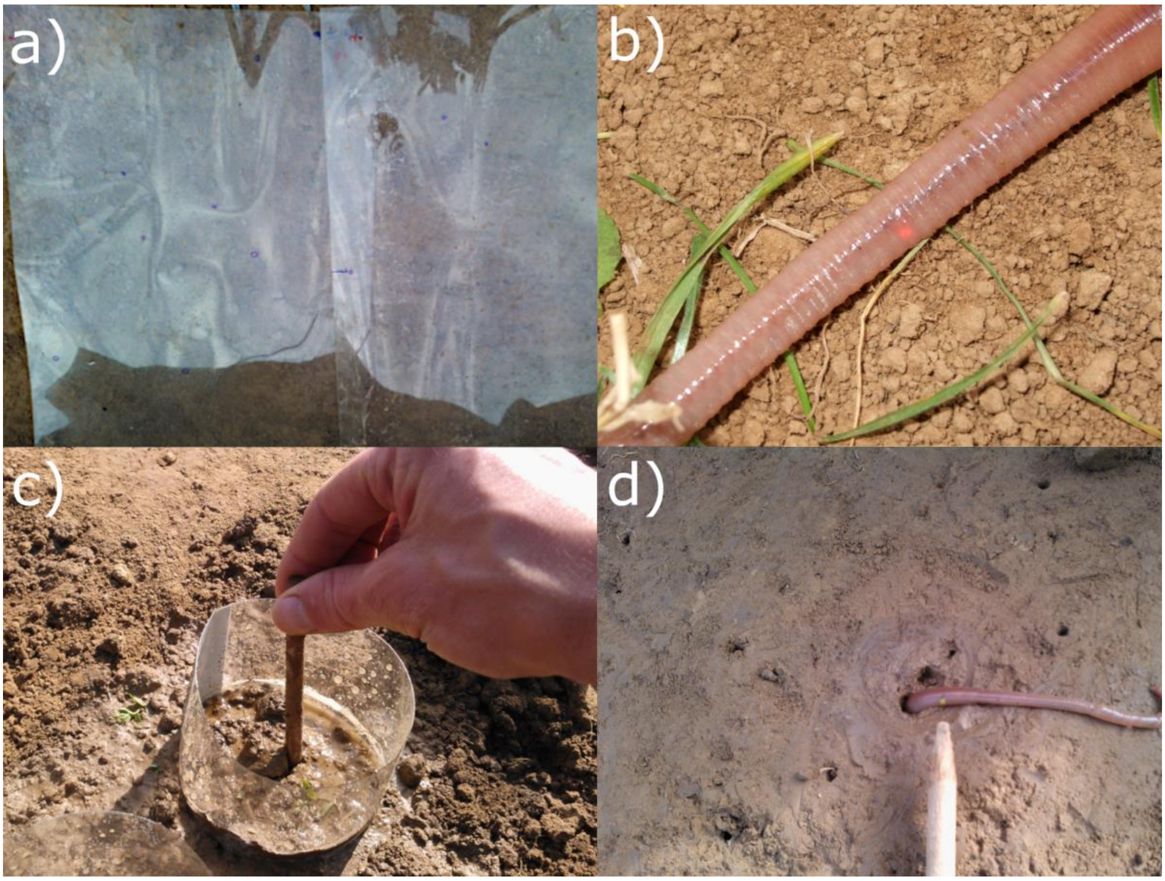

Fig. 2 *Collage illustrating the biopore formation in the field. From top left to bottom right: a) Mapping chicory roots on plastic films in 45 cm depth, b) L. terrestris featuring an elastomer tag, c) refilling the topsoil and creation of a continuous biopore from the subsoil to topsoil (wooden stick), d) tagged earthworm incubation from the original soil surface. Photos courtesy of Marcel Lüsebrink.*

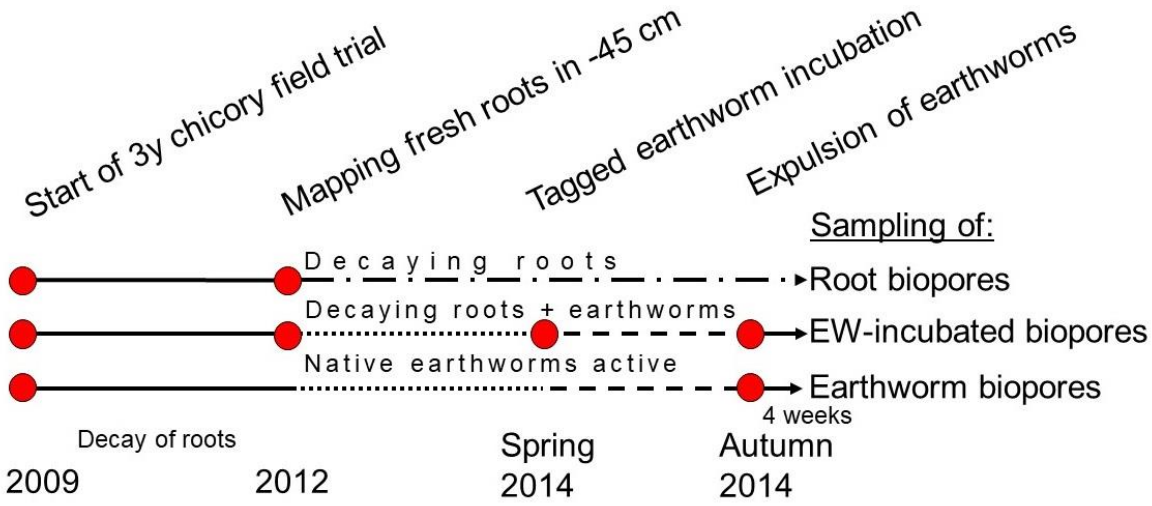
Start of 3y chicory field trial
Mapping fresh roots in -45 cm
Tagged earthworm incubation
Expulsion of earthworms
Sampling of:
Decaying roots
Root biopores
Decaying roots + earthworms
EW-incubated biopores
Native earthworms active
Earthworm biopores
4 weeks
Decay of roots
2009
2012
Spring 2014
Autumn 2014

Fig. 3 *Timeline of the field experiment. Root biopores are three-year-old chicory roots followed by two years decay. Earthworm-incubated biopores are equivalent to the root biopores but for the last six months of decay earthworms (L. terrestris) were incubated into chicory root biopores). Earthworm biopores represent the native earthworm population of the field site. Taken from Banfield et al. (2018).*

root biopores, which were incubated for six months with tagged adult earthworms (*Lumbricus terrestris* L.). Before the earthworm incubation (Fig. 2), both biopore types were identical. 'Native earthworm biopores' represent the native earthworm population. All earthworms were fed with grass-clover litter put onto the soil surface. Bulk soil samples, i.e. the fourth treatment, were taken from adjacent plots with the same treatment. At the end of the biopore formation and maturation period in autumn 2014, each biopore was opened vertically, and samples were taken by shaving off the inner biopore wall material using micro spatulas (Andriuzzi et al., 2013). Thirty-two samples were taken in total: four replicates × four treatments × two soil depths (45–75 cm; 75–105 cm). Material for each combination was pooled from about 25 individual biopores.

Plant nutrients (e.g. C, N, S) were analysed by elemental analysis (EA). Microbiological parameters were determined: microbial biomass C (MBC), metabolic quotient (qCO_2) (Anderson and Domsch, 1978; Anderson and Domsch, 2010), along with biomarker contents and their contributions to soil organic C (SOC): amino sugars (Zhang and Amelung, 1996), neutral sugars (Amelung et al., 1996), lignin-derived phenols (Hedges and Ertel, 1982), cutin/suberin-derived lipids (Spielvogel et al., 2014), phospholipids (Apostel et al., 2013), and, free lipids. A comprehensive overview of the studied biomarker classes can be found in Table 1, next page. The relative contributions of the biomarkers make up its fingerprint. SOC normalisation, i.e. dividing biomarker contents by the sample's total organic carbon (TOC) content, unveiled the biomarkers' contribution to the biopore OC pool. Biomarker SOC contributions close to the bulk soil value indicate a late decomposition stage of the tissue represented by the biomarker. The respective sections on the statistics are 2.1.2.7, 2.2.2.3, 2.3.2.6, and 2.4.2.7.

Table 1 *Overview of the biomarker approaches used to characterise OM sources, turnover and microbial communities.*

	Biomarker	Description	Turnover marker	Sample preparation
Carbohydrates	**Amino sugars**	Monomers of microbial cell walls components (n-acetylglucosamine, n-acetylmuramic acid)-heteropolymer; chitin (polyglucosamine)		6 M HCl hydrolysis (105 °C, 8 h), iron precipitation, derivatisation to aldononitrile acetates
	Neutral sugars (microbial hexoses, plant-derived pentose), acidic sugars (hexuronic acids)	Monomers of plant hemicelluloses (arabinose, xylose); microbial polysaccharides (mannose + ribose + fucose)	∑(galactose + mannose) / ∑(arabinose + xylose) ∑(mannose + ribose + fucose) / ∑(arabinose + xylose)	TFA digestion (105 °C, 8 h), DOWEX W X8 solid phase extraction (SPE), derivatisation to aldononitrile acetates, or, trimethyl silylated uronic acids (BSTFA)
Aromatics	**VSC-lignin** (vanillyl, syringyl, cinnamyl phenols)	Lignin-derived phenolic monomers	Ratio of acidic / aldehyde V, S or C phenol Ratio of syringyl / vanillyl lignin phenols	CuO oxidation, humic acid precipitation, silylation of phenols (BSTFA)
Lipids	**Cutin/Suberin-derived monomers** (ω-hydroxy fatty acids, alcohols, diacids, fatty acids)	Ester-bound ω-hydroxy fatty acids (C16-C24) + α,ω-diacids (C16-C26)), alcohols and fatty acids	Ratio of ∑ free / ∑ (bound ω-hydroxy fatty acids; (C16-C24) + α,ω-diacids acids (C16-C26)); Ratio of ∑ free / ∑ bound fatty acids (C20-C30)	Removal of free lipids by Soxhlet pre-extraction. Alkaline pressure digestion (2 M KOH:MeOH at 170 °C), liquid-liquid separation; Acetylation of hydroxyl groups (pyridine : Ac$_2$O), methylation of carboxyl groups (BF$_3$ in MeOH)
	Free lipids (n-alkanes, n-alkenes, ketones, n-alcohols, fatty acids, hydroxy fatty acids)	Decomposition products of cutin / suberin, stabilised soil lipids of various origin (e.g. cuticles, fungal neogenesis)	∑ n-alkenes (≥C14) / ∑ n-alkanes (≥C26)	Soxhlet extraction, liquid liquid separation, silica gel SPE. Acetylation of hydroxyl groups (pyridine : Ac$_2$O), methylation of carboxyl groups (BF$_3$ in MeOH)
	Phospholipid-derived fatty acids (PLFAs)	Microbial group-specific fatty acids derived from phospholipids allowing broad characterisation of the microbial community composition		Bligh/Dyer extraction; Purification by liquid-liquid extraction, elution of polar lipids from silical gel SPE by MeOH, cleaving off head groups by KOH:MeOH; methylation of carboxyl groups to FAMEs

The degree of OM turnover can be inferred from biomarker ratios (turnover proxies), which relate, e.g. plant-derived sugar monomers to microbial sugar monomers (GM/AX, Table 1) or oxidised to reduced lignin phenols. **Microbial processing** (Fig. 4, blue and red arrows) is the increase of an OM turnover proxy value from the source biomass value (red horizontal bars) to the value at the date of sampling. All changes brought about by earthworms or roots, e.g. in biomarker contents relative to the bulk soil value are summarised as **earthworm effect** or **root effect** (Fig. 4, green lines/brackets). Note that, before roots or earthworms were active in a soil volume, the same volume was bulk soil.

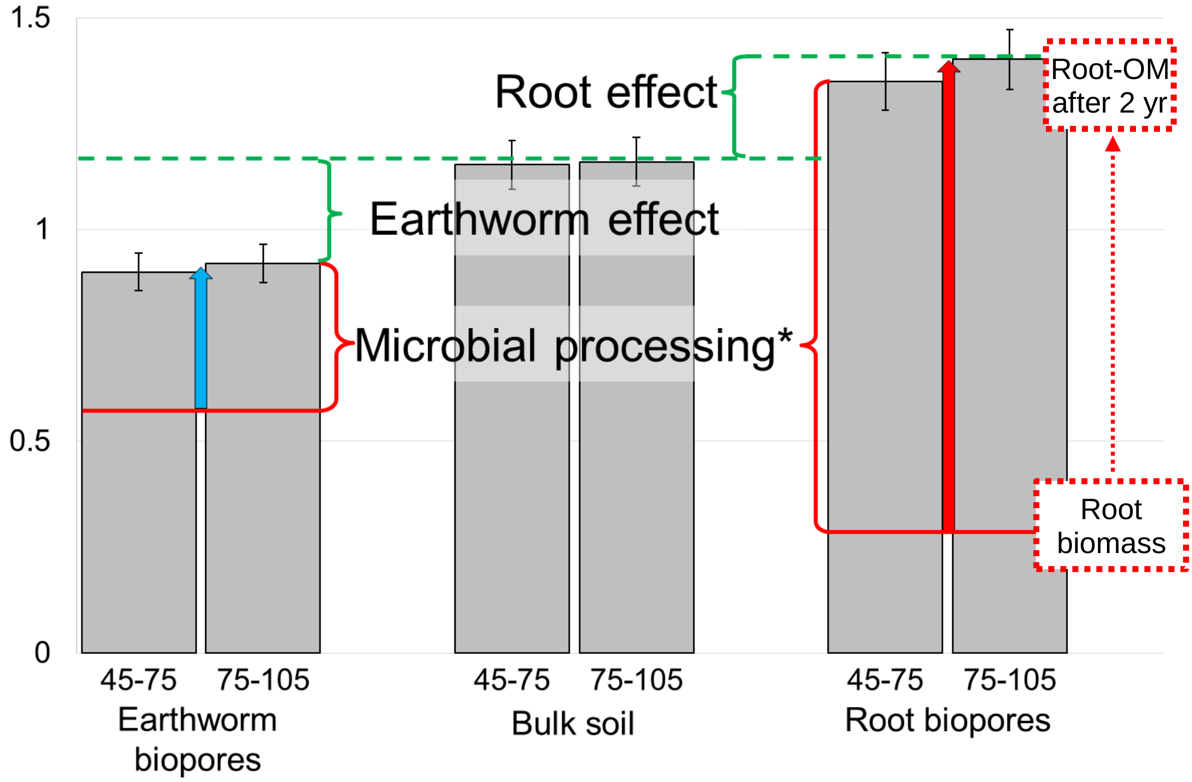

Fig. 4 *Illustration of the earthworm and root effects, i.e. the changes of the mean biomarker content or turnover proxy relative to bulk soil. In case of the turnover proxies*, the change from the undecomposed source biomasses (shown as vertical red lines) during biopore formation is the microbial processing of OM (blue and red arrows).*

1.2.2 Lab experiment 1: A proof-of-concept tool for biopore re-use

Up to now, no technique existed to study biopore re-use without disturbing the soil massively. This lab experiment established a novel technique based on dual radionuclide labelling, which for the first time enabled studying biopores and roots in a crop rotation without disturbing the soil. The method permits to evaluate the biopore re-use and couple it to potentially positive effects.

For a proof of concept, alfalfa (*Medicago sativa* L.) and chicory (*Cichorium intybus* L.) were grown in 5-cm pots and simultaneously labelled with $^{14}CO_2$ in an airtight chamber and with $^{137}CsCl$ through cut leaves (leaf feeding). Both radionuclides were allocated

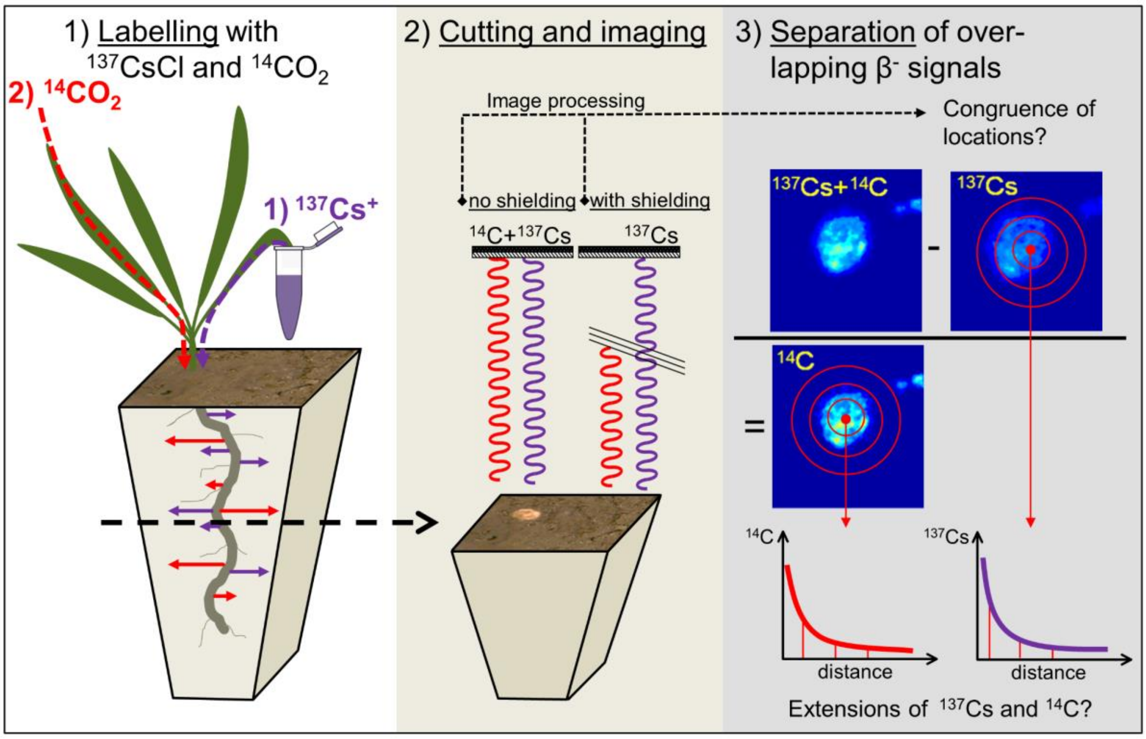
1) Labelling with
137CsCl and 14CO2
2) 14CO2
1) 137Cs+
2) Cutting and imaging
Image processing
no shielding
with shielding
14C+137Cs
137Cs
3) Separation of over-
lapping β- signals
Congruence of
locations?
137Cs+14C
-
137Cs
=
14C
14C
137Cs
distance
distance
Extensions of 137Cs and 14C?

Fig. 5 *Illustration of the ^{137}Cs labelling and imaging feasibility study (Banfield et al., 2017b). Three steps (from left to right): Labelling with $^{14}CO_2$ in an airtight chamber and ^{137}CsCl leaf feeding at the same time to simulate biopore re-use, i.e. ^{137}Cs and ^{14}C in the same rhizosphere. Cutting the soil core in 5 cm depth and two-step phosphor imaging (with and without shielding of weaker ^{14}C). Image processing, i.e. separating activities by subtraction of the attenuation-corrected ^{137}Cs image from the unshielded image, i.e. ^{14}C+^{137}Cs. Finally, checking for overlap of activities.*

belowground into the same root channel, which simulates biopore re-use. Conceptually, in a crop rotation, pre-crop biopores would be labelled by ^{137}Cs leaf feeding, while the main crop roots would be labelled through ^{14}C photosynthate exudation (after one year of soil rest). A two-step phosphor imaging approach was tested to separate the contributions of both nuclides and test for spatial overlap, i.e. biopore re-use. In the first step, phosphor imaging without shielding captured both the ^{14}C and the ^{137}Cs β^- signals together. In the second step, the β^- signal of ^{14}C was shielded off by 320 µm of polypropylene plastic film, so only the ^{137}Cs β^- signal is captured. Through image analysis, the signals of ^{14}C and ^{137}Cs are corrected, separated and give two spatial representations of the nuclides.

1.2.3 Lab experiment 2: Two-year crop rotation under controlled conditions

Twelve undisturbed subsoil cores (45–115 cm soil depth) from the location of the field experiment were taken. On six cores, the pre-crops tap-rooted *Cichorium intybus* L. var. Puna and six with fibrous *Phacelia tanacetifolia* Benth. var. Maja KWS were cultivated for three months. All pre-crops were labelled with ^{137}Cs through leaf feeding. Half of the soil cores cultivated with chicory or phacelia were labelled with $K^{15}NO_3$ by foliar application to label the biopores with ^{15}N after plant death. The pre-crops were cut after three months

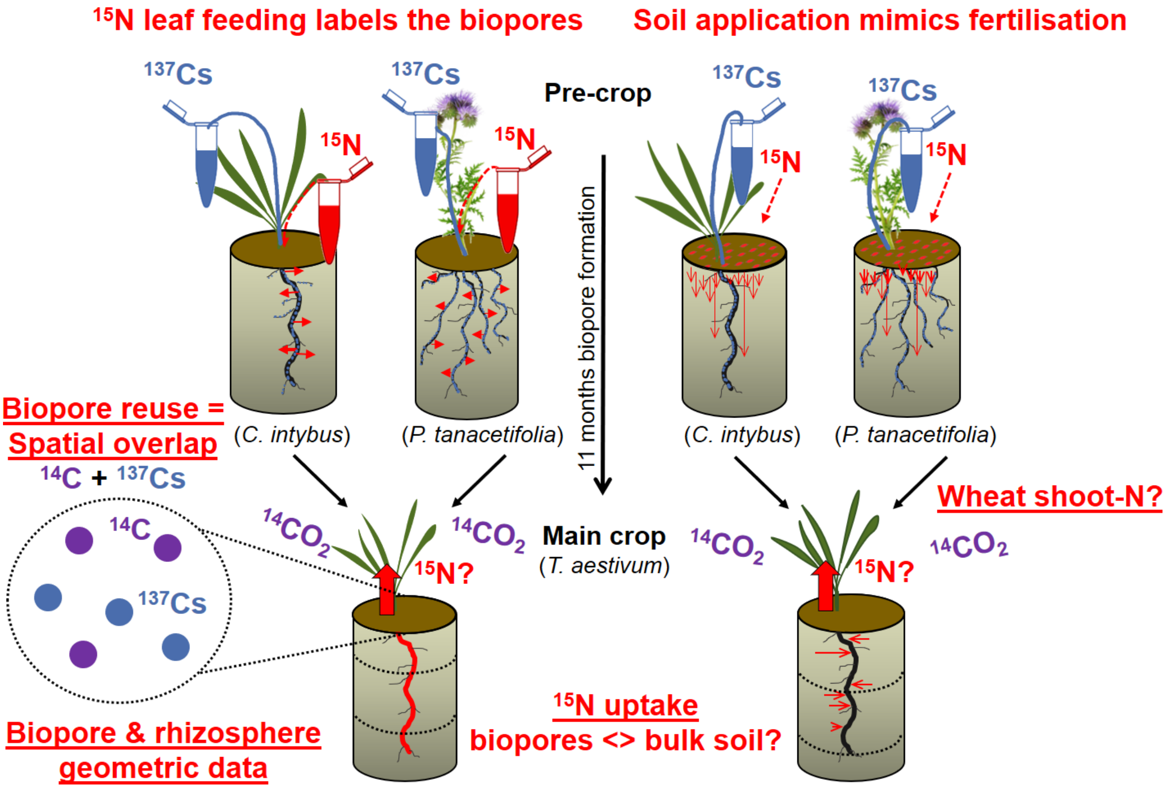
15N leaf feeding labels the biopores
Soil application mimics fertilisation
137Cs
15N
Pre-crop
11 months biopore formation
(C. intybus)
(P. tanacetifolia)
Biopore reuse = Spatial overlap
14C + 137Cs
14C
137Cs
14CO2
15N?
Main crop
(T. aestivum)
Wheat shoot-N?
15N uptake biopores <> bulk soil?
Biopore & rhizosphere geometric data

Fig. 6 *Second lab experiment 'Crop rotation': Two different pre-crops (C. intybus, P. tanacetifolia) were cultivated on soil cores. After seven weeks all plants were labelled by ^{137}Cs leaf feeding, and half of the plants were labelled by ^{15}N leaf feeding. On the other half of plants, the same amount of ^{15}N was applied to the soil surface as fertiliser. After 12 weeks, the pre-crops were cut and killed, soil cores were stored at 7 °C for root biopore formation for 11 months (last two months at 20 °C). Wheat (T. aestivum) was grown for 12 weeks and labelled six times with 3 MBq $^{14}CO_2$. Soil cores were cut three times and biopore re-use, biopore statistics and ^{15}N uptake were determined.*

and killed by herbicide application. The other half of the soil cores received a similar pulse of the same tracer by pipetting it onto the soil surface to simulate fertiliser application. The soil cores were stored at 7 °C for nine months, followed by two months at 18 °C to allow decomposition of the roots. After the pre-crop phase, wheat (*Triticum aestivum* L.) was grown under the same conditions for three months and received six $^{14}CO_2$ pulses of 3 MBq each. The soil cores were cut, and biopore re-use was quantified by two-step phosphor imaging (details see study 5). ^{15}N uptake into wheat shoots stemming from pre-crop ^{15}N was determined by an elemental analyser coupled to an isotope ratio mass spectrometer (EA-IRMS) and using an isotopic two-pool mixing model. Biopores were destructively sampled, and the isotopic composition of biopores and bulk soil was determined.

1.3 Results and Discussion

This section is split into two parts representing the main scientific disciplines' perspective on biopores. While the first part deals with the biogeochemistry of different biopore types and implications for subsoil C turnover, the second part discusses the relevance of root biopores from the perspective of agricultural soil science.

Table 2 *Overview of the studies of this dissertation*

Study	Objectives	Main results and conclusions
Study 1: "Biopores as carbon highways into the subsoil: organic matter origin and differentiation in microbial hotspots"	Detailed characterisation of OM of three different biopore types *vs* bulk soil.	Roots and earthworms strongly accumulate C in subsoils (>+100% TOC contents). Only lignin and suberin were enriched in biopore OC pool relative to bulk soil, thus limited alteration of OC pool by roots and earthworms. However, OM quality was changed (+30% substrate diversity relative to bulk soil).
Study 2: "Microbial processing of plant residues in the subsoil – The role of biopores"	Characterisation of OM decomposition in the same three biopore types to assess biopore-specific OM dynamics.	Strong OM accumulation was weakly processed in earthworm biopores. Readily available OM preferentially turned over in biopores, structural OM relatively enriched in case of frequent inputs. OM dynamics discern biopores much better than OM composition.
Study 3: "Biopore history determines the microbial community composition in subsoil hotspots"	Characterisation of the microbial community composition in the same three biopore types *vs* bulk soil to assess biopore-specific communities.	Higher C availability boosted microbial biomass >26 times relative to bulk soil. Clear link from OM quality to microbial community: Earthworms increased fungal and Gram-negative PLFAs. Root detritus increased Gram-positive PLFAs. Six months of earthworm activities overrode former root biomarker signature, i.e. earthworms are the strongest factor for the community. Biopores are important hotspots in the subsoil.
Study 4: "Six months of *L. terrestris* L. activity in root-formed biopores increases nutrient availability, microbial biomass and enzyme activity"	Assessment of the enzyme activity in the same three biopore types. Determination of nutrient stocks in biopore walls.	Root biopore formation increased plant nutrients and enzyme activities (>+100% rel. to bulk soil). Short-term earthworm activity further increased availability of C, N, P and S (+200% relative to bulk soil). Biopores are nutrient reservoirs with strong nutrient cycling in the subsoil, from which crops should benefit.
Study 5: "Labelling plants in the Chernobyl way: A new ^{137}Cs and ^{14}C foliar application approach to investigate rhizodeposition and biopore reuse"	Development of a biopore re-use quantification tool.	^{137}Cs leaf feeding and $^{14}CO_2$ labelling both label root biomass. β^- decay of both nuclides can be separated by shielding during two-step phosphor imaging. Biopore re-use quantification successfully proved to work, which enables upscaling of biopore relevance to the field scale.
Study 6: "Subsoil exploitation: The re-use of root biopore hotspots in crop rotations"	Characterisation of biopore re-use of wheat in biopores of either fibrous or tap-rooted pre-crops.	Biopore re-use likely positive for crops as it was three times higher than stochastically expected, increases with depth and bulk density. Twelve weeks cultivation of phacelia and chicory provided equal opportunities for subsoil exploration. Re-use positively correlated with N contents of the main crop.
Study 7: "The fate of pre-crop nitrogen: Biopores as hotspots for interannual nitrogen transfer in crop rotations?"	Assessment of the importance of pre-crop N for the next crop.	^{15}N leaf feeding labels biopores and bulk soil equally. Pre-crop ^{15}N not preferentially taken up by subsequent wheat. Biopore effect not caused by last-year pre-crop N, but rather less mobile nutrients like P and K.

1.3.1 Biogeochemistry of root and earthworm biopores

The field experiment in an agricultural Haplic Luvisol allows an assessment of the effects of tap-root detritus, anecic earthworm burrowing and their combination on OM dynamics in subsoils.

1.3.1.1 The effects of earthworms and tap-roots on sum parameters of OM (Study 1)

Decaying chicory tap-roots and earthworm burrowing represented large OM inputs into the subsoils and, thus, sharply increased the TOC contents and microbial biomass in their biopores. Root biopores featured only chicory root detritus but no other OM inputs. After two years of root decay, the TOC and TN contents were still increased by 100% relative to the bulk soil (Table 3). Biopores inhabited by the native earthworm population had 200% higher TOC and TN contents than bulk soil. Introducing earthworms into root biopores for six months, i.e. combining two C sources for a limited time, increased the TOC contents more than either root detritus or earthworms individually. The TOC content decreased in bulk soil with depth, while in biopores it remained constant. Thus, the biopores relevance for C cycling increases in the deeper subsoil. A constant TOC content from 45–105 cm in biopores suggests similarly strong allocation of root-C and earthworm-C into both depths.

The biopore OM was not only quantitatively but also qualitatively enhanced, namely by a 30% higher substrate richness relative to the bulk soil. Earthworm incubation (roots + earthworms) did not induce a higher substrate diversity than >2.5-year-old native earthworm biopores. Percolation likely contributed to the downward transport of C in root biopores because the count of identified compounds and TOC contents increased with depth (Kaiser and Kalbitz, 2012). Apart from a higher substrate diversity, the C/N ratio, a broad proxy for the past turnover of SOM (Wallander et al., 2003), was significantly wider in biopores than in bulk soil — hinting to weak degradation of biopore OM. The $\delta^{13}C$, a proxy for SOM turnover (Dorodnikov et al., 2007; Gunina and Kuzyakov, 2014), was significantly lighter in earthworm biopores. Therefore, accumulation of more diverse, wider C/N ratio and isotopically lighter OM underlined that biopore OM was less decomposed than bulk soil (Wilkinson et al., 2009). An absence of $\delta^{13}C$ differences between root biopores and bulk soil suggested that root biopore OM was more decomposed than the earthworm biopore OM. The lowest C content and narrow C/N ratio (~7) in bulk soil reflected the low amounts of DOC inputs (Kalbitz and Kaiser, 2008; Rumpel et al., 2004; Schulz et al., 2012), long-term SOM turnover and accumulation of microbial necromass with a narrow C/N ratio (Rumpel and Kögel-Knabner, 2011).

1.3.1.2 Characterisation of OM biomarkers in bulk soil and biopores (Study 1)

The findings of the previous section were fundamentally confirmed by the biomarker contents (Table 4). The principal component analysis (PCA, Fig. 7 on page 18, right) of all biomarkers expanded our understanding of biopore OM. Both soil depths of one treatment were separated despite vertical burrowing of earthworms redistributing OM. Samples of both earthworm-influenced biopore types were overlapping, which indicated that earthworm incubation overrode the biomarker signature of the former root presence within six months. The root biopore samples were partly overlapping with earthworm biopores but were located between earthworm biopores and bulk soil. The root detritus had neither the composition of ‘old’ bulk subsoil nor the composition of ‘fresh’ earthworm biopores. Importantly, this showed that biopores and bulk soil can be differentiated by a combination of biomarkers (Amelung et al., 2008).

Among the treatments, the **bulk soil** had the lowest contents of plant-derived OM (e.g. determined as Σ lignin, Σ cutin/suberin; Table 4) and the lowest microbial biomass (Table 3). Substrate diversity was lowest among all treatments. Neither the number of identified compounds nor their relative occurrences differed between soil depth — suggesting that most C turnover in bulk soil happens in the topsoil and not in the deep subsoil. Without prior turnover of OM in the topsoil, compounds may not be leached into the

Table 3 *Basic soil and microbiological parameters of the field experiment at Klein-Altendorf: Means ± SEM of TOC, TN, MBC, C/N, $\delta^{13}C$, ∑ PLFA g^{-1} soil, ∑ PLFA g^{-1} SOC. Letters/asterisks indicate significant differences between treatments and between soil depth. Modified after Banfield et al. (2017).*

	Root biopores		**EW-incubated biopores**		**Earthworm biopores**		**Bulk soil**	
	45-75 cm	**75-105 cm**	**45-75 cm**	**75-105 cm**	**45-75 cm**	**75-105 cm**	**45-75 cm**	**75-105 cm**
Total organic carbon [%]	0.81 ± 0.03^{b}	0.93 ± 0.06^{A}	1.16 ± 0.04^{c}	$1.07 \pm 0.04^{A*}$	1.17 ± 0.05^{c}	1.05 ± 0.04^{A}	0.41 ± 0.02^{a}	0.35 ± 0.05^{B}
Total nitrogen [%]	0.09 ± 0.00^{b}	0.10 ± 0.01^{A}	0.12 ± 0.00^{c}	0.11 ± 0.01^{A}	0.11 ± 0.00^{c}	0.10 ± 0.01^{A}	0.06 ± 0.00^{a}	$0.05 \pm 0.00^{B*}$
Microbial biomass carbon [µg g^{-1} soil]	181 ± 6^{a}	170 ± 9^{a}	820 ± 38^{b}	593 ± 88^{b}	463 ± 28^{c}	384 ± 38^{b}	33 ± 1^{d}	22 ± 3^{c}
C/N	8.6 ± 0.2^{a}	9.7 ± 0.5^{A}	9.6 ± 0.1^{b}	9.9 ± 0.4^{A}	10.3 ± 0.2^{c}	10.3 ± 0.5^{A}	7.2 ± 0.1^{d}	7.7 ± 0.9^{A}
$\delta^{13}C$ [‰]	-25.66 ± 0.46^{ab}	-23.87 ± 1.17^{A}	-26.47 ± 0.21^{a}	-25.55 ± 0.51^{A}	-25.30 ± 0.25^{ab}	-23.76 ± 0.66^{A}	-25.00 ± 0.05^{b}	-23.51 ± 0.75^{A}
Σ PLFAs [µg g^{-1} soil]	16.7 ± 1.0^{a}	23.0 ± 3.3^{A}	33.5 ± 2.1^{b}	25.5 ± 9.1^{A}	36.6 ± 3.4^{b}	26.4 ± 3.9^{A}	$1.1 \pm 0.5^{\dagger}$	$0.7 \pm 0.1^{\dagger}$

† not tested, assumptions not met subsoil (Kalbitz and Kaiser, 2008; Schulz et al., 2012). Bulk soil OM was a broad mixture of substance classes (Rumpel et al., 2012) — but not mostly root-C (Mendez-Millan et al., 2010).

The initial OM input by the perennial chicory tap-roots fuelled the **root biopores** for at least two years (Table 4). All microbial and plant biomarker contents were 33% lower than in the earthworm biopores. Relative to the bulk soil, the root biopores were enriched in lignin, hemicelluloses (75–105 cm), root suberin lipids and microbial residues (amino sugars), i.e. compounds often considered as residual C. This suggests a late decomposition stage and an accumulation of microbial residues lowered the C/N ratio (Rumpel et al., 2012; Wallander et al., 2003). After two years, the root effect was weaker than the earthworm effect.

Earthworm-incubated biopores combined two C sources (Table 4). Within six months *L. terrestris* had nearly completely overridden the biomarker signature of the former root. The combination of root, shoot and earthworm OM increased the substrate richness by 33% compared to bulk soil. The OM fingerprint matched well with the clover-grass source biomass (Table S7, Study 1), suggesting weak processing of the inputs (Jégou et al., 2000). The root/shoot biomarker ratio of the OM was highest among all treatments in root-influenced biopores (root biopores, earthworm-incubated biopores). The incubation tripled the hemicellulose contents, doubled n-alkane and lignin contents but did not change cutin/suberin contents relative to the root biopores. Relative to the bulk soil, the lignin contents were 15 times higher, which was by far the strongest increase compared to the other biomarkers. The microbial necromass dynamics appeared decoupled from the plant biomarker accumulation because the highest plant biomarker contents did not lead to equally high amounts of necromass.

The **native earthworm biopores** were very similar to the earthworm-incubated biopores due to the strong earthworm influence and the same food sources (Table 4). Even though the ‘native’ earthworms had been active much longer than the ‘incubated’ earthworms, the mean TOC and biomarker contents were lower. The longer the earthworms had been active, the less pronounced the effect of the soil depth became. Biomarkers representing tissues with shorter turnover times showed more discernible depth effects.

Table 4 *Biomarker contents [g^{-1} soil] and contributions to SOC [g^{-1} SOC]. Shown are means ± SEM. Letters indicate significant differences (one-way ANOVA, large: 45–75 cm, small 75–105 cm). Asterisks given in 75–105 cm show significant differences between both soil depth.*

	Biomarker contents [µg g^{-1} soil]				**SOC contribution [mg g^{-1} SOC]**			
45-75 cm	**Bulk soil**	**Earthworm pores**	**EW-incubated pores**	**Root pores**	**Bulk soil**	**Earthworm pores**	**EW-incubated pores**	**Root pores**
Σ Amino sugars	762 ± 164A	1933 ± 464A	1073 ± 84A	689 ± 176A	188 ± 39A	161 ± 34A	95 ± 7A	85 ± 20A
Σ Cutin/suberin	4.4 ± 0.7A	37.9 ± 1.3C	21.7 ± 0.6B	21.4 ± 2.0B	1.1 ± 0.2A	3.3 ± 0.1C	1.8 ± 0.1AB	2.5 ± 0.2BC
Σ VSC	21.0 ± 0.5A	197.7 ± 12.0C	267.5 ± 2.3D	120.8 ± 13.5B	4.9 ± 0.2A	16.9 ± 1.0B	21.8 ± 1.2C	16.7 ± 0.7B
Σ Plant pentoses	98 ± 6A	338 ± 16AB	457 ± 9B	167 ± 5AB	23 ± 0AB	32 ± 2AB	38 ± 2B	21 ± 1A
Σ Microbial hexoses	99 ± 9A	289 ± 14AB	353 ± 9B	187 ± 6AB	23 ± 0AB	26 ± 2AB	29 ± 1B	25 ± 1A
Σ Neutral sugars	346 ± 35A	1249 ± 13AB	1461 ± 34B	706 ± 27AB	74 ± 3A	107 ± 2AB	116 ± 5B	85 ± 3AB
Σ n-alkanes	118 ± 19A	412 ± 99A	407 ± 87A	203 ± 46A	35 ± 7A	35 ± 7A	35 ± 6A	25 ± 5A
incl. n-alkanes > C26	63 ± 8	258 ± 63	307 ± 69	113 ± 25	18 ± 4A	22 ± 5A	26 ± 5A	14 ± 3A
Σ n-alkenes	86 ± 7A	162 ± 48A	209 ± 43A	186 ± 39A	20 ± 2A	14 ± 4A	18 ± 3A	23 ± 5A
Σ ketones / alcohols	6 ± 0A	13 ± 2AB	15 ± 2B	10 ± 1AB	2 ± 0A	1 ± 0A	1 ± 0A	1 ± 0A
Σ fatty acids	1 ± 0A	6 ± 1A	8 ± 1A	4 ± 1A	0 ± 0A	1 ± 0A	1 ± 0A	0 ± 0A
Σ hydroxy fatty acids	15 ± 1A	31 ± 15A	19 ± 4A	27 ± 10A	4 ± 0A	3 ± 1A	2 ± 0A	3 ± 1A
Σ Free lipids	227 ± 11A	624 ± 158A	658 ± 125A	429 ± 79A	56 ± 3A	54 ± 14A	56 ± 9A	53 ± 10A
Root / shoot biomarkers	0.6 ± 0.1B	18 ± 0.1AB	2.2 ± 0.0A	2.8 ± 0.5A				
75-105 cm								
Σ Amino sugars	606 ± 56a	1230 ± 195a	1010 ± 77a*	1600 ± 340a	184 ± 34a	118 ± 19a	103 ± 6a*	178 ± 45a
Σ Cutin/suberin	1.7 ± 0.4a*	14.8 ± 1.6b*	17.9 ± 4.3b	11.8 ± 2.6ab	0.6 ± 0.1a*	1.4 ± 0.2a*	1.7 ± 0.4a	1.3 ± 0.3a
Σ VSC	12.5 ± 2.5a	185 ± 13.6ab	231.2 ± 18.0b	123 ± 19.0ab	4.1 ± 0.2a	17.8 ± 1.2b	21.8 ± 1.8b	13.6 ± 1.8b
Σ Plant pentoses	76 ± 1a	281 ± 23a	383 ± 22b	170 ± 7a	25 ± 1a	25 ± 3a*	36 ± 2b	18 ± 1a
Σ Microbial hexoses	74 ± 3a	243 ± 15ab	341 ± 11b	200 ± 11a	24 ± 2a	22 ± 2a	32 ± 2b	22 ± 1a
Σ Neutral sugars	267 ± 10a	1065 ± 59a	1266 ± 63a*	759 ± 37a	83 ± 6ab	89 ± 8ab	113 ± 7b	77 ± 3a
Σ n-alkanes	156 ± 13a*	287 ± 28a	330 ± 63a*	219 ± 47a	45 ± 5a*	27 ± 3a	31 ± 5a*	25 ± 9a
incl. n-alkanes > C26	84 ± 8a	163 ± 13a	199 ± 35a	112 ± 22a	24 ± 3a	15 ± 1a	18 ± 3a	13 ± 4a
Σ n-alkenes	70 ± 1a*	113 ± 15a	119 ± 26a	92 ± 26a	20 ± 3a	10 ± 1a	11 ± 2a*	11 ± 4a
Σ ketones / alcohols	7 ± 0a*	10 ± 1a	12 ± 2a	9 ± 3a	2 ± 0a	1 ± 0a	1 ± 0a	1 ± 1a
Σ fatty acids	2 ± 1a	4 ± 2a	7 ± 2a	6 ± 2a	1 ± 0a	0 ± 0a	1 ± 0a	1 ± 0a
Σ hydroxy fatty acids	20 ± 4a	35 ± 14a	45 ± 26a	44 ± 17a	6 ± 2a	3 ± 1a	4 ± 2a	5 ± 2a
Σ Free lipids	255 ± 10a*	449 ± 52a	514 ± 111a*	371 ± 86a	74 ± 10a	41 ± 5a	47 ± 8a*	43 ± 15a
Root / shoot biomarkers	0.4 ± 0.1b	2.1 ± 0.2a	2.3 ± 0.4a	2.3 ± 0.4a				

1.3.1.3 The contributions of biomarkers to SOC composition (Study 1)

Long-term native earthworm presence (> 2.5 years) and two years of tap-root decay only weakly affected biopore OM on the level of substance classes (Table 4, right). After TOC normalisation, only lignin was significantly enriched in the OC pool of all biopores compared to bulk soil, and cutin/suberin was significantly enriched in native earthworm and root biopore OM. Among the biopores, only earthworm incubation into root biopores changed the composition of the SOM strongly, i.e. additional enrichment of hemicelluloses and microbial sugars relative to bulk soil. On the individual substance level, the fingerprints of the three biopores were similar to each other but different to the bulk soil (shown by a similarity analysis; ANOSIM). The OM inputs were biopore-specific but the resulting OM after biopore-specific processing was not drastically different to the other biopore types.

1.3.1.4 Turnover of biopore OM (Study 2)

The isotopic composition, C/N ratio and SOC contribution of substance classes implied that relative to bulk soil there was little C turnover in earthworm biopores and considerably more in root biopores, which were approaching the decomposition stage of bulk soil. The PCA of the turnover proxies (Fig. 7, left) clearly differentiated fresh C input treatments (both earthworm biopore types) from older C, more degraded OM treatments (bulk soil, root biopores). The PCA of the turnover proxies (Fig. 7, left) separated the treatments much better than the PCA of all biomarkers (Fig. 7, right). The most discriminating individual biomarkers were markers for microbial stress and OM degradation. Thus, in biopores, OM turnover is more defining than the OM composition.

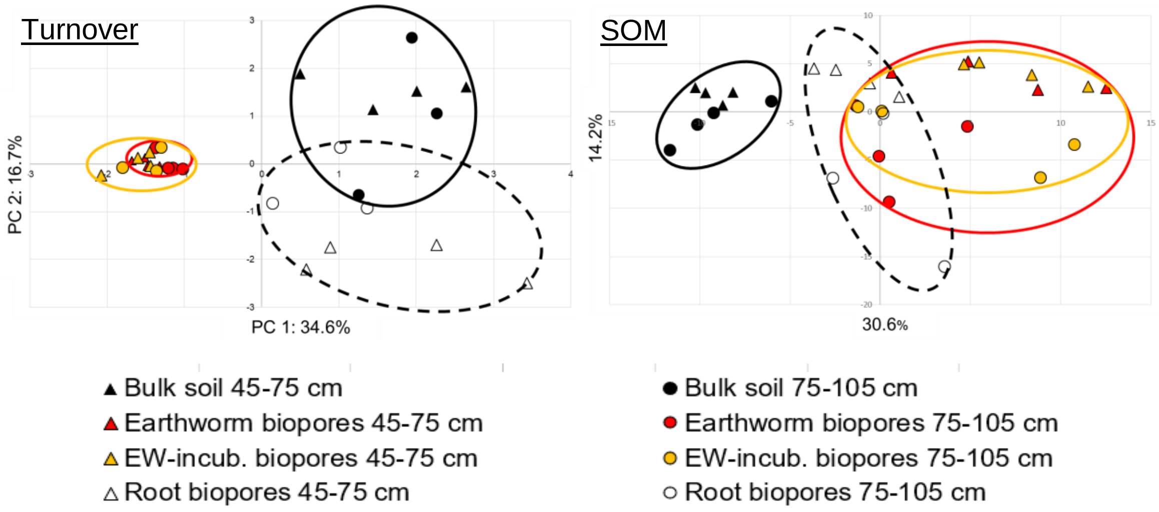

Fig. 7 *Two PCAs of turnover proxies (left) and the SOM fingerprints (~160 compounds; right). The left PCA describing OM turnover separated the bulk soil and root biopores better than the PCA of the SOM fingerprints, and explained a higher proportion of the total variance. OM turnover, which includes the interaction of the biota with the soil, characterises biopores better than the composition of SOM. In both cases, earthworm-influenced biopores featured much smaller within-group variance than bulk soil or root biopores, and the x-axis separated samples with frequent C inputs from those with infrequent C inputs.*

1.3.1.5 The effects of earthworms, roots and soil depth on the decomposition stage of biopore OM (Study 2)

The overall decomposition of the OM in earthworm biopores was much less advanced than in bulk soil due to the fresh, weakly pre-processed OM brought into their burrows (earthworm effect). This underlines the immense role of earthworms as ecosystem engineers (Curry and Schmidt, 2007; Jones et al., 1996). In particular, hemicelluloses, lignin vanillyl subunits, suberin and n-alkanes were less degraded than in bulk soil. In contrast, the root effect was much weaker, and after two years, only suberin and lignin vanillyl subunits were not as degraded as bulk soil OM, suggesting like the PCA, biomarker contents and SOC contributions, that root biopores and bulk soil featured similarly degraded OM. The soil depth played a minor role when earthworms were active (Fig. 7) as earthworms vertically redistributed OM in their burrows (Jégou et al., 2000). The separation of root biopore samples in the PCA (Fig. 7, left) from both soil layers underlines that root detritus was more degraded in the deeper subsoil (Fig. 8).

1.3.1.6 Microbial processing of OM inputs in biopores (Study 2)

The microbial processing (illustrated in Fig. 4 and Fig. 8, next page) was negatively connected with the frequency of C inputs. Consequently, the OM in root biopores was generally most strongly processed among the biopores. The processing was substance class-specific: e.g. in all biopores, hemicelluloses (Fig. 8) were more strongly processed than lignin during the same period (Fig. 9) as hemicelluloses are more easily decomposable than lignin (Haider and Martin, 1979; Lorenz and Lal, 2007; Marhan and Scheu, 2006). The vanillyl subunits of lignin were almost untouched in earthworm biopores — probably they were not microbially attacked as vanillyl subunits represent parts of the lignin macromolecule, which are in the centre of the molecule (Thevenot et al., 2010). Consequently, earthworm activity relatively enriched less bioavailable lignin and suberin in their burrows. In the subsoil, intact suberin is mainly limited to biopores since in bulk soil the highest ratio of free/bound hydroxy fatty acids were found.

At least four more factors influence the degree of processing. 1) Earthworms mix ingested soil with OM, thereby bringing chemical functional groups in contact with each other (von Luetzow et al., 2006). Such physicochemical stabilisation is not expected to be as strong in root biopores, as the root detritus is not actively incorporated into the surrounding soil (Lubbers et al., 2017; Schmidt et al., 2011). 2) Functional groups of the substance govern the interaction of OM with mineral surfaces, e.g. n-alkanes feature no functional groups as compared to hemicelluloses (hydroxyl groups) (Amelung et al., 2008).

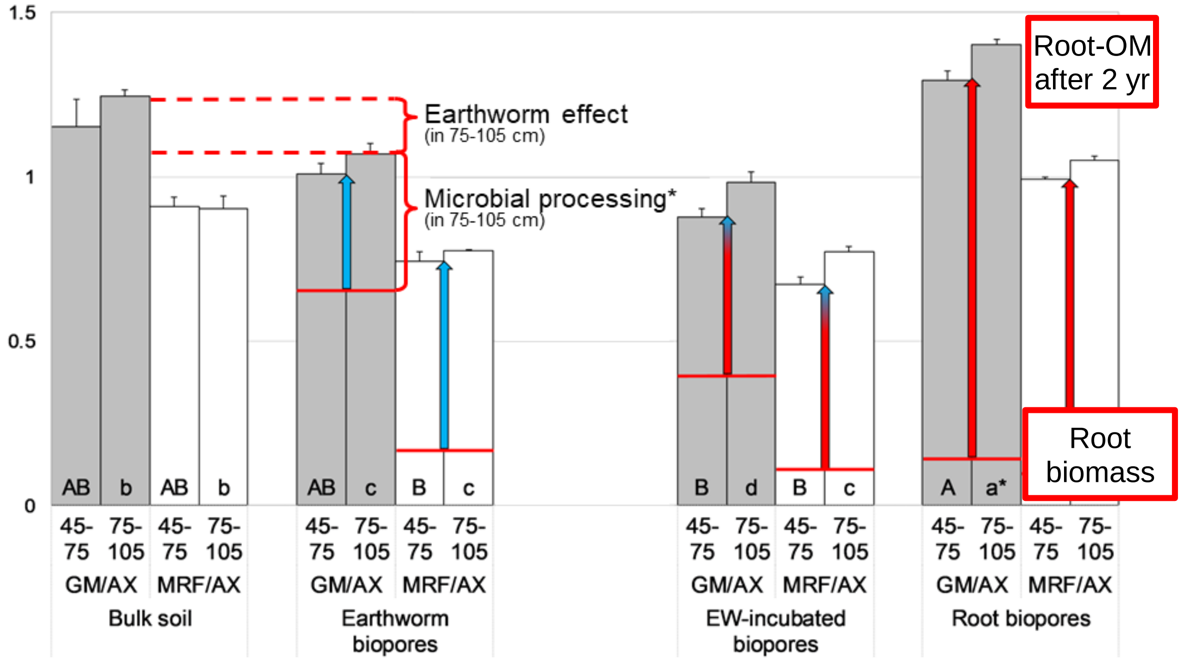

Fig. 8 *Ratio of microbial-derived galactose and mannose to plant-derived arabinose and xylose (GM/AX; grey bars) and as white bars, the ratio of mannose + fucose + ribose to arabinose and xylose (MRF/AX), both are markers for the turnover of hemicelluloses. The difference between the bulk soil mean and, e.g. the earthworm biopore mean is the '****earthworm effect****' (on bulk soil). '****Microbial processing****' is illustrated by the red and blue arrows and defined as the increase of the initial, undecomposed source biomass (vertical red line) during biopore formation. After Banfield et al. (2018).*

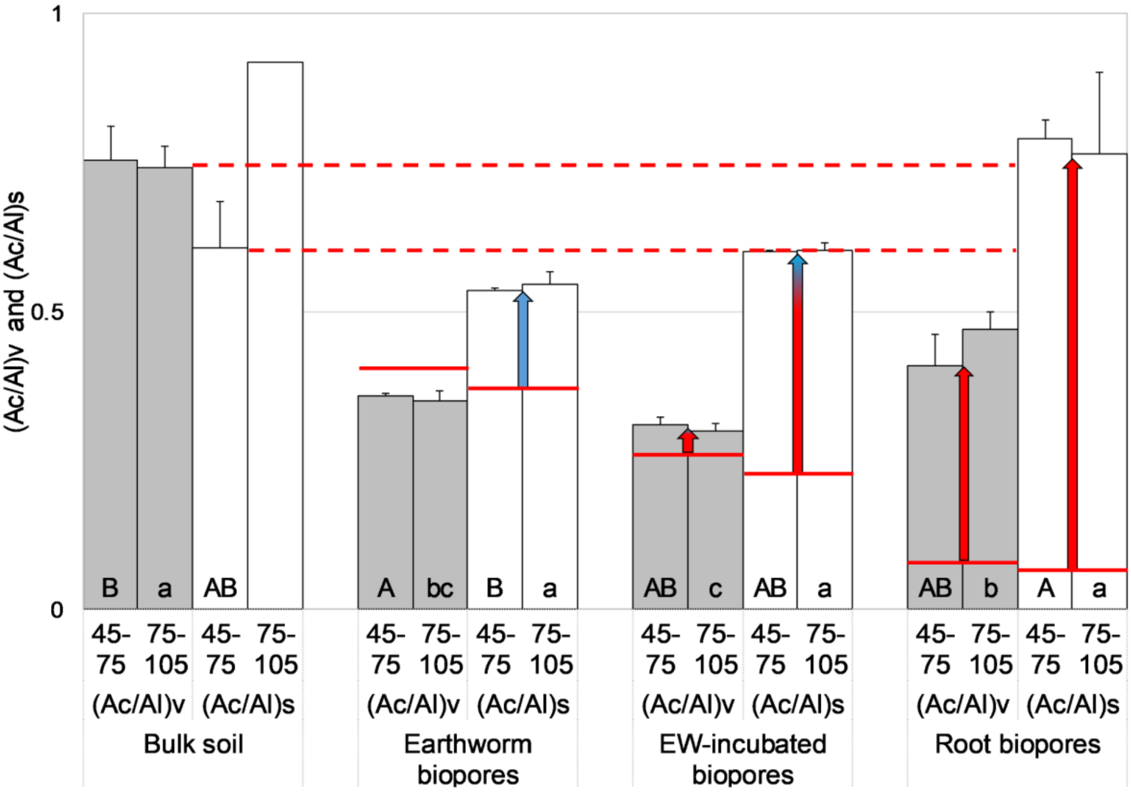

Fig. 9 *The ratios of the acidic phenol to the aldehyde phenol for lignin-derived subunits (grey bars Ac:Alv for the vanillyl phenols; white bars for Ac:Als for the syringyl phenols) are proxies for the oxidation state of the lignin molecule. Red lines indicate the respective ratios of the source biomasses prior to decomposition. Taken from Banfield et al. (2018).*

3) The higher decomposition of root hemicelluloses in the deeper subsoil may result from a lower degree of lignification (Barros et al., 2015) or from a lower degree of cross-linking of hemicelluloses to lignin of the younger root parts (Amin et al., 2014; Bertrand et al., 2005; Moorhead et al., 2014). 4) The effect of soil depth on processing was little and was only discernible in root biopores (Fig. 7, left). These facts suggest that the processing of OM was not strongly influenced by preferential OM inputs (e.g. by favoured earthworm activity in 45–75 cm). Biota likely had the most significant effect on microbial processing: in the PCA by far the smallest within-group variance was in both earthworm biopore types, illustrating the strong role of earthworms as ecosystem engineers (Jones et al., 1996).

1.3.1.7 Microbial community composition (Study 3)

The previous sections showed that the OM in earthworm biopores was not only ‘more’ but also ‘more diverse’ and ‘more available’ since it was frequently replenished. Preferential processing caused little need for microorganisms to consume less bioavailable compounds like lignin. In contrast, root biopores feature 33% less C but of an ‘older’ quality, i.e. later decomposition stage.

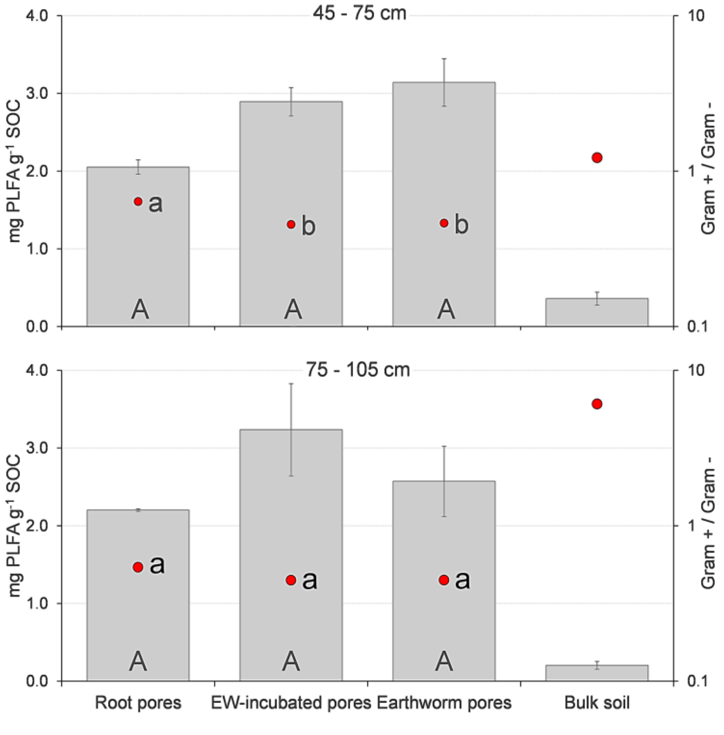

Fig. 10 *Microbial biomass g SOC^{-1} (grey bars) as determined by its proxy ∑ PLFAs, and the ratio of Gram-positive/Gram-negative PLFAs (red dots). Letters indicate significant differences on α 0.05, separately tested for each depth Banfield et al. (2017a).*

The microbial community structure was a result of rooting/earthworm activities and the frequency and quality of inputs (frequent pre-digested shoot *vs* infrequent root inputs). The C inputs led to 26–35 times higher microbial biomass contents (∑ phospholipid-derived fatty acids g^{-1} soil, ∑ PLFA), relative to bulk soil (Fig. 10). The highest Σ PLFA and MBC were found in both earthworm biopore types. Thus, the highest C and nutrient turnover were expected. The Σ PLFA g^{-1} SOC was 33% lower in root biopores than in earthworm biopores (Fig. 10).

The quality of the OM was linked to the microbial community (Sanaullah et al., 2016; Zhou et al., 2002). Its composition can be modelled from environmental variables by RDA. When the variable δ^{13}C was included in the RDA model, the ordination improved considerably (Fig. 4 on page 128). Therefore, C and N contents and C quality were likely the main factors governing the community composition. Gram-positive bacteria including actinobacteria were more abundant in root biopores than in earthworm biopores. Gram-positive bacteria are known to include decomposers of structural and not readily available C (Goodfellow and Williams, 1983). Most readily available OM was already respired at this late decomposition stage in root biopores, leaving behind less bioavailable suberin and lignin. In contrast, both earthworm biopore types featured regular fresh litter input of a higher C availability than the older root detritus, promoting preferential growth of Gram-negative bacteria and fungi (Gram-positive/Gram-negative bacteria ratio in Fig. 10). First, earthworm gut bacteria are mostly Gram-negative (Sampedro et al., 2006). Regular inputs of readily available shoot-C promoted a community of Gram-negative bacteria. Thus, the less bioavailable, structural OM (lignin, suberin) was weakly processed. Earthworms in root biopores shifted the composition of the microbial community entirely and effectively turned root biopores into earthworm biopores within six months of incubation — like the biomarkers describing the OM composition (Study 1). Certainly, environmental factors cannot be completely ruled out for shaping the communities, e.g. drier root biopores (relative to earthworm biopores) may be giving advantage to biofilm-dwellers (Vu et al., 2009). However, C input quality and frequency were most strongly affected the community composition. Such a connection between C quality and input frequency on microbial communities was previously described for top and subsoils (change from Gram-negative in topsoil to Gram-positive in subsoil (Fierer et al., 2003; Kramer and Gleixner, 2008), as well as for the decomposition of root OM over time (change from Gram-positive to Gram-negative over three years of root decay; (Sanaullah et al., 2016).

The overall connection between microbial communities (Study 3), C quality (Studies 1, 2) and the effect of earthworms was corroborated by the PLFA fingerprints (pattern of 27 PLFAs). Fingerprints of both earthworm biopore types were not distinguishable from each other by ANOSIM or PCA, but both earthworm biopore types were different to root biopores.

1.3.1.8 Microbial activity and nutrient supply (Study 4)

Along with higher MBC, much higher enzyme activities were apparent in biopores (Fig. 11). A sharply increased qCO_2 in bulk soil points to less efficient and more stressed microbial biomass in bulk soil compared to biopores (Anderson and Domsch, 2010). C cycling releases nutrients from OM and mineral-bound nutrients by enzymes as catalysts (Tabatabai, 2007). The contents of C, N, P, and, S were at least doubled in the biopore walls of both soil depths compared to bulk soil (Study 4, Table 1). Plant-available P was 10–15 times enriched in earthworm-incubated biopores and 7.5–10 times in root biopores. In bulk soil, the contents of TN and sulphur (TS) decreased with depth, while total phosphorus (TP) increased with depth. There were no depth effects in root biopores, but in earthworm biopores preferential burrowing led to higher TN and TP contents in the upper soil layer. Enzyme activities of the C cycle (cellobiohydrolase, ß-glucosidase and xylanase) and the N cycle (chitinase, chitotriosidase, leucine aminopeptidase) were increased in earthworm (2.9–5.6 times and 3–11 times, respectively), and less pronounced in root biopores relative to bulk soil (1.5–2 times and 2.5–3 times, respectively). N-cycling enzyme activities were more increased than C-cycling enzyme activities, suggesting that the biopore-N was being mineralised more rapidly than biopore-C. Also, mobilisation of nutrients is more likely in biopores than in bulk soil — potentially providing nutrients to crops that re-use biopores in crop rotations.

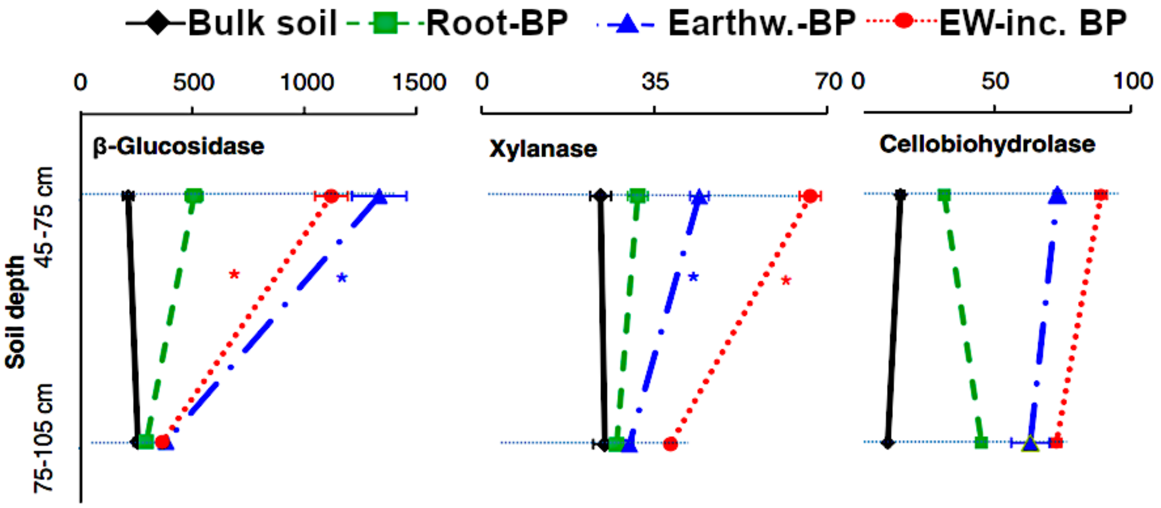

Fig. 11 *Enzyme activities of β-glucosidase, xylanase and cellobiohydrolase (nmol g^{-1} MUF h^{-1} or nmol g^{-1} AMC h^{-1}) at two soil depths (45–75 and 75–105 cm) in three biopores types (abbreviated BP) and bulk soil. The asterisk (*) illustrated a significant effect of soil depth for one enzyme. Modified after Hoang et al. (2016).*

1.3.2 The relevance of root biopores in crop rotations

The previous section on biogeochemistry showed that subsoil biopores are clearly hotspots, which are enriched in C and N, contain considerable nutrient pools (P), and cycle valuable nutrients — especially N — at much higher rates than the surrounding bulk soil. All of this makes biopores an attractive option for organic farming, which relies more on nutrient mobilisation in the subsoil than conventional agriculture (Kopke et al., 2015). Previous research pointed to physical benefits for plants such as faster subsoil access (Passioura, 2002). Biopores are seemingly beneficial as roots grow within them (Athmann et al., 2013; Nakamoto, 2000; Rasse and Smucker, 1998). However, from the viewpoint of agricultural soil science, just because biopores are microbial hotspots, and roots grow within them, does not necessarily mean that biopores increase yields (Han et al., 2015b) — albeit correlations between biopore densities and crop yields were modelled (Gaiser et al., 2013; Jakobsen and Dexter, 1988) or occasionally found (Volkmar, 1996). Conceptually, for biopores to be *potentially* relevant for plant nutrition, roots need to grow preferentially in them and in contact with the biopore wall to take up nutrients. Biopore re-use has never been quantified pre-crop-specifically (only root growth in macropores) despite it being the prerequisite for the relevance of biopores. As in the field, the majority of biopores are induced by tap-rooted crops (Dinter et al., 2013; Han et al., 2015a; Kautz et al., 2014), a method to quantify root biopore re-use was developed and tested (Studies 5, 6; lab experiment 1) and subsequently applied to study plant nutrition in order to assess the relevance of biopores in a crop rotation (Studies 6, 7, lab experiment 2). If the hypothesis of a beneficial biopore re-use holds true, then the biopore properties become very relevant for nutrient storage and uptake. Larger biopores may contain more nutrients, but in smaller biopores, the wall-root contact may be more intimate. Thus, geometric data of biopores are invaluable for upscaling studies.

1.3.2.1 Method development (Studies 5 and 6)

Identification and tracking of biopores in crop rotations requires an easily detectable label, which is immobile after biopore formation and re-use in the following years. ^{137}Cs fulfils these requirements, as it is only negligibly taken up by microbes and strongly binds to mineral phases. Its high maximum β^- decay energy, chemical behaviour similar to potassium, and, half-life of 30.2 years make it an excellent label for biopores, with quantification by phosphor imaging (IAEA, 1995; Zapata, 2003). ^{137}Cs given through cut leaves of chicory (*Cichorium intybus* L.) and alfalfa (*Medicago sativa* L.) was distributed throughout the plant and roots. About 10% of the ^{137}Cs activity was allocated into the roots — irrespective of the plant species and its root system. Hence, ^{137}Cs is a unique and long-term stable tracer for roots, which was established herein for the first time. Of the $^{14}CO_2$

photoassimilates, about 33% was recovered below ground. The β$^-$ decay signal of ^{14}C photoassimilates was successfully separated from the ^{137}Cs β$^-$ signal by shielding the ^{14}C radiation off during the two-step imaging procedure (with and without shielding ^{14}C). 320 µm of polypropylene films shielded off the 156 keV ^{14}C β$^-$ radiation (Amato and Lizio, 2009) while allowing transmission of a large part of the 512 keV ^{137}Cs β$^-$ decay radiation. The two images from the imaging procedure were successfully registered pixel by pixel, activity-dependent attenuation of ^{137}Cs by the shielding was corrected (by a separate ^{137}Cs calibration with eight plastic films), and the images were subtracted from each other (Fig. 12). This procedure resolved the separate spatial distributions of both radionuclides. The approach, with both labels applied at the same time, shows the feasibility of the approach (Study 5). Coupling the new ^{137}Cs approach to the already established ^{14}C labelling of roots (Pausch and Kuzyakov, 2011), offers exciting new opportunities for upscaling and long-term fate of biopores.

This feasibility study only implied but did not yet prove that the ^{137}Cs is released from the roots upon death, nor that the ^{137}Cs signal would be stable after biopore formation and re-use. These questions were resolved by the second lab experiment (Study 6). ^{137}Cs was released from the root detritus and bound to the biopore walls, resulting in strong β$^-$ signals after 11 months decomposition and three months of wheat cultivation. Upscaling from 10-cm pots to 70-cm soil cores did not require multiple pulse labelling, but only application of higher ^{137}Cs activities. The approach labels biopore *in situ* and enables studying re-use of individual biopores in crop rotations without disturbing the soil between crops and on larger scales. It is only limited by the size of the imaging plates. Importantly, the studies proved that the new ^{137}Cs application by leaf feeding, with exclusion of litterfall, cutting the shoot and determining its activity, does indirectly label individual biopores with specific amounts of the tracer. This principle was also used to label biopores with ^{15}N in study 7.

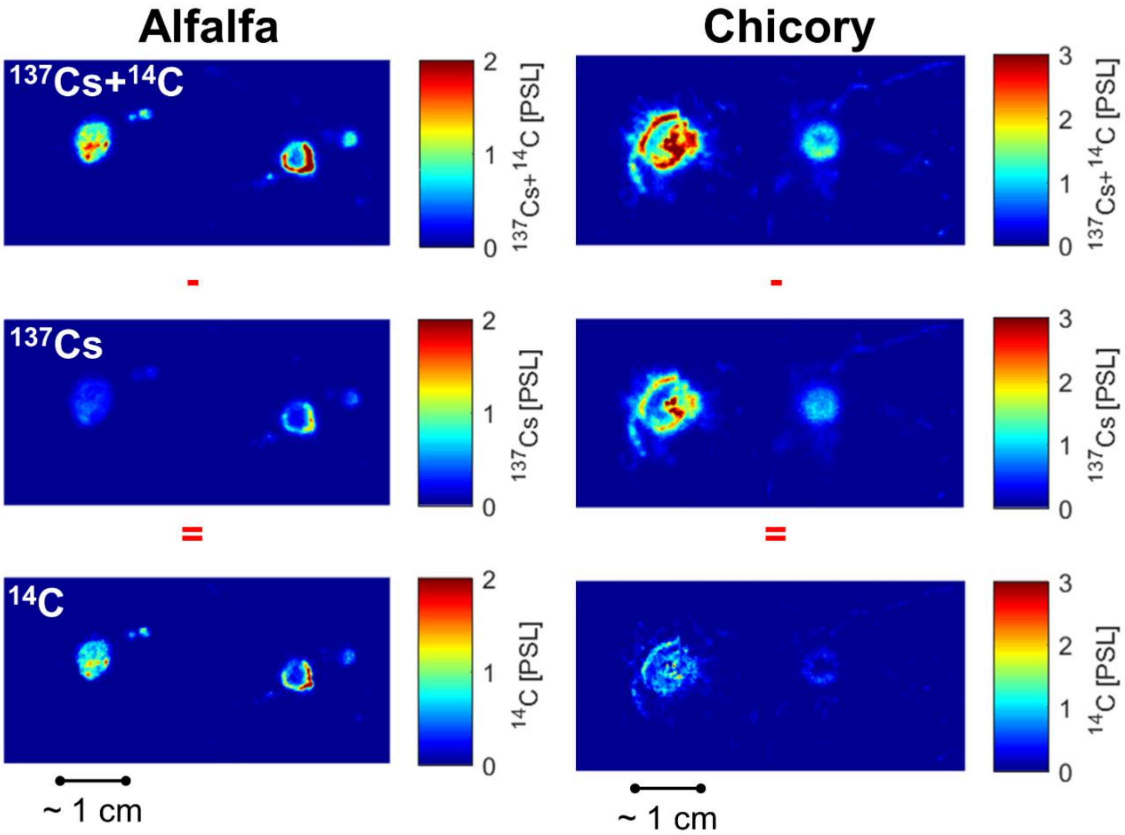

Fig. 12 *Imaging processing from Study 5. Two examples are shown for chicory and alfalfa, respectively, shown are the main root locations. The first row shows the total activity of* ^{137}*Cs and* ^{14}*C, while the second row shows just the* ^{137}*Cs activity. The last row shows the calculated* ^{14}*C activity as explained in the text. From Banfield et al. (2017b).*

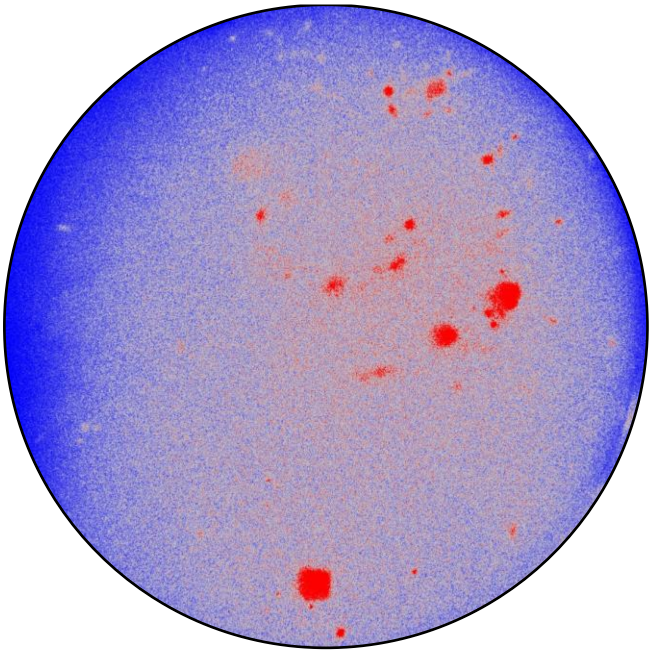

Fig. 13 *Phosphor imaging of a soil core in 25 cm depth after one year of root decomposition (Study 6).* ^{14}*C was shielded off by 320 µm of polypropylene plastic films. Red patches refer to* ^{137}*Cs activity which was supplied to the preceding crop about one year before. Consequently, red patches are* ^{137}*Cs-labelled biopores.*

1.3.2.2 Biopore re-use in crop rotations (Study 6)

Biopores were re-occupied by wheat roots much more often (up to 75%) than stochastically expected from the contribution of biopores to the total soil volume (20%) or previously assumed (Nakamoto, 2000). Most wheat roots (65%) were growing in biopores, and only 20-30% of roots were growing in bulk soil (Fig. 14, far right). The constant proportion of roots in the bulk soil (Fig. 14, centre left) suggests that plants cannot fulfil their entire resource demand from biopores alone (nutrients, water). Biopores became less frequent with depth (Fig. 14, far left) but the remaining biopores were more frequently re-used with depth. The re-use correlated positively with the bulk density which increased concomitantly from 0–50 cm depth (cf. Table 1 on page 231). This fact highlights the higher relevance of biopores for nutrient uptake in deeper subsoil. The re-use, which was three times above the stochastically expected value, clearly showed that biopores are beneficial to crops — and not random. Biopore re-use was positively correlated with TN contents of wheat (Spearman correlation coefficient 0.65-0.71), which was the motivation to study ^{15}N uptake from biopores. Increasing biopore re-use by plant breeding, or because of deteriorated topsoil conditions (Dresemann et al., 2018; Kopke et al., 2015), could offer further plant nutritional benefits.

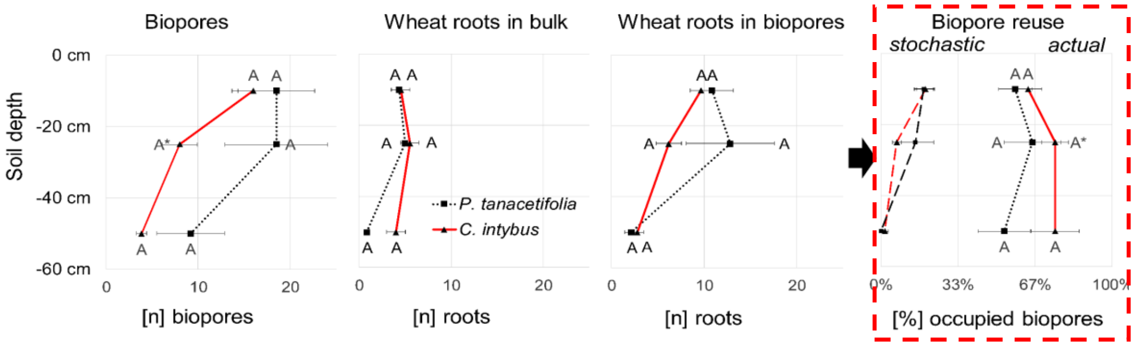

Fig. 14 *Differentiation of biopores and roots growing inside or outside biopores; determination of biopore reuse. From left to right: Count of biopores across depths; wheat roots in bulk soil; wheat roots in biopores and biopore re-use (%). Red lines and black (dotted) lines represent chicory and phacelia pre-crops, respectively.*

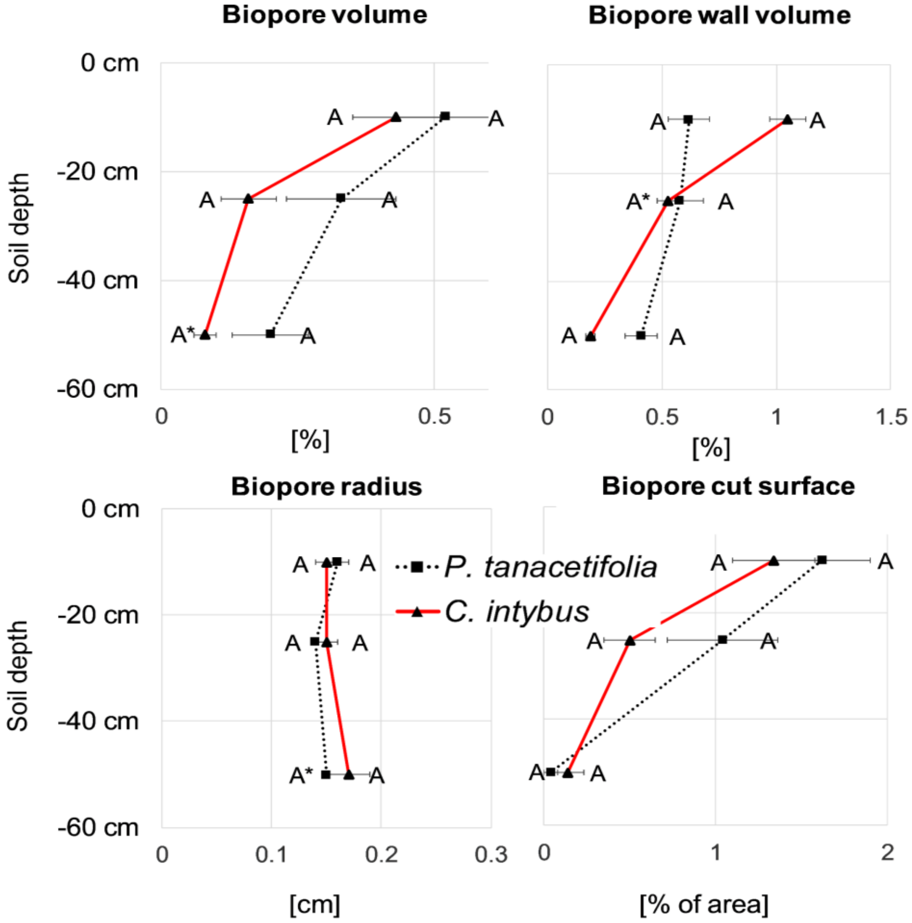

Fig. 15 *Selected biopore properties: volume, wall volume, radius and cut surface for the biopores of the two pre-crops chicory (dotted, black) and phacelia (red solid lines) down to 60 cm soil depth.*

1.3.2.3 Biopore properties and their effect on the root system of wheat (Study 6)

The biopore properties (volume, radius, wall volume; Fig. 15) were similar between the two chosen pre-crops phacelia (fibrous) and chicory (tap-rooted) after 12 weeks of cultivation and 11 months of decay. Longer pre-cropping durations might have caused stronger differences in biopore abundance and geometry (Uteau et al., 2013). However, economic pressure in agriculture may in many cases only allow one season of pre-cropping. Thus, short-term effects of pre-cropping, as in this study, are very relevant for agricultural management.

A larger biopore volume, larger radius and a higher biopore abundance make biopore re-use more likely (Gaiser et al., 2013; Perkons et al., 2014). Tap-rooted pre-cops may thus induce biopores which are more stable and more frequently re-used. The biopore wall volume characterises the physical size of the OM pool. Thus, such biopores characteristics have important implications for the choice of pre-crop species (root system, duration of cover cropping). Pre-cropping has profound effects on biochemical properties of biopores: TOC contents were 150% larger (largest for tap-rooted chicory), and TN contents were 70% higher than in bulk soil at the end of the experiment (Fig. 16). However,

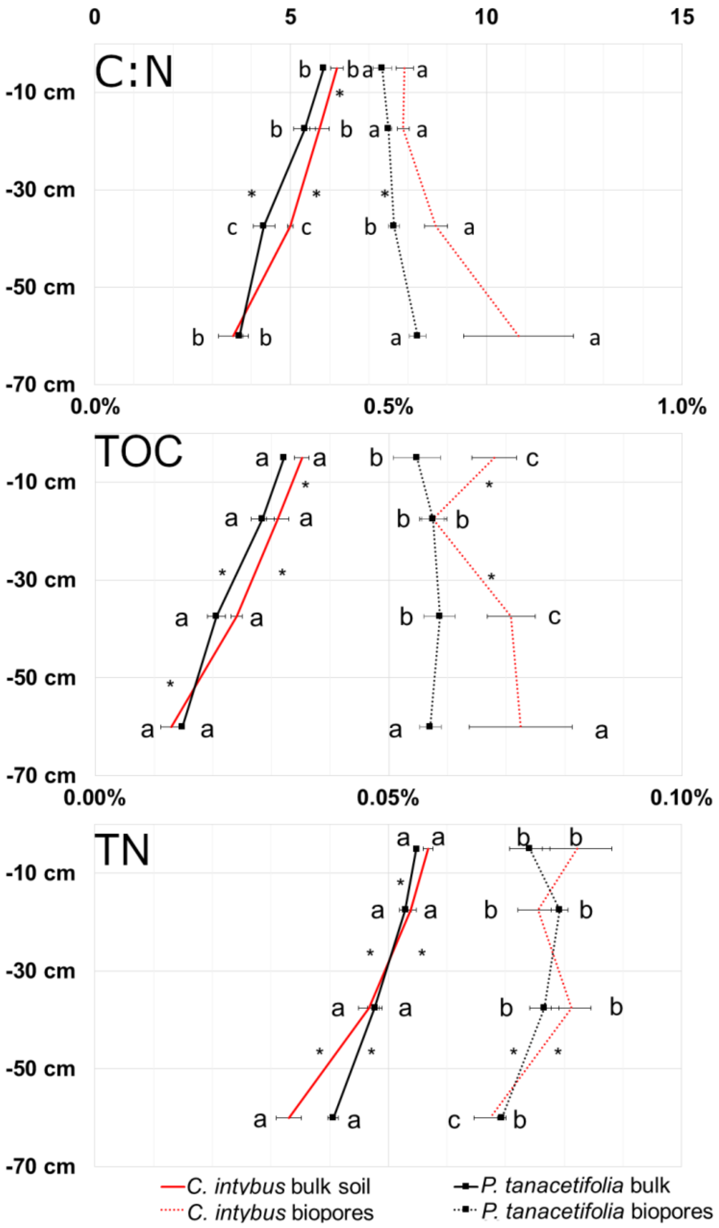

Fig. 16 *C/N ratio, TOC and TN contents inside (dotted lines) and outside (solid lines) the biopore walls of chicory (red) and phacelia (black lines, squares). Letters indicate significant differences in one soil layer (two-way ANOVA: factors pre-crop; soil compartment).*

the C/N ratio (~8) points towards lower OM decomposability of the biopore wall than of bulk soil OM (~5).

Identical root system parameters of wheat (e.g. radius, volume) suggest that the pre-crops had no positive or negative influence on the root system of wheat. Thus, one season of pre-cropping did not induce physically different biopores, nor did it influence the root system parameters of wheat. Since the identical physical biopore properties did not induce any preference of wheat for distinct biopores, it is plausible that also the chemical biopore properties were comparable between chicory and phacelia biopores.

1.3.2.4 N nutrition in crop rotations (Study 7)

The translocation of leaf-fed nutrients into roots and the subsequent biopore labelling was successfully applied for ^{137}Cs (Studies 5, 6). However, ^{15}N leaf feeding did not exclusively label the biopores (Fig. 17, top), but also the bulk soil, likely because of exudation via fine roots into the bulk soil, higher mobility of N-exudates and redistribution by fungal hyphae (Frey et al., 2000). Even though ^{15}N was similarly distributed between bulk soil and biopores, wheat was preferentially rooting in biopores. The TN content of wheat was positively correlated with biopore re-use (Spearman correlation coefficient 0.65–0.71). However, the TN content increase in wheat was not due to pre-crop-^{15}N, which was taken up less after leaf feeding compared to the ^{15}N fertiliser application on the soil surface. The organic ^{15}N stemming from the last-year pre-crop residues was less available than fertiliser ^{15}N (Evans et al., 2001). There was no significant difference in residue quality between chicory and phacelia. Accordingly, the positive biopore effects are nutrient-specific and may not be based on the pre-crop N but on older N (deposited before the experiment started) or physical factors. The importance of biopore nutrients may be much higher for immobile nutrients like K or P.

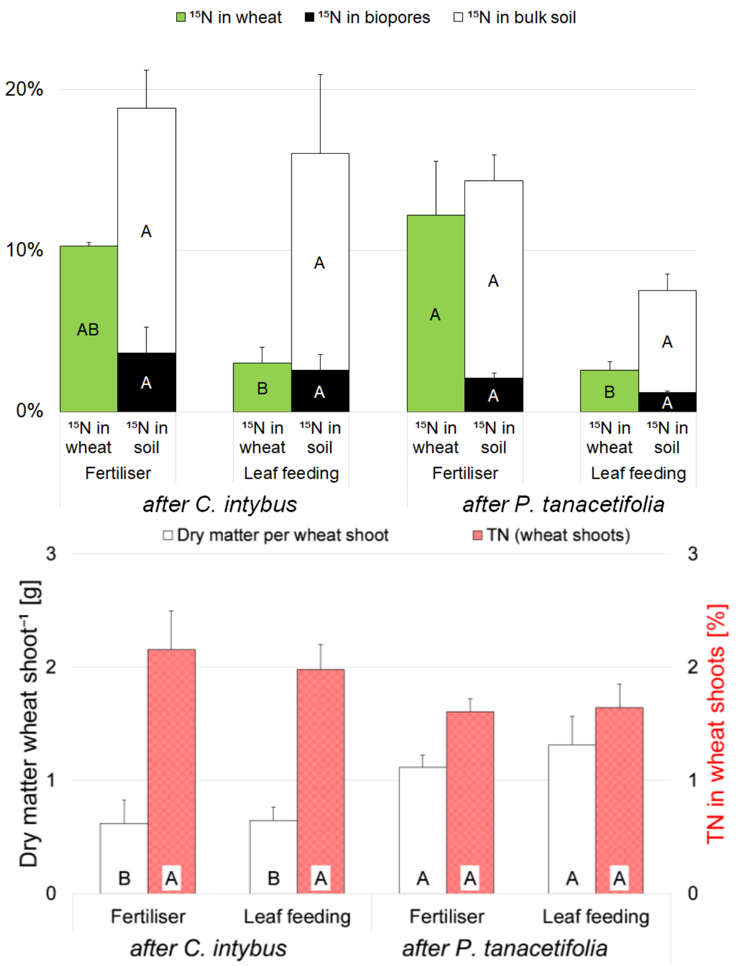

Fig. 17 *Fate of ^{15}N applied during the pre-crop phase (top) and plant productivity of wheat, both depending on the pre-crop species and mode of ^{15}N application(bottom). Letters indicate significant differences (Two-way ANOVA).*

1.4 Conclusions

Biopores have at least dual functionality, which becomes apparent at different time scales. Their long-term effects on C dynamics are mainly considered in organic geochemistry, while their short and medium-term effects on nutrient dynamics are relevant issues in agricultural soil science.

1.4.1 The relevance of biopores in organic geochemistry

The subsoil presents a large and potentially unsaturated C sink (Rumpel et al., 2012; Stockmann et al., 2013). C dynamics of this reservoir need to be better understood to enable appropriate C storage. Most C turnover in the subsoil is believed to occur in hotspots like biopores. Especially in the subsoil, the contrast between hotspots and bulk soil is much more pronounced than in the topsoil (e.g. hotspot lignin contents 15 times and MBC 30 times higher than in bulk soil). Consequently, all assessments of C inputs, stabilisation or remobilisation need to focus on hotspots, of which biopores — alongside preferential flow pathways like cracks — are the largest and most prominent.

The previously uncharacterised OM of the three most relevant biopore types (formed by roots and/or earthworms under identical field conditions) were assessed biogeochemically across depth and compared to bulk subsoil OM for the first time in this thesis. A comprehensive OM characterisation revealed that years of biopore formation increased substrate richness by 30% (based on individual compounds), but only weakly affected the overall composition of the OC pool (based on the pattern of substance classes; Study 1). Short-term earthworm activities had by far the strongest influence on C contents and biomarker patterns, even overriding years of tap-root presence within six months (Studies 1, 2). Through biomarkers, the three biopore types could be differentiated from each other. Consequently, biomarker combinations can be used to identify biopores of unknown origin in the field, which allows upscaling their abundance, properties and potential functions (e.g. nutrient stocks; Study 1).

The frequency and to a smaller degree the quality of the OM inputs governed the microbial biomass size and the microbial community in biopores, i.e. enrichment of fast-growing Gram-negatives in earthworm biopores as compared to general decomposers / Gram-positives in root biopores. Readily available OM is preferentially consumed in all biopores with the less available parts relatively accumulating — unless the frequency is too low, in which case all inputs are eventually consumed (Studies 2, 3).

Biopores facilitate the C input into the deeper subsoil as they are preferential rooting channels into the subsoil (Study 6). Tap-rooted chicory was shown to deposit especially large amounts of OM into the subsoil (Study 1), i.e. more OM than phacelia (Study 7).

Anecic earthworms may deposit OM of high microbial availability at great depths (4-5 m). Weakly processed OM containing large parts of less bioavailable or easily stabilised OM (e.g. long chain n-alkanes, aromatic compounds, or metabolites sorbed to mineral surfaces such as amino sugars) ends up in the deep subsoil (Studies 1, 2). Larger and more diverse inputs (Study 1) increase the total chance for C stabilisation, but large amounts of younger C may induce priming and therefore loss of old C. It is an open question under which circumstances the increased C allocation belowground outweighs priming losses. A higher substrate diversity should maintain a higher microbial diversity through additional niches and, therefore, contribute to more resilient soil microbial functioning.

Irrespective of the equilibrium of priming *vs* stabilisation, biopores very likely support C sequestration *at least* indirectly by a positive feedback loop through nutrient dynamics and provision of subsoil resources (soil water), which increases the total C input and the plant survival under stress. Given its immense global land use, cropped land could strongly contribute to C sequestration in subsoils.

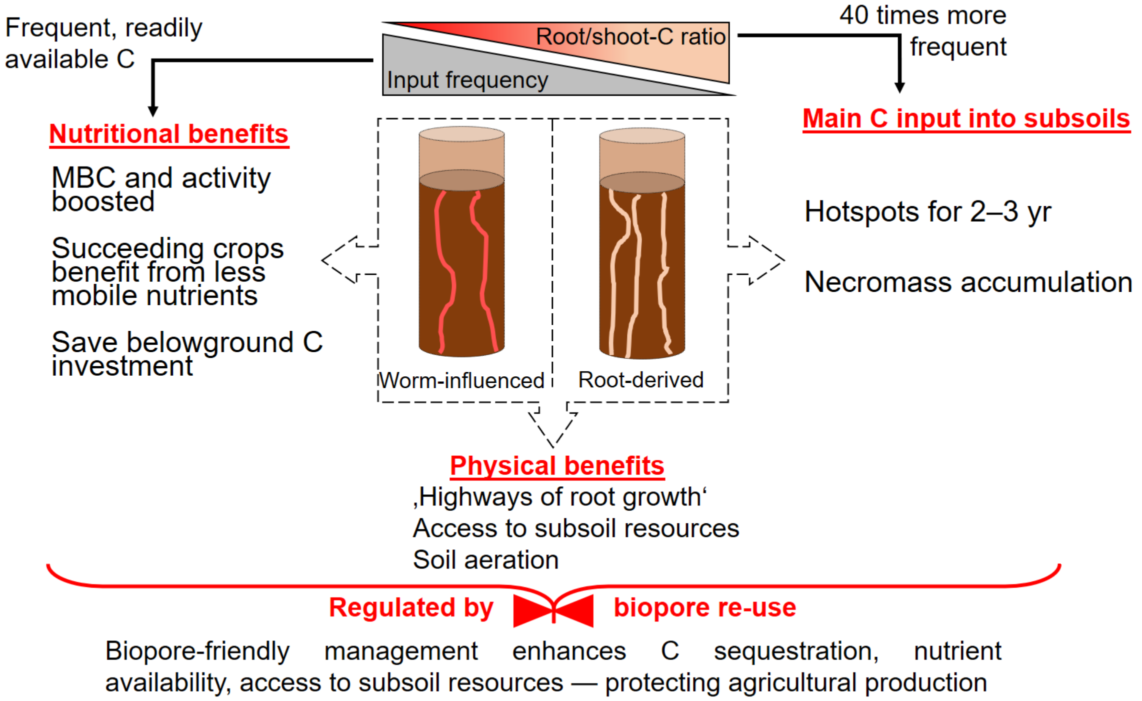
Frequent, readily available C
Root/shoot-C ratio
Input frequency
40 times more frequent
Nutritional benefits
MBC and activity boosted
Succeeding crops benefit from less mobile nutrients
Save belowground C investment
Main C input into subsoils
Hotspots for 2–3 yr
Necromass accumulation
Worm-influenced
Root-derived
Physical benefits
‚Highways of root growth'
Access to subsoil resources
Soil aeration
Regulated by
biopore re-use

Biopore-friendly management enhances C sequestration, nutrient availability, access to subsoil resources — protecting agricultural production

Fig. 18 *The relevance of biopores comprises nutritional benefits, increased C input into subsoils and physical benefits, in total governed by biopore re-use.*

The main biogeochemical effects of biopores depend on the input frequency and bioavailability of the OM input (Studies 1, 2, 3 and 4). As root biopores are on average 40 times more frequent than earthworm biopores, they govern the main C input into the agricultural subsoil. Root-C may be more easily stabilised than shoot-C. Thus, root biopores are primarily responsible for C sequestration. The high frequency of shoot-C inputs causes a strongly boosted substrate availability in earthworm biopores and thus induces significantly higher C turnover and microbial activity in earthworm biopores than in root biopores (Study 4). Consequently, earthworm biopores mostly feature nutrient cycling and mobilisation and are very likely of highest relevance for the agricultural perspective of biopores.

This more profound understanding of subsoil C turnover in very contrasting hotspots is crucially important for managing the subsoil functions. This dissertation demonstrated that promoting biopores in cropland, especially formed by tap-rooted crops, is a strategy to increase subsoil C stocks.

1.4.2 The relevance of biopores in agricultural soil science

As compared to organic geochemistry, agricultural soil science usually studies shorter time scales, e.g. nutrient carry over and mobilisation within the time scales of crop rotations.

OM inputs into biopores strongly increased microbial biomass and activity — especially in earthworm biopores with its fresh aboveground litter, thus boosting mobilisation of mineral and OM-bound nutrients (Study 4). Subsequent crops potentially benefit from the elevated biopore nutrient pools, which was confirmed by the observation that crops preferentially root in biopores (200% over the stochastically expected re-use, Study 6). A newly developed dual labelling approach with ^{137}Cs and ^{14}C and two-step phosphor imaging with selective shielding for the first time enabled differentiation of biopore creation (^{137}Cs), roots (^{14}C) and biopore re-use (^{14}C+^{137}Cs) — without any disturbance during the experiment (Studies 5, 6). This method characterises biopores physically and, thus, enables optimisation of biopore management with regard to optimal biopore diameters and densities, e.g. for nutrient uptake. Further adaption to earthworm biopores is easily possible.

Wheat was preferentially growing in biopores, and biopore re-use was positively correlated with shoot TN contents. However, wheat did not preferentially mobilise pre-crop-^{15}N from leaf feeding, and no significant increase in N content of wheat after chicory compared to phacelia was found (Study 7). Hence, the beneficial effects of biopores are not primarily based on pre-crop N, but rather on other nutrients. The relevance of biopores for nutrient storage and release may be higher for less mobile N species (amino sugars) or less mobile nutrients (P, K; Study 7). In future, the importance of K cycling in biopores will be quantified from ^{137}Cs uptake (a K analogue) into wheat shoots.

Root growth in biopores potentially saves C investment assuming improved nutrient uptake from biopores. Fewer roots would be sufficient to fulfil nutritional demands, allowing plants to invest more C in aboveground biomass and yields increase. If this held true, two management strategies are favourable: 1) increasing the number of biopores by tap-rooted pre-crops and earthworm-friendly, i.e. reduced, tillage practices and 2) breeding new crop varieties to enhance biopore re-use as 30% of biopores remained not re-used (Study 6).

If the findings are confirmed especially with regard to advantages for crop nutrition of less mobile nutrients, biopore-friendly management practices (e.g. reduced tillage, perennial cover cropping) could be part of smart subsoil management. Faster access to subsoil water and concentrated biopore nutrients safeguard agricultural production — especially in times of rising fertiliser costs (both monetary and environmental) and more frequent droughts.

1.5 References

- Abiven, S., Recous, S., Reyes, V., Oliver, R., 2005. Mineralisation of C and N from root, stem and leaf residues in soil and role of their biochemical quality. Biology and Fertility of Soils 42, 119–128.
- Amato, E., Lizio, D., 2009. Plastic materials as a radiation shield for β − sources. A comparative study through Monte Carlo calculation. Journal of Radiological Protection 29, 239–250.
- Amelung, W., Brodowski, S., Sandhage-Hofmann, A., Bol, R., 2008. Chapter 6 Combining Biomarker with Stable Isotope Analyses for Assessing the Transformation and Turnover of Soil Organic Matter, in: Sparks, D.L. (Ed.), Advances in agronomy. Volume 100. Elsevier; Academic Press, San Diego, pp. 155–250.
- Amelung, W., Cheshire, M.V., Guggenberger, G., 1996. Determination of neutral and acidic sugars in soil by capillary gas-liquid chromatography after trifluoroacetic acid hydrolysis. Soil Biology and Biochemistry 28, 1631–1639.
- Amin, B.A.Z., Chabbert, B., Moorhead, D., Bertrand, I., 2014. Impact of fine litter chemistry on lignocellulolytic enzyme efficiency during decomposition of maize leaf and root in soil. Biogeochemistry 117, 169–183.
- Anderson, J.P.E., Domsch, K.H., 1978. A physiological method for the quantitative measurement of microbial biomass in soils. Soil Biology and Biochemistry 10, 215–221.
- Anderson, T.-H., Domsch, K.H., 2010. Soil microbial biomass: The eco-physiological approach. Knowledge gaps in soil C and N interactions 42, 2039–2043.
- Andrist-Rangel, Y., Simonsson, M., Andersson, S., Öborn, I., Hillier, S., 2006. Mineralogical budgeting of potassium in soil. A basis for understanding standard measures of reserve potassium. Journal of Plant Nutrition and Soil Science 169, 605–615.
- Andriuzzi, W.S., Bolger, T., Schmidt, O., 2013. The drilosphere concept. Fine-scale incorporation of surface residue-derived N and C around natural Lumbricus terrestris burrows. Soil Biology and Biochemistry 64, 136–138.
- Apostel, C., Dippold, M.A., Glaser, B., Kuzyakov, Y., 2013. Biochemical pathways of amino acids in soil: Assessment by position-specific labeling and 13C-PLFA analysis. Soil Biology and Biochemistry 67, 31–40.
- Athmann, M., Kautz, T., Pude, R., Köpke, U., 2013. Root growth in biopores—evaluation with in situ endoscopy. Plant and Soil 371, 179–190.
- Banfield, C.C., Dippold, M.A., Pausch, J., Hoang, D.T.T., Kuzyakov, Y., 2017a. Biopore history determines the microbial community composition in subsoil hotspots. Biology and Fertility of Soils 9, 54.
- Banfield, C.C., Pausch, J., Kuzyakov, Y., Dippold, M.A., 2018. Microbial processing of plant residues in the subsoil – The role of biopores. Soil Biology and Biochemistry 125, 309–318.
- Banfield, C.C., Zarebanadkouki, M., Kopka, B., Kuzyakov, Y., 2017b. Labelling plants in the Chernobyl way. A new 137Cs and 14C foliar application approach to investigate rhizodeposition and biopore reuse. Plant and Soil 29, 239.

- Bertrand, I., Chabbert, B., Kurek, B., Recous, S., 2005. Can the Biochemical Features and Histology of Wheat Residues Explain their Decomposition in Soil? Plant and Soil 281, 291–307.
- Bird, J.A., Herman, D.J., Firestone, M.K., 2011. Rhizosphere priming of soil organic matter by bacterial groups in a grassland soil. Special Issue: Knowledge gaps in soil C and N interactions. Soil Biology and Biochemistry 43, 718–725.
- Bonkowski, M., Scheu, S., 2004. Biotic Interactions in the Rhizosphere: Effects on Plant Growth and Herbivore Development, in: Weisser, W.W. (Ed.), Insects and ecosystem function. With 12 tables. Springer, Berlin, Heidelberg, New York, pp. 71–91.
- Brown, G.G., 1995. How do earthworms affect microfloral and faunal community diversity? Springer, Dordrecht, Netherlands.
- Carminati, A., 2013. Rhizosphere wettability decreases with root age: a problem or a strategy to increase water uptake of young roots? Frontiers in Plant Science, 298.
- Collins, H.P., Elliott, E.T., Paustian, K., Bundy, L.G., Dick, W.A., Huggins, D.R., Smucker, A.J.M., Paul, E.A., 2000. Soil carbon pools and fluxes in long-term corn belt agroecosystems. Soil Biology and Biochemistry 32, 157–168.
- Cresswell, H.P., Kirkegaard, J.A., 1995. Subsoil amelioration by plant-roots - the process and the evidence. Australian Journal of Soil Research 33, 221.
- Curry, J.P., Byrne, D., Schmidt, O., 2002. Intensive cultivation can drastically reduce earthworm populations in arable land. European Journal of Soil Biology 38, 127–130.
- Curry, J.P., Schmidt, O., 2007. The feeding ecology of earthworms – A review. Pedobiologia 50, 463–477.
- Deshmukh, A.P., Simpson, A.J., Hadad, C.M., Hatcher, P.G., 2005. Insights into the structure of cutin and cutan from Agave americana leaf cuticle using HRMAS NMR spectroscopy. 2008 Australian Organic Geochemistry Conference: A national conference held in association with the International Humic Substances Society and the Natural Organic Matter Interest Group 36, 1072–1085.
- Devliegher, W., Verstraete, W., 1997. Microorganisms and soil physico-chemical conditions in the drilosphere of Lumbricus terrestris. Soil Biology and Biochemistry 29, 1721–1729.
- Dinter, A., Oberwalder, C., Kabouw, P., Coulson, M., Ernst, G., Leicher, T., Miles, M., Weyman, G., Klein, O., 2013. Occurrence and distribution of earthworms in agricultural landscapes across Europe with regard to testing for responses to plant protection products. Journal of Soils and Sediments 13, 278–293.
- Don, A., Steinberg, B., Schöning, I., Pritsch, K., Joschko, M., Gleixner, G., Schulze, E.-D., 2008. Organic carbon sequestration in earthworm burrows. Soil Biology and Biochemistry 40, 1803–1812.
- Dorodnikov, M., Fangmeier, A., Kuzyakov, Y., 2007. Thermal stability of soil organic matter pools and their δ13C values after C3–C4 vegetation change. Soil Biology and Biochemistry 39, 1173–1180.
- Dresemann, T., Athmann, M., Heringer, L., Kautz, T., 2018. Effects of Continuous Vertical Soil Pores on Root and Shoot Growth of Winter Wheat: A Microcosm Study. Agricultural Sciences 09, 750–764.

- Dungait, J.A.J., Hopkins, D.W., Gregory, A.S., Whitmore, A.P., 2012. Soil organic matter turnover is governed by accessibility not recalcitrance. Global Change Biology 18, 1781–1796.
- Edwards, C.A., Bohlen, P.J., 1996. Biology and ecology of earthworms. Springer Science & Business Media.
- Ellerbrock, R.H., Gerke, H.H., 2004. Characterizing organic matter of soil aggregate coatings and biopores by Fourier transform infrared spectroscopy. European Journal of Soil Science 55, 219–228.
- Evans, J., McNeill, A.M., Unkovich, M.J., Fettell, N.A., Heenan, D.P., 2001. Australian Journal of Experimental Agriculture 41, 347.
- FAOSTAT, 2017. Agri-environmental indicators—Land Use. http://www.fao.org/faostat/en/#data/EL, last accessed 3 Jan 2018.
- Fierer, N., Schimel, J.P., Holden, P.A., 2003. Variations in microbial community composition through two soil depth profiles. Soil Biology and Biochemistry 35, 167–176.
- Frey, S.D., Elliott, E.T., Paustian, K., Peterson, G.A., 2000. Fungal translocation as a mechanism for soil nitrogen inputs to surface residue decomposition in a no-tillage agroecosystem. Soil Biology and Biochemistry 32, 689–698.
- Frostegård, Å., Tunlid, A., Bååth, E., 2011. Use and misuse of PLFA measurements in soils. Soil Biology and Biochemistry 43, 1621–1625.
- Gaiser, T., Perkons, U., Küpper, P.M., Kautz, T., Uteau-Puschmann, D., Ewert, F., Enders, A., Krauss, G., 2013. Modeling biopore effects on root growth and biomass production on soils with pronounced sub-soil clay accumulation. Ecological Modelling 256, 6–15.
- Gaiser, T., Perkons, U., Küpper, P.M., Puschmann, D.U., Peth, S., Kautz, T., Pfeifer, J., Ewert, F., Horn, R., Köpke, U., 2012. Evidence of improved water uptake from subsoil by spring wheat following lucerne in a temperate humid climate. Field Crops Research 126, 56–62.
- Goodfellow, M., Williams, S.T., 1983. Ecology of actinomycetes. Annual review of microbiology 37, 189–216.
- Gunina, A., Kuzyakov, Y., 2014. Pathways of litter C by formation of aggregates and SOM density fractions: Implications from 13C natural abundance. Soil Biology and Biochemistry 71, 95–104.
- Hagedorn, F., Bundt, M., 2002. The age of preferential flow paths. Geoderma 108, 119–132.
- Haider, K., Martin, P., 1979. Abbau und Umwandlung von Pflanzenrückständen und ihren Inhaltsstoffen durch die Mikroflora des Bodens. Zeitschrift für Pflanzenernährung und Bodenkunde 142, 456–475.
- Han, E., Kautz, T., Huang, N., Köpke, U., 2017. Dynamics of plant nutrient uptake as affected by biopore-associated root growth in arable subsoil. Plant and Soil 415, 145–160.
- Han, E., Kautz, T., Köpke, U., 2016. Precrop root system determines root diameter of subsequent crop. Biology and Fertility of Soils 52, 113–118.
- Han, E., Kautz, T., Perkons, U., Lüsebrink, M., Pude, R., Köpke, U., 2015a. Quantification of soil biopore density after perennial fodder cropping. Plant and Soil 394, 73–85.

- Han, E., Kautz, T., Perkons, U., Uteau, D., Peth, S., Huang, N., Horn, R., Köpke, U., 2015b. Root growth dynamics inside and outside of soil biopores as affected by crop sequence determined with the profile wall method. Biology and Fertility of Soils 51, 847–856.
- Hedges, J.I., Ertel, J.R., 1982. Characterization of lignin by gas capillary chromatography of cupric oxide oxidation products. Analytical Chemistry 54, 174–178.
- Hirth, J.R., McKenzie, B.M., Tisdall, J.M., 2005. Ability of seedling roots of Lolium perenne L. to penetrate soil from artificial biopores is modified by soil bulk density, biopore angle and biopore relief. Plant and Soil 272, 327–336.
- Hoang, D.T.T., Pausch, J., Razavi, B.S., Kuzyakova, I., Banfield, C.C., Kuzyakov, Y., 2016. Hotspots of microbial activity induced by earthworm burrows, old root channels, and their combination in subsoil. Biology and Fertility of Soils 52, 1105–1119.
- IAEA (Ed.), 1995. Nuclear techniques in soil plant studies for sustainable agriculture and environmental preservation. Proceedings of an International Symposium on Nuclear and Related Techniques in Soil Plant Studies on Sustainable Agriculture and Environmental Preservation jointly org. by the IAEA and the FAO and held in Vienna, 17 - 21 October 1994, Vienna.
- IUSS Working Group WRB, 2008. World reference base for soil resources 2006. Ein Rahmen für internationale Klassifikation, Korrelation und Kommunikation, 1st ed,. BGR, Hannover.
- Jakobsen, B.E., Dexter, A.R., 1988. Influence of biopores on root growth, water uptake and grain yield of wheat (Triticum aestivum) based on predictions from a computer model. Biology and Fertility of Soils 6, 315–321.
- Jastrow, J., Amonette, J., Bailey, V., 2007. Mechanisms controlling soil carbon turnover and their potential application for enhancing carbon sequestration. Climatic Change 80, 5–23.
- Jégou, D., Cluzeau, D., Hallaire, V., Balesdent, J., Tréhen, P., 2000. Burrowing activity of the earthworms Lumbricus terrestris and Aporrectodea giardi and consequences on C transfers in soil. European Journal of Soil Biology 36, 27–34.
- Jones, C., Lawton, J., Shachak, M., 1996. Organisms as Ecosystem Engineers, in: Samson, F.B., Knopf, F.L. (Eds.), Ecosystem management. Selected readings. Springer, New York, pp. 130–147.
- Jones, D.L., Nguyen, C., Finlay, R.D., 2009. Carbon flow in the rhizosphere: carbon trading at the soil–root interface. Plant and Soil 321, 5–33.
- Kaiser, K., Kalbitz, K., 2012. Cycling downwards – dissolved organic matter in soils. Soil Biology and Biochemistry 52, 29–32.
- Kalbitz, K., Kaiser, K., 2008. Contribution of dissolved organic matter to carbon storage in forest mineral soils. Journal of Plant Nutrition and Soil Science 171, 52–60.
- Kautz, T., Amelung, W., Ewert, F., Gaiser, T., Horn, R., Jahn, R., Javaux, M., Kemna, A., Kuzyakov, Y., Munch, J.-C., Pätzold, S., Peth, S., Scherer, H.W., Schloter, M., Schneider, H., Vanderborght, J., Vetterlein, D., Walter, A., Wiesenberg, G.L.B., Köpke, U., 2013. Nutrient acquisition from arable subsoils in temperate climates: A review. Soil Biology and Biochemistry 57, 1003–1022.

- Kautz, T., Lüsebrink, M., Pätzold, S., Vetterlein, D., Pude, R., Athmann, M., Küpper, P.M., Perkons, U., Köpke, U., 2014. Contribution of anecic earthworms to biopore formation during cultivation of perennial ley crops. Pedobiologia 57, 47–52.
- Kell, D.B., 2012. Large-scale sequestration of atmospheric carbon via plant roots in natural and agricultural ecosystems: why and how. Phil Trans R Soc B 367, 1589–1597.
- Kögel-Knabner, I., 2002. The macromolecular organic composition of plant and microbial residues as inputs to soil organic matter. Soil Biology and Biochemistry 34, 139–162.
- Kopke, U., Athmann, M., Han, E., Kautz, T., 2015. Optimising cropping techniques for nutrient and environmental management in organic agriculture. Sustainable Agriculture Research 4, 15.
- Kramer, C., Gleixner, G., 2008. Soil organic matter in soil depth profiles. Distinct carbon preferences of microbial groups during carbon transformation. Soil Biology and Biochemistry 40, 425–433.
- Kuhlmann, H., Baumgärtel, G., 1991. Potential importance of the subsoil for the P and Mg nutrition of wheat. Plant and Soil 137, 259–266.
- Kuzyakov, Y., 2010. Priming effects: Interactions between living and dead organic matter. Soil Biology and Biochemistry 42, 1363–1371.
- Kuzyakov, Y., Blagodatskaya, E., 2015. Microbial hotspots and hot moments in soil: Concept & review. Soil Biology and Biochemistry 83, 184–199.
- Lambin, E.F., Meyfroidt, P., 2011. Global land use change, economic globalization, and the looming land scarcity. Proceedings of the National Academy of Sciences 108, 3465–3472.
- Liang, C., Balser, T.C., 2008. Preferential sequestration of microbial carbon in subsoils of a glacial-landscape toposequence, Dane County, WI, USA. Geoderma 148, 113–119.
- Logsdon, S.D., Linden, D.R., 1992. INTERACTIONS OF EARTHWORMS WITH SOIL PHYSICAL CONDITIONS INFLUENCING PLANT GROWTH. Soil Science 154.
- Lorenz, K., Lal, R., 2007. The Depth Distribution of Soil Organic Carbon in Relation to Land Use and Management and the Potential of Carbon Sequestration in Subsoil Horizons, in: Sparks, D.L. (Ed.), Advances in agronomy. Academic Press, San Diego, Calif, London, pp. 35–66.
- Lorenz, K., Lal, R., Shipitalo, M.J., 2011. Stabilized Soil Organic Carbon Pools in Subsoils under Forest Are Potential Sinks for Atmospheric CO2. Forest Science 57, 19–25.
- Lubbers, I.M., Pulleman, M.M., van Groenigen, J.W., 2017. Can earthworms simultaneously enhance decomposition and stabilization of plant residue carbon? Soil Biology and Biochemistry 105, 12–24.
- Marhan, S., Scheu, S., 2005. Effects of sand and litter availability on organic matter decomposition in soil and in casts of Lumbricus terrestris L. Geoderma 128, 155–166.
- Marhan, S., Scheu, S., 2006. Mixing of different mineral soil layers by endogeic earthworms affects carbon and nitrogen mineralization. Biology and Fertility of Soils 42, 308–314.

- Marschner, P., Marhan, S., Kandeler, E., 2012. Microscale distribution and function of soil microorganisms in the interface between rhizosphere and detritusphere. Soil Biology and Biochemistry 49, 174–183.
- McCallum, M.H., Kirkegaard, J.A., Green, T.W., Cresswell, H.P., Davies, S.L., Angus, J.F., Peoples, M.B., 2004. Improved subsoil macroporosity following perennial pastures. Australian Journal of Experimental Agriculture 44, 299.
- Mendez-Millan, M., Dignac, M.-F., Rumpel, C., Rasse, D.P., Derenne, S., 2010. Molecular dynamics of shoot vs. root biomarkers in an agricultural soil estimated by natural abundance 13C labelling. Soil Biology and Biochemistry 42, 169–177.
- Miltner, A., Bombach, P., Schmidt-Brücken, B., Kästner, M., 2012. SOM genesis: microbial biomass as a significant source. Biogeochemistry 111, 41–55.
- Moorhead, D., Lashermes, G., Recous, S., Bertrand, I., 2014. Interacting microbe and litter quality controls on litter decomposition. A modeling analysis. PloS one 9, e108769.
- Nakamoto, T., 2000. The Distribution of Wheat and Maize Roots as Influenced by Biopores in a Subsoil of the Kanto Loam Type. Plant Production Science 3, 140–144.
- Oades, J.M., 1984. Soil organic matter and structural stability. Mechanisms and implications for management. Plant and Soil 76, 319–337.
- Partsch, S., Milcu, A., Scheu, S., 2006. Decomposers (Lumbricidae, Collembola) affect plant performance in model grasslands of different diversity. Ecology 87, 2548–2558.
- Passioura, J.B., 2002. Soil conditions and plant growth. Plant, Cell & Environment 25, 311–318.
- Paul, E.A., Follett, R.F., Leavitt, S.W., Halvorson, A., Peterson, G.A., Lyon, D.J., 1997. Radiocarbon dating for determination of soil organic matter pool sizes and dynamics. Soil Science Society of America Journal 61, 1058–1067.
- Pausch, J., Kuzyakov, Y., 2011. Photoassimilate allocation and dynamics of hotspots in roots visualized by 14C phosphor imaging. Journal of Plant Nutrition and Soil Science 174, 12–19.
- Perkons, U., Kautz, T., Uteau, D., Peth, S., Geier, V., Thomas, K., Lütke Holz, K., Athmann, M., Pude, R., Köpke, U., 2014. Root-length densities of various annual crops following crops with contrasting root systems. Soil and Tillage Research 137, 50–57.
- Rasse, D.P., Rumpel, C., Dignac, M.-F., 2005. Is soil carbon mostly root carbon? Mechanisms for a specific stabilisation. Plant and Soil 269, 341–356.
- Rasse, D.P., Smucker, A.J.M., 1998. Root recolonization of previous root channels in corn and alfalfa rotations. Plant and soil 204, 203–212.
- Rumpel, C., Chabbi, A., Marschner, B., 2012. Carbon Storage and Sequestration in Subsoil Horizons: Knowledge, Gaps and Potentials, in: Lal, R., Lorenz, K., Hüttl, R.F., Schneider, B.U., Braun, J. von (Eds.), Recarbonization of the Biosphere. Ecosystems and the Global Carbon Cycle. Springer Netherlands, Dordrecht, pp. 445–464.
- Rumpel, C., Eusterhues, K., Kögel-Knabner, I., 2004. Location and chemical composition of stabilized organic carbon in topsoil and subsoil horizons of two acid forest soils. Soil Biology and Biochemistry 36, 177–190.

- Rumpel, C., Kögel-Knabner, I., 2011. Deep soil organic matter—a key but poorly understood component of terrestrial C cycle. Plant and Soil 338, 143–158.
- Rumpel, C., Kögel-Knabner, I., Bruhn, F., 2002. Vertical distribution, age, and chemical composition of organic carbon in two forest soils of different pedogenesis. Organic Geochemistry 33, 1131–1142.
- Salome, C., Nunan, N., Pouteau, V., Lerch, T.Z., Chenu, C., 2010. Carbon dynamics in topsoil and in subsoil may be controlled by different regulatory mechanisms. Global Change Biology 16, 416–426.
- Sampedro, L., Jeannotte, R., Whalen, J.K., 2006. Trophic transfer of fatty acids from gut microbiota to the earthworm Lumbricus terrestris L. Soil Biology and Biochemistry 38, 2188–2198.
- Sanaullah, M., Chabbi, A., Maron, P.-A., Baumann, K., Tardy, V., Blagodatskaya, E., Kuzyakov, Y., Rumpel, C., 2016. How do microbial communities in top-and subsoil respond to root litter addition under field conditions? Soil Biology and Biochemistry 103, 28–38.
- Schimel, D.S., 1995. Terrestrial ecosystems and the carbon cycle. Global Change Biology 1, 77–91.
- Schmidt, M.W.I., Torn, M.S., Abiven, S., Dittmar, T., Guggenberger, G., Janssens, I.A., Kleber, M., Kögel-Knabner, I., Lehmann, J., Manning, D.A.C., Nannipieri, P., Rasse, D.P., Weiner, S., Trumbore, S.E., 2011. Persistence of soil organic matter as an ecosystem property. Nature 478, 49–56.
- Schulz, S., Giebler, J., Chatzinotas, A., Wick, L.Y., Fetzer, I., Welzl, G., Harms, H., Schloter, M., 2012. Plant litter and soil type drive abundance, activity and community structure of alkB harbouring microbes in different soil compartments. The ISME Journal 6, 1763–1774.
- Schwertmann, U., Huith, M., 1975. Erosionsbedingte Stoffverteilung in zwei hopfengenutzten Kleinlandschaften der Hallertau (Bayern). Zeitschrift für Pflanzenernährung und Bodenkunde 138, 397–405.
- Spielvogel, S., Prietzel, J., Leide, J., Riedel, M., Zemke, J., Kögel-Knabner, I., 2014. Distribution of cutin and suberin biomarkers under forest trees with different root systems. Plant and soil 381, 95–110.
- Stirzaker, R.J., Passioura, J.B., Wilms, Y., 1996. Soil structure and plant growth: Impact of bulk density and biopores. Plant and Soil 185, 151–162.
- Stockmann, U., Adams, M.A., Crawford, J.W., Field, D.J., Henakaarchchi, N., Jenkins, M., Minasny, B., McBratney, A.B., Courcelles, Vivien de Remy de, Singh, K., Wheeler, I., Abbott, L., Angers, D.A., Baldock, J., Bird, M., Brookes, P.C., Chenu, C., Jastrow, J.D., Lal, R., Lehmann, J., O'Donnell, A.G., Parton, W.J., Whitehead, D., Zimmermann, M., 2013. The knowns, known unknowns and unknowns of sequestration of soil organic carbon. Agriculture, Ecosystems & Environment 164, 80–99.
- Stromberger, M.E., Keith, A.M., Schmidt, O., 2012. Distinct microbial and faunal communities and translocated carbon in Lumbricus terrestris drilospheres. Soil Biology and Biochemistry 46, 155–162.
- Tabatabai, M.A., 2007. Soil Enzymes, in: Bitton, G. (Ed.), Encyclopedia of environmental microbiology. Wiley, New York, Weinheim [u.a.], p. 97.
- Thevenot, M., Dignac, M.-F., Rumpel, C., 2010. Fate of lignins in soils. A review. Soil Biology and Biochemistry 42, 1200–1211.

- Uteau, D., Pagenkemper, S.K., Peth, S., Horn, R., 2013. Root and time dependent soil structure formation and its influence on gas transport in the subsoil. Soil and Tillage Research 132, 69–76.
- van Groenigen, J.W., Lubbers, I.M., Vos, H.M.J., Brown, G.G., Deyn, G.B. de, van Groenigen, K.J., 2014. Earthworms increase plant production: a meta-analysis. Scientific reports 4, 6365.
- Vetterlein, D., Kühn, T., Kaiser, K., Jahn, R., 2013. Illite transformation and potassium release upon changes in composition of the rhizophere soil solution. Plant and Soil 371, 267–279.
- Volkmar, K.M., 1996. Effects of biopores on the growth and N-uptake of wheat at three levels of soil moisture. Canadian Journal of Soil Science 76, 453–458.
- von Luetzow, M., Kögel-Knabner, I., Ekschmitt, K., Matzner, E., Guggenberger, G., Marschner, B., Flessa, H., 2006. Stabilization of organic matter in temperate soils. Mechanisms and their relevance under different soil conditions - a review. European Journal of Soil Science 57, 426–445.
- Vu, B., Chen, M., Crawford, R.J., Ivanova, E.P., 2009. Bacterial Extracellular Polysaccharides Involved in Biofilm Formation. Molecules 14, 2535–2554.
- Wallander, H., Nilsson, L.O., Hagerberg, D., Rosengren, U., 2003. Direct estimates of C:N ratios of ectomycorrhizal mycelia collected from Norway spruce forest soils. Soil Biology and Biochemistry 35, 997–999.
- White, R.G., Kirkegaard, J.A., 2010. The distribution and abundance of wheat roots in a dense, structured subsoil--implications for water uptake. Plant, Cell & Environment 33, 133–148.
- Wilkinson, M.T., Richards, P.J., Humphreys, G.S., 2009. Breaking ground: Pedological, geological, and ecological implications of soil bioturbation. Earth-Science Reviews 97, 257–272.
- Wuest, S.B., 2001. Soil biopore estimation: effects of tillage, nitrogen, and photographic resolution. Soil and Tillage Research 62, 111–116.
- Zapata, F., 2003. Handbook for the Assessment of Soil Erosion and Sedimentation Using Environmental Radionuclides. Springer Netherlands, Dordrecht.
- Zhang, X., Amelung, W., 1996. Gas chromatographic determination of muramic acid, glucosamine, mannosamine, and galactosamine in soils. Soil Biology and Biochemistry 28, 1201–1206.
- Zhou, J., Xia, B., Treves, D.S., Wu, L.-Y., Marsh, T.L., O'Neill, R.V., Palumbo, A.V., Tiedje, J.M., 2002. Spatial and Resource Factors Influencing High Microbial Diversity in Soil. Applied and Environmental Microbiology 68, 326–334.

1.6 Contributions to the included manuscripts and publications

Manuscript 1:

Title: *“Biopores as carbon highways into the subsoil: Organic matter origin and differentiation in microbial hotspots”*

Status at date of thesis submission: to be submitted to Science of the Total Environment

Status at date of thesis defense: n.a.

Contributors:

Callum C. Banfield	50%	Sampling, biomarker analyses (all but lignin and neutral sugars), data analysis, statistics, preparation of figures, tables and manuscript
Kristina Osina	20%	Biomarker analyses (lignin and neutral sugars), comments to manuscript
Michaela A. Dippold	10%	Comments and suggestions to manuscript
Sandra Spielvogel	10%	Comments and suggestions to manuscript
Yakov Kuzyakov	10%	Comments and suggestions to manuscript

Manuscript 2:

Title: “*Microbial processing of plant residues in the subsoil – The role of biopores*”

Status at date of thesis submission: published in Soil Biology and Biochemistry

Status at date of thesis defense: published in Soil Biology and Biochemistry (Vol. 125, 309–318)

https://doi.org/10.1016/j.soilbio.2018.08.004

Contributors:

Callum C. Banfield	65%	Sampling, biomarker analyses, data analysis, preparation of figures, tables and manuscript
Johanna Pausch	10%	Comments and suggestions to manuscript
Yakov Kuzyakov	10%	Comments and suggestions to manuscript
Michaela A. Dippold	15%	Comments and suggestions to manuscript

Manuscript 3:

Title: „*Biopore history determines the microbial community composition in subsoil hotspots*“

Status at date of thesis submission: published in Biology and Fertility of Soils

Status at date of thesis defense: published in Biology and Fertility of Soils (Vol. 53, 573-588).

https://doi.org/10.1007/s00374-017-1201-5

Contributors:

Callum C. Banfield	50%	Sampling, biomarker analyses, data analysis, preparation of figures, tables and manuscript
Michaela A. Dippold	15%	Comments and suggestions to manuscript
Johanna Pausch	10%	Comments and suggestions to manuscript
Duyen T. T. Hoang	5%	Comments to manuscript
Yakov Kuzyakov	10%	Comments and suggestions to manuscript

Manuscript 4:

Title: „*Six months of L. terrestris L. activity in root-formed biopores increases nutrient availability, microbial biomass and enzyme activity*“

Status at date of thesis submission: published in Applied Soil Ecology

Status at date of thesis defense: published in Applied Soil Ecology (Vol. 120, 135–142)

https://doi.org/10.1016/j.apsoil.2017.08.015

Contributors:

Miriam Athmann	20%	Sampling, analyses, preparation of figures/tables, preparation and suggestions to manuscript
Timo Kautz	10%	Experimental design, sampling, analyses, preparation of figures/tables, preparation and suggestions to manuscript
Callum C. Banfield	10%	Sampling, analyses, preparation of figures/tables, preparation and suggestions to manuscript
Sara Bauke	10%	Sampling, analyses, preparation of figures/tables, preparation and suggestions to manuscript
Duyen T.T. Hoang	10%	Sampling, analyses, preparation of figures/tables, preparation and suggestions to manuscript
Marcel Lüsebrink	10%	Sampling, analyses, preparation of figures/tables, preparation and suggestions to manuscript
Johanna Pausch	7.5%	Comments and suggestions to manuscript
Wulf Amelung	7.5%	Comments and suggestions to manuscript
Yakov Kuzyakov	7.5%	Comments and suggestions to manuscript
Ulrich Köpke	7.5%	Comments and suggestions to manuscript

Manuscript 5:

Title: „*Labelling plants in the Chernobyl way: A new ^{137}Cs and ^{14}C foliar application approach to investigate rhizodeposition and biopore reuse*"

Status at date of thesis submission: published in Plant and Soil

Status at date of thesis defense: published in Plant and Soil (Vol. 417, 301-315)

https://doi.org/10.1007/s11104-017-3260-7

Contributors:

Callum C. Banfield	65%	Concept, lab work, phosphor imaging, data analysis, preparation of figures, tables and manuscript
Mohsen Zarebanadkouki	20%	Data analysis, comments and suggestions to manuscript
Bernd Kopka	5%	Comments and suggestions to manuscript
Yakov Kuzyakov	10%	Comments and suggestions to manuscript

Manuscript 6:

Title: *"Subsoil exploitation: The re-use of root biopore hotspots in crop rotations."*

Status at date of thesis submission: submitted to New Phytologist

Status at date of thesis defense: n.a.

Contributors:

Callum C. Banfield	50%	Sampling, analyses, data analysis, preparation of figures, tables and manuscript
Michaela A. Dippold	10%	Comments and suggestions to manuscript
Johanna Pausch	10%	Comments and suggestions to manuscript
Mohsen Zarebanadkouki	15%	Comments and suggestions to manuscript
Bernd Kopka	5%	Sampling, comments, suggestions to manuscript
Yakov Kuzyakov	10%	Comments and suggestions to manuscript

Manuscript 7:

Title: *„The fate of pre-crop nitrogen: Biopores as hotspots for interannual nitrogen transfer in crop rotations?"*

Status at date of thesis submission: to be submitted to Agriculture, Ecosystems and Environment

Status at date of thesis defense: n.a.

Contributors:

Callum C. Banfield	55%	Sampling, data analysis, preparation of manuscript
Magdalena Holzapfel	15%	Preparation of samples for IRMS measurement, preparation of figures and tables
Michaela A. Dippold	10%	Comments and suggestions to manuscript
Johanna Pausch	10%	Comments and suggestions to manuscript
Yakov Kuzyakov	10%	Comments and suggestions to manuscript

2 Publications and Manuscripts

2.1 Study 1: Biopores as carbon highways into the subsoil: Organic matter origin and differentiation in microbial hotspots

Authors and affiliations

Callum C. Banfield[1*±]; Kristina Osina[2, ±], Michaela A. Dippold[1,3], Sandra Spielvogel[3], Yakov Kuzyakov[,4,5]

[1] Georg-August-University of Goettingen, Biogeochemistry of Agroecosystems, Buesgenweg 2, 37077 Goettingen, Germany

[2] Tula State University, Department of Chemistry, Tula, 300012, Russian Federation

[3] Christian-Albrechts-University Kiel, Institute for Plant Nutrition and Soil Science, Hermann-Rodewald-Str. 2, 24118 Kiel, Germany

[4] Georg-August-University of Goettingen, Department of Agricultural Soil Science, Buesgenweg 2, 37077 Goettingen, Germany

[5] Georg-August-University of Goettingen, Institute for Soil Science of Temperate Ecosystems, Buesgenweg 2, 37077 Goettingen, Germany

[±] Authors have equally contributed to this work.

Corresponding author: callumba@gmail.com

Telephone: +49 1578 4527077

Fax: +49 551 3933310

Role of the funding source: DFG KU 1184/29-1

Conflicts of interest: The authors declare no conflicts of interest.

Keywords: Cutin, suberin, lignin, neutral sugars, hexoses, pentoses, free lipids, bound lipids, amino sugars, biopores, detritusphere, drilosphere, field study, source partitioning, subsoil

Abstract

Root growth and earthworm burrowing accumulate considerable organic matter (OM) in distinct biopores in subsoils. Apart from elevated C and nutrient contents, chemical characterisation of these crucial subsoil hotspots of C sequestration and nutrient cycling is missing. The specific OM inputs and transformations were assessed for native earthworm biopores (>2.5 years earthworms) *vs* root biopores (2 years decomposition) *vs* the combination of both (1.5 years root decomposition + 0.5 years active earthworms). Most substance classes had merely higher contents in biopores, but their contributions to soil organic carbon were the same as in the bulk soil except for lignin and cutin/suberin. Years of biopore formation increased the proportion of less readily available parts of soil OM and substrate diversity by 30%. Relative to the non-hotspot bulk soil, earthworms tripled C contents by feeding on plant litter and importing cell wall material (lignin, hemicelluloses), which boosted microbial biomass (microbial hexoses and lipids) – irrespective of the duration of earthworm activity. In root biopores, C and biomarker contents were 33% lower than in earthworm biopores. Residual root biomass markers (lignin, suberin) and microbial residues (amino sugars) made up the 100% higher C contents in root biopores than bulk soil. Only six months of earthworm incubation nearly completely overrode the original biomarker fingerprint of the root biopores and made them molecularly indistinguishable from native earthworm biopores. However, a molecular toolset differentiating root from earthworm biopores could be identified and points towards a higher relevance of pore-specific turnover proxies than source-related markers for the identification of specific biopores types.

2.1.1 Introduction

Roots and earthworms in subsoils release a great deal of carbon (C) within an environment of very low C content, high radiocarbon age (Don et al., 2008; Rethemeyer et al., 2005) and long C mean residence time (Paul et al., 1997). These properties led to the consideration of the subsoils as C sinks for climate change mitigation. Subsoils may have the potential to store even more C than their current stock of 50% of the terrestrial C (Kell, 2012; Kuhlmann and Baumgärtel, 1991; Rumpel and Kögel-Knabner, 2011; Salome et al., 2010). C reaches the subsoil mainly by leaching as dissolved organic carbon (DOC), (Kalbitz and Kaiser, 2008). Due to the slow nature of this process, the multitude of C sources, the long distance and interactions along, highly processed, microbial-C enriched compounds are found in the subsoils (Rumpel and Kögel-Knabner, 2011). Alternatively, large amounts of C are transported into the subsoil faster and less processed within biopores, i.e. in long, tubular and vertical macropores created by roots or earthworms (Jakobsen and Dexter, 1988; Stirzaker et al., 1996).

Agriculture as the largest global land use (Betts et al., 2007) could play a significant role in climate change mitigation. Smart agricultural management promoting biopores could enhance C contents in the subsoils and thus possibly promote long-term C storage (Rumpel et al., 2012). Tap-rooted pre-crops like chicory quantitatively create large biopores (*Cichorium intybus* L., (Ehlers et al., 1983; Perkons et al., 2014). Upon plant death and decomposition, the rhizosphere turns into the detritusphere, and a void is formed. Alternatively, anecic earthworms such as *Lumbricus terrestris* form large vertical biopores. They feed on plant litter near the soil surface and deposit digested, litter-containing faeces, casts, and mucus within their burrows, creating the drilosphere (Bouché, 1975; Jégou et al., 1998). As tillage destroys biopores, they mostly persist under no-till management or below the ploughed horizon, i.e. in the subsoil.

Considering the large organic matter (OM) accumulations by roots and earthworms, biopores are not merely shortcuts for C into the subsoil, but they become microbial hotspots (Banfield et al., 2017a; Kuzyakov and Blagodatskaya, 2015). As their inner walls are coated in OM, microbial growth and enzyme activities are induced (Hoang et al. 2016). A disproportionally large part of the subsoil OM turnover, transformation and nutrient release is assumed to take place in such hotspots (Kuzyakov and Blagodatskaya, 2015; Rumpel et al., 2012). The composition of the OM reflects the C dynamics in the course of biopore formation. Even though, the inputs of biopores are conceptually known, especially in long-lived biopores different inputs may be combined, and microbial turnover may lead to biopore-specific SOM fingerprints. However, a comprehensive SOM characterisation of different hotspot types is lacking and is urgently needed to understand subsoil C dynamics better.

Here, we comprehensively describe the SOM composition in earthworm- and root-induced biopores created under identical field conditions - after determining more than 200 compounds of 16 substance classes. In a field experiment over five years (Fig. XY), three biopore types were induced by either I) growing chicory for three years followed by two years of fallow, II) ≥ 2.5 years of native earthworm activities with defined food sources, or III) a combination of growing chicory for three years, 1.5 years of root decay and 6 months of earthworm incubation. The inner walls of the biopores were sampled and analysed for contents of lignin-derived phenols, cutin/suberin-derived lipids (fatty acids, hydroxy fatty acids and alcohols), hexoses and pentoses, amino sugars and free lipids including n-alkanes to characterise the specific C sources. In root biopores, the primary C source is the root detritus comprising of cellulose, hemicelluloses, suberin and lignin (Kögel-Knabner, 2002). In case of earthworm colonisation, decaying root tissues and earthworm-digested C from the soil surface are combined, i.e. root biomarkers and aboveground biomass markers such as cutin and n-alkanes. We aim at identifying a characteristic subset of biomarker molecules allowing molecular differentiation of biopores of various origin and OM sources.

2.1.2 Material and Methods

The study was conducted on Campus Klein-Altendorf experimental research station near Bonn, Germany. The site has a mean annual temperature of 9.6 °C, mean annual precipitation of 625 mm and features a Haplic Luvisol (Hypereutric, Siltic) developed from loess (IUSS Working Group WRB, 2008). C contents of the bulk soil were 0.41 ± 0.02% and 0.35 ± 0.05% for the 45–75 and the 75–105 cm layers, respectively. A full soil characterisation was given in Vetterlein et al. (2013).

The full sampling set-up was previously described in Banfield et al. (2017a). Briefly, from 2009 to 2012 Common chicory (*Cichorium intybus* L., var. Puna) was grown to induce intensive root penetration into the subsoil. Three biopore types were induced in the field: root biopores, earthworm-incubated biopores and (native) earthworm biopores (Banfield et al., 2017a). The treatments represent conditions found in agricultural fields after two years of no-till or fallow, i.e. earthworm burrowing and decaying roots.

1) *Root biopores:* in 2012, the topsoil was removed and three-year-old chicory roots larger than 5 mm were mapped in 45 cm depth. The topsoil was filled back, the plots were kept fallow, and roots decayed until sampling in autumn 2014.

2) *Earthworm-incubated biopores*: After 1.5 years of root decomposition, tagged earthworms (*Lumbricus terrestris* L.) were incubated into a subset of 25 root biopores per field replicate for six months (one earthworm per root biopore). A red elastomer tag was injected into the earthworm body to allow relocation of the earthworms (Butt and Lowe, 2007). Earthworms were fed with clover-grass put on the soil surface.
3) *Native earthworm biopores* were treated like the incubated earthworm biopores, i.e. the sites were kept fallow from 2012, grass-clover litter was put on the soil surface for six months from spring 2014, and they were expelled in autumn 2014. For this, a horizontal soil surface was prepared in 45 cm depth and covered with plant litter for three full days. Biopores with visible earthworm middens were considered colonised with native earthworms and labelled. The main difference to the incubated biopores is the length of the earthworm influence (6 months vs > 2 years).
4) *Bulk soil* samples, i.e. soil not containing any biopores, were taken from the sides of the profile wall.

2.1.2.1 Analysis of neutral sugars

Depending on C content, 600-900 mg of dried and ground soil was hydrolysed according to Zhang and Amelung et al. (1996). Myo-inositol (500 µg) was added as the first internal standard (IS). The hydrolysate was filtered through glass fibre filters GF6 (Whatman, GE Healthcare, Freiburg, Germany) and the filtrate was reduced to dryness in a rotary evaporator at 40 °C. The residue was re-dissolved in 5 mL of Millipore water and transferred to DOWEX 50W X 8 solid phase extraction (SPE) columns (conditioned with 2 M NaOH, water, 2 M HCl, water until the pH was 7). DOWEX exchange resins were used to remove cations such as iron and amino sugars. The organic phase was filtered through columns filled with anhydrous Na_2SO_4 and dried under N_2 and finally, dissolved in 185 µl of ethyl acetate-hexane (1:1, v/v), 15 µg methyl tridecanoate were added as the IS 2. For quantification, a standard mixture containing 25, 50, 100, 200, 400 and 800 µg of external standard stock solution (monosaccharides galactose, glucose, mannose, ribose, rhamnose, fucose, arabinose, xylose and myo-inositol) was prepared and derivatised with the samples.

Separation was performed on the Agilent 7820A GC system equipped with a flame ionisation detector and Optima® 17 MS column (Macherey Nagel, Dueren, Germany; phenylmethyl polysiloxane, 50 % phenyl, 30 m × 0.25 mm inner diameter with 0.5 µm film thickness). The injected sample volume was 1 µl. The temperature program was as follows: the initial column temperature of 100 °C was held for 1 min and increased at 20 °C min^{-1}

to 175 °C, held for 3 min. The temperature was increased again at 4 °C min^{-1} to 225 °C, held for 3 min, and finally increased at 50 °C min^{-1} to 300 °C and held for 7 min. Helium was used as a carrier gas at a flow rate of 1.1 ml min$^{-1,}$ and the split ratio was 30:1. The injector temperature was set to 250 °C, and the temperature of the detector was 300 °C.

2.1.2.2 Analysis of lignin-derived phenols

Depending on the C content, 250 – 400 mg of soil were analysed for their lignin phenol content according to Hedges and Ertel (1982). Ethyl vanillin (10 µg) was added as the IS 1. After cooling, the hydrolysate was centrifuged for 15 min at 3000 rpm. Humic substances were precipitated by adding 6 M HCl until pH 1.8 – 2.2 was reached. After 60 min, samples were centrifuged at 4000 rpm for 25 min. The supernatant was transferred to preconditioned C18 SPE columns. After drying under N_2, lignin monomers were eluted from the SPE columns by applying 10 x 0.5 mL ethyl acetate into reaction vials. Dry samples were re-dissolved in derivatisation reagent (0.3 ml), containing 200 µL BSTFA and 100 µL pyridine, and were heated at 60 °C for 20 min. After derivatization, samples were transferred to 250 µl GC vials containing 25 µg n-tetradecane as the IS 2. An external standard mixture containing 30, 60, 120, 240, 360, 480 and 600 µl of external standard stock solution (2.5 mg lignin monomers in 100 ml methanol) was used for quantification. Lignin-derived phenols were separated on the GC-FID system described above. The temperature program started at 100 °C (isothermal for 0.5 min) and increased to 160 °C at 10 °C min^{-1}, held for 6 min. Subsequently, the oven temperature was increased at 20 °C min^{-1} to 250 °C, and again at 50 °C min^{-1} to the final temperature of 300 °C, which was held for 5 minutes. The split ratio was 33:1. The injector temperature was set to 250 ° C, and the injected sample volume was 1 µl.

2.1.2.3 Analysis of amino sugars

For a full method description including the GC parameters, please see Banfield et al. (2017a), adapted from Zhang and Amelung (1996). In short, 500 mg of dried, ground soil were hydrolysed in 6 M HCl at 105 °C for eight hours. Iron was removed by centrifugation after adjusting the sample to pH 6.7. The dried sample was re-dissolved in MeOH and centrifuged to remove salts. Derivatisation to aldononitriles was in 4-dimethylamino-pyridine and hydroxylamine at 75 °C for 30 min and subsequent derivatisation to aldononitrile acetates in acetic anhydride at 75 °C for 30 min. The samples were separated on the GC-FID system described above for the neutral sugars.

2.1.2.4 Analysis of hexuronic acids

Samples were treated as the neutral sugars; however, silylated for GC measurement. Dried samples were re-dissolved in N-methyl-2-pyrrolidone containing 50 µg of IS methyl-glucose. To this, 200 µl of the derivatisation reagent methoxyamine hydrochloride (4 mg in 200 µl) were added and heated to 75 °C for 30 min. After cooling down, 400 µl N,O-bis(trimethylsilyl)trifluoroacetamide (BSTFA) were added and heated to 75 °C for 5 min. Before injection, 50 µg pentadecane were spiked to each sample. External standards at concentrations of 10, 20, 40, 80 and 160 µg μl^{-1} were prepared and derivatised with the samples for the quantification.

Samples were measured on an Agilent 7890A gas chromatograph coupled to an Agilent 7000A triple quadrupole mass spectrometer (both Agilent Waldbronn, Germany, equipped with a DB-5MS column (30 m x 250 µm coated with 0.25 µm 5% phenyl-methyl siloxane). Injection volume was 2 µl. Helium carrier gas flow was at 2.25 ml s^{-1}. The mass spectrometer was set to the selected ion mode: selected m/z were 73, 147, 160, 205, 261, 292 and 333, dwell time was 40 ms and 5 cycles per second. 1 µL amounts were injected in split mode (10:1), and injection temperature was 250°C. The total measured flow was 1.18 mL/min. The oven programme started at 145°C, held for one minute, increased at 5 °C min^{-1} to 160°C, and increased again at 6 °C min^{-1} to 185 °C, which was held for 3 min. To the final temperature of 300 °C heating was at 40 °C min^{-1} and was held for 0.5 min.

2.1.2.5 Analysis of cutin- and suberin-monomers

Three g of dried, sieved and ground soil were pre-extracted in a Soxhlet apparatus for 36 h in a mixture of dichloromethane and methanol (2:1) to remove all free lipids. With 500 mg of the pre-extracted soil, a digestion in 1 M KOH in MeOH at 100 °C for 3 h was performed to cleave bound lipids. Lipids were extracted once with MeOH: KOH, twice with MeOH: DCM and once with DCM. Supernatants were combined, internal standards (deuterated stearic acid, deuterated hexadecenoic acid and 17-hydroxy heptadecanoic acid) were spiked and water was added to create two phases. The pH of the aqueous phase was adjusted to pH 1 by diluted hydrochloric acid. After shaking and complete phase separation overnight, the lower phase was dried and derivatised. Methylation was by addition of 500 µl 1.3 M BF_3 in MeOH solution and heating to 80 °C for 15 min. Derivatives were extracted by hexane, dried and subsequently acetylated in acetic anhydride: pyridine (400 µl, 1:1) over night. Residual derivatisation agent and water were removed by passing the samples through sodium sulphate. Samples were dissolved in 185 µl toluene and 15 µg IS 2 methyl tricedanoate (1 µg μl^{-1}) was added before measurement. 50, 100, 200, 300 and 400 µl (~ 1 µg μl^{-1}) of the external standard mixture containing nine fatty acids, one diacid and two n-alkanols (after Spielvogel et al. (2014)) were derivatised together with the samples.

Samples were measured on the GC-MS system used for hexuronic acids, however in scan mode (50-550 amu), 1 µl injection volume into the splitless inlet. The oven programme started at 80°C, held for one minute, increased at 10 °C min^{-1} to 150 °C. Until 275 °C heating was at 1 °C min^{-1}, and finally at 10 °C min^{-1} to 300 °C.

2.1.2.6 Analysis of free lipids

Free lipids extracted during the Soxhlet procedure were spiked with internal standards (hexatriacontane for n-alkanes, pentadecanone for ketones, nonadecanol for n-alkanols, nervonic acid for the fatty acids, 12-OH stearic acid for hydroxy fatty acids). 20 ml of water were added to the samples and pH was adjusted to pH 10 by NaOH in MeOH. Three liquid-liquid extractions with chloroform were collected and the extracts were pipetted onto SPE columns (activated silica gel in n-hexane, biopore size 63-200 µm, Sigma-Aldrich, Munich, Germany). Alkanes did not bind to the gel and were washed out with 30 ml of hexane. Ketones and n-alkanols were eluted by 30 ml of DCM and 50 ml of MeOH, acetylated and prepared for measurement as described above in the cutin and suberin section. After the first liquid-liquid extraction at pH 10, the pH was adjusted to pH 2, and the acidic fractions were extracted three times with chloroform. Dried extracts were methylated with 1.3 M BF_3 : MeOH solution and subsequently separated on a silica gel SPE from the hydroxy fatty acids by DCM. The hydroxy fatty acid fraction was eluted with MeOH, and the hydroxyl groups were acetylated as the n-alkanols. Samples were dried and re-dissolved in 185 µl toluene and 15 µg second IS methyl tridecanoate (1 µg $µl^{-1}$) was added before injection. External standard mixes for each lipid fraction containing 20 n-alkanes (C17 to C36) or 27 n-alkanols and 8 ketones or 28 fatty acids or 18 hydroxy fatty acids were derivatised like the corresponding samples and used for quantification.

2.1.2.7 Statistical analyses

Principal components analysis (PCA) was performed to screen for ordination, i.e. similarity of treatments and underlying factors, after removal of compounds which had more than 10% missing data. Outliers between field replicates were identified using Nalimov's test (Lozán and Kausch, 1998). No more than one outlier was removed. One-way analyses of variance (ANOVA) were carried out for each depth and significances were calculated by Tukey's Honest Significance Difference test on $\alpha < 0.05$ level. Levene's test was used to test for homogenous variances. Normality of the residues was visually checked in Q-Q plots. Pairwise t-tests for dependent samples were used to determine differences between soil depths within each biopore type. Error bars in all charts were calculated as standard errors of the mean (SEM). In case assumptions were not met, non-parametric Kruskal-Wallis ANOVAs were calculated instead, followed by post-hoc comparisons of mean ranks of all pairs of groups (Kruskal-Wallis test). Error bars reported are SEM. Wilcoxon matched pair tests for dependent samples were used to determine differences between soil depths within each biopore type.

Analysis of similarity (ANOSIM) was performed on the outlier-corrected, treatment-grouped biomarker dataset. A Bray-Curtis similarity matrix was calculated as the basis for the non-parametric ANOSIM with 9999 permutations. Results are given as Bonferroni-corrected p-values.

228 variables were describing 32 cases of four categories, creating multicollinearities. Traditional discriminant analysis failed because of computation errors due to collinearities. Dimension reduction and determination of suitable predictor variables was achieved by partial least squares (PLS) classification. The biopore type was chosen as a categorical dependent variable and the 228 biomarker variables as continuous predictors. We also included a previous data set on 27 phospholipid-derived fatty acids (Banfield et al., 2017a). Cases were dropped if more than 80% of variables were missing. Variables were dropped if no variance was detected or if more than 80% of cases were missing. Biomarker variables were sorted by VIP (variance importance in projection), and the eight variables with the highest importance were chosen as regressors for a linear discriminant analysis. Calculated were discriminant functions, classification functions from these ten variables (all effects) and the factor structure for the first two roots. Canonical scores were plotted as XY scatterplots to show the significant classification.

All statistical analyses were performed in Statistica Version 13.3 (TIBCO Inc., Palo Alto, CA, U.S.A.) and PAST 3.20 (Hammer et al., 2001).

2.1.3 Results

The count of individually identified compounds was 33% lower in bulk soil (~ 80 compounds; Table 1) compared to the biopores (~ 120 compounds). Only in root biopores, the number of identified compounds increased with depth, whereas in the other treatments the count was constant with depth. A comprehensive substance list of > 200 compounds and their contents can be found in Table S8 (Supplementary material). The characterisation of the primary inputs can be found in Table S1 and S7 (supplementary material).

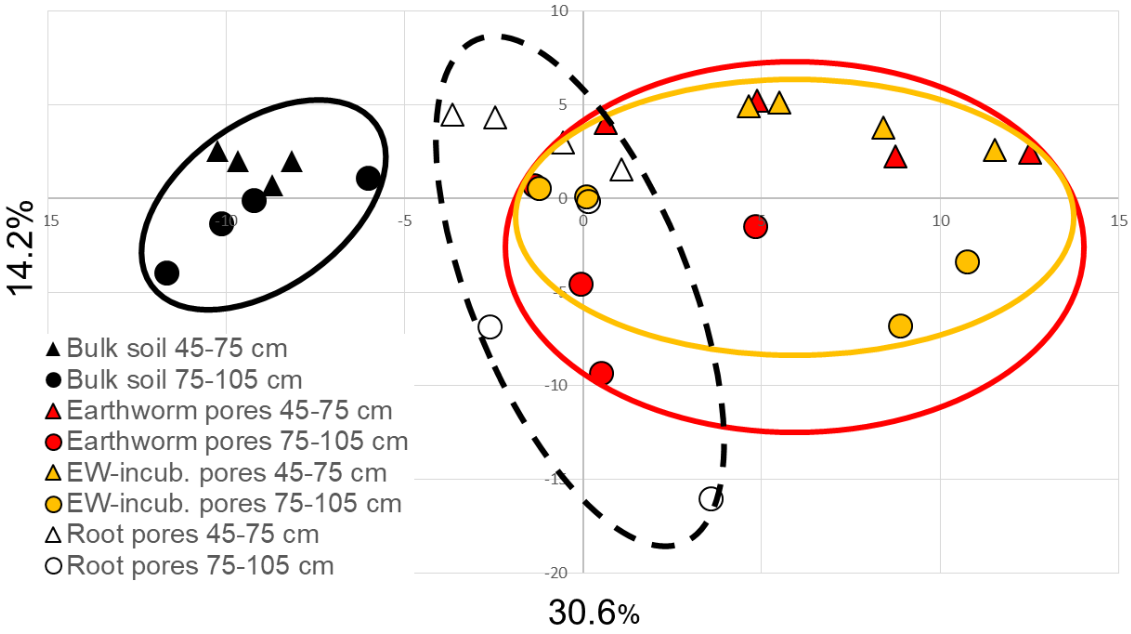

Fig. 1 *Principal components analysis (PCA) based on correlation of the entire biomarker dataset. Triangles represent samples from 45–75 cm, while circles present samples form 75–105 cm. Principal component (PC) 1 (x-axis) explained 39% of the inertia, while PC 2 explained further 15%.*

The first two principal components (PC) of the PCA (Fig. 1) based on 160 biomarkers explained 31 and 14 % of the total variance, respectively. The grouping showed that the OM was different between soil depths, i.e. samples of each soil depth grouped together but were separated along PC 2 (y-axis) from the other soil depth. Therefore, PC 2 likely represents soil depth. All three biopore types were at least partly overlapping and were separated from the bulk soil along PC 1 (x-axis). Both earthworm biopore types were overlapping almost perfectly. Root biopores grouped between bulk soil and both earthworm biopore types, indicating that among all biopore types, root biopores were similar to both bulk soil and biopores.

The root biomarker content was significantly higher in the biopores than in the bulk soil (Table 1). The ratio of root/shoot biomarkers was lowest in the bulk soil among all treatments. However, the ratio of microbial/shoot biomarkers was highest in bulk soil, indicating that the root-C is strongly microbially colonised in bulk subsoil. No such trend was found for the ratio of microbial/shoot biomarkers.

Based on the ANOSIM, the biomarker fingerprints of the three biopore types were statically similar to each other (Table 2), i.e. the substance lists could not be differentiated between the three biopore types. However, the fingerprints were different to the bulk soil, which is in excellent agreement with the PCA (Fig. 1) grouping.

Table 1 *Means ± SEM of total organic carbon (TOC), total nitrogen (TN), microbial biomass (MBC, taken from Hoang et al. (2016)), count of identified compounds, matches/overlaps with the source biomass fingerprints, root/shoot biomass ratio, microbial/shoot biomass ratio and microbial/root biomass ratio; for two soil depths (45-75 cm (top) and 75-105 cm (below). Small and capital letters each indicate significant differences among treatments of one soil depth (one-way ANOVA, Tukey's HSD on α 0.05; separated for contents and SOC contributions). Asterisks given in the lower soil depth indicate significant differences between soil depth (Two sample t-test for paired samples on α 0.05).*

45-75 cm	**Bulk soil**	**Earthworm pores**	**EW-incubated pores**	**Root pores**
TOC	0.41 ± 0.02A	1.17 ± 0.05C	1.16 ± 0.04C	0.81 ± 0.03B
TN	0.06 ± 0.00A	0.11 ± 0.00C	0.12 ± 0.00C	0.09 ± 0.00B
MBC	33 ± 1D	463 ± 28c	820 ± 38b	181 ± 6a
# of compounds	80 ± 7B	118 ± 4A	123 ± 2A	91 ± 1B
Matches: chicory roots	57 ± 4A	79 ± 4A	76 ± 3A	61 ± 3A
Matches: earthworm bodies	62 ± 5A	72 ± 4A	72 ± 3A	62 ± 3A
Matches: clover-grass	35 ± 4A	67 ± 3A	63 ± 2A	44 ± 2A
Root biomarkers	0.01 ± 0.00B	0.04 ± 0.00A	0.06 ± 0.01A	0.05 ± 0.01A
Root / shoot biomass	0.6 ± 0.1B	1.8 ± 0.1AB	2.2 ± 0.0A	2.8 ± 0.5A
Microbial / shoot biomarkers	39 ± 9A	29 ± 8A	19 ± 2A	31 ± 7A
Microbial / root biomarkers	37 ± 15A	15 ± 4A	8 ± 0A	12 ± 3A
75-105 cm				
TOC	0.35 ± 0.05b	1.05 ± 0.04a	1.07 ± 0.04a*	0.93 ± 0.06a
TN	0.05 ± 0.00b*	0.10 ± 0.01a	0.11 ± 0.01a	0.10 ± 0.01a
MBC	22 ± 3c	384 ± 38b	593 ± 88b	170 ± 9a
# of compounds	82 ± 6b	117 ± 3a	122 ± 4a	120 ± 1a
Matches: chicory roots	63 ± 6a	84 ± 2a	79 ± 2a	84 ± 2a
Matches: earthworm bodies	74 ± 8a	77 ± 2a	77 ± 2a	82 ± 2a
Matches: clover-grass	35 ± 4a	68 ± 2a	64 ± 2a	64 ± 1a
Root biomarkers	0.01 ± 0.00c	0.04 ± 0.00ab	0.06 ± 0.01a	0.03 ± 0.01bc
Root / shoot biomass	0.4 ± 0.1b	2.1 ± 0.2a	2.3 ± 0.4a	2.3 ± 0.4a
Microbial / shoot biomarkers	33 ± 5a	33 ± 6a	21 ± 9a	61 ± 15a
Microbial / root biomarkers	88 ± 4a	16 ± 3b	8 ± 3b	28 ± 7b

Table 2 *ANOSIM results based on 9999 permutations (p 0.0001). Shown are pairwise Bonferroni-corrected p-values in a matrix describing the similarity of biopore types and bulk soil. Significant p-values denote significantly different treatments.*

	Root biopores	**Roots + Earthworms**	**Earthworm biopores**	**Bulk soil**
Root biopores	-			
Roots + Earthworms	p > 0.05	-		
Earthworm biopores	p > 0.05	p > 0.05	-	
Bulk soil	*	*	*	-

2.1.3.1 Lignin

Roots and earthworms imported large amounts of lignin into the subsoil: while roots increased the lignin stock (Σ lignin-derived phenols of VSC subunits g^{-1} soil) moderately after two years, i.e. six times compared to bulk soil (Fig. 2, Table S2), earthworms imported much more lignin than roots, i.e. 10 times higher contents compared to bulk soil. Highest lignin stocks were brought about by the combination of roots and earthworms, which led to a 13-fold increase in VSC subunits ($p< 0.05$ relative to bulk soil). All contents tended to decrease from 45–75 cm to 75–105 cm, especially in biopores with short-term earthworm incubation (-40%, $p< 0.05$). The average lignin contents in both earthworm biopore types (mean values from 45–105 cm) were similar (500 *vs* 380 µg g^{-1} soil, Table S2). Vanillyl (V) and syringyl (S) subunits occurred at a ~ 1:1 ratio in all treatments. The cinnamyl (C) subunit was only present (5–10%) in earthworm biopores. Since chicory roots did not contain C subunits (<1%), these have to originate from the earthworm diet (Table S7, Supplementary material). Earthworm bodies and the clover-grass material used to feed earthworms during the biopore differentiation contained 30–60% C subunits.

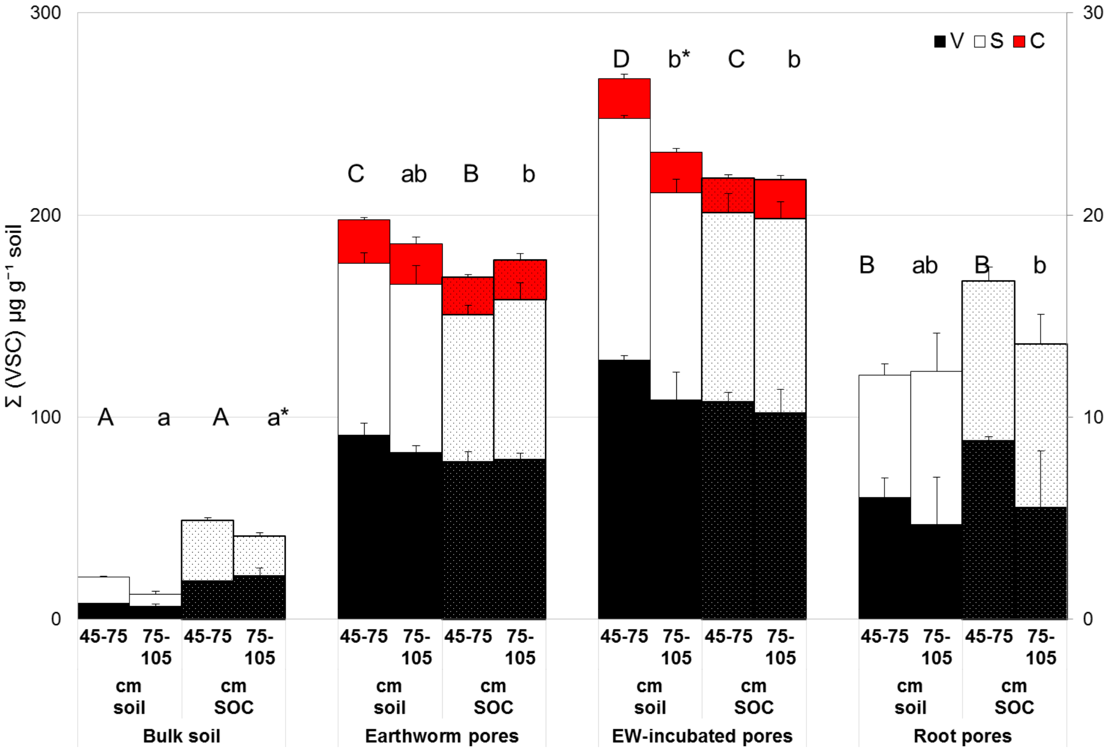

Fig. 2 *Mean VSC-lignin contents ± SEM (two left bars of each treatment; µg g^{-1} soil) and their contributions to SOC ± SEM (two right bars; mg g^{-1} SOC) of the three biopore types and bulk soil in two subsoil depths (45–75 cm, 75–105 cm). Colours represent vanillyl (V), syringyl (S) and cinnamyl (C) subunits released during lignin CuO oxidation. Small and capital letters each indicate significant differences among treatments of one soil depth (one-way ANOVA, Tukey's HSD on α 0.05; separated for contents and SOC contributions). Asterisks given in the lower soil depth indicate significant differences between soil depth (Two sample t-test for paired samples on α 0.05). Full and dashed red lines represent the level of the bulk soil contents and OM, respectively, to illustrate biopore effects.*

The contribution of lignin to soil organic carbon (Fig. 2) generally followed the trend of the stocks (Fig. 2), and all contributions were significantly higher than in bulk soil. It was again highest in both earthworm biopore types, reflecting the large inputs of lignin-rich plant material by earthworms - irrespective of the duration of their presence (Fig. 2). In root biopores, a considerable part of the lignin had to be already decomposed, since the biomass characterisation revealed extremely high lignin contents in roots.

2.1.3.2 Carbohydrates: Neutral sugars, hexuronic acids and amino sugars

The two mainly **plant-derived sugars** arabinose and xylose made up 25-30% of the total neutral sugars (Table S3): their contents (Fig. 3, Table S3) followed the pattern of the lignin contents (Fig. 2). Lowest contents in 45–75 cm were found for the bulk soil (Fig. 3), intermediate contents for root biopores (+70% compared to bulk soil) and highest in both earthworm biopores (+ 250% and 350% for native and incubated treatments compared to bulk soil, respectively). The trends remained the same in 75–105 cm. With depth, contents decreased in incubated biopore types ($p< 0.05$, shown by the asterisks), which was in line with lignin pattern and hinted to preferential earthworm activities in 45–75 cm. The

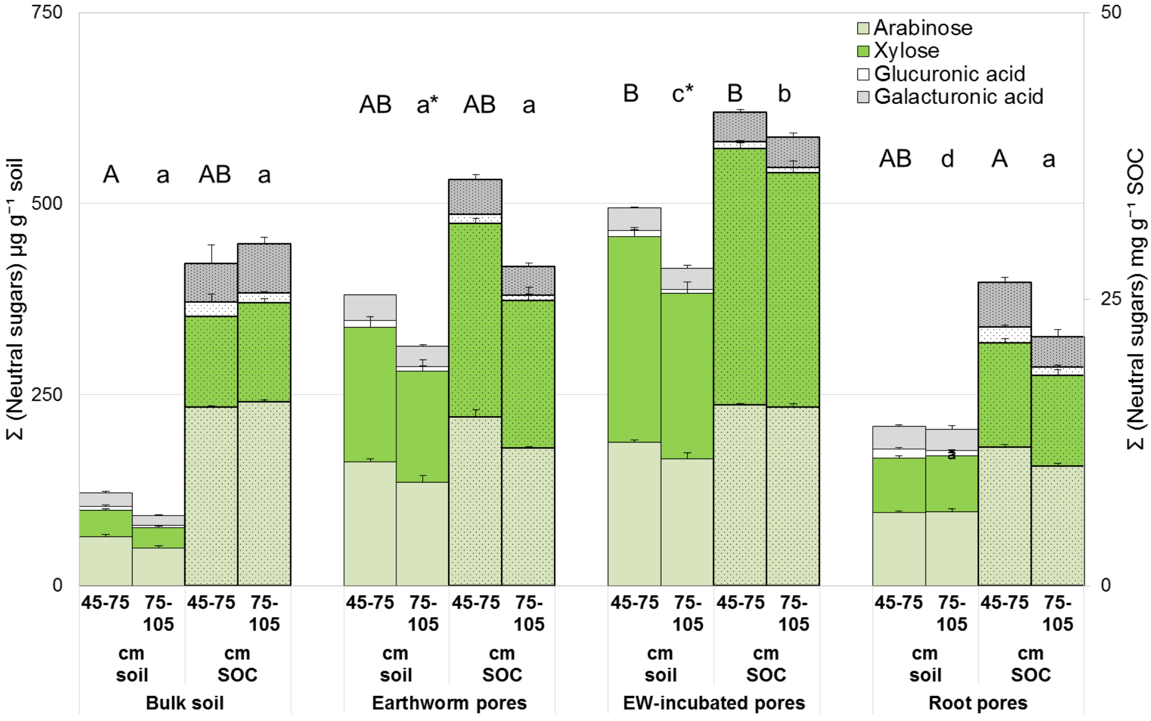

Fig. 3 *Mean hemicellulose and hexuronic acids contents ± SEM (two left bars of each treatment; µg g^{-1} soil) and their contributions to SOC ± SEM (two right bars; mg g^{-1} SOC) of the three biopore types and bulk soil in two subsoil depths (45–75 cm, 75–105 cm). Colours represent sugar monomers. Small and capital letters each indicate significant differences among treatments of one soil depth (one-way ANOVA, Tukey's HSD on α 0.05; separated for contents and SOC contributions). Asterisks given in the lower soil depth indicate significant differences between soil depth (Two sample t-test for paired samples on α 0.05).*

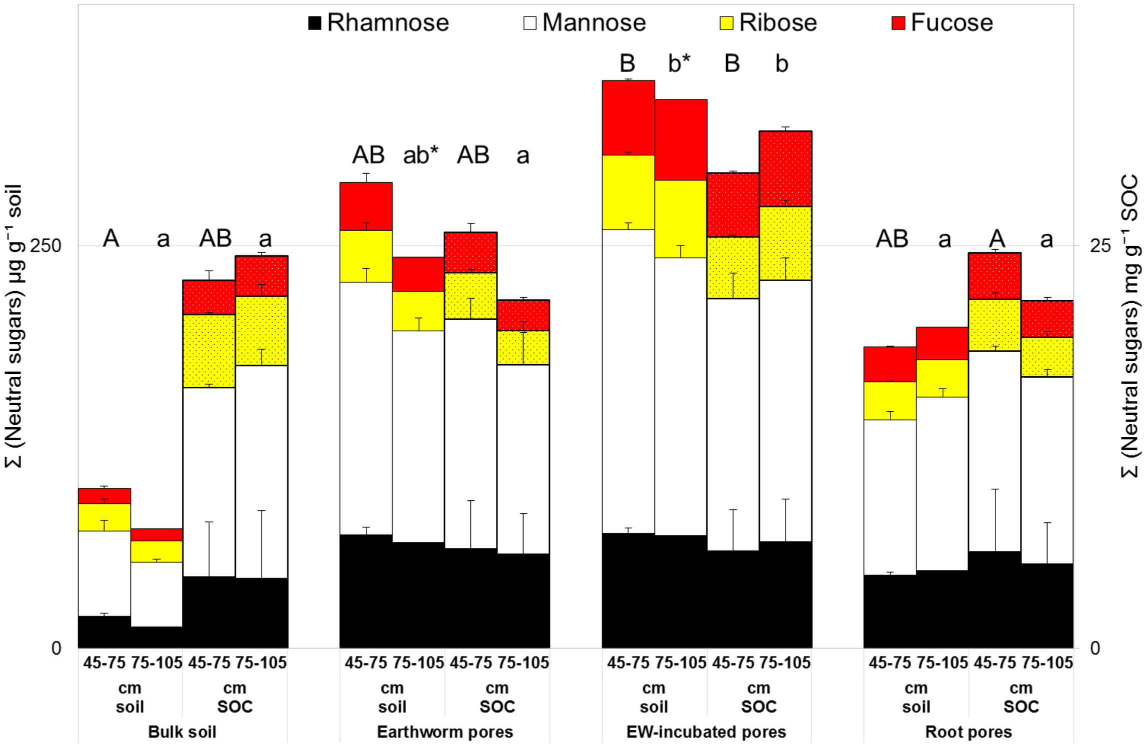

Fig. 4 *Mean microbial hexoses contents ± SEM (two left bars of each treatment; µg g^{-1} soil) and biomarker contributions to SOC ± SEM (two right bars; mg g^{-1} SOC) of the three biopore types and bulk soil in two subsoil depths (45–75 cm, 75–105 cm). Colours represent sugar monomers of microbial origin. Small and capital letters each indicate significant differences among treatments of one soil depth (one-way ANOVA, Tukey's HSD on α 0.05; separated for contents and SOC contributions). Asterisks given in the lower soil depth indicate significant differences between soil depth (Two sample t-test for paired samples on α 0.05).*

contribution of arabinose and xylose to SOC (Fig. 3, two right columns) was the same in the biopores and bulk soil, which indicates that hemicelluloses have already been decomposed to the level of the bulk soil. In this case, biopores merely feature higher SOC contents, but no SOC enrichment in hemicelluloses.

Hexuronic acids followed the trend of neutral sugars and accounted for 5% of neutral sugars (Fig. 3, Table S3). Galacturonic acid was recovered in higher amounts than glucuronic acid, likely representing residual pectin from plant cell walls. Galacturonic acid was significantly enriched only in earthworm biopores in 45–75 cm, while glucuronic acid was only enriched in root biopores in 45–75 cm.

We considered rhamnose, mannose, ribose and fucose as **microbial sugars** (Moers 1990, Tanaka 1990), as we did not find them in relevant amounts in our plant biomass. However, galactose had to be excluded from that list due to high galactose contents in the chicory biomass (for the biomass characterisation see Table S1). The treatment effects of the Σ microbial sugars (Fig. 4) and Σ arabinose + xylose (Fig. 3) were similar. Contents significantly decreased with depth in the earthworm biopore, indicating preferential earthworm activities in the upper soil compartment. Despite a 100% increased stock compared to bulk soil, normalised to SOC neither root biopores nor native earthworm biopores were significant enriched in the SOC pool. Incubated earthworm biopores, however, had significantly increased contents (+250%) and contribution to SOC in both depths.

The combined stock of the **amino sugars** glucosamine, mannosamine, galactosamine and muramic acid (Fig. 5, Table S4) represents microbial cell walls, i.e. predominantly microbial necromass. Only the amino sugars contents of root biopores in 75–105 cm showed significant enrichment relative to bulk soil. The contribution of amino sugars to SOC was in both earthworm biopore types smaller than in bulk soil, hinting to fast turnover of microbial cell residues in these biopores. A dependency on soil depth was found for the root biopores and, less pronounced, in incubated biopores, i.e. treatments with former roots. No depth effect was apparent in native earthworm biopores.

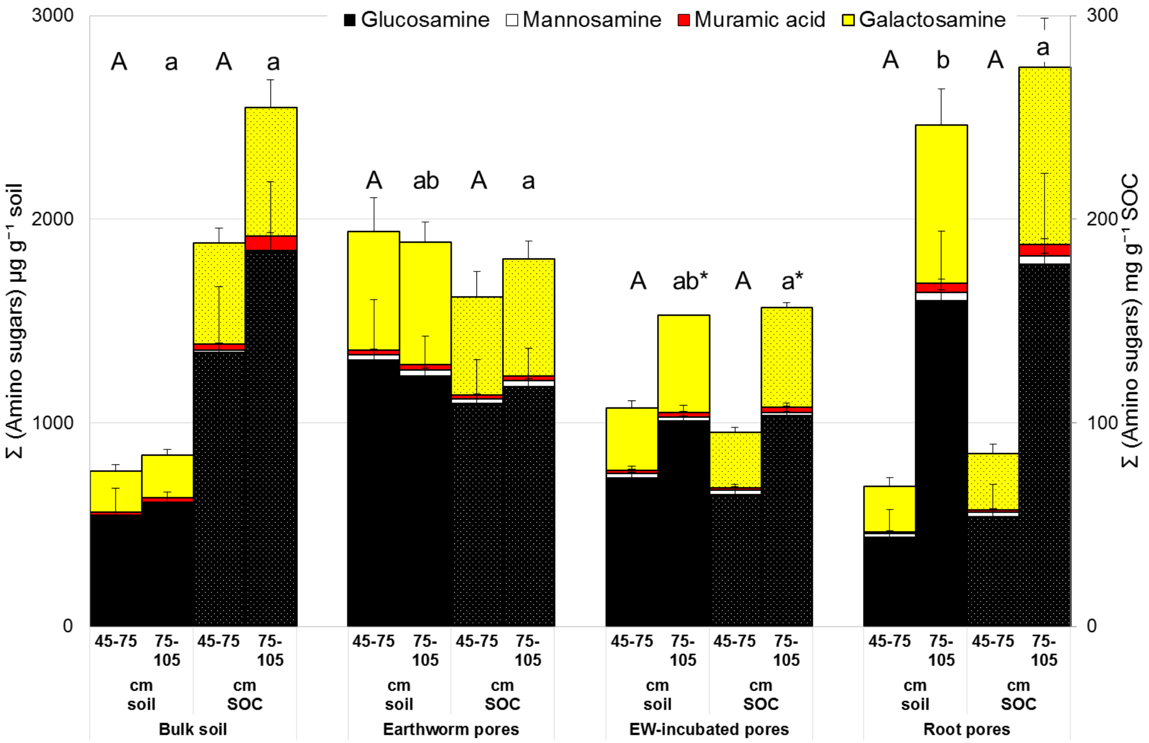

Fig. 5 *Mean amino sugars contents ± SEM (two left bars of each treatment; µg g^{-1} soil) and their contributions to SOC ± SEM (two right bars; mg g^{-1} SOC) of the three biopore types and bulk soil in two subsoil depths (45–75 cm, 75–105 cm). Colours represent amino sugar monomers of microbial origin (cell walls). Small and capital letters each indicate significant differences among treatments of one soil depth (one-way ANOVA, Tukey's HSD on α 0.05; separated for contents and SOC contributions). Asterisks given in the lower soil depth indicate significant differences between soil depth (Two sample t-test for paired samples on α 0.05).*

2.1.3.3 Free lipids: n-alkanes, n-alkenes, n-alkanols, ketones, fatty acids and hydroxy fatty acids

The total contents of the free lipids did not differ among treatments (Fig. 6, Table S5). Neither was there any higher contribution to biopore SOC relative to bulk soil.

Among all treatments, n-alkanes and n-alkenes had by far the highest contents within the free lipids (Table S5). N-alkanes were considered to derive from plants starting from a chain length of C26 as indicated by the pronounced odd-over-even ratio for n-alkanes >C26 found in soil and the biomasses (Fig. S1, Table S1). Despite lacking statistical confirmation, earthworms imported large amounts of long-chain n-alkanes from plants into their burrows (Fig. 6). The contribution of n-alkanes to SOC appeared smaller than in bulk soil in 75–105 cm. *N-alkenes* as degradation products of n-alkanols or conversion products of n-alkanes were recovered at roughly 60% of the n-alkane fraction (Fig. 6). In 45–75 cm, the ratio of n-alkanes to n-alkenes was highest in root biopores (0.90) and bulk soil (0.75), and the lowest in earthworm biopores with fresh input (0.40). In contrast, in 75–105 cm, the ratios were much narrower among all treatments (36–45%). The contents of ∑ n-alkanols + ketones were significantly higher in the incubated biopores than in bulk soil (Table S5).

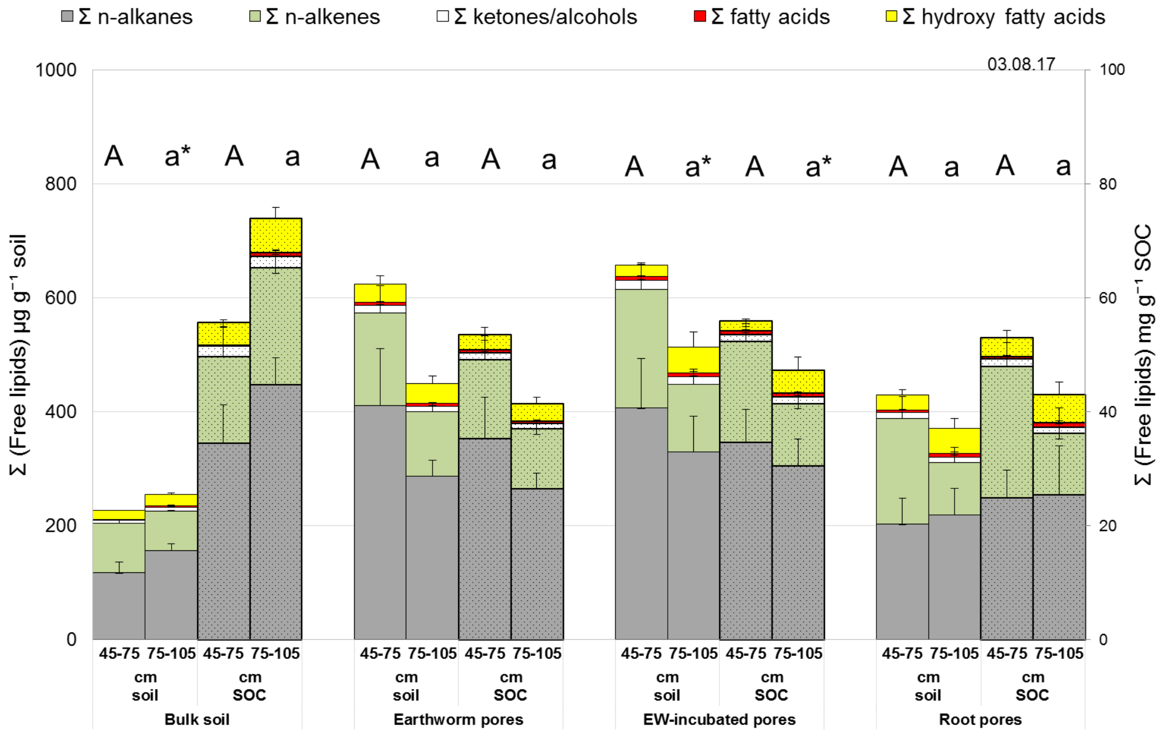

Fig. 6 *Mean free lipids contents ± SEM (two left bars of each treatment; µg g^{-1} soil) and their contributions to SOC ± SEM (two right bars; mg g^{-1} SOC) of the three biopore types and bulk soil in two subsoil depths (45–75 cm, 75–105 cm). Colours represent lipid fraction: n-alkanes, ketones/alcohols, fatty acids and hydroxy fatty acids. Small and capital letters each indicate significant differences among treatments of one soil depth (one-way ANOVA, Tukey's HSD on α 0.05; separated for contents and SOC contributions). Asterisks given in the lower soil depth indicate significant differences between soil depth (Two sample t-test for paired samples on α 0.05).*

Like the other lipid fractions, the contents of free fatty acids appeared larger in the biopores in 45–75 cm than in bulk soil, and to a smaller degree, this was also the case in 75–105 cm (Table S5). Their contribution to SOC was also generally lower in biopores than in bulk soil, hinting at their relatively rapid turnover under increased microbial activity. Stemming from mostly cutin and suberin, free hydroxy fatty acids may be indicative of the turnover and ongoing decomposition of these polymers (Table S5). Contents tended to increase with depth in all treatments, but more strongly in the treatments with roots previously growing in, i.e. root biopores and earthworm-incubated biopores.

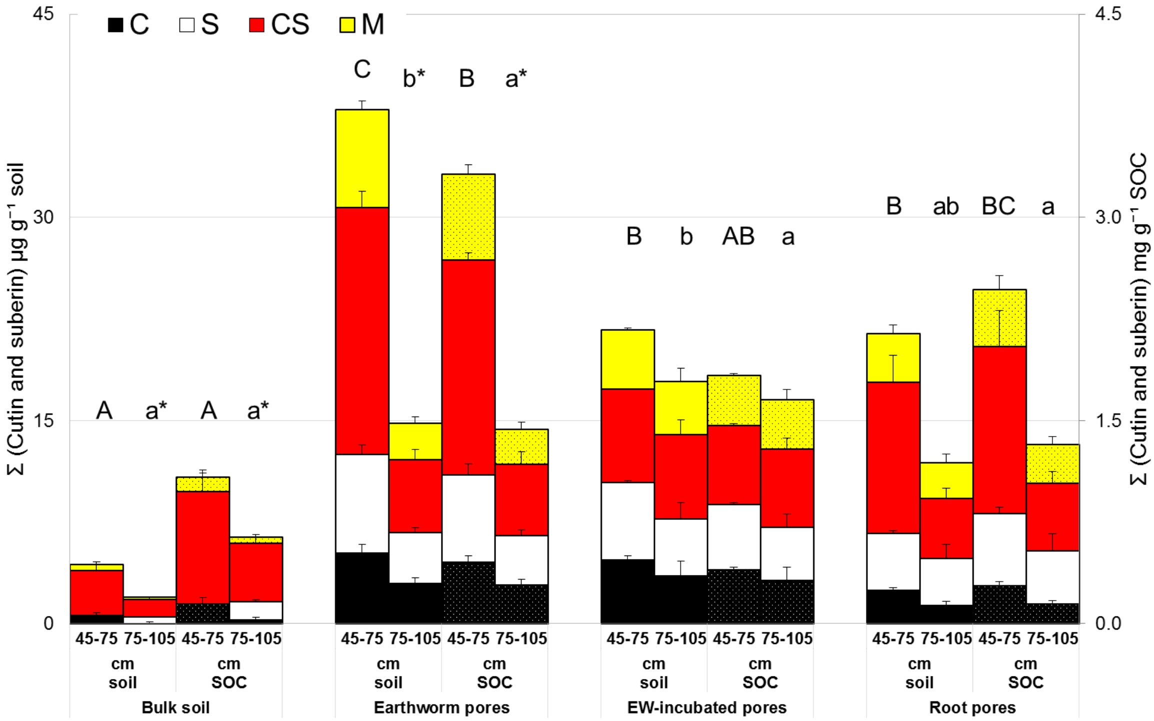

Fig. 7 *Mean cutin/suberin contents ± SEM (two left bars of each treatment; µg g^{-1} soil) and their contributions to SOC ± SEM (two right bars; mg g^{-1} SOC) of the three biopore types and bulk soil in two subsoil depths (45–75 cm, 75–105 cm). Different colours represent cutin (C), suberin (S), unspecific (CS) and microbial (M) fractions. Small and capital letters each indicate significant differences among treatments of one soil depth (one-way ANOVA, Tukey's HSD on α 0.05; separated for contents and SOC contributions). Asterisks given in the lower soil depth indicate significant differences between soil depth (Two sample t-test for paired samples on α 0.05).*

2.1.3.4 Hydrolysable lipids: Cutin and suberin-derived monomers

Monomers studied herein derive from either cutin, suberin, both (i.e. non-specific lipids) or are of microbial origin. In 45–75 cm, root and incubated biopores had five times higher contents, and native earthworm biopores had nine times higher contents than bulk soil (Fig. 7, Table S6). The total contents from 45–105 cm of both native and incubated earthworm biopores were comparable (~ 53 vs 40 µg g^{-1} soil), hinting to a comparable extent of earthworm activities in these two biopore types. In 75–105 cm, contents in biopores increased relative to bulk soil six times (root biopores), 7.5 times (native earthworm biopores), and nine times (incubated biopores). Cutin/suberin contents and their contributions to SOC showed strong decreases with depth in bulk soil and native earthworm biopores (both $p<0.05$). The contents of the individual groups (cutin- *vs* suberin-derived *vs* microbial) were differentiated. Mainly unspecific markers characterised bulk soils, i.e. markers neither representing cutin or suberin, whereas among the biopores the ratio of cutin, suberin, unspecific and microbial lipids hardly changed. The microbial lipid content was strongly correlated with the microbial community structure reported in Banfield et al. (2017a) and was the lowest in bulk soil and the highest in earthworm biopores. In 45–75 cm, suberin- and also cutin-derived markers were significantly enriched in all biopores compared to bulk soil. In the deeper soil, even though none of the individual fractions were different from bulk soil, the total stock of all earthworm-influenced biopores were higher than the bulk soils. The SOC contribution of biopores was 2.5 times larger (45–75 cm and 75–105 cm) than bulk soils' and decreased with depth in all treatments. While no differences of fractions were found in 75–105 cm among the treatments, cutin contribution was larger in the both earthworm-influenced biopore types than in the root biopores or bulk soil in the upper soil layer.

2.1.3.5 Identification of a biomarker subset to characterise unknown biopores

The PLS procedure returned an ordered list of best predictors (Table 3, left), from which we have taken the top ten. The model returned 14 components with 54% cumulative variance explained by the first two and 99.9% of the variance explained by all. Linear discriminant analysis (LDA) on the reduced data set returned significant roots explaining 51% and 41% of total discrimination. The classification functions, which can be used for a direct classification, can be found in Table 3 (right). The factor structure (Table 3, centre) and the LDA biplot (Fig. 8) show that root 2 (y-axis) separated the biopores from the bulk soil. Since all ten variables correlate positively and similarly with root 2, this root may mostly represent the TOC content. Root 1 (x-axis), which was most positively correlated with C subunits of lignin and negatively with actinobacteria (10Me 16:0), separated both earthworm biopores from root biopores.

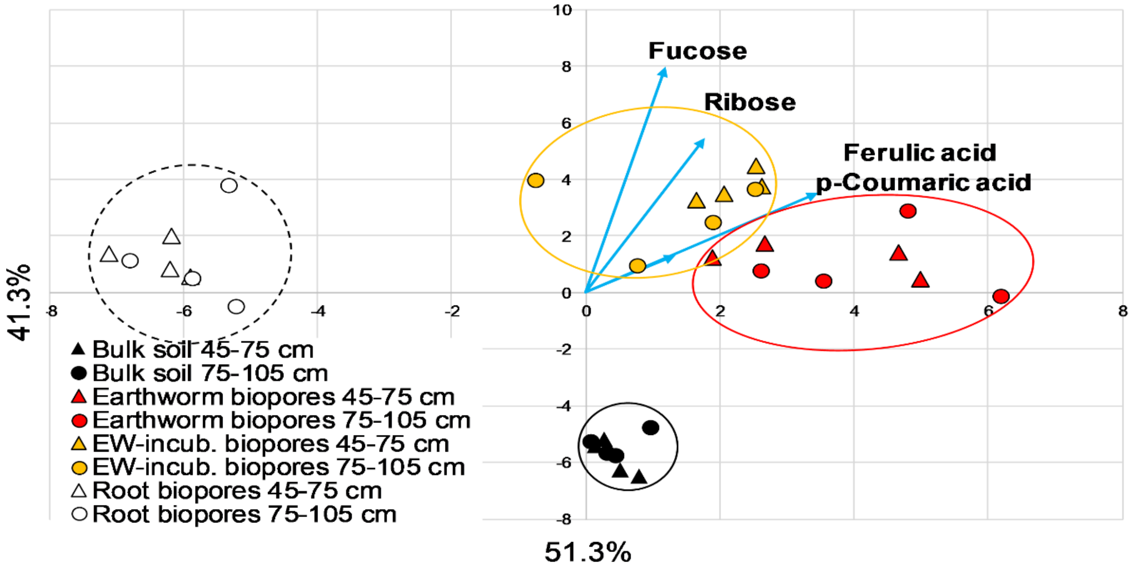

Fig. 8 *LDA biplot showing the discrimination scores as an XY scatterplot (triangles: samples from 45–75 cm, circles: samples from 75–105 cm) and the four variables with the highest discriminatory power (because of visibility).*

Table 3 *Dimension reduction by partial least squares (PLS) classification (left) and linear discriminant analysis (LDA). The ten variables with the highest VIP from the PLS analysis were used to calculate linear discriminant functions, their factor structure and classification functions.*

PLS VIP			**Discriminant functions**		**Factor structure**		**Classification functions**			
Variable	**VIP**	**Rank (of 228)**	**Root 1**	**Root 2**	**Root 1**	**Root 2**	**Root biopores**	**EW-inc. biopores**	**Earthw. biopores**	**Bulk soil**
10Me16:0	2.06	1	-0.49	0.45	-0.25	0.31	48.38	17.11	14.95	-4.19
Ferulic acid	1.67	2	1.13	0.57	0.60	0.61	-1.45	2.41	3.59	-0.14
Ketone (unknown)	1.65	3	-0.70	0.92	-0.16	0.04	66.90	43.73	14.06	-10.33
cy19:0	1.53	4	-0.59	0.33	-0.11	0.39	18.08	6.46	0.72	0.17
Fucose	1.48	5	-1.53	1.08	0.04	0.29	1.17	0.41	-0.29	-0.36
p-Coumaric acid	1.47	6	-0.08	0.01	0.30	0.30	0.16	-0.25	-0.23	-0.21
20:4w6c	1.42	7	0.58	-0.29	0.13	0.24	-138.96	-8.37	-33.66	9.23
Ribose	1.40	8	0.93	-1.32	0.07	0.20	-0.82	-0.49	0.10	0.53
22-Hydroxydocosanoic acid	1.40	9	0.11	0.07	-0.08	0.26	3.86	6.98	10.33	4.20
Octacosanic acid (C28:0)	1.37	10	-0.52	1.13	0.04	0.30	22.39	21.74	6.04	-5.85
Residuals							-42.38	-37.46	-30.81	-4.17
Eigenvalue			15.78	12.68						
Wilks' λ			0.001	0.022						
p			< 0.000	< 0.000						

2.1.4 Discussion

The main differences between the biopores arise from the frequency and the properties of the C inputs and sources: continuous earthworm activities, i.e. repeated shoot-C inputs, are to be distinguished from the large single root C input. Chicory induced root biopores filled with detritus of a defined age (Hafner and Kuzyakov, 2016), equivalent to a two-year fallow after three years of cover cropping. In the field, under natural conditions, root biopores would be colonised by earthworms. Root biopores are abundant in the subsoil (Gaiser et al., 2013) and earthworm colonisation is likely. We emulated the earthworm colonisation by **incubation** of *Lumbricus terrestris* into root biopores for one growing season. Supplying them with defined food sources reveals the short-term effects of earthworms. To compare the short-term *vs* long-term earthworm presence, **native earthworm biopores** were sampled. **Bulk subsoil** samples were not subject to any experimental alteration and represented bulk subsoil conditions, i.e. long-term stabilised C and absence of hotspots due to low carbon inputs (Rumpel and Kögel-Knabner, 2011).

2.1.4.1 Bulk soil

In bulk subsoil, abiotic decomposition conditions and OM inputs are not as favourable as in the biopore hotspots (e.g. lower oxygen supply) (Brown, 1995; Gliński and Lipiec, 1990; Rumpel et al., 2012). The pathways of OM from the soil surface into the subsoil as DOM are slow, so compounds are heavily modified, and get partly respired (Kalbitz and Kaiser, 2008; Rumpel et al., 2004; Schulz et al., 2012). Besides lower C contents, substrate richness was 33% lower in bulk soil than in earthworm biopores. The relative occurrences of substances to the substances classes did not change with soil depth – hinting to most dominant C turnover processes in the topsoil. This unspecific SOM pattern was further reflected by the low specificity of cutin-/suberin-derived lipids (Fig. 7, Table S6) caused by microbial modifications like depolymerisation, oxidation, breaking off side chains or desaturation (Engelking et al., 2007; Thevenot et al., 2010). Intact and unprocessed OM is therefore not to be expected in the deeper subsoil, in contrast to the biopores. The fundamental difference in C sources was discernible from the full OM fingerprints (>160 substances): ANOSIM (Table 2) and PCA (Fig. 1) showed that the OM of bulk soil was statistically separated from the biopore OM. This fact suggests that intensive DOC processing and alteration is a key process causing the OM composition of the bulk soil.

Despite low absolute biomarker content in bulk soil, some biomarker classes contributions to SOC were equal to the root biopores' contribution (e.g. hemicelluloses, Fig. 3) or even all biopores (free lipid fractions, Fig. 6). Either the tissues represented by these biomarkers are fast-cycling in biopores, or they are stabilised in the bulk subsoil. Increases of SOC contribution with depth may be due to stronger physical stabilisation and less favourable decomposition conditions in the bulk subsoil. Especially aliphatic compounds like n-alkanes may be persistent (Rumpel et al., 2012). N-alkane contents dominated the free lipid fraction (Fig. 6) (Jaffé et al., 1996; Marseille et al., 1999; Wiesenberg et al., 2004).

Plant inputs will be eventually respired or immobilised as microbial necromass (Miltner et al., 2012). The highest ratios of microbial / root biomarkers were found in the bulk soil (Table 1, 75–105 cm), where plant inputs are highly processed and plant biomarkers are largely decomposed while the resulting microbial necromass remains. The higher OM degradation was confirmed by the lower substrate richness and the lower C/N ratio in the bulk soil than the biopores (Table 1). Bulk subsoil C is thought to be of root origin, rather processed, depleted in plant matter and enriched in microbial residues (Rumpel and Kögel-Knabner, 2011). Whereas we could confirm a high contribution of microbial residues, bulk soil OM was less enriched in root OM (lower root biomarkers, Table 1). Residues include amino sugars (monomers of microbial cell walls) and the neutral sugars fucose, mannose, rhamnose and ribose (Basler et al., 2015; Oades, 1984; Paul, 2016) in exopolymeric substances (EPS, biofilms (Vu et al., 2009) and lipopolysaccharides (LPS, components of Gram-negative cell membranes, Zelles et al., 1995). Due to strong interactions with mineral surfaces, amino and microbial neutral sugars accumulate after cell death (Gleixner et al., 1999; Miltner et al., 2012). The increased the contribution of microbial amino sugars to SOC with depth points to higher stabilisation on mineral phases in 75–105 cm and is very likely correlated with less saturated mineral phases in the deeper subsoil (Six et al., 2002). The microbial neutral sugars (Fig. 4) only partly replicated the trend of the amino sugars (Fig. 5), hinting to deviating stabilisation and decomposability of microbial residues. Summarising, the bulk soil OM comprises a mixture of compounds of varying decomposability (Liang and Balser, 2008) and is less diverse than the biopore OM. Its sources are relative to biopores less likely root-derived.

2.1.4.2 Root biopores

After two years of root decay and lack of recent C inputs, the sizeable initial root biomass was still apparent in the root biopores from I) high root/shoot biomarker ratio (Table 1) and II) all biomarkers contents were on average a third lower than in the earthworm biopores (Figs. 2–7, Tables S2–6). Root biopores had mostly increased contents of polymeric plant biomarkers ∑ (cutin + suberin) and lignin (Figs. 2, 7). The root biopore OM fingerprint did not match the intact root biomass fingerprint because the OM processing was rather advanced (Table 1). From the PCA (Fig. 1), the soil depths were more separated than in the other biopores or bulk soil, and the count of identified substances increased sharply with depth (Table 1) — possibly less favourable decomposition conditions in the deeper soil or percolation contributed to this phenomenon.

Before decomposition, chicory roots featured the largest lignin content of all source biomasses (Table S1). Consequently, roots were clearly the largest single contributor to lignin in the subsoil biopores. Despite the low initial bioavailability of the lignin macromolecule (Větrovský et al., 2014), within two years the most substantial part of lignin was decomposed in the root biopores, and only a fraction remained. The hemicellulose (arabinoxylan) signature got lost during root decomposition. In bulk soils and biopores, a 1:1 instead of the 5:1 ratio of xylose to arabinose was found (Rumpel et al., 2010). Such preferential respiration of xylose may be due to the crosslinking of the arabinoxylan (Amin et al., 2014). Chicory is commercially cultivated for inulin and pectin, i.e. polymeric homogalacturonic acid (Robert et al., 2008; Street et al., 2013). The use of uronic acids as specific and natural abundance biomarkers is challenging due to its widespread occurrence in nature. They derive from EPS, plant mucilage, from LPS or glycosaminoglycans containing glucuronic acid from earthworms, e.g. *Eisenia andrei* (Bouché, 1975). Due to this ubiquitous origin (Fig. 3) the uronic acids contents only weakly differentiated between treatments.

After normalisation to SOC, the root biopores start telling a different story: the treatment effects of most biomarker contents disappeared — except for lignin and cutin/suberin. Some substance classes behaved differently during decomposition in root biopores: ∑ (cutin/suberin) and lignin were in contrast to n-alkanes and hemicelluloses enriched in the root biopore SOC pool, thus implying higher decomposability of two latter. After two years of decomposition, the contributions of hemicelluloses (Fig. 3), microbial sugars (Fig. 4) and n-alkanes to SOC (Fig. 6) were equal or lower than in the bulk soil. In the course of the decomposition, gradually the SOC pattern is approached – unless the biopore is re-used (Banfield et al., 2017b). No lower SOC contributions than in the bulk soil were expected since bulk soil OM is deemed long-term stabilised. Selective priming of such biomarker classes during OM turnover seems to be a plausible explanation (Kuzyakov, 2010), e.g. episodic priming driven by percolated C (Kuzyakov, 2002, 2010).

Root biopores and bulk soil have similar soil physical parameters (Pagenkemper et al., 2014). This fact and the late decomposition stage explain why the molecular characterisation of root biopores gave similar results like bulk soil. Even though the remaining OM was not particularly bioavailable (lignin and microbial residues), enzyme activities and the microbial biomass were still considerably increased relative to the bulk soil (Banfield et al., 2017a; Hoang et al., 2016). Contents of microbial lipids (Fig 8) and microbial hexoses (Fig. 4) closely followed the pattern of MBC and Σ PLFAs (Banfield et al., 2017a; Hoang et al., 2016).

2.1.4.3 Earthworm-incubated biopores

Combining two C sources, i.e. active earthworms and root detritus, in the 'earthworm-incubated biopores' led to the highest C accumulation among all biopore types (Table 1) — within six months of earthworm incubation. Conceptually, the OM composition in earthworm-influenced biopores depends on, e.g. the palatability of the food sources, the earthworm's gut microbiome and the interactions of the inputs with the mineral phase during the gut passage (Bouché, 1975; Brown et al., 2000; Curry and Schmidt, 2007). Earthworms almost completely overrode the molecular structure of the former root detritus OM within six months. The resulting similar substrate quality between incubated and native earthworm biopores was underlined by an identical count of identified compounds (Table 1), overlap in the PCA (Fig. 1) and by the fact that ANOSIM did not differentiate both (Table 2). The earthworms' specific biomarker signature stems from a combination of the earthworm bodies (especially through mucus secretion) and the earthworm food (clover grass; Table 1) since both earthworm-influenced biopore types showed the most matches with these source biomasses. Preferential earthworm activities were discernible from decreases with depths (lignin -15% from first to the second horizon, cutin/suberin -18%). Short-term incubation might have favoured preferential earthworm activities in 45–75 cm, which are likely to equalise over longer time spans.

Earthworms in root channels did not increase substrate richness further than native earthworm biopores. *Before* the earthworm incubation, the root detritus contents were identical in the root biopores and the earthworm-incubated biopores. Six months of earthworm activities tripled the contents of hemicelluloses and doubled contents n-alkanes and lignin relative to root biopores but did not affect cutin/suberin contents. Six months of earthworms in root biopores accumulated more lignin than years of native earthworm activity (Fig. 2). The quality of the lignin changed with incubation: cinnamyl subunits were only recovered in the earthworm biopores. They stem from the earthworm forage of ryegrass and clover, which lignin fraction contained up to 60% ferulic acid, i.e. a cinnamyl derivative (Table S2, Supplementary material). This finding shows the utility of characterising the primary inputs to identify C sources. Earthworms may not easily digest lignin (Brown et al., 2004; Lee, 1985; Satchell, 1967), but support lignin degradation by priming through additional moisture and available C from the mucus (Al-Maliki and Scullion, 2013; Kuzyakov, 2010). Nevertheless, lignin was most resistant to the decomposition in biopores, as it was most strongly enriched in all biopores SOC pools.

The free lipid contents in all subsoil biopore hotspots were in the range of agricultural bulk topsoils previously reported by Wiesenberg et al. (2004). However, despite the high enrichment of biomarker contents in the incubated biopores, free lipids were not significantly enriched relative to bulk (Fig. 6). Free lipids are nevertheless of great diagnostic value: I) the relative amounts of ∑ n-alkanes + n-alkanols and hydroxy fatty acids could be useful molecular turnover proxies of shoots and roots in the presence of earthworms, respectively (Vidal 2016) and II) the average chain length of n-alkanes could be a second proxy for plant OM turnover (Wiesenberg et al., 2004). High microbial turnover over time was linked to low lipid contents in soil (Fridland, 1976), as was the case in all earthworm biopores.

Evidently, the plant cuticles were the primary source not only for cutin-derived lipids but also for most free lipids. Cutin *vs* suberin in biopores reflected the food sources of earthworms (Fig. 7, Table S6, Supplementary material). Cutin contents were significantly larger than in root biopores, while suberin was not higher in incubated biopores. This is easily explained by the cutin-only forage of the incubated earthworms and the same root detritus in both root-affected biopore types. Thus, earthworm food sources left behind a significant molecular fingerprint in the biopores after six months of incubation.

In the earthworm-incubated biopores, most plant biomarkers had higher contributions to SOC than bulk soil as these biopores are made from a combination of two large C sources (Table 1). However, the highest plant biomarker accumulation among biopores did not lead to the highest amount of microbial necromass: the amino sugars contribution to SOC was not larger than in bulk soil, but it led to significantly higher microbial hexoses per SOC (Fig. 4). Apparently, both biomarkers represent differently stabilised microbial compounds in soil.

2.1.4.4 Native earthworm biopores

The ‘native earthworm biopores’ represent the long-term (> 2.5 years) earthworm burrowing. The biomarker contents were very comparable to the earthworm-incubated biopores likely because all earthworms were fed with the same forage. In contrast to the other two biopore types, there was no known former root influence in these biopores for at least two years. Earthworms introduced much more C into the subsoil than roots alone (+28%; Table 1). Preferential earthworm activities were also found in the native earthworm biopores albeit weaker than in earthworm-incubated biopores. Without pre-existing root detritus, the lignin decrease with depth was weaker than in the incubated biopores (Fig. 2). Over longer time spans, earthworm activities more likely equalise lignin contents in both soil depths, suggesting that periodic events (e.g. droughts) force earthworms to dig deeper into the subsoil. In contrast, Σ (cutin + suberin) showed a much stronger depth effect than lignin. Cutin and suberin are likely more bioavailable than lignin, which means preferential earthworm activities in the immediate time before sampling may have become more apparent.

Even though earthworms were at least two years longer active in native earthworm biopores than the incubated ones, the biomarker contents were usually lower than in the earthworm-incubated biopores, suggesting lower overall activity. As native earthworm biopores did not feature a drastically different SOM composition (Figs. 2–7) than bulk soil, rather intensive processing and a lower recent input than in the incubated biopores is likely. Consequently, lacking regular, active OM input earthworm biopores are during 2–3 years already converge to bulk soil. Therefore, an active biopore management and their re-use and re-fill of the C stocks is required in case their unique features and potentially beneficial roles in agroecosystems shall be maintained.

2.1.4.5 Identification of unknown biopores

To assess the importance of biopores on the larger field scale, the origin of unknown biopores need to be identified. This will allow large-scale assessment of the relative contributions of roots and earthworms to biopores. As this is seldom visually possible, biopores need to be identified by biomarkers. However, analysis of > 16 substance classes including > 220 substances requires not only large amounts of very scarce biopore wall material but also time. For a successful differentiation, only a couple of compounds may be necessary. In our data set, the PLS algorithm assigned variables a high VIP which were recovered in all replicates of a biopore type, but not in others. The best predictors stem from lignin, neutral sugars, phospholipids and hydroxy fatty acids (Table 3). Thus, multiple biomarker analyses may be necessary to differentiate biopores. Microbial metabolites, stress markers and compounds stemming from OM decomposition, i.e. markers of OM dynamics, are much more relevant for the characterisation of hotspots than biomarkers describing OM sources. This points towards the fact that the unique turnover dynamics of biopores is heavily contributing to its molecular fingerprint and that OM sources are rapidly overridden by the high OM turnover (Banfield et al., 2018).

The subsequent discriminant analysis with its discriminant functions consequently enables differentiation by ten variables (Table 3). Comparing the cases' canonical scores with the ten variables in a biplot (Fig. 8) reveals that fucose and ribose feature high loadings on the Y-axis, separating the biopores from bulk soil. The lignin phenols p-coumaric acid and ferulic acid (both C subunits) had high loadings on the x-axis, separating the root biopores from the earthworm biopores. Consequently, neutral sugars and lignin analyses may be a good starting point for biopore differentiation, if analytical effort needs to be minimised.

The PLFA 20:4ω6 was previously discussed as an earthworm marker (Sampedro and Whalen, 2007; Stromberger et al., 2012), which was also among the top ten predictors. The vectors of the p-coumaric acid, ferulic acid and PLFA 20:4ω6 were overlapping in the biplot (Fig. 8), suggesting all three are markers for earthworms. However, the loadings of p-coumaric acid and ferulic acid were much higher, and lignin C subunits are more likely of plant-origin. Therefore, p-coumaric acid and ferulic acid were valid earthworm markers here due to their food sources (which were only applied to earthworms), but PLFA 20:4ω6 may be a more general marker for earthworms. Hence, we recommend comparing biomarker candidates with source biomass characterisation to differentiate earthworm biomarkers from earthworm food biomarkers.

2.1.5 Conclusions

A comprehensive compound-specific description of the OM in biopores and the deep bulk subsoil was direly needed to help disentangle C source contributions and C dynamics in subsoil hotspots. Earthworms and perennial tap-roots are immense sources of weakly processed C, which increased C contents up to three times in distinct subsoil biopores and enhanced substrate diversity relative to bulk soil. Over time, earthworms and roots distributed OM within their biopores, forming rather homogenous habitats. Macropore flow contributed to the C transport downwards – presumably strongest in root channels where no earthworms might have transported C up again. The biomarker contents in biopores reflected their specific C inputs: incubated earthworms fed on clover grass shoots until sampling, thus contents of C, hemicelluloses, cutin and lignin accumulated. Six months of earthworm incubation were sufficient to override former root detritus molecular fingerprint nearly. In root biopores, two years after the last C input, contents of less bioavailable cutin/suberin and especially lignin were larger than in bulk soil but a third lower than in both earthworm biopores – suggesting more advanced decomposition. While C inputs enhanced microbial biomass, turnover in earthworm biopores decreased microbial necromass, possibly through N recycling or priming. Despite the prominently increased biomarker contents in biopores, the contributions of biomarkers to SOC were only in few cases higher than in bulk soil. So even in the long-term, earthworms and roots only weakly altered the SOM structure (i.e. relative abundances of compound classes relative to bulk soil) but mainly increase OM stocks.

Subsoil hotspot OM was undoubtedly *quantitatively* a very attractive C source for microorganisms, being highly concentrated in the very C poor surrounding. However, the SOM was also *qualitatively* different: for instance, biopore OM was 33% more diverse, which might I) bring metabolic advantages especially for recycling of complex compounds from SOM, II) imply a higher resilience towards changing environmental conditions and III) enhance C sequestration as a higher number of different compounds increases the probability of C stabilisation. All these aspects require further investigations of the ecological relevance of OM complexity and biopores may serve as a practical example where such a topic might have field-scale relevance up to the level of agricultural production.

We conclude that promoting earthworms or cultivation of tap-rooted crops even for one vegetation period only, is an effective management tool to transport large amounts of weakly processed and diverse OM into the subsoil, whose origin and turnover can be traced by biomarker approaches at least over several years.

Acknowledgements

We would like to thank Tilman de la Haye for statistical advice, Timo Kautz and the colleagues from Institute of Organic Agriculture of the University of Bonn for establishing and managing the field trial Klein-Altendorf, and the German Research Foundation for their financial support for DFG KU 1184/29, PAK 888 and INST 186/1006-1 /P.

2.1.6 References

- Al-Maliki S, Scullion J. Interactions between earthworms and residues of differing quality affecting aggregate stability and microbial dynamics. Appl Soil Ecol 2013;64:56–62.
- Amin BAZ, Chabbert B, Moorhead D, Bertrand I. Impact of fine litter chemistry on lignocellulolytic enzyme efficiency during decomposition of maize leaf and root in soil. Biogeochemistry 2014;117(1):169–83. http://link.springer.com/content/pdf/10.1007%2Fs10533-013-9856-y.pdf.
- Banfield CC, Dippold MA, Pausch J, Hoang DTT, Kuzyakov Y. Biopore history determines the microbial community composition in subsoil hotspots. Biol Fertil Soils 2017a;9:54.
- Banfield CC, Pausch J, Kuzyakov Y, Dippold MA. Microbial processing of plant residues in the subsoil – The role of biopores. Soil Biol Biochem 2018;125:309–18.
- Banfield CC, Zarebanadkouki M, Kopka B, Kuzyakov Y. Labelling plants in the Chernobyl way: A new 137Cs and 14C foliar application approach to investigate rhizodeposition and biopore reuse. Plant Soil 2017b;29:239.
- Basler A, Dippold M, Helfrich M, Dyckmans J. Microbial carbon recycling – an underestimated process controlling soil carbon dynamics – Part 1: A long-term laboratory incubation experiment. Biogeosciences 2015;12(20):5929–40.
- Betts RA, Falloon PD, Goldewijk KK, Ramankutty N. Biogeophysical effects of land use on climate: Model simulations of radiative forcing and large-scale temperature change. Agricultural and Forest Meteorology 2007;142(2-4):216–33.
- Bouché MB. Action de la faune sur les états de la matière organique dans les écosystèmes. In: Gilbertus K, Reisinger O, Mourey A, Cancela da Fonseca JA, editor. Biodegradation et Humification. Sarreguemines, France: Pierron Editeur; 1975. p. 157–168.
- Brown GG. How do earthworms affect microfloral and faunal community diversity? Dordrecht, Netherlands: Springer, 1995.
- Brown GG, Barois I, Lavelle P. Regulation of soil organic matter dynamics and microbial activityin the drilosphere and the role of interactionswith other edaphic functional domains. Eur J Soil Biol 2000;36(3-4):177–98.
- Brown GG, Doube BM, Edwards CA. Functional interactions between earthworms, microorganisms, organic matter, and plants. Earthworm ecology 2004:213–39.
- Butt KR, Lowe CN. A viable technique for tagging earthworms using visible implant elastomer. Appl Soil Ecol 2007;35(2):454–7.
- Curry JP, Schmidt O. The feeding ecology of earthworms – A review. Pedobiologia 2007;50(6):463–77.
- Don A, Steinberg B, Schöning I, Pritsch K, Joschko M, Gleixner G et al. Organic carbon sequestration in earthworm burrows. Soil Biol Biochem 2008;40(7):1803–12.
- Ehlers W, Köpke U, Hesse F, Böhm W. Penetration resistance and root growth of oats in tilled and untilled loess soil. Soil Till Res 1983;3(3):261–75.
- Engelking B, Flessa H, Joergensen RG. Shifts in amino sugar and ergosterol contents after addition of sucrose and cellulose to soil. Soil Biol Biochem 2007;39(8):2111–8.

- Fridland YE. Lipid (alcohol benzene) fraction of organic matter in different soil groups. Soviet soil science 1976.
- Gaiser T, Perkons U, Küpper PM, Kautz T, Uteau-Puschmann D, Ewert F et al. Modeling biopore effects on root growth and biomass production on soils with pronounced sub-soil clay accumulation. Ecological Modelling 2013;256:6–15.
- Gleixner G, Bol R, Balesdent J. Molecular insight into soil carbon turnover. Rapid Commun. Mass Spectrom. 1999;13(13):1278–83.
- Gliński J, Lipiec J. Soil physical conditions and plant roots. Boca Raton, FL, USA: CRC Press; 1990.
- Hafner S, Kuzyakov Y. Carbon input and partitioning in subsoil by chicory and alfalfa. Plant Soil 2016;406(1):29–42.
- Hammer Ø, Harper DAT, Ryan PD. PAST. Palaeontol Electron 2001;4(1):9.
- Hoang DTT, Pausch J, Razavi BS, Kuzyakova I, Banfield CC, Kuzyakov Y. Hotspots of microbial activity induced by earthworm burrows, old root channels, and their combination in subsoil. Biol Fertil Soils 2016;52:1105–19.
- IUSS Working Group WRB. World reference base for soil resources 2006: Ein Rahmen für internationale Klassifikation, Korrelation und Kommunikation. 1st ed. Hannover: BGR; 2008.
- Jaffé R, Elismé T, Cabrera AC. Organic geochemistry of seasonally flooded rain forest soils: Molecular composition and early diagenesis of lipid components. Organic Geochemistry 1996;25(1-2):9–17.
- Jakobsen BE, Dexter AR. Influence of biopores on root growth, water uptake and grain yield of wheat (Triticum aestivum) based on predictions from a computer model. Biol Fertil Soils 1988;6(4):315–21.
- Jégou D, Cluzeau D, Balesdent J, Tréhen P. Effects of four ecological categories of earthworms on carbon transfer in soil. Appl Soil Ecol 1998;9(1-3):249–55.
- Kalbitz K, Kaiser K. Contribution of dissolved organic matter to carbon storage in forest mineral soils. Journal of Plant Nutrition and Soil Science 2008;171(1):52–60.
- Kell DB. Large-scale sequestration of atmospheric carbon via plant roots in natural and agricultural ecosystems: why and how, 2012. Phil Trans R Soc B;367:1589–97.
- Kögel-Knabner I. The macromolecular organic composition of plant and microbial residues as inputs to soil organic matter. Soil Biol Biochem 2002;34(2):139–62.
- Kuhlmann H, Baumgärtel G. Potential importance of the subsoil for the P and Mg nutrition of wheat. Plant Soil 1991;137(2):259–66.
- Kuzyakov Y. Review: Factors affecting rhizosphere priming effects. J. Plant Nutr. Soil Sci. 2002;165(4):382–96.
- Kuzyakov Y. Priming effects: Interactions between living and dead organic matter. Soil Biol Biochem 2010;42(9):1363–71.
- Kuzyakov Y, Blagodatskaya E. Microbial hotspots and hot moments in soil: Concept & review. Soil Biol Biochem 2015;83:184–99.
- Lee KE. Earthworms: Their ecology and relationships with soils and land use. Earthworms: their ecology and relationships with soils and land use 1985.

- Liang C, Balser TC. Preferential sequestration of microbial carbon in subsoils of a glacial-landscape toposequence, Dane County, WI, USA. Geoderma 2008;148(1):113–9.
- Lozán JL, Kausch H. Angewandte Statistik für Naturwissenschaftler. Singhofen, Germany: Parey Buchverlag; 1998.
- Marseille F, Disnar JR, Guillet B, Noack Y. n-Alkanes and free fatty acids in humus and A1 horizons of soils under beech, spruce and grass in the Massif-Central (Mont-Lozère), France. Eur J Soil Sci 1999;50(3):433–41. http://onlinelibrary.wiley.com/doi/10.1046/j.1365-2389.1999.00243.x/full.
- Miltner A, Bombach P, Schmidt-Brücken B, Kästner M. SOM genesis: microbial biomass as a significant source. Biogeochemistry 2012;111(1-3):41–55.
- Oades JM. Soil organic matter and structural stability: Mechanisms and implications for management. Plant Soil 1984;76(1-3):319–37.
- Pagenkemper SK, Athmann M, Uteau D, Kautz T, Peth S, Horn R. The effect of earthworm activity on soil bioporosity – Investigated with X-ray computed tomography and endoscopy. Soil Till Res 2014(146A):79–88. http://www.sciencedirect.com/science/article/pii/S0167198714000981.
- Paul EA. The nature and dynamics of soil organic matter: Plant inputs, microbial transformations, and organic matter stabilization. Soil Biol Biochem 2016;98:109–26.
- Paul EA, Follett RF, Leavitt SW, Halvorson A, Peterson GA, Lyon DJ. Radiocarbon dating for determination of soil organic matter pool sizes and dynamics. Soil Science Society of America Journal 1997;61(4):1058–67.
- Perkons U, Kautz T, Uteau D, Peth S, Geier V, Thomas K et al. Root-length densities of various annual crops following crops with contrasting root systems. Soil Till Res 2014;137:50–7.
- Rethemeyer J, Kramer C, Gleixner G, John B, Yamashita T, Flessa H et al. Transformation of organic matter in agricultural soils: radiocarbon concentration versus soil depth. Mechanisms and regulation of organic matter stabilisation in soils 2005;128(1–2):94–105.
- Robert C, Emaga TH, Wathelet B, Paquot M. Effect of variety and harvest date on pectin extracted from chicory roots (Cichorium intybus L.). Food chemistry 2008;108(3):1008–18.
- Rumpel C, Chabbi A, Marschner B. Carbon Storage and Sequestration in Subsoil Horizons: Knowledge, Gaps and Potentials. In: Lal R, Lorenz K, Hüttl RF, Schneider BU, Braun J von, editors. Recarbonization of the Biosphere: Ecosystems and the Global Carbon Cycle. Dordrecht: Springer Netherlands; 2012. p. 445–464.
- Rumpel C, Eusterhues K, Kögel-Knabner I. Location and chemical composition of stabilized organic carbon in topsoil and subsoil horizons of two acid forest soils. Soil Biol Biochem 2004;36(1):177–90.
- Rumpel C, Eusterhues K, Kögel-Knabner I. Non-cellulosic neutral sugar contribution to mineral associated organic matter in top- and subsoil horizons of two acid forest soils. Soil Biol Biochem 2010;42(2):379–82.
- Rumpel C, Kögel-Knabner I. Deep soil organic matter—a key but poorly understood component of terrestrial C cycle. Plant Soil 2011;338(1-2):143–58.

- Salome C, Nunan N, Pouteau V, Lerch TZ, Chenu C. Carbon dynamics in topsoil and in subsoil may be controlled by different regulatory mechanisms. Glob Change Biol 2010;16(1):416–26.
- Sampedro L, Whalen JK. Changes in the fatty acid profiles through the digestive tract of the earthworm Lumbricus terrestris L. Appl Soil Ecol 2007;35(1):226–36.
- Satchell JE. Lumbricidae. In: BURGES A, RAW F, editors. Soil biology; 1967.
- Schulz S, Giebler J, Chatzinotas A, Wick LY, Fetzer I, Welzl G et al. Plant litter and soil type drive abundance, activity and community structure of alkB harbouring microbes in different soil compartments. The ISME Journal 2012;6(9):1763–74.
- Six J, Conant RT, Paul EA, Paustian K. Stabilization mechanisms of soil organic matter: implications for C-saturation of soils. Plant and soil 2002;241(2):155–76.
- Spielvogel S, Prietzel J, Leide J, Riedel M, Zemke J, Kögel-Knabner I. Distribution of cutin and suberin biomarkers under forest trees with different root systems. Plant and soil 2014;381(1):95–110. https://doi.org/10.1007/s11104-014-2103-z.
- Stirzaker RJ, Passioura JB, Wilms Y. Soil structure and plant growth: Impact of bulk density and biopores. Plant Soil 1996;185(1):151–62.
- Street RA, Sidana J, Prinsloo G. Cichorium intybus: Traditional Uses, Phytochemistry, Pharmacology, and Toxicology. Evidence-based complementary and alternative medicine eCAM 2013;2013:579319.
- Stromberger ME, Keith AM, Schmidt O. Distinct microbial and faunal communities and translocated carbon in Lumbricus terrestris drilospheres. Soil Biol Biochem 2012;46:155–62.
- Thevenot M, Dignac M-F, Rumpel C. Fate of lignins in soils: A review. Soil Biol Biochem 2010;42(8):1200–11.
- Větrovský T, Steffen KT, Baldrian P. Potential of cometabolic transformation of polysaccharides and lignin in lignocellulose by soil Actinobacteria. PloS one 2014;9(2):e89108.
- Vetterlein D, Kühn T, Kaiser K, Jahn R. Illite transformation and potassium release upon changes in composition of the rhizophere soil solution. Plant Soil 2013;371(1-2):267–79.
- Vu B, Chen M, Crawford RJ, Ivanova EP. Bacterial Extracellular Polysaccharides Involved in Biofilm Formation. Molecules 2009;14(7):2535–54. http://www.mdpi.com/1420-3049/14/7/2535/pdf.
- Wiesenberg GLB, Schwarzbauer J, Schmidt MWI, Schwark L. Source and turnover of organic matter in agricultural soils derived from n-alkane/n-carboxylic acid compositions and C-isotope signatures. Advances in Organic Geochemistry 2003. Proceedings of the 21st International Meeting on Organic Geochemistry 2004;35(11–12):1371–93.
- Zelles L, Rackwitz R, Bai QY, Beck T, Beese F. Discrimination of microbial diversity by fatty acid profiles of phospholipids and lipopolysaccharides in differently cultivated soils: Springer Netherlands, 1995. http://link.springer.com/content/pdf/10.1007%2F978-94-011-0479-1_9.pdf.
- Zhang X, Amelung W. Gas chromatographic determination of muramic acid, glucosamine, mannosamine, and galactosamine in soils. Soil Biol Biochem 1996;28(9):1201–6.

2.1.7 Supplementary Material

Table S1 Count data of identified substances and their contents [g^{-1} dry matter] in all samples and for the primary plant inputs: shoots and roots of *Cichorium intybus* L., shoots of *Trifolium* repens L., *T. pratense* L. and *Lolium perenne* L. and *L. terrestris* bodies

	Lumbricus terrestris	**Cichorium intybus shoots**	**Cichorium intybus roots**	**Lolium perenne shoots**	**Trifolium pratense shoots**	**Trifolium repens shoots**
# of compounds	142	125	118	122	142	106
# of cutin/suberin-derived lipids	23	17	21	30	33	35
# of lignin-derived phenols	8	8	8	8	8	8
# of n-alkanes	25	26	18	3	14	0
# of neutral and acidic sugars	8	8	8	8	8	0
# of free alcohols/ketones	12	5	8	12	13	10
# of free fatty acids	29	31	27	27	25	33
# of free hydroxy fatty acids	37	30	28	34	41	20
Contents of cutin/suberin-derived lipids	1361	1846	2404	7349	9507	12029
Contents of lignin-derived phenols	3717	3274	42363	12150	6723	7648
Contents of n-alkanes	11301	13868	5250	247	1021	0
Contents of neutral and acidic sugars	21640	84588	64182	52545	130954	0
Contents of free alcohols/ketones	814	478	589	255	254	279
Contents of free fatty acids	135	593	254	155	93	140
Contents of free hydroxy fatty acids	2509	1961	4117	3701	10061	4236

Table S2 Contents ± SEM of lignin-derived phenols [µg g^{-1} soil] and their contribution to SOC ± SEM [mg g^{-1} SOC] in the biopore types and bulk soil. V, S and C represent vanillyl, syringyl and cinnamyl subunits. Letters state significant differences in one soil depth (Capital letters: 45-75 cm; small letters: 75-105 cm; One-way ANOVA with Tukey's HSD post hoc test, α 0.05). Significant differences between two soil depths are shown by asterisks (t test for dependent samples)

	Biomarker contents [µg g^{-1} soil]				**SOC contribution [mg g^{-1} SOC]**			
45-75 cm	**Bulk soil**	**Earthworm pores**	**EW-incubated pores**	**Root pores**	**Bulk soil**	**Earthworm pores**	**EW-incubated pores**	**Root pores**
V	8.0 ± 0.1A	91.1 ± 6.0C	128.2 ± 2.4D	60.3 ± 9.8B	1.9 ± 0.0A	7.8 ± 0.5B	10.8 ± 0.4C	8.8 ± 0.2B
S	13.0 ± 0.5A	84.8 ± 5.3C	119.7 ± 1.3D	60.5 ± 5.4B	3.0 ± 0.1A	7.3 ± 0.5B	9.3 ± 1.0B	7.9 ± 0.7B
C	n.d.	21.8 ± 0.9A	19.6 ± 2.3A	n.d.	n.d.	1.9 ± 0.1A	1.7 ± 0.1A	n.d.
Σ VSC	21.0 ± 0.5A	197.7 ± 12.0C	267.5 ± 2.3D	120.8 ± 13.5B	4.9 ± 0.2A	16.9 ± 1.0B	21.8 ± 1.2C	16.7 ± 0.7B
75-105 cm								
V	6.3 ± 1.2a	82.7 ± 3.2ab	108.7 ± 13.5b	46.9 ± 23.5ab	2.2 ± 0.4a	7.9 ± 0.3ab	10.2 ± 1.2b	8.3 ± 0.9ab
S	6.2 ± 1.5a	83.0 ± 9.1ab	102.1 ± 6.7b	75.9 ± 19.0ab	2.0 ± 0.2a	7.9 ± 0.8ab	9.6 ± 0.8b	8.1 ± 1.5ab
C	n.d.	20.0 ± 3.2a	20.3 ± 1.7a	n.d.	n.d.	1.9 ± 0.3a*	1.9 ± 0.2a	n.d.
Σ VSC	12.5 ± 2.5a	185.8 ± 13.6ab	231.2 ± 18.0b	122.8 ± 19.0ab	4.1 ± 0.2a	17.8 ± 1.2b	21.8 ± 1.8b	13.6 ± 1.8b

Table S3 Contents ± SEM of the neutral sugars [µg g^{-1} soil] and their contribution to SOC ± SEM [mg g^{-1} SOC]. Letters state significant differences in one soil depth (Capital letters: 45-75 cm; small letters: 75-105 cm; One-way ANOVA with Tukey's HSD post hoc test, α 0.05). Significant differences between two soil depths are shown by asterisks (t test for dependent samples)

	Biomarker contents [µg g^{-1} soil]				**SOC contribution [mg g^{-1} SOC]**			
45-75 cm	**Bulk soil**	**Earthworm pores**	**EW-incubated pores**	**Root pores**	**Bulk soil**	**Earthworm pores**	**EW-incubated pores**	**Root pores**
Rhamnose	20 ±	70 ± 5C	71 ± 3C	45 ± 2B	4 ± 0A	6 ± 0A	6 ± 0A	6 ± 0A
Ribose	17 ±	32 ± 5AB	47 ± 2B	24 ±	5 ± 1A	3 ± 1A	4 ± 0A	3 ± 0A
Fucose	10 ±	30 ± 6AB	46 ± 1B	21 ±	2 ± 0A	3 ± 1A	4 ± 0A	3 ± 0A
Arabinose	64 ±	162 ± 4AB	188 ± 3B	95 ±	16 ±	15 ± 0AB	16 ± 0B	12 ± 0A
Xylose	34 ±	176 ± 14AB	269 ± 12B	72 ±	8 ± 0A	17 ± 1AB	22 ± 2B	9 ± 0A
Mannose	53 ±	157 ± 9AB	189 ± 4B	97 ±	12 ±	14 ± 1AB	16 ± 1B	13 ±
Glucose	71 ±	389 ± 23B	401 ± 35B	199 ±	15 ±	35 ± 2B	33 ± 2B	25 ±
Galactose	60 ±	190 ± 6C	213 ± 4D	116 ±	14 ±	17 ± 0AB	18 ± 1B	15 ±
Uronic acids	23 ± 6A	42 ± 5A	37 ± 3A	37 ± 8A	5 ± 2A	4 ± 0A	3 ± 0A	5 ± 1A
Σ Plant pentoses	98 ± 6A	338 ± 16AB	457 ± 9B	167 ± 5AB	23 ± 0AB	32 ± 2AB	38 ± 2B	21 ± 1A
Σ Microbial hexoses	99 ± 9A	289 ± 14AB	353 ± 9B	187 ± 6AB	23 ± 0AB	26 ± 2AB	29 ± 1B	25 ± 1A
Σ Neutral sugars	346 ± 35A	1249 ± 13AB	1461 ± 34B	706 ± 27AB	74 ± 3A	107 ± 2AB	116 ± 5B	85 ± 3AB
75-105 cm								
Rhamnose	13 ±	66 ± 4c	70 ± 2c	48 ± 3b	4 ± 1a	6 ± 1a	7 ± 0a	5 ± 0a
Ribose	13 ±	25 ± 2a	48 ± 0a	23 ± 2a	4 ± 0b	2 ± 0a	5 ± 0b	2 ± 0a
Fucose	8 ±	21 ± 1a	50 ± 1a	21 ± 2a	3 ± 0a	2 ± 0a	5 ± 0b	2 ± 0a
Arabinose	49 ±	135 ± 8a	165 ± 8a	96 ± 4a	16 ±	12 ± 1ab	16 ± 1bc	10 ± 1a
Xylose	26 ±	145 ± 15a	217 ± 14a	74 ± 4a	9 ± 1a	13 ± 2a*	20 ± 1b	8 ± 0a
Mannose	40 ±	131 ± 8b	173 ± 8c	108 ±	13 ±	12 ± 1a	16 ± 1a	12 ± 0a
Glucose	54 ±	341 ± 10c	319 ±	227 ±	18 ±	31 ± 2b	30 ± 2b	24 ±
Galactose	47 ±	167 ± 11c	191 ± 8d	131 ±	16 ±	15 ± 1a	18 ± 1a	14 ± 1a
Uronic acids	15 ± 2a	33 ± 2a	33 ± 4a	32 ± 5a	5 ± 1a	3 ± 0a	3 ± 0a	4 ± 1a
Σ Plant pentoses	76 ± 1a	281 ± 23a	383 ± 22b	170 ± 7a	25 ± 1a	25 ± 3a*	36 ± 2b	18 ± 1a
Σ Microbial hexoses	74 ± 3a	243 ± 15ab	341 ± 11b	200 ± 11a	24 ± 2a	22 ± 2a	32 ± 2b	22 ± 1a
Σ Neutral sugars	267 ± 10a	1065 ± 59a	1266 ± 63a*	759 ± 37a	83 ± 6ab	89 ± 8ab	113 ± 7b	77 ± 3a

Table S4 Contents ± SEM of the amino sugars [µg g^{-1} soil] and their contribution to SOC ± SEM [mg g^{-1} SOC]. Letters state significant differences in one soil depth (Capital letters: 45-75 cm; small letters: 75-105 cm; One-way ANOVA with Tukey's HSD post hoc test, α 0.05). Significant differences between two soil depths are shown by asterisks (t test for dependent samples)

	Biomarker contents [µg g^{-1} soil]				**SOC contribution [mg g^{-1} SOC]**			
45-75 cm	**Bulk soil**	**Earthworm pores**	**EW-incubated pores**	**Root pores**	**Bulk soil**	**Earthworm pores**	**EW-incubated pores**	**Root pores**
Glucosamine	544 ± 133A	1308 ± 296A	729 ± 57A	437 ± 138A	135 ± 32A	109 ± 22A	65 ± 5A	54 ± 16A
Mannosamine	3 ± 1A	26 ± 2B	23 ± 4B	18 ± 2B	1 ± 0A	2 ± 0B	2 ± 0B	2 ± 0B
Muramic acid	13 ± 2A	22 ± 8A	15 ± 4A	9 ± 4A	3 ± 0A	2 ± 1A	1 ± 0A	1 ± 0A
Galactosamine	203 ± 32A	583 ± 167A	306 ± 34A	225 ± 43A	50 ± 7A	48 ± 12A	27 ± 3A	28 ± 4A
Σ Amino sugars	762 ± 164A	1933 ± 464A	1073 ± 84A	689 ± 176A	188 ± 39A	161 ± 34A	95 ± 7A	85 ± 20A
75-105 cm								
Glucosamine	606 ± 56a	1230 ± 195a	1010 ± 77a*	1600 ± 340a	184 ± 34a	118 ± 19a	103 ± 6a*	178 ± 45a
Mannosamine	1 ± 0a	28 ± 9a	17 ± 6a	42 ± 13a	0 ± oka	3 ± 1a	2 ± 0a	4 ± 1a
Muramic acid	23 ± 5a	25 ± 5a	23 ± 5a	44 ± 21a	7 ± 2a	2 ± 0a	2 ± 1a	5 ± 3a
Galactosamine	209 ± 30b	605 ± 98ab	477 ± 5ab*	776 ± 177b	63 ± 14a	58 ± 9a	49 ± 2a*	87 ± 24a
Σ Amino sugars	838 ± 85a	1875 ± 296ab	1527 ± 81ab*	2451 ± 529b	255 ± 49a	179 ± 28a	157 ± 7a*	273 ± 71a

Table S5 Contents ± SEM of the free lipid fractions n-alkanes, ketones/n-alkanols, fatty acids and hydroxy fatty acids [µg g^{-1} soil] and their contribution to SOC ± SEM [mg g^{-1} SOC]. Letters state significant differences in one soil depth (Capital letters: 45-75 cm; small letters: 75-105 cm; One-way ANOVA with Tukey's HSD post hoc test, α 0.05). Significant differences between two soil depths are shown by asterisks (t test for dependent samples)

	Biomarker contents [µg g^{-1} soil]				**SOC contribution [mg g^{-1} SOC]**			
45-75 cm	**Bulk soil**	**Earthworm pores**	**EW-incubated pores**	**Root pores**	**Bulk soil**	**Earthworm pores**	**EW-incubated pores**	**Root pores**
Σ n-alkanes	118 ± 19A	412 ± 99A	407 ± 87A	203 ± 46A	35 ± 7A	35 ± 7A	35 ± 6A	25 ± 5A
incl. n-alkanes > C26	63 ± 8A	258 ± 63A	307 ± 69A	113 ± 25A	18 ± 4A	22 ± 5A	26 ± 5A	14 ± 3A
Σ n-alkenes	86 ± 7A	162 ± 48A	209 ± 43A	186 ± 39A	20 ± 2A	14 ± 4A	18 ± 3A	23 ± 5A
Σ ketones / alcohols	6 ± 0A	13 ± 2AB	15 ± 2B	10 ± 1AB	2 ± 0A	1 ± 0A	1 ± 0A	1 ± 0A
Σ fatty acids	1 ± 0A	6 ± 1A	8 ± 1A	4 ± 1A	0 ± 0A	1 ± 0A	1 ± 0A	0 ± 0A
Σ hydroxy fatty acids	15 ± 1A	31 ± 15A	19 ± 4A	27 ± 10A	4 ± 0A	3 ± 1A	2 ± 0A	3 ± 1A
Σ Free lipids	227 ± 11A	624 ± 158A	658 ± 125A	429 ± 79A	56 ± 3A	54 ± 14A	56 ± 9A	53 ± 10A
75-105 cm								
Σ n-alkanes	156 ± 13a*	287 ± 28a	330 ± 63a*	219 ± 47a	45 ± 5a*	27 ± 3a	31 ± 5a*	25 ± 9a
incl. n-alkanes > C26	84 ± 8a	163 ± 13a	199 ± 35a	112 ± 22a	24 ± 3a	15 ± 1a	18 ± 3a	13 ± 4a
Σ n-alkenes	70 ± 1a*	113 ± 15a	119 ± 26a	92 ± 26a	20 ± 3a	10 ± 1a	11 ± 2a*	11 ± 4a
Σ ketones / alcohols	7 ± 0a*	10 ± 1a	12 ± 2a	9 ± 3a	2 ± 0a	1 ± 0a	1 ± 0a	1 ± 1a
Σ fatty acids	2 ± 1a	4 ± 2a	7 ± 2a	6 ± 2a	1 ± 0a	0 ± 0a	1 ± 0a	1 ± 0a
Σ hydroxy fatty acids	20 ± 4a	35 ± 14a	45 ± 26a	44 ± 17a	6 ± 2a	3 ± 1a	4 ± 2a	5 ± 2a
Σ Free lipids	255 ± 10a*	449 ± 52a	514 ± 111a*	371 ± 86a	74 ± 10a	41 ± 5a	47 ± 8a*	43 ± 15a

Table S6 Contents ± SEM of the cutin and suberin-derived lipids [µg g^{-1} soil] and their contribution to SOC ± SEM [mg g^{-1} SOC]. C, CS, S and M represent cutin-, cutin or suberin-, suberin-, or, microbial-derived lipids as determined after characterisation of plant inputs. Letters state significant differences in one soil depth (Capital letters: 45-75 cm; small letters: 75-105 cm; One-way ANOVA with Tukey's HSD post hoc test, α 0.05). Significant differences between two soil depths are shown by asterisks (t test for dependent samples)

	Biomarker contents [µg g^{-1} soil]				**SOC contribution [mg g^{-1} SOC]**			
45-75 cm	**Bulk soil**	**Earthworm pores**	**EW-incubated pores**	**Root pores**	**Bulk soil**	**Earthworm pores**	**EW-incubated pores**	**Root pores**
C	0.6 ± 0.2A	5.2 ± 0.7C	4.7 ± 0.3BC	2.4 ± 0.2AB	0.1 ± 0.1A	0.4 ± 0.0B	0.4 ± 0.0AB	0.3 ± 0.0AB
S	n.d.	7.3 ± 0.7B	5.7 ± 0.1AB	4.2 ± 0.2A	0.0 ± 0.0	0.6 ± 0.1A	0.5 ± 0.0A	0.5 ± 0.0A
CS	3.3 ± 0.6A	18.2 ± 1.2D	6.9 ± 0.0B	11.1 ± 2.0C	0.8 ± 0.2A	1.6 ± 0.1A	0.6 ± 0.0A	1.2 ± 0.3A
M	0.4 ± 0.2A	7.2 ± 0.7B	4.4 ± 0.1AB	3.6 ± 0.6AB	0.1 ± 0.0A	0.6 ± 0.1B	0.4 ± 0.0AB	0.4 ± 0.1AB
Σ Cutin/suberin	4.4 ± 0.7A	37.9 ± 1.3C	21.7 ± 0.6B	21.4 ± 2.0B	1.1 ± 0.2A	3.3 ± 0.1C	1.8 ± 0.1AB	2.5 ± 0.2BC
75-105 cm								
C	0.1 ± 0.1a	3.0 ± 0.4a*	3.5 ± 1.1a*	1.3 ± 0.3a	0.0 ± 0.0a	0.3 ± 0.0a	0.3 ± 0.1a	0.1 ± 0.0a
S	0.4 ± 0.0a	3.8 ± 0.3a	4.2 ± 1.2a	3.5 ± 1.1a	0.1 ± 0.0a	0.4 ± 0.0a	0.4 ± 0.1a	0.4 ± 0.1a
CS	1.3 ± 0.2a*	5.4 ± 0.7a*	6.2 ± 1.1a	4.5 ± 0.8a*	0.4 ± 0.1a	0.5 ± 0.1a*	0.6 ± 0.1a	0.5 ± 0.1a*
M	0.1 ± 0.0a	2.7 ± 0.5a	4.0 ± 1.0a	2.6 ± 0.7a*	0.0 ± 0.0a	0.3 ± 0.1a	0.4 ± 0.1a	0.3 ± 0.1a*
Σ Cutin/suberin	1.7 ± 0.4a*	14.8 ± 1.6b*	17.9 ± 4.3b	11.8 ± 2.6ab	0.6 ± 0.1a*	1.4 ± 0.2a*	1.7 ± 0.4a	1.3 ± 0.3a

Table S7 Full dataset of the biopore contents [µg g^{-1} soil]

All compounds, only uploaded as Excel spreadsheet (200 x 32 data points)

See CD attached

2.2 Study 2: Microbial processing of plant residues in the subsoil – The role of biopores

Authors and affiliations

Callum C. Banfield[1,*], Johanna Pausch[2], Yakov Kuzyakov[3], Michaela A. Dippold[1]

[1]University of Goettingen, Biogeochemistry of Agricultural Ecosystems, Buesgenweg 2, Goettingen, 37077, Germany.
[2]University of Bayreuth, Agroecology, Universitätsstrasse 30, 95440 Bayreuth.
[3]University of Goettingen, Department of Soil Science of Temperate Ecosystems, Department of Agricultural Soil Science, Buesgenweg 2, 37077 Goettingen, Germany.

*__Corresponding author:__ callumba@gmail.com
Telephone: +49 1578 4527077
Fax: +49 551 3933310

Role of the funding source: DFG KU 1184/29-1

Conflicts of interest: The authors declare no conflict of interest.

Keywords: detritusphere; drilosphere; earthworm tagging; source partitioning

Highlights

- Subsoil C turnover in hotspots was evaluated using biomarkers as proxies
- The hotspot type (earthworm *vs* root biopores) governs OM processing
- Degree of OM processing highest in bulk subsoil, lower in biopores
- Stronger processing of hemicelluloses than of lignin in biopores
- Short-term anecic earthworm activities effectively renew biopore OM

Abstract

Most subsoil carbon (C) turnover occurs in biopore hotspots such as root channels and earthworm burrows. Biopores allocate large C amounts into the subsoil, where a vast capacity for long-term C sequestration is predicted. We hypothesise that organic matter (OM) cycling in biopores depends on their origin.

Earthworm and root biopores were induced under field conditions and were sampled from the subsoil (45–75 and 75–105 cm) after two years of biopore formation. The effects of biopore formation on OM decomposition were studied by biomarkers: neutral sugars, cutin and suberin-derived lipids, lignin-derived phenols and free lipids. The degradation stage of OM was biopore type-specific but was only governed by the soil depth in root biopores. Degradation of OM increased from earthworm biopores to root biopores and bulk soil. Hemicelluloses (GM/AX ratio) were more strongly degraded than lignin side-chains (relative change from initial values). Two years of microbial processing during biopore formation increased the GM/AX ratio in earthworm biopores from 0.65 to 1.05 and in root biopores from 0.15 to 1.35 (both relative to source biomasses). Root biopores and bulk soil had the highest GM/AX ratios (1.2 – 1.3), hinting to rapid processing of plant residues and accumulation of microbial residues. The regular, frequent OM inputs by earthworms stimulated microbial growth and processing of mostly bioavailable OM and, thus, relatively enriched more persistent OM (e.g. lignin). Syringyl subunits of lignin underwent low (ratio changed from 0.35 to 0.55 relative to initial input) and vanillyl subunits underwent almost no processing in earthworm biopores indicating the preferential microbial utilisation of the easily available compounds frequently replenished by earthworm activity. After two years of decomposition of the root detritus, mainly structural plant material was enriched in root biopores. Short periods (6 months) of earthworm activity effectively recharged the highly processed OM in root biopores with fresh OM.

In total, deep-rooting catch crops and short-term earthworm activities promote C accumulation in the subsoil followed by biopore-specific microbial processing predominantly governed by the C input frequency. As root biopores are up to 40 times more common than earthworm biopores, they dominate the OM input into subsoils. Such C inputs create several years lasting hotspots for preferential root growth and nutrient mobilisation in the subsoil. We conclude that root- and earthworm-derived biopores are vertical pathways for plant C from the soil surface into the subsoil and for intensive processing of litter C and sequestration of microbial necromass.

2.2.1 Introduction

Steadily increasing carbon (C) dioxide concentrations in the atmosphere are driving global climate change (IPCC, 2014). Its prominent projected consequences such as rising global mean temperatures and more variable precipitation (Li et al., 2009; Pal et al., 2004) are deemed unfavourable by society and therefore are to be mitigated (Tompkins et al., 2010; Urry, 2015). Sequestering carbon dioxide from the atmosphere in soils is being discussed as a viable option for reducing carbon dioxide concentrations (Lal et al., 2015; Poeplau and Don, 2015). Soils are the largest pool in the terrestrial C cycle (Scharlemann et al., 2014; Schimel, 1995) and are comparatively easy to manage in comparison to geological or marine pools. This holds particularly true for croplands as they are under management. Usually, mostly the topsoils are considered for plant nutrition in arable fields as the main C cycling and nutrient pools are found in the top part of the soil (Kautz et al., 2013). Recently, the subsoils, i.e. the soil below the ploughed horizon, have been pushed into the centre of attention of soil science. Subsoils have the capacity of storing large amounts of C when their mineral phases (clay, iron oxides) are not saturated (Kell, 2012). The large land cover of cropland (FAOSTAT, 2017), their manageability and the potential C storage capacity of subsoils make them attractive as long-term C sinks (Dignac et al., 2017; Torres-Sallan et al., 2017). However, for successful C sequestration, the dynamics of C in subsoils need to be better understood first.

Carbon reaches the subsoil predominantly through leaching as dissolved organic carbon (Kalbitz and Kaiser, 2008; Kindler et al., 2011). It involves potentially strong microbial modifications to the leached C compounds (e.g. respiration) and depends on the water solubility of the allocated compounds (Kaiser and Kalbitz, 2012). Large amounts of C may be also brought into the subsoils by roots or soil fauna such as earthworms, i.e. in biopores (Kautz, 2015; Stirzaker et al., 1996). Compared to leaching, organic matter (OM) ends up faster in the subsoil (Munyankusi et al., 1994), but in defined vertical macropores. They feature not just elevated C stocks, but also strong and intense microbial activity relative to the non-biopore bulk soil (Hoang et al., (2016). Hence, they are considered as hotspots, i.e. small soil volumes with much higher microbial processing rates than the average soil conditions (Kuzyakov and Blagodatskaya, 2015). The bulk subsoil is characterised by low C stocks, high radiocarbon age and slow microbial cycling (Rumpel et al., 2002; Rumpel and Kögel-Knabner, 2011). Biopores could contribute to higher C stocks in the subsoil because with higher C inputs, more C may remain stabilised as soil organic matter (SOM). Conversely, more easily available C may cause priming of older, potentially stabilised SOM, which would cause a loss of C (Fontaine et al., 2007; Kuzyakov, 2010). Studies on microbial communities and their residues in biopores have hinted to different functions of biopores, i.e. nutrient cycling *vs*. C sequestration – depending on their genesis, i.e. root vs earthworm-derived biopores (Banfield et al., 2017). C stabilisation may vary mechanistically among different hotspot types. Earthworms may change the texture of the soil in their burrows through selective feeding (Zhang and Schrader, 1993) and OM is strongly physically and chemically modified during the gut passage (Cheshire and Griffiths, 1989; Thakuria et al., 2010). Depending on the biopore-specific C inputs, the resulting microbial necromass may further contribute to long-term C sequestration (Miltner et al., 2012; Six et al., 2006). If C turnover depends on the biopore type, this will have consequences for the total subsoil C turnover, which mainly takes place in hotspots (Kuzyakov and Blagodatskaya, 2015).

The chemical composition of OM, its sources and degradation can be assessed by biomarkers (Amelung et al., 2008; Simoneit, 2005). Biomarkers are organic molecules whose detection indicates presence of an organism, tissue, secreted metabolites or their past presence. For instance, root influence is reflected by the contents of mid-chain *ω*-hydroxy alkanoic acids and lignin-derived phenols (Armas-Herrera et al., 2016; Spielvogel et al., 2008; Thevenot et al., 2010). The degradation stage of the OM is assessed by biomarker ratios, e.g. contents of oxidised / reduced lignin-derived phenols (Thevenot et al., 2010). Ideally, undecomposed source biomasses (e.g. crop shoots as earthworm food) are collected before the experiment and characterised for their biomarker composition together with the soil samples (Gunina and Kuzyakov, 2015). The change of the biomarker pattern of the undecomposed source biomass to the biomarker pattern in soil can be related to the experiment duration, herein termed ‘microbial processing’.

To better understand C dynamics in hotspots and their relevance for subsoil C turnover, we conducted a biomarker study to link the biopore type and soil depth with C processing. Biomarker ratios known to characterise the degradation state of plant residues were used to reconstruct microbial processing by relating them to microbial biomarkers. In a field experiment over five years, three biopore types were induced by either I) growing tap-rooted chicory (*Cichorium intybus* L.) for three years followed by two years of fallow (root biopores), II) at least ≥ 3 years of earthworm activities (native earthworm biopores) or III) 6 months of earthworm incubation into root biopores (earthworm-incubated biopores). We sampled the material on the inner walls of the biopores and analysed it for lignin-derived phenols, cutin and suberin-derived biomarkers, neutral sugars and free lipids. Proxies describing the processing of plant residues were calculated from these data and compared among the biopore types.

2.2.2 Material and methods

2.2.2.1 Sampling

The study was conducted on the Campus Klein-Altendorf experimental research station near Bonn, Germany. The location had a mean annual temperature of 9.6 °C, a mean annual precipitation of 625 mm and featured a Haplic Luvisol (Hypereutric, Siltic; (IUSS Working Group WRB, 2008). A characterisation of the soil and its genetic horizons was given in Vetterlein et al. (2013). The experimental set-up was previously described in Banfield et al. (2017). In short, three biopore types were induced in the field and studied in two subsoil depths (45-75 cm; 75-105 cm), namely root biopores, native earthworm biopores and a combination of both: earthworm-incubated biopores (Fig. S1, Supplementary Material). Each treatment combination was replicated four times in different locations of the same agricultural field.

1) *Root biopores:* from 2009 to 2012 chicory (*Cichorium intybus* L., var. Puna) was grown to induce taproots of at least 4 mm diameter in the subsoil. In 2012, the topsoil (0-45 cm) was temporarily removed and live roots were mapped in 45 cm depth. After filling the disturbed topsoil back, the plots were kept fallow and did not receive any clover-grass. Roots had two years to decay until sampling in autumn 2014.
2) *Earthworm-incubated biopores*: after 1.5 years of root decomposition, earthworms (*Lumbricus terrestris* L.), a native earthworm species in Central Europe, were inserted into a subset of at least 25 root biopores per field replicate for six months. In spring 2012, the topsoil (0-45 cm) was temporarily removed, and earthworms were incubated into previously identified and mapped 1.5-year-old root pores. Prior to incubation, an elastomer tag was injected into each earthworm body to allow re-discovery of the earthworms (Butt and Lowe, 2007). Earthworms were fed with clover-grass (shoots of *Trifolium repens* L., *T. pratense* L. and *Lolium perenne* L.) put on the soil surface until four weeks prior to sampling.
3) *Native earthworm biopores* (colonised with predominately *L. terrestris*) were treated similarly to the earthworm-incubated biopores: plots were kept fallow from 2012 on and grass-clover material was placed on the soil surface as food. Native earthworm biopores were identified at the end of the experiment in September 2014 as follows: after removing the topsoil, a new soil surface was prepared in -45 cm and covered with litter for three days. Biopores with visible earthworm middens were considered colonised with earthworms.

4) *Bulk soil* samples, i.e. soil not containing any macroscopic biopores, were taken from areas next to the biopore plots. These plots were kept fallow and did not receive any clover grass amendment.

In September 2014, after removing the topsoil down to -45 cm, soil around each identified biopore was manually removed first down to -75 cm, then to -105 cm. The biopores were opened vertically and the inner wall coating was sampled by shaving it off with micro spatulas once, i.e. approximately 1 mm (Andriuzzi et al., 2013). Thirty-two samples were taken: four field replicates were taken from each treatment (three biopore types + bulk soil) and from two subsoil depths (45–75 cm; 75–105 cm). Each sample was pooled from about 25 biopores.

2.2.2.2 Biomarker analyses

Contents of *neutral sugars* from hemicelluloses and microbial polysaccharides were determined after 4 M trifluoroacetic acid hydrolysis of 500 mg dried soil, followed by sample clean-up on DOWEX 50W X8 exchange resin and derivatization to aldononitrile acetates after Zhang and Amelung (1996). *Lignin-derived phenols* were determined after alkaline CuO oxidation, sample purification (precipitation of humic acids and C18 solid phase extraction columns, SPE), derivatisation of the lignin-derived phenols to trimethylsilylates by N,O-Bis(trimethylsilyl)trifluoroacetamide. To separate *bound* and *free lipids*, 3 g of dried and ground soil were extracted in a Soxhlet apparatus for 36 h in a 2:1 (v:v) mixture of dichloromethane and methanol. The extracted soil was used for cutin/suberin analyses, while the solvent extract was used for the free lipid analysis. The extracted soil was hydrolysed in methanolic KOH to cleave monomers off the bound lipids *cutin and suberin*, cleaned up by liquid-liquid extraction at pH 1 and finally derivatized in two steps (methylation by BF_3: MeOH, 1.3.M, and acetylation by acetic anhydride: pyridine). The *free lipids* consisted of the free *n*-alkanes, *n*-alkenes, *n*-alkanols + alkanones, *n*-alkanoic acids, *α,ω*-alkanedioic acids and *ω*-hydroxy alkanoic acids. Liquid-liquid extraction at two pH values separated the acidic from the neutral fraction, while silica gel SPE separated the substance classes. Carboxylic groups were methylated (cf. above), while hydroxyl groups were acetylated (cf. above). All analyses included internal standards to correct for analyte loss during preparation and for autosampler injection volume. Five to seven volumes of external standard solutions were derivatized with the samples of each biomarker approach and the regressions of the resulting peak areas and the concentrations of standards were used for analyte quantification. The samples were measured by gas chromatography on Agilent 7820A or 7890A GCs fitted with DB-5MS (lipids) or OV-17 (carbohydrates) columns coupled to mass selective detectors (Agilent 7000A) or flame ionisation detectors (all Agilent Technologies, Waldbronn, Germany). Full details about oven programmes, GC and

MS parameters can be found in the Table S1 (Supplementary Material). The following proxies were calculated (Table 1):

- The ratio of microbial sugars to plant-derived sugars ∑ (galactose + mannose) / ∑ (arabinose + xylose), in short: GM/AX, is a general proxy for the decomposition of plant material (Oades, 1984). With processing the proportion of plant-derived sugars decreases, whereas the proportion of microbial sugars successively increases.
- A source-adapted ratio of ∑ (mannose + ribose + fucose) / ∑ (arabinose + xylose), in short MRF/AX, was calculated after characterisation of the source biomasses. Into the biopores, e.g. root residues of chicory or shoot litter of clover grass was introduced. The source biomasses were analysed like the samples to receive their 'undecomposed' biomarker pattern. Substances were only used as plant biomarkers if they were identified in substantial amounts (> 10% of ∑) in the plant source biomasses such as chicory roots or clover shoots (Gunina and Kuzyakov, 2015; Moers et al., 1990; Oades, 1984; Rumpel et al., 2010). Hexoses were assumed to be microbial markers only if they were known in the literature (Tanaka et al., 1990) and if they were absent in the source biomasses (Gunina and Kuzyakov, 2015).
- The ratios of the lignin-derived syringyl/vanillyl phenols (S/V) or cinnamyl/vanillyl phenols (Ci/V) describe the lignin decomposition since syringyl and cinnamyl subunits are preferentially decomposed (Thevenot et al., 2010).
- The ratio of the acidic phenol to the aldehyde phenol for each lignin-derived subunit, e.g. (Ac/Al)v for the vanillyl phenols, is a proxy for the side chain oxidation state of the lignin macromolecule (Thevenot et al., 2010).
- The ratio of ∑ free / ∑ bound (ω-hydroxy alkanoic acids + α,ω-alkanedioic acids), i.e. solvent extractable suberin-derived molecules, describes the breakdown of polymeric plant tissues (mostly root suberin), which are the quantitatively most relevant source for free hydroxy alkanoic acids ≥ C16 (Armas-Herrera et al., 2016; Bull et al., 2000; Kolattukudy, 1984), i.e. depolymerisation products (Naafs and van Bergen, 2002). Albeit minor sources include oxidative degradation of free alkanoic acids (Quenea et al., 2004), relating the contents of free to suberin-derived ω-hydroxy alkanoic acids was suggested to be a biomarker for suberin degradation (Otto and Simpson, 2007).
- Analogous to the above, the ratio of ∑ free / ∑ bound saturated alkanoic acids was calculated as a potentially meaningful proxy for the cleavage of suberin. Longer alkanoic acids (≥ C20) were suggested to be mainly derived from suberins (Bull et al., 2000; Kolattukudy, 1980; Naafs and van Bergen, 2002; Vidal et al., 2016).

- The ratio of ∑ *n*-alkenes / ∑ *n*-alkanes ≥ C26 (both odd and even chain length) was calculated as a proxy for the microbial processing of cuticles and root tissues (Amblès et al., 1994; Vidal et al., 2016) (Naafs and van Bergen, 2002). Long-chain *n*-alkanes derive from plant waxes (Lichtfouse, 1997; Wiesenberg et al., 2004), while *n*-alkenes are microbial products (Amblès et al., 1994; Lichtfouse et al., 1998).
- The C/N ratio and bulk isotopic composition ($\delta^{13}C$) are broad proxies for SOM processing (Balesdent et al., 1987).

These proxies needed to be related to the intact source biomasses since prior to decomposition the source biomasses already differ in their proxy values (Table S2, Supplementary material). We characterised the biomasses of *L. terrestris* bodies, *C. intybus* shoots, *C. intybus* roots, *Lolium perenne* shoots, *Trifolium pratense* shoots and *T. repens* shoots. Data on the bulk isotopic composition ($\delta^{13}C$), as well as C and nitrogen (N) contents of the same treatments, were taken from Banfield et al. (2017).

Table 1 Overview of the biomarker proxies used to evaluate the microbial processing and degradation of plant inputs in biopores

Biomarker	**Abbreviation**	**Description**	**References**
∑(galactose + mannose) / ∑(arabinose + xylose)	GM/AX	Processing of plant-derived hemicelluloses	(Gunina and Kuzyakov, 2015; Moers et al., 1990; Oades, 1984; Rumpel et al., 2010)
∑(mannose + ribose + fucose) / ∑(arabinose + xylose)	MRF/AX	Processing of plant-derived hemicelluloses, source-adapted	Source adaption (Gunina and Kuzyakov, 2015)
Ratio of syringyl / vanillyl lignin phenols	S/V	Processing of lignin-derived phenols (subunit-specific)	(Rasse et al., 2006; Thevenot et al., 2010)
Ratio of cinnamyl / vannilyl lignin phenols			
Ratio of acidic / aldehyde phenol for each lignin subunit	(Ac/Al)v (vanillyl); (Ac/Al)s (syringyl)	Oxidative degradation state of lignin-derived phenols	(Rasse et al., 2006; Thevenot et al., 2010)
Ratio of ∑ free / ∑ (bound ω-hydroxy alkanoic acids (C16-C24) + α,ω-alkanedioic acids (C16-C26))	HO-AA	Processing of suberin and root lipids	(Ertel and Hedges, 1984; Hedges and Ertel, 1982; Thevenot et al., 2010)
Ratio of ∑ free / ∑ bound n-alkanoic acids (C20-C30)	AA	Processing of suberin and root lipids	(Bull et al., 2000; Vidal et al., 2016)
∑ n-alkenes (≥C14) / ∑ n-alkanes (≥C26)	APR (alkene/ precursor ratio)	Processing of epicuticular waxes (≥C26) to n-alkenes (≥C14)	(Kolattukudy, 1980; Naafs and van Bergen, 2002)

These proxies needed to be related to the intact source biomasses since prior to decomposition the source biomasses already differ in their proxy values (Table S2, Supplementary material). We characterised the biomasses of *L. terrestris* bodies, *C. intybus* shoots, *C. intybus* roots, *Lolium perenne* shoots, *Trifolium pratense* shoots and *T. repens* shoots. Data on the bulk isotopic composition ($\delta^{13}C$), as well as C and nitrogen (N) contents of the same treatments, were taken from Banfield et al. (2017a).

2.2.2.3 Statistical evaluation

Each dataset containing the proxy values was screened for outliers by Nalimov's test and maximum one outlier per treatment combination and proxy was removed. A principal component analysis (PCA) based on correlations was performed on the combined dataset of all proxies. For the treatments, factor coordinates were calculated from the two principal components with the highest eigenvalues. Likewise, for the variables (biomarker ratios), a correlation circle was calculated. The MRF/AX ratio was excluded due to collinearity with the GM/AX ratio. The grouping variable was the treatment (three biopore types and bulk soil). Data given in the tables and figures are mean values ± standard errors. Significant differences of means among biopore types were tested by one-way analyses of variance (ANOVA) for each depth separately since the two soil depths provide paired samples. Levene's test was used to test for homogenous variances. Normality of the residues was checked in Q-Q plots. Post-hoc comparisons were by Tukey's Honest Significant Differences Test. If assumptions were not met, non-parametric ANOVA (Kruskal-Wallis ANOVA) including post-hoc comparisons of mean ranks were used instead. Pairwise two-sample t-tests for dependent samples were used to determine differences between soil depths for each biopore type and proxy. All statistical analyses were performed in Statistica 13.2 (StatSoft Inc., Tulsa, OK, U.S.A.).

2.2.3 Results

The PCA calculated from seven variables explained 51% of the total variance (Fig. 2). All variables, i.e. biomarker proxies, were positively correlated with the principal component (PC) 1 (x-axis, Fig. 2, right). The GM/AX and (Ac/Al)v ratios were most strongly correlated with PC 1, which separated the earthworm biopores from root biopores and bulk soil (Fig. 2, left). Both earthworm biopore types showed little in-group variance and were overlapping. Earthworm incubation for six months obscured the former root presence by incorporation of fresh material. Bulk soil and root biopores showed much higher in-group variance along PC 2, which separated root biopore samples from to -45–75 cm and form of -75–105 cm. The effect of the soil depth was most strongly represented by the lignin biomarkers (S/V, (Ac/Al)s, (Ac/Al)v ratios; Fig. 2, right). Long-term and short-term earthworm activities in the earthworm biopores obscured any soil depth effect. The other proxies were equally correlated with both principal components. As the Ci/V ratio correlated only weakly with either axis, it was only included in the supplementary material (Fig. S2).

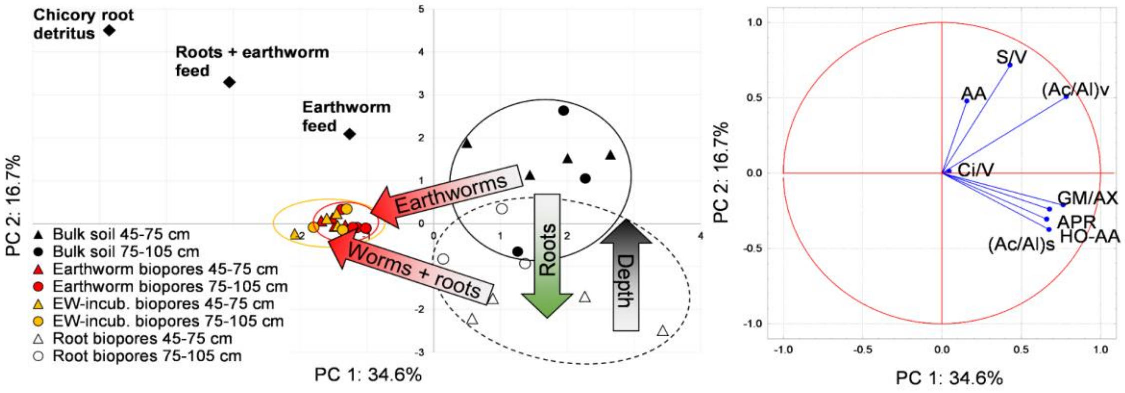

Fig. 1 ***Left:*** *Principal component analysis of seven proxies describing the degree of processing: GM/AX, Ac/Al for S and V subunits, S/V and Ci/V ratios; free/bound ω-hydroxy alkanoic acids or alkanoic acids ratios, as well as the n-alkene / n-alkanes ratio. Source biomasses were added as supplementary data (black diamonds): earthworm feed, chicory root detritus and a combination of both. Different colours represent the four treatments (bulk soil vs native vs earthworm (EW)-incubated biopores vs root biopores). Triangles represent samples from 45–75 cm, while circles are samples from 75–105 cm. Ellipses show the within-group variance. PC 1 and 2 explained 35% and 17% of the inertia, respectively. The arrows illustrate the effects of earthworms (corresponding to PC 1, i.e. x-axis), soil depth (mainly corresponding to PC 2, i.e. y-axis), earthworm incubation and tap roots.* ***Right:*** *Correlation circle describing the correlation between biomarker ratios and the two PC.*

2.2.3.1 Neutral sugar ratios

The sugar ratios values did not differentiate the biopores types from the bulk soil in 45–75 cm but in 75–105 cm (Fig. 2). Earthworms decreased the degradation stage of the hemicelluloses in the deeper subsoil (relative to bulk soil, i.e. ‘earthworm effect’ illustrated exemplarily in Fig. 2), while after two years of root decay in the root biopores the hemicelluloses were as degraded as in bulk soil. Relative to the source biomasses, native earthworm activity increased the GM/AX ratio from 0.65 (clover grass) to 1.0, while short-term earthworm incubation in root biopores increased it from 0.42 (50% clover grass + 50% roots) to 0.95. So, the means of the earthworm biopores were close to the source biomasses, suggesting that polysaccharides in earthworm biopores had undergone the least microbial processing among the biopores. In comparison, the GM/AX ratio after two years decomposition was 1.3 in root biopores, while the undecomposed root necromass had a GM/AX ratio of 0.2, which underlines the strong processing of polysaccharides compared to the earthworm biopores. The high GM/AX ratio of bulk soil reflected the long-term turnover. Equivalent results were found for the MRF/AX ratio.

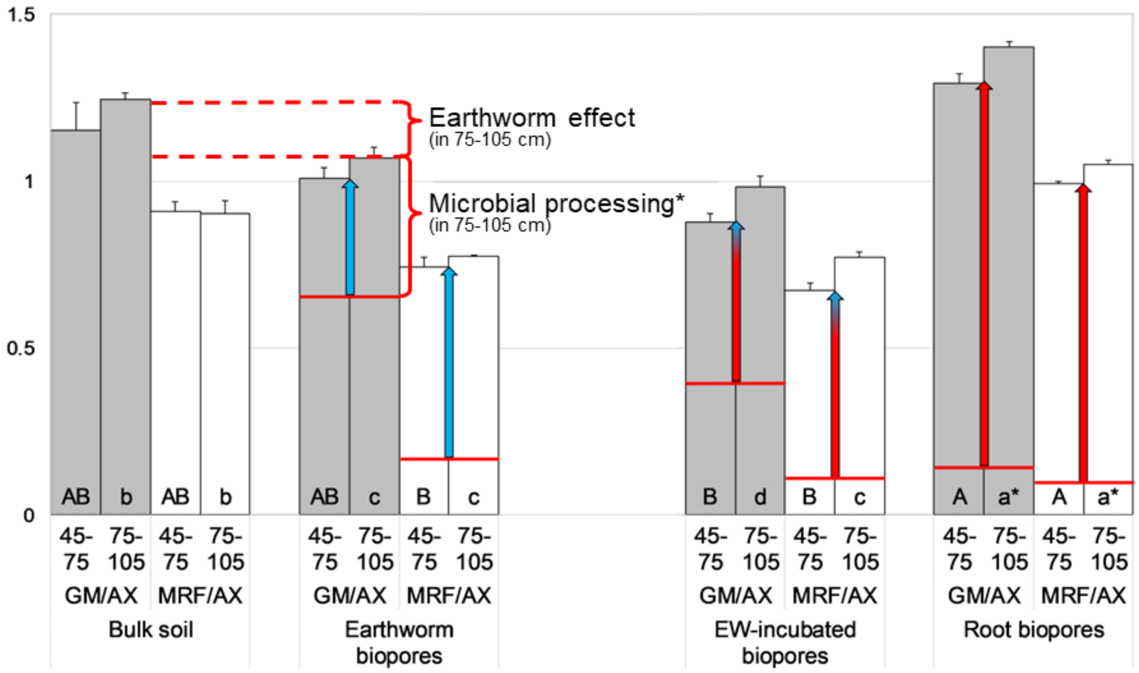

Fig. 2 *Proxies for hemicelluloses: the GM/AX ratio ∑ (galactose + mannose) / ∑ (arabinose + xylose) as grey bars and the source-adapted MRF/AX ratio as white bars ∑ (mannose + ribose + fucose) / ∑ (arabinose + xylose). Shown are means ± standard errors of all four treatments. Capital letters indicate significant differences for 45–75 cm (one-way ANOVA, Tukey's HSD test on α 0.05), whereas small letters indicate significant differences for 75–105 cm. Asterisks indicate significant differences of a variable between both soil depths according to t-test for dependent samples. Red lines indicate the values of the source biomasses, i.e. plant litter or residue inputs prior to decomposition (earthworm biopores: clover grass only; EW-incubated biopores: 50% clover grass + 50% roots; root biopores: root detritus only). The red and blue arrows indicate the effects of biopore-specific microbial processing, which in the case of earthworms (*) also includes earthworm / gut microflora processing. The difference to the bulk indicates the effects of roots and/or earthworms, respectively (shown as an example of interpretation, red dashed line as a visual guide).*

2.2.3.2 Processing of the lignin macromolecule

The oxidation state of the lignin side chains (Fig. 3) confirmed the degree of OM processing in biopores previously seen in the polysaccharides – irrespective of the subunit studied (Fig. 2). Relative to bulk soil, the lignin oxidation state in earthworm biopores was lower in both subsoil depths. However, lignin in root-influenced biopores was only less oxidised in the 75–105 cm horizon. Highest oxidation was apparent in bulk soil. Both earthworm biopores had the lowest lignin oxidation state and also the least microbial processing during biopore formation (oxidation state increased from initial 0.4 → 0.55 for (Ac/Al)s). Vanillyl subunits underwent almost no processing in any of the earthworm biopore types. Like in the case of sugars, root biopore lignin underwent the strongest processing among biopores. The S/V ratio showed stronger processing in bulk soil than in earthworm biopores (Fig. S2, Supplementary material), especially in 45–75 cm. The Ci/V could only be applied to the earthworm biopore types since only in them cinnamyl subunits were recovered, which stem from the clover-grass feed. Preferential earthworm activities may be deduced from the Ci/V ratio since significant differences were only found in 45–75 cm between both earthworm biopore types.

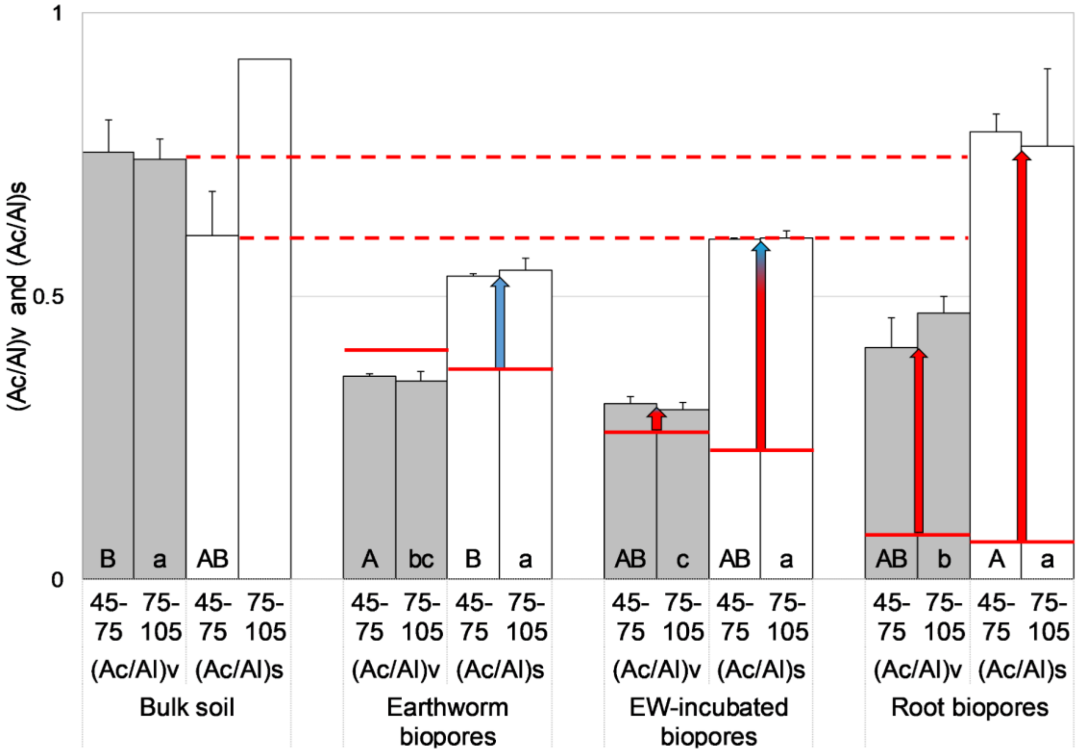

Fig. 3 *Oxidation state of the lignin side chains. Ratios of vanillic acid/vanillin (Ac/Al)v as grey bars and syringic acid/syringaldehyde (Ac/Al)s as white bars. Shown are means ± standard errors of all four treatments. Capital letters indicate significant differences for 45–75 cm (one-way ANOVA, Tukey's HSD test on α 0.05), whereas small letters indicate significant differences for 75–105 cm. (Ac/Al)s for bulk soil represents only one value. Red lines indicate the values of the source biomasses, i.e. plant inputs prior to decomposition. The red and blue arrows indicate the effects of biopore-specific microbial processing. The difference to the bulk indicates the effects of roots and/or earthworms, respectively. The red dashed lines correspond to the bulk soil degradation state as a visual guide.*

2.2.3.3 Lipid-derived proxies

The HO-AA ratio, describing the depolymerisation of suberin to free ω-hydroxy alkanoic acids, was highest in bulk soil ($p<0.05$ in 75–105 cm, Fig. 4). Suberin in earthworm biopores remained rather intact relative to bulk soil. The effects of root decay, earthworm incubation and earthworm burrowing on the depolymerisation state of suberin were similar in 75–105 cm, however, no data was available for 45–75 cm. Significant differences among biopores were found for the AA ratio, describing the depolymerisation of suberin to free alkanoic acids: highest values were found in the root biopores relative to native earthworm biopores (75–105 cm). The ratio of *n*-alkenes to their pre-cursors *n*-alkanes (describing the degradation of epicuticular waxes) had a similar behaviour among treatments like the GM/AX ratio: the highest degree of processing in bulk soil and root biopores, lowest in both earthworm biopore types. However, both root detritus-influenced biopore types featured a lower degree of degradation of waxes with depth ($p<0.05$). Summarising, the proxies for the hemicelluloses, suberin and lignin showed increasing OM processing in the order: earthworm biopore < root biopores < bulk soil.

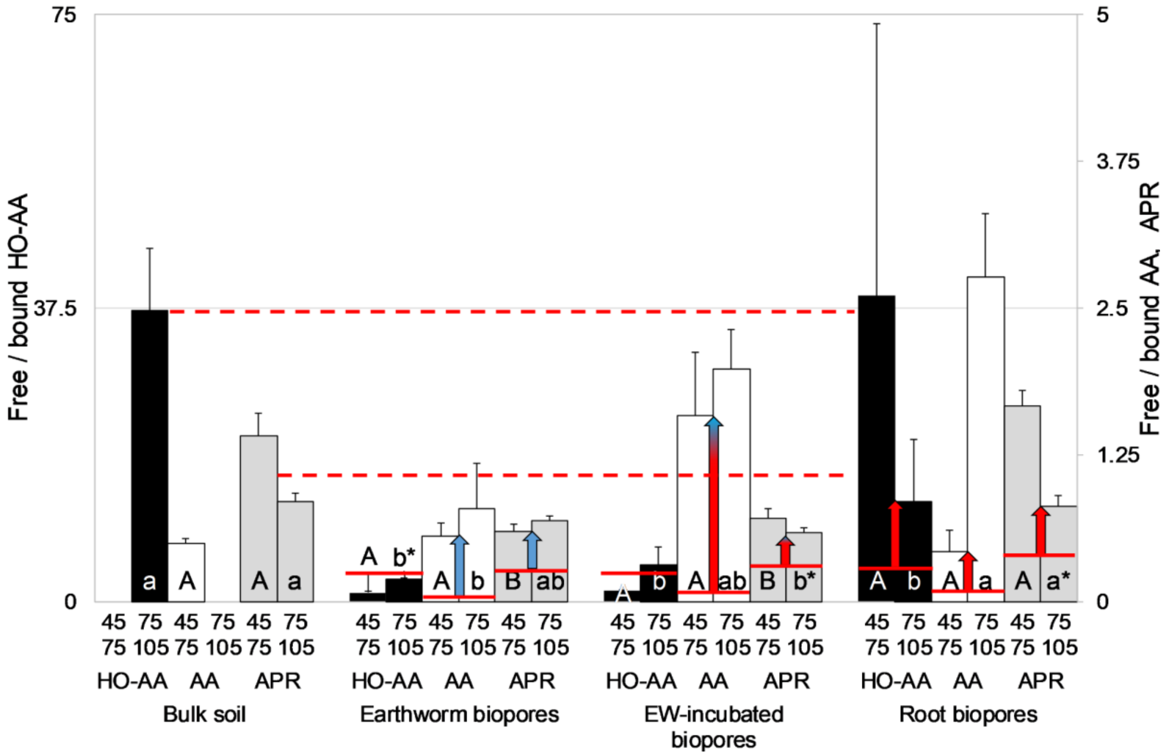

Fig. 4 Lipid-based proxies: free/bound ω-hydroxy alkanoic acids (HO-AA) as black bars on the left y-axis; free/bound alkanoic acids (AA) as white bars and ∑ n-alkenes / ∑ n-alkanes as grey bars, both on the right y-axis. Shown are means ± standard errors of all four treatments. Capital letters indicate significant differences for 45–75 cm (one-way ANOVA, Tukey's HSD test on α 0.05), whereas small letters indicate significant differences in 75–105 cm. Asterisks indicate significant differences of a variable between both soil depths (Two sample t-test for dependent samples). Red lines indicate the values of the source biomasses, i.e. plant inputs prior to decomposition. The red and blue arrows indicate the effects of biopore-specific microbial processing. The difference to the bulk indicates the effects of roots and/or earthworms, respectively. The red dashed lines correspond to the bulk soil degradation state as a visual guide.

Table 2 General soil properties and information regarding the biopores. Shown are mean values ± standard errors of TOC and TN contents, C/N ratios and $\delta^{13}C$ for root biopores, EW-incubated biopores, native earthworm biopores and bulk soil. Capital letters indicate significant differences for 45–75 cm (one-way ANOVA, Tukey's HSD test on α 0.05), whereas small letters correspond to 75–105 cm. Asterisks indicate significant differences of a variable between both soil depths (two sample t-test for dependent samples). Taken from Banfield et al. (2017a).

	Bulk soil		**Earthworm pores**		**EW-incubated pores**		**Root pores**	
	45-75 cm	**75-105 cm**	**45-75 cm**	**75-105 cm**	**45-75 cm**	**75-105 cm**	**45-75 cm**	**75-105 cm**
Total organic carbon [%]	0.41 ± 0.02^{A}	0.35 ± 0.05^{b}	1.17 ± 0.05^{C}	1.05 ± 0.04^{a}	1.16 ± 0.04^{C}	1.07 ± 0.04^{a*}	0.81 ± 0.03^{B}	0.93 ± 0.06^{a}
Total nitrogen [%]	0.06 ± 0.00^{A}	0.05 ± 0.00^{b*}	0.11 ± 0.00^{C}	0.10 ± 0.01^{a}	0.12 ± 0.00^{C}	0.11 ± 0.01^{a}	0.09 ± 0.00^{B}	0.10 ± 0.01^{a}
C : N	7.2 ± 0.1^{D}	7.7 ± 0.9^{a}	10.3 ± 0.2^{C}	10.3 ± 0.5^{a}	9.6 ± 0.1^{B}	9.9 ± 0.4^{a}	8.6 ± 0.2^{A}	9.7 ± 0.5^{a}
$\delta^{13}C$ [‰]	-25.0 ± 0.05^{B}	-23.5 ± 0.75^{a}	-25.3 ± 0.25^{AB}	-23.8 ± 0.66^{a}	-26.5 ± 0.21^{A}	-25.6 ± 0.51^{a}	-25.7 ± 0.46^{AB}	-23.4 ± 1.17^{a}

2.2.4 Discussion

2.2.4.1 Applicability of biomarker-derived proxies

This study employed biomarkers ratios to determine the degree of microbial processing of biopore OM and the effects of soil biota. Biomarker ratios have been used extensively in the past to study OM dynamics (Glaser et al., 2004; Otto and Simpson; Spielvogel et al., 2007). As with many biomarkers, their sources are frequently generalised and thus not always undoubted or specific (Amelung et al., 2008; Frostegård et al., 2011), e.g. in the case of neutral sugars (Gunina and Kuzyakov, 2015). Thus, we characterised the input biomasses (e.g. chicory roots, clover grass) to get source-adapted biomarkers. The lignin, suberin and hemicellulose markers represent the main structural components of shoot litter and root residues (Bull et al., 2000; Kögel-Knabner, 2002). They reflect medium and long-term decomposition processes and are not appropriate to characterise the very early stages of litter decomposition (Haider and Martin, 1979; Schöning et al., 2005).

As the time points of the last C input into different biopore types were not identical in our study, a direct comparison of the decomposition rates in the biopores is not quantitatively possible (Figs. 2, 3, 4). As under field management conditions inputs into different biopores also occur at different times of the cropping season (Eriksen-Hamel et al., 2009), our design features representative conditions for biopores in agricultural soils. Therefore, our findings can be generalised: the conditions described herein, i.e. earthworm burrowing and decaying roots, are common in arable fields under fallow or no-till (Chan, 2001). Certainly, the OM input amounts were not identical among the biopore types. By calculating biomarker ratios, the absolute biomarker contents are taken out of the equation and the decomposition stage under field conditions becomes evident.

At a glance, all proxies present a certain degree of degradation of the biopore OM. The biopore development was intensive enough to affect all proxies irrespective of the analytical method and suggested mutual validation of the proxies (also visible in the correlation circle of Fig. 1, right). However, comparing e.g. lignin and *n*-alkane proxies in root biopores (Figs. 3, 4), a depth effect was apparent only for the latter. Therefore, it is crucial to compare proxies for multiple substance classes to get the ‘big picture’, i.e. the compound and hotspot-specific OM transformations. Apart from the biomarker-derived proxies, the microbial processing also impacted the bulk isotopic composition ($\delta^{13}C$) and the C/N ratio through the relative increase of microbial necromass relative to the successively decomposed plant material (Table 2). As less pronounced treatment effects were apparent relative to the biomarkers, $\delta^{13}C$ was clearly a less sensitive marker for the processing of OM compared to the biomarker ratios.

The distinction between the GM/AX ratio and the source-adapted MRF/AX ratio was not immediately obvious in case of the investigated hotspots (Fig. 2). The similarity of both ratios underlines that both are suitable for C dynamics studies due to the same methodological background (Gunina and Kuzyakov, 2015). However, the MRF/AX ratio is less biased than the GM/AX ratio in our setup: a high galactose content in chicory roots and other plants (Angers and Mehuys, 1990), raises concerns if the frequently applied GM/AX ratio is always the best ratio. Galactose found in biopores of chicory may be mostly root-derived and not microbial. We, therefore, recommend checking the primary inputs for confounding sugar contents and calculating source-adapted biomarkers.

Reduced explanatory power may result from sampling: the bulk soil and the soil ingested by earthworms contains native lipids and carbohydrates (Gunina and Kuzyakov, 2015; Kögel-Knabner et al., 2008). This potentially influences the apparent degree of processing at the end of the experiment. In our setup, this effect is not expected to play a major role for two reasons. First, the lipid and carbohydrate contents in the deep bulk subsoil were rather low and the C inputs into the biopores were orders of magnitude larger resulting already after two years in a threefold higher C content (Banfield et al., 2017). Second, no or only little bulk soil was sampled with the biopore linings. Care was taken not to take all biopore linings by shaving off the inner walls only once with a micro spatula. Earthworm biopores are expected to be influenced by carbohydrate-containing mucus produced by the earthworms (Brown et al., 2000; Curry and Schmidt, 2007).

2.2.4.2 The effects of earthworms, roots and soil depth on the decomposition stage of biopore OM

The PCA illustrated the similarities between both earthworm biopore types and between root biopores and the bulk soil (Fig. 1, left): earthworm-influenced biopore types were fully overlapping with each other, and the root biopores were partly overlapping with the bulk soil. Earthworm activities were discernible in the PCA from smaller within-group variance than the other biopores or bulk soil. This already anticipated some important conclusions of the experiment: I) the strong and fast impact of earthworms on OM dynamics and II) the late stage of residue turnover in root biopores and their similarity to bulk soil after two years of decomposition. Principal component 1 clearly distinguished the ‘fresh input’ (earthworm influence; Fig. 1) from the ‘old C’ samples (no recent C input in bulk soil and root biopores). As earthworms were fed with clover grass during the entire experiment, they brought new C into the biopores and induced the ‘earthworm effect’. The earthworm effect is most strongly correlated with GM/AX and (Ac/Al)v ratios apparently indicative for low processed clover grass. Figure 2 exemplarily illustrates I) microbial processing, i.e. the red arrow shows the increase of the biomarker ratio from the undecomposed source biomass during biopore development, and II) the earthworm effect, i.e. less decomposed earthworm biopore OM relative to bulk soil. Microbial processing includes processing in the earthworm gut by microflora, which is predominantly derived from soil microflora, and also enzymes produced by the earthworm itself (Brown et al., 2000; Curry and Schmidt, 2007). Earthworms replenished the OM, i.e. hemicelluloses (Fig. 2), lignin (V subunits, Fig. 3) and suberin and *n*-alkanes (Fig. 4) were less degraded than in bulk soil. This underlines the immense role of earthworms as ecosystem engineers (Jones et al., 1996).

The effect of the soil depth on both native earthworm and earthworm-incubated biopores was little: the degradation state was almost identical between soil depths and the variance of the proxies was smallest among the biopores (smallest ellipses in Fig. 1; Figs. 2, 3, 4). Therefore, even short-term earthworm burrowing for six months effectively added and redistributed OM within the burrows and equalised depth effects (Jégou et al., 2000). Earthworm incubations are almost independent of their duration beneficial for C and nutrient accumulation in the subsoil and could be easily implemented by reduced tillage (Athmann et al., 2017; Rumpel et al., 2012). While the soil depth had little effect on the OM in earthworm biopores, it was apparent for the root biopores along PC 2 (Fig. 1). Root detritus was more decomposed in the lower subsoil (Fig. 2, Table 2 C/N). The higher decomposition of root hemicelluloses (Fig. 2) may either result from a lower degree of lignification (Barros et al., 2015) or from a lower degree of cross-linking (arabinoxylan to lignin) of the younger root detritus in the deeper subsoil (Amin et al., 2014; Bertrand et al., 2005; Moorhead et al., 2014).

The root effect on all biomarker ratios was weaker than the earthworm effect (Figs. 2, 3, 4) and appeared to be wearing off after two years of root decomposition: only suberin and lignin (V subunits) were not yet as decomposed as the bulk SOM (Figs. 3, 4). Root biopores had not yet fully reached the decomposition state, nor the C contents of the bulk SOM (Table 2). Thus, until less bioavailable inputs will be fully turned over at least 1-2 years more of accelerated C and nutrient turnover may be expected in the root biopores (Schöning et al., 2005).

2.2.4.3 OM processing in the biopores

The microbial processing (illustrated by the red and blue arrows in Figs. 2, 3 and 4) in the biopore hotspots was lowest with the highest frequency of C input. First, taproot residues underwent the strongest microbial processing among biopores. Residues were probably only weakly incorporated into the surrounding soil as compared to earthworms' ingesting and casting (Lubbers et al., 2017). This limits the contact between root residues and mineral surfaces and, therefore, limits physicochemical C stabilisation (Schmidt et al., 2011). In contrast, intimate mixing of partly processed OM in the earthworm gut brings polar functional groups in contact with mineral surfaces and generates aggregates stabilised by organo-mineral interactions (Jégou et al., 2000; von Luetzow et al., 2006). It may be speculated that such protection might have contributed to the lower degree of processing of OM in earthworm biopores compared to root biopores (Figs. 2, 3, 4). For instance, the proxies of hemicelluloses and *n*-alkanes showed divergent trends with depth in root-influenced biopores (Figs. 2, 4). The microbial processing of polysaccharides and lipids is, therefore, not governed by the same factors. Likely the varying interaction with the mineral phases due to oxidation state and functional groups as well as the low bioavailability of *n*-alkanes can help explain this behaviour (Rumpel et al., 2010; Rumpel et al., 2012; Vidal et al., 2016).

The frequent OM inputs by earthworms regularly replenished the decaying pool of easily bioavailable C (hemicelluloses) - fuelling a large-size microbial community of fast-growing Gram-negative bacteria, which preferentially grow on easily available C (Banfield et al., 2017; Curry and Schmidt, 2007; Hoang et al., 2016). The less bioavailable, structural OM (lignin, suberin) is then, consequently, only weakly decomposed (Figs. 3, 4). In the case of the single OM input in the root biopores, a gradual conversion of plant biomass into more stabilised microbial necromass is likely (Puget and Le Drinkwater, 2001). The OM in root biopores enriched the microbial community in Gram-positive bacteria and actinobacteria (Banfield et al., 2017), i.e. slowly growing decomposers of structural and not easily available C (Větrovský et al., 2014).

As hemicelluloses, suberin and lignin derive from primary and secondary plant cell walls and have similar functions and locations in plants (Kögel-Knabner et al., 2008), it was expected that they are decomposed at similar stages of decomposition (Cotrufo et al., 2013). However, the GM/AX ratio was more increased than the lignin oxidation state or HO-AA (relative to the inputs) demonstrating that the processing of hemicelluloses was faster than of lignin or suberin (Figs. 2, 3, 4). Therefore, the more easily available C of the hemicelluloses was preferentially processed.

OM processing in earthworm pores is dominated by two contrasting processes: I) high microbial activity due to fresh C inputs likely caused intensive microbial processing of the biopores OM, and, II) the biomarker ratios of earthworm biopores might be vastly dominated by the high frequency of imported 'unprocessed' OM from which only the highly bioavailable parts were utilised by microorganisms. Our observation of lower microbial processing especially of less bioavailable substance classes (lignin) points toward the dominance of the second process. The two processes of I) increased microbial processing by high activity *vs* II) dominance of frequent input of 'unprocessed' biomass can also be distinguished by the $\delta^{13}C$ value of the biopore OM. When earthworms accelerate the turnover of OM, increased fractionation processes take place leading to an increase of the $\delta^{13}C$ (Werth and Kuzyakov, 2010). In contrast, the imported fresh shoot litter (clover grass) decreased the $\delta^{13}C$ of biopore OM by the input of 'unprocessed' OM. This process is enhanced by the microbial preference for easily decomposable substance classes (Blagodatskaya et al., 2009), which are isotopically heavier. This results from processes during plant biomass synthesis (Hobbie and Werner, 2004; Park and Epstein, 1961) where lignin undergoes many fractionating reaction steps during its biosynthesis and becomes isotopically lighter than sugars which remain longer in the unreacted photosynthate pool and undergo fewer reaction steps to hemicelluloses (Boerjan et al., 2003; Pauly et al., 2013). The lower ^{13}C abundance of earthworm-incubated biopores (Table 2) confirms the relative accumulation of isotopically lighter substances (e.g. lignin) in biopores by the preferential decomposition of the isotopically heavier parts of the fresh clover grass litter as e.g. hemicelluloses (Figs. 2, 3). Presumably, as soon as the C input ceases – e.g. in the root biopores – microorganisms would use all forms of C or even re-use, e.g. in the case of the bulk soil where the supply is very limited (Fierer et al., 2003; Richter and Markewitz, 1995), resulting in the higher $\delta^{13}C$ value of bulk SOM (Table 2).

The strong processing of bulk SOM indicated by its $\delta^{13}C$ value is also confirmed by highest (Ac/Al)v ratios for bulk soil lignin. The bulk SOM derives from a wide range of inputs and was highly oxidised which is likely a pre-requisite for stabilisation of lignin (Vidal et al., 2016). The subunit-specific processing of lignin was similar in bulk soil and biopores: syringyl subunits were oxidised faster than vanillyl subunits (Heim and Schmidt, 2007;

Thevenot et al., 2010). Although Banfield et al. (2017) found higher fungal / bacterial ratios in earthworm-incubated biopores, there was no indication that lignin processing in the biopore hotspots was mechanistically different from the bulk subsoil (Rasse et al., 2006). This may most likely be explained by the high functional redundancy of the microbial community in hotspots (Delmont et al., 2014) and the scarcity of specialists capable of co-metabolically attacking the lignin backbone (Tuomela et al., 2000; Větrovský et al., 2014). Suberin-derived lipids are also discussed as parts of the rather resistant SOM pool (Mendez-Millan et al., 2010). However, in bulk subsoil only very little intact suberin was recovered and the ratio of free depolymerisation products to suberin was highest (Fig. 4). Consequently, such long decomposition times as observed in bulk soil illustrated the intensive suberin decomposition of agricultural SOM and showed that intact suberin in the subsoil is mainly limited to hotspots.

2.2.4.4 The relevance of the biopore C turnover in the subsoil

Microbial hotspots are central to the understanding of subsoil C turnover (Kuzyakov and Blagodatskaya, 2015). Biopores are likely the largest subsoil hotspots by volume and almost all C and nutrient turnover in the subsoil is assumed to take place in hotspots (Kuzyakov and Blagodatskaya, 2015). Considering how long root biopores remained ‘hot’ (Figs. 2, 3, 4), they provide nutrients and C for time spans which are definitely long enough for subsequently grown crops to benefit from biopores’ nutrients. Due to their large number (e.g. 400 m^{-2}; Athmann et al., 2013) and considerable C contents (Table 2), root biopores are very relevant for the total C input and SOM formation especially in the subsoil (Figs. 2, 3, 4) and therefore nutrient accumulation. Catch crop practices like greening incentivised by the EU’s Common Agricultural Policy could prove to have further long-term effects as root biopores are easily induced in great numbers by deep-rooting catch crops (Kautz et al., 2013; Wuest, 2001). Biopores can facilitate the acquisition of nutrients from the subsoil via (1) increasing the root-length density in the bulk soil or (2) uptake of nutrients from the biopore wall (Gaiser et al., 2012; Han et al., 2016; Jakobsen and Dexter, 1988; Kautz, 2015).

The earthworm biopores featured considerably higher C contents (Table 2), enzyme activities and higher nutrient mobilisation than the root biopores (Athmann et al., 2017; Banfield et al., 2017; Hoang et al., 2016), so the specific relevance of earthworm biopores for nutrient mobilisation is likely higher compared to root biopores. It remains unclear if earthworms overcompensate their forty times lower count (Dinter et al., 2013; Kautz et al., 2014) and actually cause higher C turnover than root biopores on the field scale. Being voids makes biopores attractive for new root growth which may actually hold back long-term C sequestration. Potentially stabilised OM in biopores, e.g. oxidised lignin (Fig. 3;

(Kiem and Kögel-Knabner, 2003; Vidal et al., 2016), may not be out of reach of roots: priming through biopore re-use makes direct C sequestration less likely (Kuzyakov, 2010). Consequently, biopores may mostly indirectly promote long-term C sequestration by increasing the total belowground C input by boosted nutrient cycling and subsoil access. If long-term C sequestration was mainly improved indirectly, then the earthworm biopores may support plant growth more than the slow-cycling root biopores.

2.2.5 Conclusions

Biopores are the largest-size hotspots of C and nutrient turnover in the subsoil, especially when induced by earthworms. The microbial processing of the C inputs was biopore-specific. More easily available parts of the OM (e.g. hemicellulose) were preferentially processed in biopores compared to lignin. The repeated inputs by earthworms relatively enrich less bioavailable and weakly processed OM (e.g. lignin) in the biopore environment. Earthworms incubation in root biopores bring new life to the root detritus: within six months they replenished the highly processed OM of the root biopores with only weakly processed shoot litter. Earthworms in root biopores led to 60% less processed hemicelluloses relative to root biopores. Consequently, even short periods of earthworm promotion have long-lasting effects on C contents and the degree of processing of the OM. Root necromass of perennials is likely to be processed roughly in the time it took to form the biomass (3-4 years). The nutrient accumulation and boosted mobilisation in root biopores hold up at least for durations relevant for crop rotations. Despite the 50% higher C accumulation in earthworm biopores, root biopores are up to forty times more frequent and therefore they quantitatively provide most of the OM input into subsoils. This may pose further incentives for growing perennial tap-rooted catch crops (also for shorter-term ‘greening’). We conclude that all biopore hotspots remain ‘hot’ at least for several years and, therefore, likely provide valuable nutrients along their preferential root growth pathways for subsequently grown crops. Thereby, biopores likely indirectly support long-term C sequestration through boosting plant productivity creating a positive feedback on C sequestration.

Acknowledgements

We highly acknowledge the support from the German Research Foundation (DFG KU1184/29 and DFG INST 186/1006-1). We would like to thank Timo Kautz and the colleagues from Institute of Organic Agriculture of the University of Bonn for establishing and managing the field trial Klein-Altendorf. We would also like to thank the Centre for Stable Isotope Research and Analysis Goettingen for δ^{13}C determinations.

2.2.6 References

- Amblès, A., et al., 1994. n-Alkane oxidation in soil. Formation of internal monoalkenes. Geoderma 64, 111–124.
- Amelung, W., et al., 2008. Chapter 6 Combining Biomarker with Stable Isotope Analyses for Assessing the Transformation and Turnover of Soil Organic Matter, in: Sparks, D.L. (Ed.), Advances in agronomy. Volume 100. Elsevier; Academic Press, San Diego, pp. 155–250.
- Amin, B.A.Z., et al., 2014. Impact of fine litter chemistry on lignocellulolytic enzyme efficiency during decomposition of maize leaf and root in soil. Biogeochemistry 117, 169–183.
- Andriuzzi, W.S., Bolger, T., Schmidt, O., 2013. The drilosphere concept. Fine-scale incorporation of surface residue-derived N and C around natural Lumbricus terrestris burrows. Soil Biology and Biochemistry 64, 136–138.
- Angers, D.A., Mehuys, G.R., 1990. Barley and alfalfa cropping effects on carbohydrate contents of a clay soil and its size fractions. Knowledge gaps in soil C and N interactions 22, 285–288.
- Armas-Herrera, C.M., et al., 2016. Management effects on composition and dynamics of cutin and suberin in topsoil under agricultural use. European Journal of Soil Science.
- Athmann, M., et al., 2013. Root growth in biopores—evaluation with in situ endoscopy. Plant and Soil 371, 179–190.
- Athmann, M., et al., 2017. Six months of L. terrestris L. activity in root-formed biopores increases nutrient availability, microbial biomass and enzyme activity. Applied Soil Ecology 120, 135–142.
- Balesdent, J., Mariotti, A., Guillet, B., 1987. Natural 13C abundance as a tracer for studies of soil organic matter dynamics. Knowledge gaps in soil C and N interactions 19, 25–30.
- Banfield, C.C., et al., 2017. Biopore history determines the microbial community composition in subsoil hotspots. Biology and Fertility of Soils 9, 54.
- Barros, J., et al., 2015. The cell biology of lignification in higher plants. Annals of botany 115, 1053–1074.
- Bertrand, I., et al., 2005. Can the Biochemical Features and Histology of Wheat Residues Explain their Decomposition in Soil? Plant and Soil 281, 291–307.
- Blagodatskaya, E.V., et al., 2009. Contrasting effects of glucose, living roots and maize straw on microbial growth kinetics and substrate availability in soil. European Journal of Soil Science 60, 186–197.
- Boerjan, W., Ralph, J., Baucher, M., 2003. Lignin biosynthesis. Annual review of plant biology 54, 519–546.
- Brown, G.G., Barois, I., Lavelle, P., 2000. Regulation of soil organic matter dynamics and microbial activityin the drilosphere and the role of interactionswith other edaphic functional domains. European Journal of Soil Biology 36, 177–198.
- Bull, I.D., et al., 2000. Organic geochemical studies of soils from the Rothamsted classical experiments—V. The fate of lipids in different long-term experiments. Organic Geochemistry 31, 389–408.

- Butt, K.R., Lowe, C.N., 2007. A viable technique for tagging earthworms using visible implant elastomer. Applied Soil Ecology 35, 454–457.
- Chan, K., 2001. An overview of some tillage impacts on earthworm population abundance and diversity — implications for functioning in soils. Soil and Tillage Research 57, 179–191.
- Cheshire, M.V., Griffiths, B.S., 1989. The influence of earthworms and cranefly larvae on the decomposition of uniformly 14C labelled plant material in soil. Journal of Soil Science 40, 117–124.
- Cotrufo, M.F., et al., 2013. The Microbial Efficiency-Matrix Stabilization (MEMS) framework integrates plant litter decomposition with soil organic matter stabilization: do labile plant inputs form stable soil organic matter? Global Change Biology 19, 988–995.
- Curry, J.P., Schmidt, O., 2007. The feeding ecology of earthworms – A review. Pedobiologia 50, 463–477.
- Delmont, T.O., et al., 2014. Microbial community development and unseen diversity recovery in inoculated sterile soil. Biology and Fertility of Soils 50, 1069–1076.
- Dignac, M.-F., et al., 2017. Increasing soil carbon storage. Mechanisms, effects of agricultural practices and proxies. A review. Agronomy for Sustainable Development 37, 351.
- Dinter, A., et al., 2013. Occurrence and distribution of earthworms in agricultural landscapes across Europe with regard to testing for responses to plant protection products. Journal of Soils and Sediments 13, 278–293.
- Eriksen-Hamel, N.S., et al., 2009. Earthworm populations and growth rates related to long-term crop residue and tillage management. Soil and Tillage Research 104, 311–316.
- Ertel, J.R., Hedges, J.I., 1984. The lignin component of humic substances. Distribution among soil and sedimentary humic, fulvic, and base-insoluble fractions. Geochimica et Cosmochimica Acta 48, 2065–2074.
- FAOSTAT, 2017. Agri-environmental indicators—Land Use. http://www.fao.org/faostat/en/#data/EL, last accessed 3 Jan 2018.
- Fierer, N., Schimel, J.P., Holden, P.A., 2003. Variations in microbial community composition through two soil depth profiles. Soil Biology and Biochemistry 35, 167–176.
- Fontaine, S., et al., 2007. Stability of organic carbon in deep soil layers controlled by fresh carbon supply. Nature 450, 277–280.
- Frostegård, Å., Tunlid, A., Bååth, E., 2011. Use and misuse of PLFA measurements in soils. Soil Biology and Biochemistry 43, 1621–1625.
- Gaiser, T., et al., 2012. Evidence of improved water uptake from subsoil by spring wheat following lucerne in a temperate humid climate. Field Crops Research 126, 56–62.
- Glaser, B., Turrión, M.-B., Alef, K., 2004. Amino sugars and muramic acid—biomarkers for soil microbial community structure analysis. Soil Biology and Biochemistry 36, 399–407.
- Gunina, A., Kuzyakov, Y., 2014. Pathways of litter C by formation of aggregates and SOM density fractions: Implications from 13C natural abundance. Soil Biology and Biochemistry 71, 95–104.

- Gunina, A., Kuzyakov, Y., 2015. Sugars in soil and sweets for microorganisms: Review of origin, content, composition and fate. Soil Biology and Biochemistry 90, 87–100.
- Haider, K., Martin, P., 1979. Abbau und Umwandlung von Pflanzenrückständen und ihren Inhaltsstoffen durch die Mikroflora des Bodens. Zeitschrift für Pflanzenernährung und Bodenkunde 142, 456–475.
- Han, E., Kautz, T., Köpke, U., 2016. Precrop root system determines root diameter of subsequent crop. Biology and Fertility of Soils 52, 113–118.
- Hedges, J.I., Ertel, J.R., 1982. Characterization of lignin by gas capillary chromatography of cupric oxide oxidation products. Analytical Chemistry 54, 174–178.
- Heim, A., Schmidt, M.W.I., 2007. Lignin turnover in arable soil and grassland analysed with two different labelling approaches. European Journal of Soil Science 58, 599–608.
- Hoang, D.T.T., et al., 2016. Hotspots of microbial activity induced by earthworm burrows, old root channels, and their combination in subsoil. Biology and Fertility of Soils 52, 1105–1119.
- Hobbie, E.A., Werner, R.A., 2004. Intramolecular, compound-specific, and bulk carbon isotope patterns in C 3 and C 4 plants. A review and synthesis. New Phytologist 161, 371–385.
- IPCC, 2014. Climate change 2014: synthesis report. Contribution of Working Groups I, II and III to the fifth assessment report of the Intergovernmental Panel on Climate Change. IPCC, Geneva, Switzerland.
- IUSS Working Group WRB, 2008. World reference base for soil resources 2006. Ein Rahmen für internationale Klassifikation, Korrelation und Kommunikation, 1st ed,. BGR, Hannover.
- Jakobsen, B.E., Dexter, A.R., 1988. Influence of biopores on root growth, water uptake and grain yield of wheat (Triticum aestivum) based on predictions from a computer model. Biology and Fertility of Soils 6, 315–321.
- Jégou, D., et al., 2000. Burrowing activity of the earthworms Lumbricus terrestris and Aporrectodea giardi and consequences on C transfers in soil. European Journal of Soil Biology 36, 27–34.
- Jones, C., Lawton, J., Shachak, M., 1996. Organisms as Ecosystem Engineers, in: Samson, F.B., Knopf, F.L. (Eds.), Ecosystem management. Selected readings. Springer, New York, pp. 130–147.
- Kaiser, K., Kalbitz, K., 2012. Cycling downwards – dissolved organic matter in soils. Soil Biology and Biochemistry 52, 29–32.
- Kalbitz, K., Kaiser, K., 2008. Contribution of dissolved organic matter to carbon storage in forest mineral soils. Journal of Plant Nutrition and Soil Science 171, 52–60.
- Kautz, T., et al., 2013. Nutrient acquisition from arable subsoils in temperate climates: A review. Soil Biology and Biochemistry 57, 1003–1022.
- Kautz, T., et al., 2014. Contribution of anecic earthworms to biopore formation during cultivation of perennial ley crops. Pedobiologia 57, 47–52.
- Kautz, T., 2015. Research on subsoil biopores and their functions in organically managed soils: A review. Renewable Agriculture and Food Systems 30, 318–327.

- Kell, D.B., 2012. Large-scale sequestration of atmospheric carbon via plant roots in natural and agricultural ecosystems: why and how. Phil Trans R Soc B 367, 1589–1597.
- Kiem, R., Kögel-Knabner, I., 2003. Contribution of lignin and polysaccharides to the refractory carbon pool in C-depleted arable soils. Soil Biology and Biochemistry 35, 101–118.
- Kindler, R., et al., 2011. Dissolved carbon leaching from soil is a crucial component of the net ecosystem carbon balance. Global Change Biology 17, 1167–1185.
- Kögel-Knabner, I., 2002. The macromolecular organic composition of plant and microbial residues as inputs to soil organic matter. Soil Biology and Biochemistry 34, 139–162.
- Kögel-Knabner, I., et al., 2008. Organo-mineral associations in temperate soils. Integrating biology, mineralogy, and organic matter chemistry. Journal of Plant Nutrition and Soil Science 171, 61–82.
- Kolattukudy, P.E., 1980. Biopolyester membranes of plants: cutin and suberin. Science 208, 990–1000.
- Kolattukudy, P.E., 1984. Biochemistry and function of cutin and suberin. Canadian Journal of Botany 62, 2918–2933.
- Kuzyakov, Y., 2010. Priming effects: Interactions between living and dead organic matter. Soil Biology and Biochemistry 42, 1363–1371.
- Kuzyakov, Y., Blagodatskaya, E., 2015. Microbial hotspots and hot moments in soil: Concept & review. Soil Biology and Biochemistry 83, 184–199.
- Lal, R., Negassa, W., Lorenz, K., 2015. Carbon sequestration in soil. Current Opinion in Environmental Sustainability 15, 79–86.
- Li, Y., et al., 2009. Climate change and drought: a risk assessment of crop-yield impacts. Climate research 39, 31–46.
- Lichtfouse, E., et al., 1998. A novel pathway of soil organic matter formation by selective preservation of resistant straight-chain biopolymers: chemical and isotope evidence. Organic Geochemistry 28, 411–415.
- Lichtfouse, É., 1997. Heterogeneous Turnover of Molecular Organic Substances from Crop Soils as Revealed by 13 C Labeling at Natural Abundance with Zea mays. Naturwissenschaften 84, 23–25.
- Lubbers, I.M., Pulleman, M.M., van Groenigen, J.W., 2017. Can earthworms simultaneously enhance decomposition and stabilization of plant residue carbon? Soil Biology and Biochemistry 105, 12–24.
- Mendez-Millan, M., et al., 2010. Molecular dynamics of shoot vs. root biomarkers in an agricultural soil estimated by natural abundance 13C labelling. Soil Biology and Biochemistry 42, 169–177.
- Miltner, A., et al., 2012. SOM genesis: microbial biomass as a significant source. Biogeochemistry 111, 41–55.
- Moers, M., et al., 1990. Occurrence and origin of carbohydrates in peat samples from a red mangrove environment as reflected by abundances of neutral monosaccharides. Geochimica et Cosmochimica Acta 54, 2463–2472.
- Moorhead, D., et al., 2014. Interacting microbe and litter quality controls on litter decomposition. A modeling analysis. PloS one 9, e108769.

- Munyankusi, E., et al., 1994. Earthworm Macropores and Preferential Transport in a Long-Term Manure Applied Typic Hapludalf. Journal of Environmental Quality 23, 773.
- Naafs, D.F., van Bergen, P.F., 2002. A qualitative study on the chemical composition of ester-bound moieties in an acidic andosolic forest soil. Organic Geochemistry 33, 189–199.
- Oades, J.M., 1984. Soil organic matter and structural stability. Mechanisms and implications for management. Plant and Soil 76, 319–337.
- Otto, A., Simpson, M.J. Evaluation of CuO oxidation parameters for determining the source and stage of lignin degradation in soil. Biogeochemistry 80, 121–142.
- Otto, A., Simpson, M.J., 2007. Analysis of soil organic matter biomarkers by sequential chemical degradation and gas chromatography – mass spectrometry. Journal of Separation Science 30, 272–282.
- Pal, J.S., Giorgi, F., Bi, X., 2004. Consistency of recent European summer precipitation trends and extremes with future regional climate projections. Geophysical Research Letters 31.
- Park, R., Epstein, S., 1961. Metabolic fractionation of C13 & C12 in plants. Plant Physiology 36, 133.
- Pauly, M., et al., 2013. Hemicellulose biosynthesis. Planta 238, 627–642.
- Poeplau, C., Don, A., 2015. Carbon sequestration in agricultural soils via cultivation of cover crops – A meta-analysis. Agriculture, Ecosystems & Environment 200, 33–41.
- Puget, P., Le Drinkwater, 2001. Short-term dynamics of root-and shoot-derived carbon from a leguminous green manure. Soil Science Society of America Journal 65, 771–779.
- Quenea, K., et al., 2004. Variation in lipid relative abundance and composition among different particle size fractions of a forest soil. Organic Geochemistry 35, 1355–1370.
- Rasse, D.P., et al., 2006. Lignin turnover in an agricultural field: from plant residues to soil-protected fractions. European Journal of Soil Science 57, 530–538.
- Richter, D.D., Markewitz, D., 1995. How deep is soil? BioScience, 600–609.
- Rumpel, C., Chabbi, A., Marschner, B., 2012. Carbon Storage and Sequestration in Subsoil Horizons: Knowledge, Gaps and Potentials, in: Lal, R., et al. (Eds.), Recarbonization of the Biosphere. Ecosystems and the Global Carbon Cycle. Springer Netherlands, Dordrecht, pp. 445–464.
- Rumpel, C., Eusterhues, K., Kögel-Knabner, I., 2010. Non-cellulosic neutral sugar contribution to mineral associated organic matter in top- and subsoil horizons of two acid forest soils. Soil Biology and Biochemistry 42, 379–382.
- Rumpel, C., Kögel-Knabner, I., 2011. Deep soil organic matter—a key but poorly understood component of terrestrial C cycle. Plant and Soil 338, 143–158.
- Rumpel, C., Kögel-Knabner, I., Bruhn, F., 2002. Vertical distribution, age, and chemical composition of organic carbon in two forest soils of different pedogenesis. Organic Geochemistry 33, 1131–1142.
- Scharlemann, J.P.W., et al., 2014. Global soil carbon. Understanding and managing the largest terrestrial carbon pool. Carbon Management 5, 81–91.

- Schimel, D.S., 1995. Terrestrial ecosystems and the carbon cycle. Global Change Biology 1, 77–91.
- Schmidt, M.W.I., et al., 2011. Persistence of soil organic matter as an ecosystem property. Nature 478, 49–56.
- Schöning, I., Knicker, H., Kögel-Knabner, I., 2005. Intimate association between O/N-alkyl carbon and iron oxides in clay fractions of forest soils. Organic Geochemistry 36, 1378–1390.
- Simoneit, B.R.T., 2005. A review of current applications of mass spectrometry for biomarker/molecular tracer elucidations. Mass Spectrometry Reviews 24, 719–765.
- Six, J., et al., 2006. Bacterial and Fungal Contributions to Carbon Sequestration in Agroecosystems. Soil Science Society of America Journal 70, 555–568.
- Spielvogel, S., Prietzel, J., Kögel-Knabner, I., 2007. Changes of lignin phenols and neutral sugars in different soil types of a high-elevation forest ecosystem 25 years after forest dieback. Soil Biology and Biochemistry 39, 655–668.
- Spielvogel, S., Prietzel, J., Kögel-Knabner, I., 2008. Soil organic matter stabilization in acidic forest soils is preferential and soil type-specific. European Journal of Soil Science 59, 674–692.
- Stirzaker, R.J., Passioura, J.B., Wilms, Y., 1996. Soil structure and plant growth: Impact of bulk density and biopores. Plant and Soil 185, 151–162.
- Tanaka, H., et al., 1990. Determination of Component Sugars in Soil Organic Matter by HPLC. Zentralblatt für Mikrobiologie 145, 621–628.
- Thakuria, D., et al., 2010. Gut wall bacteria of earthworms: a natural selection process. The ISME Journal 4, 357–366.
- Thevenot, M., Dignac, M.-F., Rumpel, C., 2010. Fate of lignins in soils. A review. Soil Biology and Biochemistry 42, 1200–1211.
- Tompkins, E.L., et al., 2010. Observed adaptation to climate change. UK evidence of transition to a well-adapting society. Global Environmental Change 20, 627–635.
- Torres-Sallan, G., et al., 2017. Clay illuviation provides a long-term sink for C sequestration in subsoils. Scientific reports 7, 45635.
- Tuomela, M., et al., 2000. Biodegradation of lignin in a compost environment: a review. Bioresource Technology 72, 169–183.
- Urry, J., 2015. Climate Change and Society, in: Michie, J., Cooper, C.L. (Eds.), Why the Social Sciences Matter. Palgrave Macmillan UK, London, pp. 45–59.
- Větrovský, T., Steffen, K.T., Baldrian, P., 2014. Potential of cometabolic transformation of polysaccharides and lignin in lignocellulose by soil Actinobacteria. PloS one 9, e89108.
- Vetterlein, D., et al., 2013. Illite transformation and potassium release upon changes in composition of the rhizophere soil solution. Plant and Soil 371, 267–279.
- Vidal, A., et al., 2016. Molecular fate of root and shoot litter on incorporation and decomposition in earthworm casts. Organic Geochemistry 101, 1–10.
- von Luetzow, M., et al., 2006. Stabilization of organic matter in temperate soils. Mechanisms and their relevance under different soil conditions - a review. European Journal of Soil Science 57, 426–445.

- Werth, M., Kuzyakov, Y., 2010. 13C fractionation at the root–microorganisms–soil interface: A review and outlook for partitioning studies. Soil Biology and Biochemistry 42, 1372–1384.
- Wiesenberg, G.L., et al., 2004. Source and turnover of organic matter in agricultural soils derived from n-alkane/n-carboxylic acid compositions and C-isotope signatures. Advances in Organic Geochemistry 2003. Proceedings of the 21st International Meeting on Organic Geochemistry 35, 1371–1393.
- Wuest, S.B., 2001. Soil biopore estimation: effects of tillage, nitrogen, and photographic resolution. Soil and Tillage Research 62, 111–116.
- Zhang, X., Amelung, W., 1996. Gas chromatographic determination of muramic acid, glucosamine, mannosamine, and galactosamine in soils. Soil Biology and Biochemistry 28, 1201–1206.
- Zhang, H., Schrader, S., 1993. Earthworm effects on selected physical and chemical properties of soil aggregates. Biology and Fertility of Soils 15, 229–234.

2.2.7 Supplementary Material

Table S1 Proxies for the main primary inputs: *L. terrestris* bodies, *C. intybus* shoots, *C. intybus* roots, *L. perenne* shoots, *T. pratense* shoots, *T. repens* shoots.

	L. terrestris *bodies*	*C. intybus* shoots	*C. intybus* roots	*L. perenne* shoots	*T. pratense* shoots	*T. repens* shoots
$\delta^{13}C$	-26.9	-32.0	-29.7	-33.9	-30.1	-30.8
C/N	4.1	19.9	33.7	18.1	19.0	14.9
GM/AX	4.0	1.0	0.19	0.27	0.77	0.89
MRF/AX	2.9	0.3	0.13	0.07	0.25	0.33
(Ac/Al)v	5.5	0.2	0.1	0.6	0.4	0.4
(Ac(Al)s	2.5	0.6	0.1	0.4	0.4	0.4
S/V	1.3	1.0	2.5	1.3	1.2	1.1
Ci/V	2.2	0.2	0.0	3.7	0.5	1.1
Free/bound ω-hydroxy alkanoic acids	4.1	28.3	4.12	1.78	7.82	3.3
Free/bound alkanoic acids	0.12	0.281	0.108	0.028	0.004	0.009
∑ *n*-alkenes / ∑ *n*-alkanes	1.3	0.79	0.37	0	0.63	0

Table S2 Instrumentation and GC measurement details

Substance class / Fraction	GC oven programme	GC + detector settings
Free lipids including n-alkanes, n-alkanoic acids, α,ω-alkanedioic acids	Identical for all free lipids fractions: Measurement on GC-MS	Setup: Agilent 7890A GC coupled to Agilent 7000A triple quadrupole mass spectrometer (both Agilent Waldbronn, Germany, equipped with a DB-5MS column (30 m x 250 µm coated with 0.25 µm 5 % phenyl-methyl siloxane). Helium carrier gas flow was 2.25 ml s^{-1}. Scan mode (50-550 amu), 2 µl injection volume into the splitless inlet at 270 °C. The oven programme started at 80°C, held for one minute, then increased at 10 °C min^{-1} to 150°C. Until 275°C heating was at 1 °C min^{-1}, and finally at 10 °C min^{-1} to 300°C.
Lignin-derived phenols	Measurement of trimethylsilylates on GC-FID, peak identification on GC-MS	Setup: Agilent 7820A GC system equipped with a flame ionization detector and Optima® 17 MS column (Macherey Nagel, Dueren, Germany; phenylmethyl polysiloxane, 50 % phenyl, 30 m × 0.25 mm inner diameter with 0.5 µm film thickness). The injected sample volume was 1 µl, split ratio was 33:1 and the injector port temperature was set to 250 ° C. The temperature programme started at 100 °C (isothermal for 0.5 min) and increased to 160 °C at 10 °C min^{-1}, then held for 6 min. Subsequently, the oven temperature was increased at 20 °C min^{-1} to 250 °C, and again at 50 °C min^{-1} to the final temperature of 300 °C, which was held for 5 minutes.
Cutin/suberin-derived lipids	Measurement on GC-MS	Identical to free lipid method
Neutral sugars	Measurement of aldononitrile acetates on GC-FID, peak identification on GC-MS	Identical to Lignin-derived phenols: the injector port temperature was set to 250 °C and the temperature of detector was 300 °C. The oven programme was as follows: the initial column temperature of 100 °C was held for 1 min and then increased at 20 °C min^{-1} to 175 °C, held for 3 min. The temperature was increased again at 4 °C min^{-1} to 225 °C, held for 3 min, and finally increased at 50 °C min^{-1} to 300 °C and held for 7 min. Helium was used as a carrier gas at a flow rate of 1.1 ml min^{-1} and the split ratio was 30:1.

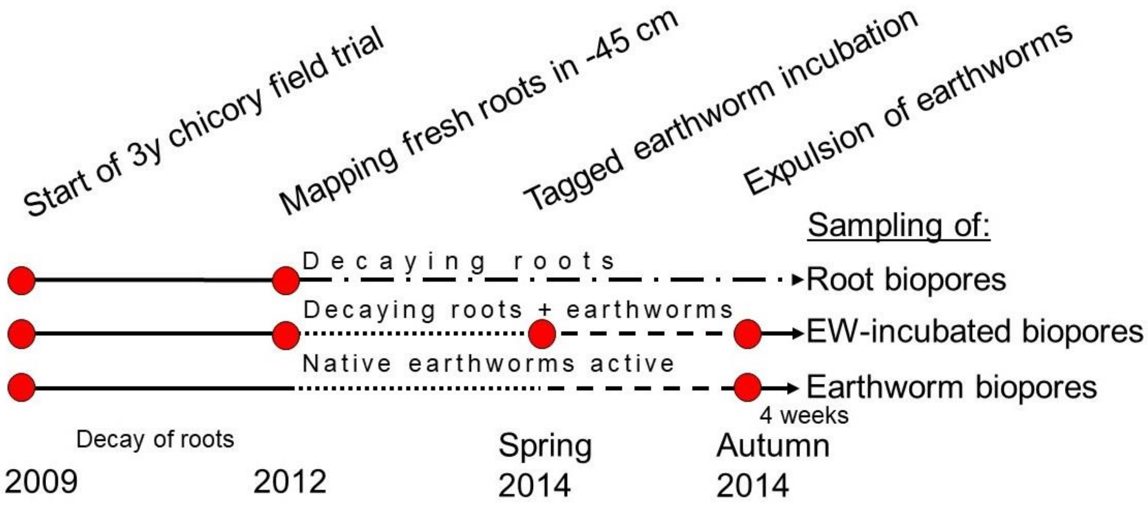
Start of 3y chicory field trial
Mapping fresh roots in -45 cm
Tagged earthworm incubation
Expulsion of earthworms
Sampling of:
Decaying roots
Root biopores
Decaying roots + earthworms
EW-incubated biopores
Native earthworms active
Earthworm biopores
4 weeks
Decay of roots
2009
2012
Spring 2014
Autumn 2014

Fig. S1 Experiment timeline: chicory was grown for three years, followed by two years of fallow. After 18 months of root decomposition, earthworms were introduced into a subset of root biopores for six months, which was compared to native earthworm biopores. Modified after Banfield et al. (2017).

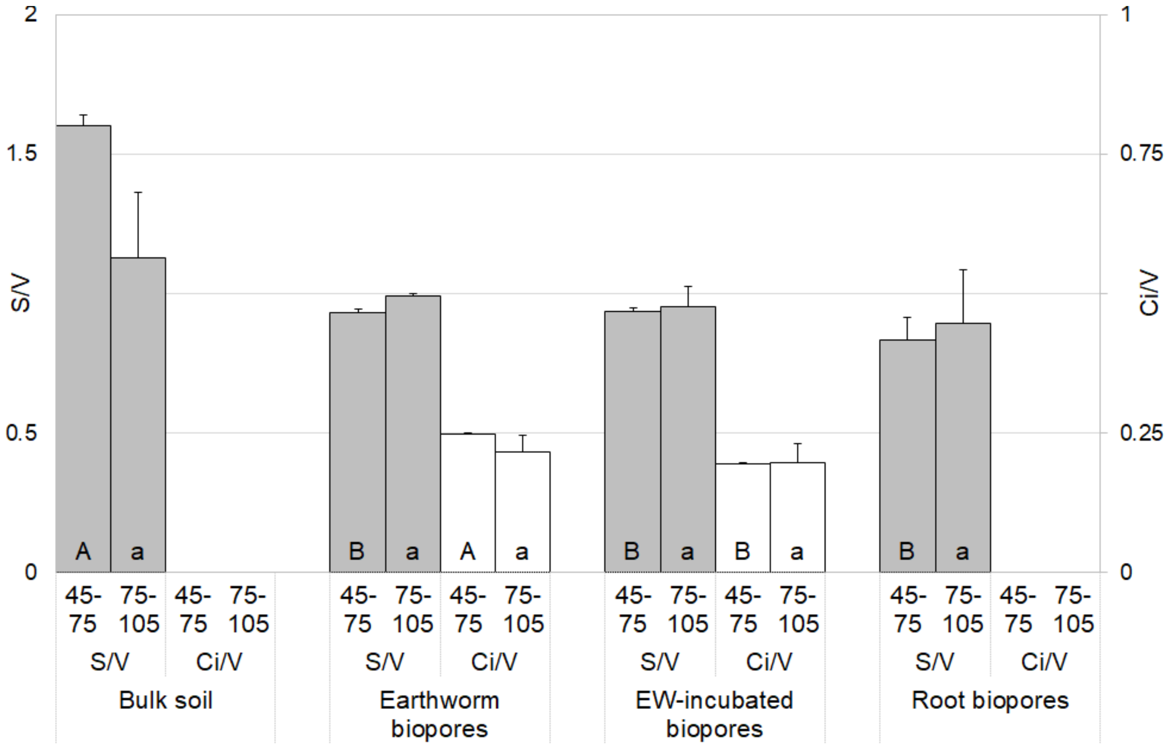

Fig. S2 Proxies relating the syringyl/vanillyl subunits as grey bars (left y-axis) and cinnamyl/vanillyl subunits as white bars (right y-axis). Shown are means ± standard errors of all four treatments. Capital letters indicate significant differences for 45-75 cm (one-way ANOVA, Tukey's HSD test on α 0.05), whereas small letters indicate significant differences for 75-105 cm. Red lines indicate the plant inputs prior to decomposition. The red and blue arrows indicate the two-year effects of roots and earthworms, respectively.

2.3 Study 3: Biopore history determines the microbial community composition in subsoil hotspots

Authors and affiliations

Callum C. Banfield[1]; Michaela A. Dippold[2], Johanna Pausch[1], Duyen T.T. Hoang[1], Yakov Kuzyakov[1,2]

[1]Department of Soil Science of Temperate Ecosystems, University of Goettingen, Buesgenweg 2, 37077 Goettingen, Germany.

[2]Department of Agricultural Soil Science, University of Goettingen, Buesgenweg 2, 37077 Goettingen, Germany

Corresponding author: callumba@gmail.com

Telephone: +49 1578 4527077

Fax: +49 551 3933310

Role of the funding source: DFG KU 1184/29-1

Conflicts of interest: The authors declare no conflicts of interest.

Keywords: Amino sugars; biomarkers; carbon sequestration; carbon turnover; detritusphere; drilosphere; phospholipid fatty acids

Abstract

Biopores are hotspots of nutrient mobilisation and shortcuts for carbon (C) into subsoils. C processing relies on microbial community composition, which remains unexplored in subsoil biopores. Phospholipid fatty acids (PLFAs; markers for living microbial groups) and amino sugars (microbial necromass markers) were extracted from two subsoil depths (45–75; 75–105 cm) and three biopore types: I) drilosphere of *Lumbricus terrestris* L., II) 2-year-old root biopores, and III) 1.5-year-old root biopores plus six months of *L. terrestris* activities. Biopore C contents were at least 2.5 times higher than in bulk soil, causing 26-35 times higher Σ PLFAs g^{-1} soil. The highest Σ PLFAs was in both earthworm biopore types, thus highest SOM and nutrient turnover were assumed. Σ PLFAs was 33% lower in root pores than in earthworm pores. The treatment affected the microbial community composition more strongly than soil depth, hinting to similar C quality in biopores: Gram-positives including actinobacteria were more abundant in root pores than in earthworm pores, probably due to lower C bioavailability in the former. Both earthworm pore types featured fresh litter input, promoting growth of Gram-negatives and fungi. Earthworms in root pores shifted the composition of the microbial community heavily and turned root pores into earthworm pores within six months. Only recent communities were affected and reflect a strong heterogeneity of microbial activity and functions in subsoil hotspots, whereas biopore-specific necromass accumulation from different microbial groups was absent.

2.3.1 Introduction

After decades of disregard, the subsoils have only recently regained interest within soil science, despite the fact they store approximately half of the terrestrial carbon (C) and contain pools of nutrients such as magnesium, calcium and phosphorus significant to plant nutrition (Kell 2012; Kuhlmann and Baumgärtel 1991; Rumpel and Kögel-Knabner 2011; Salome et al. 2010). Aside from dissolved C transport, large amounts of C are transported into the subsoil by earthworms and roots, i.e. in biopores (Don et al. 2008; Kautz 2015). Rooting plants and burrowing earthworms leave not just voids behind through which plants reach the deeper soil faster to explore soil resources (Ehlers et al. 1983; Han et al. 2015), but they additionally induce hotspots of increased microbial activity (Kautz et al. 2013; Nakamoto 2000). Apart from C transport, they have further functions such as soil organic matter (SOM) turnover or possibly C sequestration depending on their genesis.

Biopores make up about 1–10% of the total soil volume (Ehlers et al. 1983; Kuzyakov and Blagodatskaya 2015) and are only persistent in subsoils, i.e. below the ploughed horizon, or in topsoils which are not frequently tilled (Ehlers et al. 1983). Large, vertical biopores reaching into the subsoils are in particular created by crops with allorhizic root systems like common chicory (*Cichorium intybus* L.) (Ehlers et al. 1983; Perkons et al. 2014). Roots deposit large amounts of C into their surroundings, which partly remain after root death, creating the rhizo-detritusphere. Alternatively, anecic earthworms such as Lumbricus terrestris L., create earthworm biopores. They feed on plant residues near the soil surface and deposit residues, mucus and casts in their burrows, creating the drilosphere (Bouché 1975; Jégou et al. 1998). Root detritus and earthworm activities enrich the inner walls of biopores with C, N and P, which induces microbial growth, enzyme activities and, therefore, greater C and N turnover compared to the surrounding bulk soil (Graff 1967; Hoang et al. 2016; Jégou et al. 2001; Parkin and Berry 1999). This leads to nutrient release from SOM and from the solid phases, enhancing soil fertility (Jégou et al. 2001; van Groenigen et al. 2014; Volkmar 1996). C input into subsoils is usually much lower than into topsoils (Hafner and Kuzyakov 2016; Rumpel and Kögel-Knabner 2011). It is more and more questioned if subsoil C turnover is governed by the very same mechanisms as topsoil C turnover - since environmental and soil conditions are rather different in subsoils (Salome et al. 2010; Sanaullah et al. 2011; von Luetzow et al. 2006). Even though biopores are thought to be the main locations of C turnover in the subsoil, little is known about these hotspots (Kuzyakov and Blagodatskaya 2015). For climate change mitigation, it is desirable to sequester C in subsoils through biopores, e.g. by deep rooting plants or deep burrowing earthworms (Kell 2012). Prior to this, the role and relevance of biopores for C turnover and sequestration, particularly in the subsoil, need to be clarified. The importance of the microbial community composition for C turnover is frequently mentioned in the literature, but its investigation has received surprisingly little attention (Fierer et al. 2003; Schmidt et al. 2011; Struecker and Joergensen 2015). The links between the microbial community composition and C turnover are not straightforward, and microbial activity may be more important than their diversity (Nannipieri et al. 2003). Nevertheless, the microbial community composition influences the enzyme activities (Waldrop et al. 2000). So, the functional microbial groups such as fungi or Gram-positives, and their residues are key to assess the relevance of subsoil biopores for short and long-term C turnover. We characterised both by biomarkers:

1) Phospholipids are parts of microbial cell membranes and quickly decomposed after cell death, thus accounting for the living microorganisms (Frostegård and Bååth 1996; Zelles 1999). Microbial group-specific fatty acids in the phospholipids (PLFAs) allow broad characterisation of the microbial community with some limitations (Zelles 1999) and the total PLFA content (∑ PLFAs) is a proxy of the living microbial biomass (Frostegård et al. 1991).
2) Amino sugars make up microbial cell walls and are more persistent to decomposition as their polymers need to be broken up first and the resulting amino sugars are likely stabilised in soil (Amelung 2001, 2003; Glaser et al. 2004; Lauer et al. 2011; Miltner et al. 2012). Thus, they reflect mainly microbial necromass (Glaser et al. 2004; Glaser and Gross 2005; Parsons 1981). Prokaryotic bacterial cell walls consist of peptidoglycan, a polymer of N-acetylglucosamine (GlcN) and N-acetylmuramic acid (MurAc), while fungi produce chitin, an (N-acetyl) glucosamine polymer, and galactosamine (GalN) (Amelung 2001; Engelking et al. 2007; Glaser et al. 2004). The ratios of amino sugars to MurAc are used to qualitatively assess long-term changes in the microbial community composition (Glaser et al. 2004).

This work aims at better describing subsoil hotspots and their heterogeneity *in situ* through characterising functional microbial groups. We hypothesised that different biopore types featured deviating abiotic (e.g. water fluctuations, pH) and biotic factors (e.g. C content and C quality) causing a strongly different microbial community composition. However, our study mainly focussed on biotic controls to link C dynamics with microbial community composition. We assumed that the frequent C input by earthworms would lead to microbial communities adapted to abundant fresh C, i.e. mainly enrichment of Gram-negatives (Bird et al. 2011; Gunina et al. 2014; Treonis et al. 2004), while the one-time C input by roots would promote communities of more complex SOM degraders, i.e. mainly

Gram-positives including actinobacteria (Kramer and Gleixner 2008). Furthermore, we hypothesised that the necromass pattern would reflect the recent community pattern. Biopore wall coatings were sampled from root pores, earthworm pores and their combination in the subsoil and were analysed for broad taxonomic groups of microorganisms (PLFAs) and microbial residue composition (amino sugars).

2.3.2 Material and methods

The study site was the Campus Klein-Altendorf experimental research station near Bonn, Germany. The site is characterised by a maritime climate with temperate humid conditions (9.6 °C mean annual temperature, 625 mm annual precipitation). The soil type is a Haplic Luvisol (Hypereutric, Siltic) developed from loess, resulting in a loamy soil with high silt content (IUSS Working Group WRB 2008). C contents of the bulk soil were 0.41 ± 0.02% and 0.35 ± 0.05% for the 45–75 cm and the 75–105 cm layers, respectively. The soil was comprehensively described by Vetterlein et al. (2013). These layers were chosen according to the ploughing depth and our definition of the subsoil, i.e. the soil below the ploughed (Ap) horizon. In this field, the ploughing depth was 30 cm and we added another 15 cm to safely exclude any effects related to plough pans.

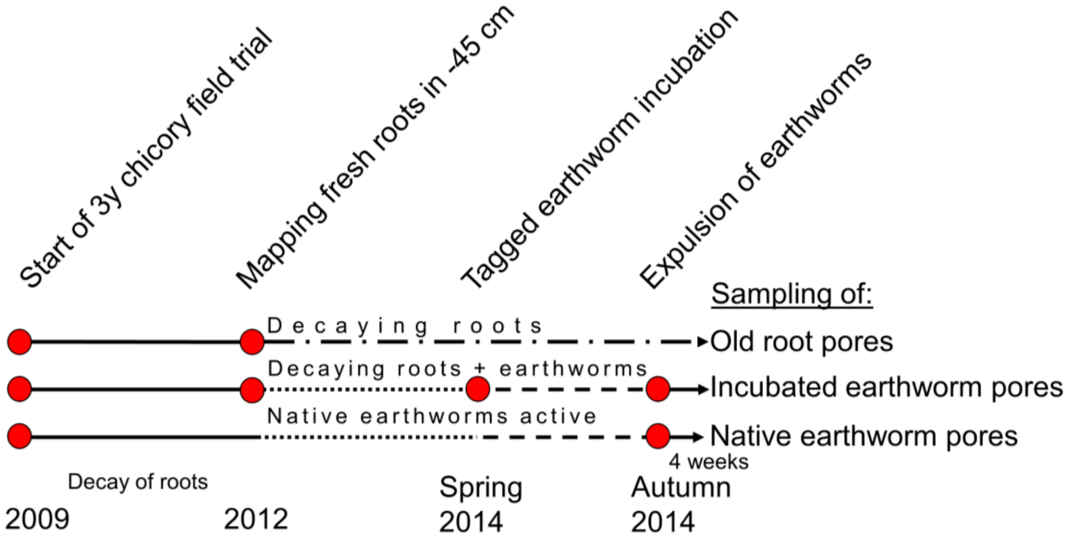
Start of 3y chicory field trial
Mapping fresh roots in -45 cm
Tagged earthworm incubation
Expulsion of earthworms
Sampling of:
Decaying roots
Old root pores
Decaying roots + earthworms
Incubated earthworm pores
Native earthworms active
Native earthworm pores
4 weeks
Decay of roots
2009
2012
Spring 2014
Autumn 2014

Fig. 1 *Timeline of the experiment. Chicory was grown for three consecutive years (2009-2012), followed by two years during which the three biopore types differentiated*

The preparation for the experiment started in 2009: common chicory (Cichorium intybus L., var. Puna) was grown for three consecutive years (2009–2012), inducing many roots in the subsoil. In 2012, the topsoil down to 45 cm depth was removed and different biopore types were induced by the experimental setup: old root pores, earthworm-incubated root pores and native earthworm pores (Fig. 1).

1) Old root pores: after excavating the topsoil in 2012, transparent plastic films were put onto the soil surface prepared in 45 cm depth. The locations of only fresh and live chicory roots ≥ 5 mm were manually mapped on plastic films by a permanent marker. Large nails were also pushed into the soil – marking the positions of the plastic films, which were then taken off the surface. The topsoil was filled back and the plots were kept fallow, i.e. weeds were manually removed, until the sampling in autumn 2014 to allow the decay of the chicory roots. For the sampling, the topsoil was removed again and the plastic films were put back onto the soil surface in 45 cm depth and aligned to match the locations of the nails. This allowed relocation of the now decayed roots. Since the last C input was the plant roots and the last input predominantly drives the microbial community differentiation, the simplified term root pores is used herein. Although these pores did not contain visible root tissue anymore, their environment can be described as detritusphere as this pore type showed enrichment in suberin and lignin (data not shown).
2) Earthworm-incubated pores: in spring 2014 after 1.5 years of fallow and root decomposition, per replicate more than twenty-five pores, which previously contained chicory roots, were incubated with tagged earthworms (Lumbricus terrestris L.). For the tagging, a red elastomer tag was injected into the earthworm body (Butt and Lowe 2007). The incubation was performed by placing tubes (8 mm diameter) containing the tagged earthworms onto the pores' opening at 45 cm depth, adding the topsoil again, and then removing the tube, thus creating a void. Earthworms were fed for 6 months with clover-grass put on the soil surface until sampling of biopores in autumn 2014. The number of earthworms incubated was chosen to be comparable to the native earthworm abundance. The pore history is well known: only 1.5 years-old root channels of chicory were incubated with earthworms of one species and fed with known food sources. Only pores were selected from which the tagged earthworms were expelled in 45 cm depth. Thus, this pore type's full description is 'root biopores incubated with earthworms for six months', or in short, earthworm-incubated pores.
3) Native earthworm pores were treated similarly to the incubated earthworm pores, i.e. the sites were kept fallow from 2012, grass-clover litter was regularly added to the soil surface for six months from spring 2014 and they were expelled in autumn 2014. For this, a horizontal soil surface was prepared in 45 cm depth and covered with plant litter for three full days. Pores with visible earthworm middens were considered colonised with native

earthworms and labelled. We assumed this pore type to be representative of the average native earthworm population in this field. Despite the large majority of earthworms identified being L. terrestris, colonisation by different earthworm species cannot be fully excluded.

4) Bulk soil samples, i.e. soil not containing any biopores, were taken from the sides of the profile wall.

In September 2014, a trench was dug next to the plots with an excavator to facilitate sampling. The location of each pore opening on the soil surface in 45 cm was labelled with a tiny flag and the soil around the pore was manually removed down to 75 cm. Each pore was opened vertically with a knife and samples were taken by carefully shaving off the inner wall coating using micro spatulas (Andriuzzi et al. 2013). Only pores with a minimum diameter of 4 mm were selected. Thirty-two samples were taken: four replicates were taken from each of the four treatments (three biopore types; bulk soil) and from two subsoil depths (45–75 cm; 75–105 cm). Sample material for each treatment combination was pooled from about 25 pores. All samples were stored at 5 °C until PLFA extraction, within three weeks. Sample material not required for the PLFA analysis was then dried at 60 °C for 48 hours to determine the soil moisture and amino sugar contents.

2.3.2.1 Phospholipid fatty acid analysis

Phospholipids were extracted by a method modified after Frostegård et al. (1991). All chemicals were of at least p.a. grade and obtained from Sigma-Aldrich Munich, Germany. Prior to extraction 25 µg of the first internal standard (IS 1) phosphatidyl cholinedinonadecanoic acid (Larodan, Sweden) was added to each sample, and additionally for the neutral lipid fraction 25 µg of dodecanoic acid triglyceride (1 µg μl^{-1}; Sigma-Aldrich Munich, Germany). About 3.5 g fresh pore wall material and 6 g of bulk soil were extracted twice with a solution of methanol, chloroform and citrate/KOH buffer (pH 4, v:v:v = 1:2:0.8) (Bligh and Dyer 1959). Following purification of phospholipids by solid phase extraction (SPE), derivatisation to fatty acid methyl esters (FAMEs) was by hydrolysation by NaOH in MeOH for 10 min at 100 °C and subsequent methylation by BF3 in MeOH (~ 1.25 M) at 80 °C for 15 min. Samples were transferred to autosampler vials after adding 15 µg of the second internal standard (IS 2; 1 µg μl^{-1}) tridecanoic acid methyl ester and measured by the GC-MS system (GC5890 with MS 5971A, Agilent Waldbronn, Germany) with a 45 m DB5-MS column (5%-Phenyl)-methylpolysiloxane, 0.25 mm I.D., 0.25 µm film thickness; Agilent Waldbronn, Germany). Stock solutions containing external standards of 27 fatty acids and IS 1 with fatty acid contents of 1, 4.5, 9, 18 and 24 µg were derivatised and measured together with the samples. The relation between the integrated peak area of each FAME and the peak area of the IS 2 was calculated. Calibration lines were determined by a linear regression from the external standard substances at five different concentrations. The quantifications of each FAME considered the losses during the sample preparation, which were corrected for by the recovery of the IS 1. The GC parameters were as follows: injection was splitless, the inlet temperature was set to 270 °C and the detector temperature to 280 °C. Column head pressure was kept constant at 0.79 bar. The initial oven temperature was 80 °C, held for 1.5 min, then increased at 10 °C min^{-1} to 167 °C and further at 0.7 °C min^{-1} to 196 °C, and finally at 10 °C min^{-1} to 300 °C and held for 8 min. The MS parameters were: Scan mode, m/z 50–550 and 1.5 cycles per second.

Single fatty acids are assigned to broad microbial groups but the relationship between the groups and the fatty acids may not be 100% accurate, e.g. because the classification of marker fatty acids to taxa comes from pure culture studies (Zelles 1999). Thus, redundancies and mismatches, e.g. due to changing environmental conditions, might occur and only cultivatable taxa are used for the classification (Frostegård et al. 2011). Briefly, branched PLFAs represent Gram-positive, while monounsaturated PLFAs mostly represent Gram-negative bacteria. Actinobacteria produce 10-methyl-branched PLFAs, whereas polyunsaturated PLFAs represent eukaryotes and PLFA 18:2ω6,9 fungi (Drenovsky et al. 2004; Fierer et al. 2003; Frostegård and Bååth 1996; Harwood and Russell 1984; Zelles 1997).

2.3.2.2 Neutral lipid analysis

During the PLFA purification, the neutral lipid fraction was collected from the SPE columns using 5 ml chloroform and subsequently derivatised like the PLFA samples. The PLFA 16:1ω5 represents arbuscular mycorrhiza fungi (AMF), but it may also be derived from Gram-negative bacteria. Therefore, Olsson (1999) suggested that the ratio of the storage lipid NLFA 16:1ω5 and the phospholipid PLFA 16:1ω5 is a more sensitive indicator for AMF. A ratio of PLFA/NLFA < 1 indicates Gram-negative origin of the PLFA 16:1ω5, while PLFA/NLFA > 1 is indicative for AMF.

2.3.2.3 Total bacterial biomass and fungal: bacterial biomass ratio

Total bacterial biomass was calculated as the sum of all bacterial PLFAs. The ratio of PLFA 18:2ω6,9 to bacterial PLFAs represents the fungal: bacterial biomass ratio in soils (Frostegård and Bååth 1996).

2.3.2.4 Amino sugar analysis

Amino sugars were extracted by a method modified after Zhang and Amelung (1996). All chemicals of at least p.a. grade were obtained from Sigma-Aldrich, Munich, Germany. About 450 mg of each dried and ground soil sample, containing ~ 0.3 mg N, were subjected to hydrolysis by 6 M HCl under N2 atmosphere for 8 h at 105 °C, filtration through glass fibre filters (Whatman GF6, GE Healthcare, Pittsburgh, PA, U.S.A), drying by a rotary evaporator with removal of the remaining acid. One hundred µg methylglucamine (MeGlcN) were added as the first internal standard (IS 1) after neutralisation. For the removal of iron and salts, pH was adjusted to 6.6–6.8 by KOH and centrifuged at 2000 g for 15 min. The supernatant was taken and lyophilized. Amino sugars were extracted from this by anhydrous methanol. Derivatisation to aldononitrile acetates was by the derivatisation reagent 32 mg ml^{-1} hydroxylamine hydrochloride and 40 mg ml^{-1} 4-(dimethylamino) pyridine in pyridine-methanol (4:1 v/v) for 30 min at 75 - 80 °C. Samples were then reheated for 30 min after adding 1 ml of acetic anhydride. Excess derivatisation agents were removed by three washing steps after addition of 2 ml dichloromethane, first by 6 M HCl and subsequently twice by 1 ml of deionised water. The organic phase was then dried under N2 and dissolved in 185 µl ethyl acetate-hexane (1:1), and 15 µl of second internal standard tridecanoic acid methyl ester (1 µg ml-^{1}) in ethyl acetate-hexane (1:1) were added. Compounds were separated gas chromatographically on a 30 m OPTIMA® 17 column (phenylmethyl polysiloxane, 50 % phenyl, 0.25 mm I.D., 0.50 µm film thickness; Macherey-Nagel, Dueren, Germany) followed by flame ionisation detection (GC-FID system Agilent GC7820A, Waldbronn, Germany). The split ratio was set to 1:10, injector temperature was 250 °C, the detector temperature was 300 °C and column flow was kept constant at 1.1 ml min^{-1}. The oven temperature programme was set as follows: initial temperature was 120 °C, held isothermal for 1 min, then increased at 5 °C min^{-1} to 250 °C, held for 2 min and increased at 10 °C min^{-1} to the final temperature 280 °C, which was held for 10 min. Peak identification was performed by analysing retention times of single amino sugar standards. Stock solutions of external standards of the amino sugars GlcN, GalN, MurAc and MeGlcN containing amounts of 25, 50, 125, 250 and 500 µg were derivatised and measured together with the samples. The relation between the peak area of each amino sugar and the peak area of the IS 2 was calculated. By a linear regression of five external standards' peak areas and their concentrations, analytes were quantified. The recovery rate was determined based on the peak area of the IS 1 and applied to the quantifications of the amino sugars.

2.3.2.5 C and N contents and δ^{13}C determination

For the analysis of C and N contents and δ^{13}C values, 40–50 mg of dried and ground sample were filled into 12 mm tin capsules (IVA, Meerbusch, Germany). The samples were measured on the FLASH 2000 CHNS/O Elemental Analyser (Thermo Fisher Scientific, Cambridge, United Kingdom) coupled by a ConFlo III interface to the Delta V Advantage isotope ratio mass spectrometer (both Thermo Fisher Scientific, Bremen, Germany). δ^{13}C may act as a proxy for SOM quality, as during SOM decomposition $\delta^{13}C$ increases as ^{12}C is preferentially lost (Werth and Kuzyakov 2010).

2.3.2.6 Statistical analyses

Outliers between field replicates were identified using Nalimov's test (Lozán and Kausch 1998). No more than one replicate was removed by the outlier test. In case only three values were available, no outlier test was carried out. Through factor analysis, microbial groups of similar statistical behaviour according to factor loadings (> 0.7) and algebraic sign were determined based on the normalised data set. Thus, ubiquitous and plant-derived fatty PLFAs were excluded from the statistical analysis. One-way analyses of variance (ANOVA) were carried out for each depth and significances were calculated by Tukey's Honest Significance Difference test on $\alpha < 0.05$ level. Levene's test was used to test for homogeneous variances. Normality of the residues was visually checked in Q-Q plots. No bulk soil data was included in the ANOVA as the assumptions were not met due to missing normal distribution of residues and missing data, so only trends regarding bulk soil were reported. All data were given as percent of Σ PLFAs, except for the two summative parameters Σ PLFAs g^{-1} soil and Σ PLFAs g^{-1} SOC. PLFA contents were normalised to SOC to express the microbial colonisation of the organic matter. Pairwise t-tests for dependent samples were used to determine differences between soil depths within each pore type. Error bars in all charts were calculated as standard errors of means (SEM). The contributions of the factors pore type, depth and their interactions to the total variance were calculated by dividing the factor's type III sum of squares by the total sum of type III sum of squares.

Constrained redundancy analysis (RDA) was performed on the relative abundances of the PLFA data set showing statistically relevant behaviour in the factor analysis, and the three explanatory environmental variables TOC, TON and $\delta^{13}C$. Response scores are reported herein as weighted average scores and type I scaling plots are shown. The RDA was performed in Addinsoft XLSTAT 2015 (Addinsoft SARL, Paris, France).

For the analysis of similarities (ANOSIM), the PLFA data set showing statistically relevant behaviour was taken. ANOSIM tests if datasets are significantly different in their species composition, i.e. the PLFA fingerprints as markers for microbial groups. A Bray-Curtis similarity matrix was calculated, which was then used to calculate the non-parametric ANOSIM. P values reported herein for ANOSIM are Bonferroni-corrected sequential p values. For this analysis, PAST 3.08 was used (Hammer et al. 2001).

For the amino sugar data, non-parametric Kruskal-Wallis ANOVAs were calculated for each depth due to missing homoscedasticity, followed by post-hoc comparisons of

Table 1 *Summary of the PLFA data, including complimentary data: Mean values (± SEM) are given. Different letters indicate statistically significant differences. Lowercase letters indicate parameters from 45–75 cm, while uppercase letters indicate parameters from 75105 cm. Differences between soil depths are significant on * = p < 0.05 – given next to the lower depth letters*

	Root pores		**EW-incubated pores**		**Earthworm pores**		**Bulk soil**	
	45–75 cm	**75–105 cm**	**45–75 cm**	**75–105 cm**	**45–75 cm**	**75–105 cm**	**45–75 cm**	**75–105 cm**
Total organic carbon [%]	0.81 ± 0.03^{b}	0.93 ± 0.06^{A}	1.16 ± 0.04^{c}	1.07 ± 0.04^{A*}	1.17 ± 0.05^{c}	1.05 ± 0.04^{A}	0.41 ± 0.02^{a}	0.35 ± 0.05^{B}
Total organic nitrogen [%]	0.09 ± 0.00^{b}	0.10 ± 0.01^{A}	0.12 ± 0.00^{c}	0.11 ± 0.01^{A}	0.11 ± 0.00^{c}	0.10 ± 0.01^{A}	0.06 ± 0.00^{a}	0.05 ± 0.00^{B*}
C : N	8.6 ± 0.2^{a}	9.7 ± 0.5^{A}	9.6 ± 0.1^{b}	9.9 ± 0.4^{A}	10.3 ± 0.2^{c}	10.3 ± 0.5^{A}	7.2 ± 0.1^{d}	7.7 ± 0.9^{A}
$\delta^{13}C$ [‰]	-25.66 ± 0.46^{ab}	-23.87 ± 1.17^{A}	-26.47 ± 0.21^{a}	-25.55 ± 0.51^{A}	-25.30 ± 0.25^{ab}	-23.76 ± 0.66^{A}	-25.00 ± 0.05^{b}	-23.51 ± 0.75^{A}
Σ PLFAs [µg g^{-1} soil]	16.65 ± 1.04^{a}	23.02 ± 3.30^{A}	33.51 ± 2.13^{b}	25.48 ± 9.11^{A}	36.61 ± 3.43^{b}	26.42 ± 3.85^{A}	1.09 ± 0.46†	0.70 ± 0.12†
Σ PLFAs [mg g^{-1} SOC]	2.05 ± 0.09^{a}	2.20 ± 0.02^{A}	2.89 ± 0.18^{b}	3.24 ± 0.59^{A}	3.14 ± 0.31^{b}	2.57 ± 0.45^{A}	0.36 ± 0.08†	0.197 ± 0.04†
Σ bacterial PLFAs [mg g^{-1} SOC]	1.09 ± 0.05^{a}	1.35 ± 0.11^{A}	1.45 ± 0.10^{b}	1.69 ± 0.32^{A}	1.56 ± 0.14^{b}	1.31 ± 0.24^{A}	0.12 ± 0.06^{c}	0.03 ± 0.01^{B}
Fungal : bacterial biomass [%]	3.6 ± 0.3^{a}	2.3 ± 0.5^{A}	8.2 ± 0.9^{b}	4.4 ± 0.1^{A}	4.9 ± 1.7a^{b}	4.1 ± 1.2^{A}	0.0 ± 0.0^{c}	*
(NLFA: PLFA) 16:1ω5	6.56 ± 0.75^{a}	5.03 ± 0.85^{A}	3.30 ± 0.32^{b}	2.85 ± 0.69^{A}	3.23 ± 0.34^{b}	3.10 ± 0.53^{A}	*	*

* too many missing data
† not tested, assumptions not

mean ranks of all pairs of groups (Kruskal-Wallis test). Error bars reported are SEM. Wilcoxon matched pair tests for dependent samples were used to determine differences between soil depths within each pore type. All other statistical analyses were performed in Statsoft Statistica Version 12.5 (StatSoft Inc., Tulsa, OK, U.S.A.).

2.3.3 Results

Σ PLFAs g^{-1} soil was similar between the two soil depths, indicating constant microbial biomass irrespective of depth (Table 1; Online Resource 1). This was also true for Σ PLFAs g^{-1} SOC (Table 1; Fig. 2). There was a close correlation between Σ PLFAs and SOC content ($R^2 = 0.85$, $p < 0.001$). Earthworm-influenced pores, i.e. after six months of earthworm presence (2.89 ± 0.18 mg g^{-1} SOC) and native earthworm pores (3.14 ± 0.31 mg g^{-1} SOC) showed ~ 33% higher PLFA amounts in 45–75 cm than root pores (2.05 ± 0.09 mg g^{-1} SOC) and ~ 8.5 times higher PLFA amounts than bulk soil (0.36 ± 0.08 mg g^{-1} SOC) (Fig. 2). Significant differences were mainly found between biopore types in 45–75 cm, indicating that pore genesis gets less relevant with depth when gradients to bulk soil increase. However, the Σ PLFAs g^{-1} SOC increased with depth in root pores and the earthworm-incubated pores (2.2 ± 0.02 mg g^{-1} SOC and 3.24 ± 0.59 mg g^{-1} SOC). Biopores in both soil depths had on average 7.5–13.5 times higher Σ PLFAs g^{-1} SOC than bulk soil (Fig. 2).

2.3.3.1 Microbial community composition

Grouping of PLFAs to functional microbial groups was achieved by combining factor analysis of the PLFA contents and literature data (Apostel et al. 2013; Gunina et al. 2014). Mean values of total bacterial biomass followed the pattern of Σ PLFAs not showing any differences between pore types in 75–105 cm (Table 1). Two distinct groups of Gram-positive bacteria (based on a15:0; i15:0 and i17:0) and one group of actinobacteria (10Me16:0 and 10Me18:0) were identified (Fig. 3). Both Gram-positive groups were predominantly found in root pores, i.e. microhabitats characterised by low amounts of available C. Based on the signature fatty acids 16:1ω7c, 18:1ω7c and cy17:0, one group of Gram-negative bacteria was identified (Fig. 3). In contrast to the Gram-positives, this group was enriched in 45–75 cm in both earthworm pores types compared to root pores and bulk soil (Fig. 3). All three pore types featured a trend towards higher Gram-negative abundance in 75–105 cm compared to 45–75 cm. Earthworm-influenced pores contained higher amounts of saprotrophic fungi (18:2ω6,9) compared to root pores (Fig. 3). For all biopores, fungal abundances decreased with soil depth, which was also represented by the corresponding fungal: bacterial biomass ratios (Table 1). The biomarker PLFA 16:1ω5 had generally lower contents in root pores compared to the other biopores (Fig. 3). However, ratios of NLFA: PLFA 16:1ω5

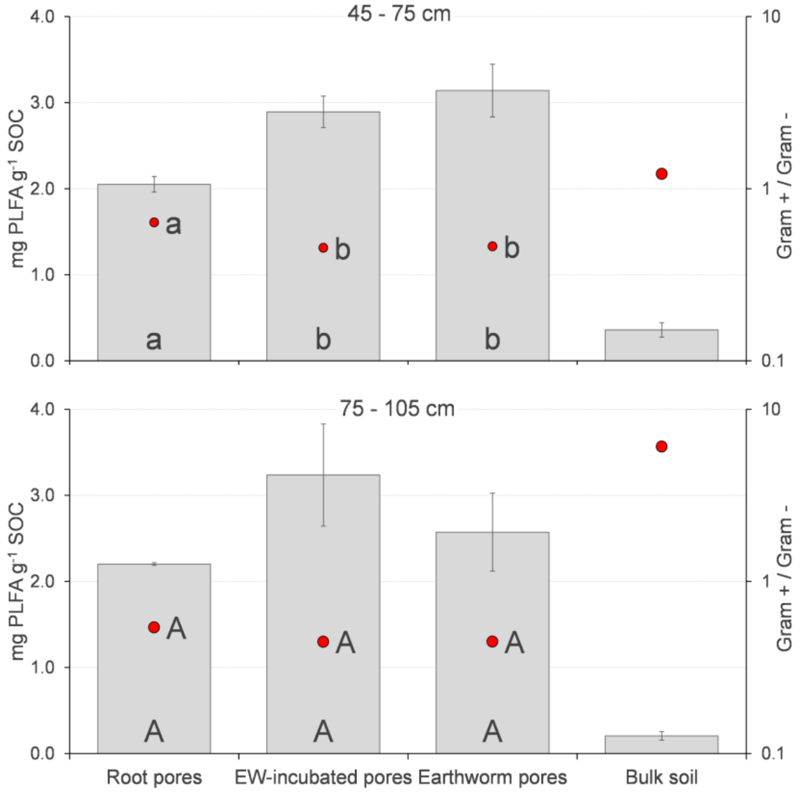

Fig. 2 *Distribution of Σ PLFAs per unit soil organic C in each biopore type (root pores, earthworm-incubated pores, native earthworm pores) and the bulk soil in two subsoil depths (4 samples x 4 treatments x 2 depths) and ratios of Gram-negative PLFAs to Gram-positive PLFAs (top: 45 – 75 cm, bottom: 75 – 105 cm). Bars show Σ PLFAs (left vertical axis), while red circles show the ratios of Σ Gram-positive / Σ Gram-negative PLFAs (right vertical axis, note the logarithmic scale). Mean values (± SEM) are given. Letters indicate significant differences between pore types in each depth ($p < 0.05$). Differences between soil depths were not significant. Σ PLFAs g^{-1} SOC in the three pore types (root pores, incubated pores, native earthworm pores) was in 45–75 cm 7.5 times, and in 75–105 cm 13.5 times higher than in bulk soil. Pores with earthworms showed higher Σ PLFAs g^{-1} SOC than root pores and bulk soil.*

indicated highest arbuscular mycorrhiza fungi contribution in root pores (~ 5.0–6.5, Table 1), and lower AMF contribution to the 16:1ω5 fatty acid in earthworm-influenced pores (~ 3). Higher Gram-negative abundance in earthworm-influenced pores explained the higher 16:1ω5 contents there.

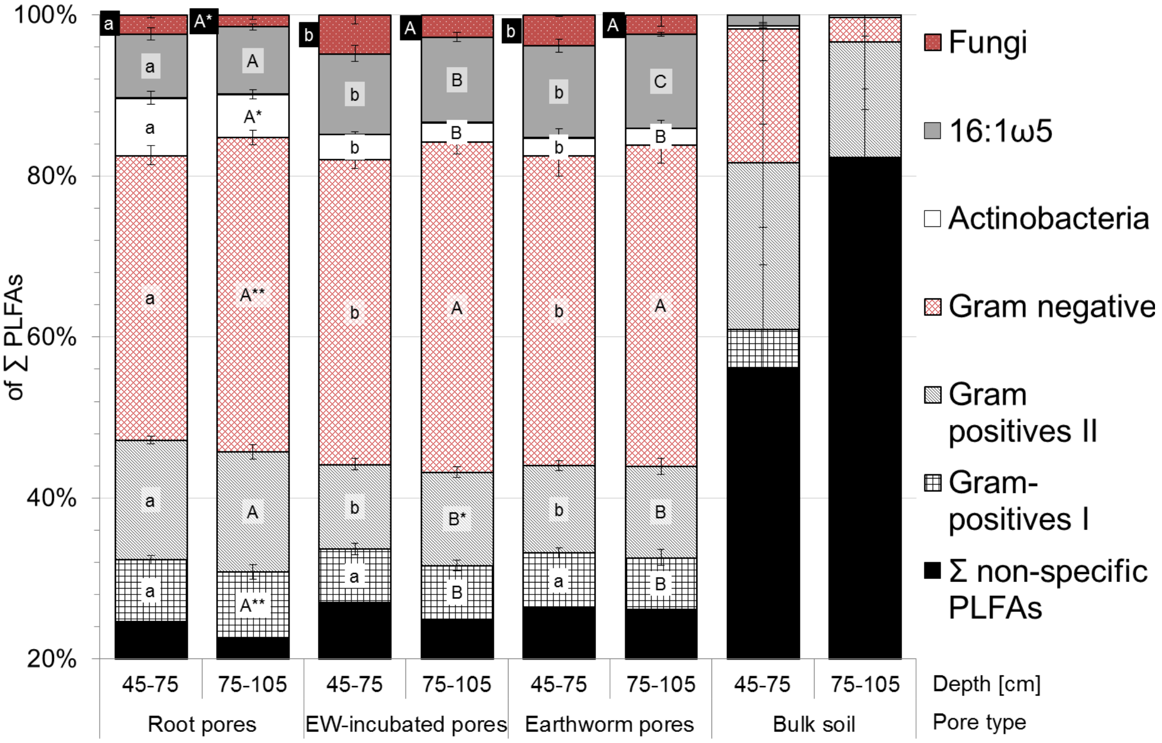

Fig. 3 *Microbial communities in the three biopore types and bulk soil from two subsoil depths (4 samples x 4 treatments x 2 depths): Note the truncated y-axis. Mean values of percentage of Σ PLFAs (± SEM) are given. Letters indicate significant differences between pore types in each depth ($p < 0.05$). Lowercase and uppercase letters indicate 45 – 75 cm and 75 – 105 cm depth, respectively. Differences between soil depths were significant on * = $p < 0.05$ and ** = $p < 0.01$ – given next to the lower depth letters. Gram-positives I and Gram-positives II are both Gram-positive groups, which, however, showed different behaviour in the factor analysis. Root pores featured enrichment of Gram-positives and actinobacteria, whereas both earthworm pore types showed enrichment of Gram-negatives and saprotrophic fungi. Note very high contribution of non-specific PLFAs to bulk soil.*

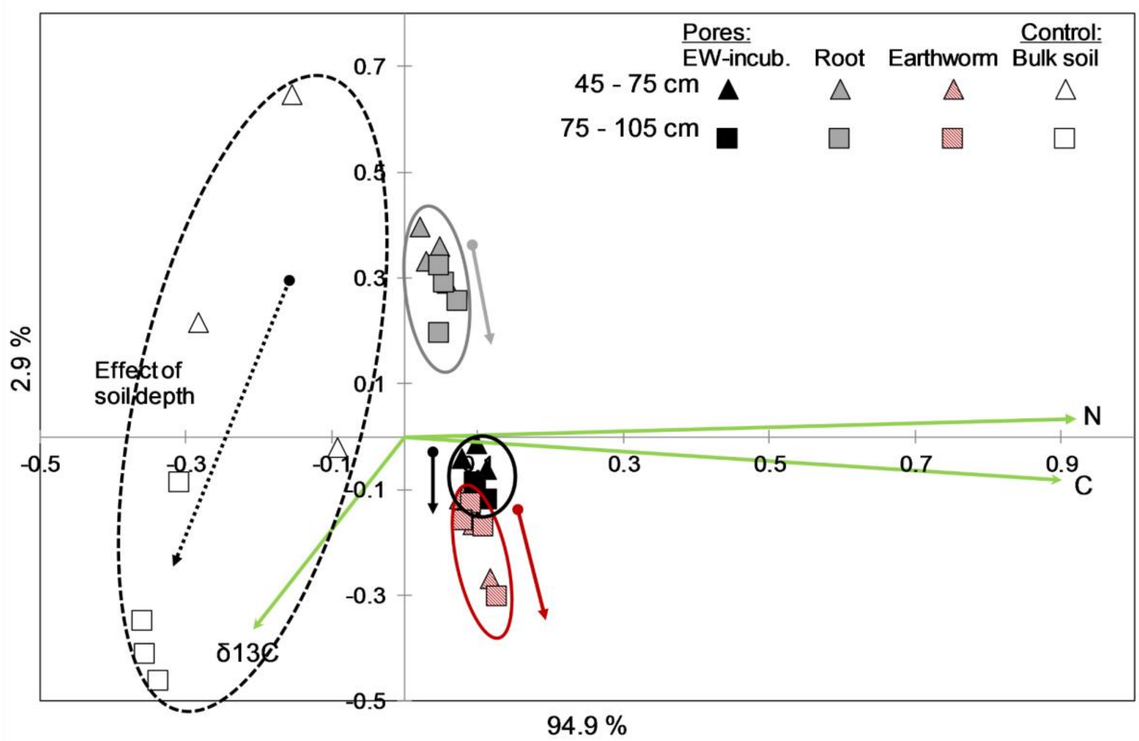

Fig. 4 *Constrained redundancy analysis on the PLFA fingerprints from Fig. 3. Response scores were calculated as weighted average scores. The overall RDA was significant based on 9999 permutations. A type I scaling (distance) plot is shown. Green vectors illustrate the explanatory variables C, N and δ^{13}C. Arrows illustrate the depth effects within a pore type. 48% of inertia is explained by the soil parameters C and N content, δ^{13}C. 52% is explained by other factors (unconstrained).*

The analysis of similarity (Table 2) showed that the microbial community fingerprints of both earthworm biopores were not different from each other, but different to the root pore fingerprint. Bulk soil showed no deviation in community composition from the three pore types. The community differentiation was also discernible in the constrained redundancy analysis (Fig. 4), which explained 48% of the inertia. A strong scattering of the bulk soil community data in the redundancy analysis indicates that bulk soil communities were affected by various biotic and abiotic factors and obviously in some cases also by macroscopically non-visible biopores (Fig. 4). It also clearly showed that the depth affects PLFA composition in bulk soil much more strongly than in the biopores. The depth effect was almost eliminated from the biopores. Both earthworm pore types were overlapping, indicating a high degree of similarity. The variability of each biopore type was smaller than the bulk soil's variability. The three biopores combined variability was also smaller than the bulk soil's. Comparing the constrained RDA with an unconstrained principal components analysis (Online Resource 4), the grouping improved considerably. The x-axis of the RDA, defined by C and N contents, clearly separated biopores from bulk soil. The y-axis defined by δ^{13}C, a proxy for SOM quality, separated the earthworm pores from the root pores.

Variance partitioning showed that most variance (> 60%) of all microbial groups, except Gram-negative and fungi, was explained by the pore type and not by soil depth (Fig. 5).

Table 2 *ANOSIM results: Values reported are Bonferroni-corrected sequential p values based on 9999 permutations on the Bray-Curtis similarity matrix of the lipid fingerprint. Differences between pores were significant on * = p < 0.05 – given next to the lower depth letters. Both earthworm types were similar. Both are, however, different from root pores. The bulk soils were not different from any pore type*

		45–75 cm				75–105 cm			
		Root pores	EW-incubated pores	Earthworm pores	Bulk soil	Root pores	EW-incubated pores	Earthworm pores	Bulk soil
45–75 cm	Root pores								
	EW-incubated pores	*							
	Earthworm pores	*							
	Bulk soil								
75–105 cm	Root pores		*	*	*				
	EW-incubated pores	*				*			
	Earthworm pores	*				*			
	Bulk soil	*	*	*	*	*	*	*	

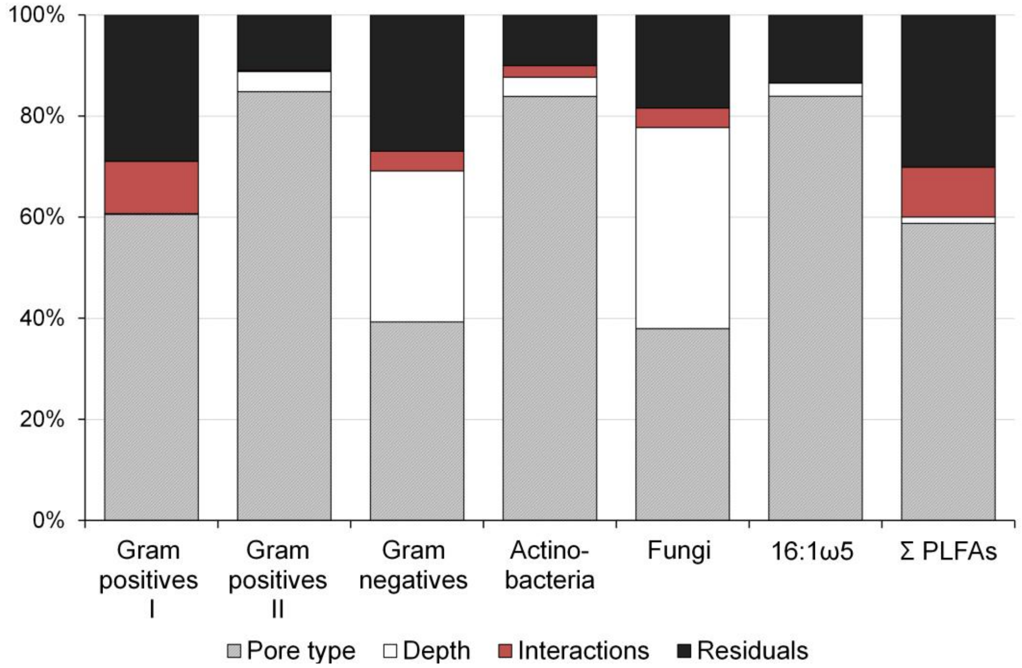

Fig. 5 *Contribution of the factors depth, pore type and their interactions to the total variance of microbial community composition. Bulk soil was not included, i.e. in total 24 samples were analysed. The contribution of the factors and their interactions to the total variance was calculated by dividing the factor's type III sum of squares by the total sum of type III sum of squares. Most variance (40-85%) of microbial groups is explained by the pore type. Gram-negatives and fungi are also influenced by soil depth.*

2.3.3.2 Amino sugars

Total mean amino sugar contents among all treatments were for the 45 - 75 cm depth 1179 ± 183 µg g^{-1}, and for 75–105 cm 1673 ± 214 µg g^{-1}, i.e. an increase of 42% with depth (Table 3; Online Resource 2). Both amino sugar ratios GalN: MurAc and GlcN: MurAc showed no different patterns among biopores (Fig. 6a, b) and gave smaller fungal: bacterial necromass ratios with depth for earthworm and root pores and bulk soil. Muramic acid contents were similar among the biopore types (Table 3). Highest bacterial contribution to the necromass was in bulk soil and earthworm-incubated pores, whereas root pores and earthworm pores showed the highest fungal contribution to the necromass (Fig. 6a, b).

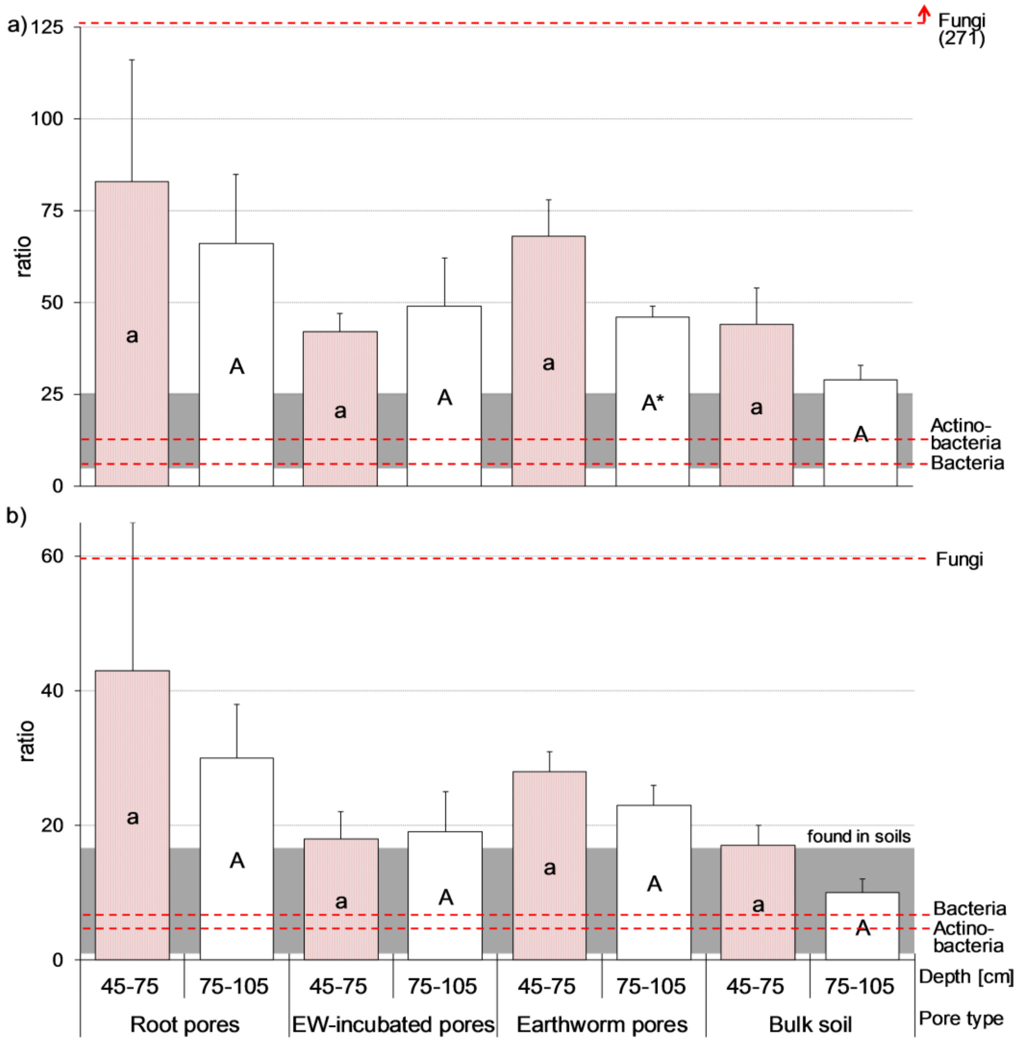

Fig. 6 *Amino sugars ratios of a) glucosamine to muramic acid, and b) galactosamine to muramic acid. Data from 4 samples x 4 treatments x 2 depths. Mean values (± SEM) are given. Letters indicate significant differences between pore types in each depth. Differences between soil depths were significant on * = $p < 0.05$ – given next to the lower depth letters. Red and white bars show 45 – 75 cm and 75 – 105 cm depth, respectively. The shaded areas indicate the ratios found in a broad range of bulk soils and the dashed lines indicate ratios of pure cultures of fungi, bacteria and actinobacteria (data taken from Glaser et al., 2004)). Both ratios represent fungal : bacterial necromass (45–75 cm, 75–105 cm). No pore effects were found.*

*Table 3 Summary of the amino sugar data: Mean values (± SEM) are given. Different letters indicate statistically significant differences. Lowercase letters indicate amino sugar contents for 45 – 75 cm. Uppercase letters indicate 75 – 105 cm. Different letters indicate significant differences. Differences between soil depths are significant on * = $p < 0.05$*

45–75 cm [µg g^{-1} soil]	**Root pores**	**EW-incubated pores**	**Earthworm pores**	**Bulk soil**	
Glucosamine	727 ± 305^{A}	729 ± 57^{A}	1308 ± 296^{A}	544 ± 133^{A}	
Mannosamine	18 ± 2^{A}	23 ± 4^{A}	26 ± 2^{A}	3 ± 1^{A}	
Muramic acid	12 ± 5^{A}	19 ± 2^{A}	22 ± 8^{A}	13 ± 2^{A}	
Galactosamine	225 ± 43^{A}	306 ± 34^{A}	583 ± 167^{A}	203 ± 32^{A}	
Σ	921 ± 264^{A}	1071 ± 86^{A}	1933 ± 464^{A}	762 ± 164^{A}	**1179 ± 183**

75–105 cm [µg g^{-1} soil]					
Glucosamine	1600 ± 340^{b}	$1010 \pm 77^{ab*}$	1230 ± 195^{ab}	606 ± 56^{a}	
Mannosamine	42 ± 13^{a}	11 ± 1^{a}	28 ± 9^{a}	1 ± 0^{a}	
Muramic acid	23 ± 7^{a}	23 ± 4^{a}	25 ± 5^{a}	23 ± 5^{a}	
Galactosamine	776 ± 177^{b}	$394 \pm 83^{ab*}$	605 ± 98^{ab}	209 ± 30^{a}	
Σ	2425 ± 516^{c}	$1517 \pm 79^{ab*}$	1875 ± 296^{b}	838 ± 85^{a}	**1673 ± 214**

2.3.4 Discussion

The decisive factors for the microbial community composition were the biopore history and the biopore properties (Fig. 5). We assumed that the heterogeneous C inputs of varying frequency (root detritus vs. digested shoot biomass of clover-grass) in the pore types have mainly driven the community development (Fig. 3) and that abiotic soil factors like the texture (Sleutel et al. 2012), pH (Rousk et al. 2010) and moisture (Chen et al. 2007) have likely contributed to this community differentiation. Earthworms and roots strongly increased the C contents in the biopores, which led to 26–35 times higher PLFA abundances than in bulk soil (Table 1). This corresponds to a larger living microbial biomass and higher activity (Hoang et al. 2016), which are often linked to increased SOM decomposition rates and C turnover. In contrast, very low PLFA contents in bulk soil indicate lower C turnover but higher mean residence times (Don et al. 2008).

The root pore community fingerprint was unique to the communities of both earthworm pore types (ANOSIM, Table 2), which was also supported by their lower PLFA contents (Fig. 2). Both earthworm pore type fingerprints were not different from each other, suggesting that earthworm activity was the strongest factor for the microbial community composition in the pore walls (Table 2). Especially the earthworm gut taxa influence the microbial composition rather strongly in the casts (Brown 1995; Sampedro and Whalen 2007). Six months of earthworm activities have been long enough to turn a root pore into an earthworm pore regarding the microbial community composition. In this experiment, this pore type was specifically designed to assess the effect of short-term earthworm activity in old root pores. This is also supported by the overlapping of the native earthworm and the earthworm-incubated pores in the RDA plot (Fig. 4).

The PLFA fingerprints remained constant with depth (Table 2), indicating that depth is a minor factor for the microbial community composition in continuous pores due to root detritus and earthworm activities throughout the burrows. The contrast between pores and bulk soil increased with soil depth, as pore PLFA contents remained constant but bulk soil contents decreased with depth. This emphasises the importance of such hot spots, especially in the deeper subsoil. Very comparable findings for the bulk soil and native drilosphere using 16S rRNA gene fingerprinting were reported for the same chicory-planted soil (Uksa et al. 2014). Such mutual validation underlines the power of the PLFA analysis, even though it comes with some pitfalls and uncertainties (Frostegård et al. 2011). The bulk soil PLFA fingerprint was not statistically different from the biopores. This might be explained by the high variability of the bulk soil, especially in 45-75 cm. This high variability might also be caused by small, non-visible biopores in the bulk soil subsample, which may not have been 100% excluded, as compared to the lower subsoil layer. Additionally, due to the C inputs - which are pore-specific, but partly similar - certain microbial groups preferentially grew in pores. Thus, pores can be differentiated from each other, but they are not necessarily different from bulk soil regarding their community composition.

Irrespective of the reasons for this, biopores increase or decrease variability depending on the scale: they increase the overall ecological variability in soil (Ehlers et al. 1983; Stromberger et al. 2012), but among biopores, it is considerably lower and even lower within one biopore. Therefore, different types of biopores presumably increase habitat diversity (as a function of substrate quality, input frequency, moisture, texture, aggregation or pH) – even if individual pores are along their vertical axis less diverse. Vertical variability of one biopore is rather low, as the defining factors e.g. C quality, oxygen availability (Gliński and Lipiec 1990) and moisture controlling their properties remain rather constant along the biopore. The variability between biopores and bulk soil increases with soil depth, as the bulk soils variability decreases while the pore's properties remain constant (Zhou et al. 2002). This increased variability is linked to higher resilience, a classic ecosystem property – in this case attributed to soils (Ponge 2015). As biopores can be re-used, different subsequent crops may cause further variability in e.g. C quality. Likewise, earthworms facilitate the introduction of species from the soil surface into the subsoil.

Multivariate statistics considerably improved the grouping of the principal component analysis (Online resource 4) as soon as the explanatory variable $\delta^{13}C$ was included in the analysis (Fig. 4). $\delta^{13}C$, a proxy accounting for SOM quality and related to turnover and decomposability, separated the upper bulk soil from the lower bulk soil reflecting the increased C processing with depth. However, also the lower bulk soil was clearly separated from the pore habitats by the RDA along the $\delta^{13}C$ vector suggesting a difference in C quality between biopores and bulk soil in 75-105 cm (Dorodnikov et al. 2007; Gunina and Kuzyakov 2014). Thus, the differences in microbial community composition between bulk soil and biopores also depend on SOM decomposability. A clear separation was also visible between root and earthworm-influenced pores which was partially along the $\delta^{13}C$ vector, i.e. explained by SOC quality. However, as the second axis describes a much lower proportion of the variance, this effect is much weaker than the difference between pores and bulk soil. To summarise, biopores featured 26-35 times higher PLFA abundances than bulk soil, and earthworm activities induced microbial communities unique to the root pores within six months.

2.3.4.1 Microbial community composition

Bacterial abundances

The bacterial group patterns are well explained by the organic matter input history and assumed quality. The root pores' most recent input of C was two years prior to sampling, so the more easily degradable C has been largely mineralised, having left behind less available compounds. The two groups of Gram-positive bacteria (I and II) and actinobacteria were enriched in the root pores and in the bulk soil compared to other microbial groups (Fig. 3). Two Gram-positive groups were distinguished as they showed statistically different behaviour from each other (Fig. 3), but more precise taxonomic description is not possible with PLFAs. In both habitats, older, more complex and more processed SOM is expected, of which Gram-positive and actinobacteria are frequently described to be decomposers of (Brant et al. 2006; Heuer et al. 1997; Kramer and Gleixner 2008; McCarthy and Williams 1992). The root pores in 75-105 cm were also significantly drier than the earthworm pores (data not shown). Soil moisture modulates the activity of bacteria, but it is not yet known how the microbial communities react to moisture fluctuations in biopores, e.g. through physiological adaptions to episodic macropore flow (Chen et al. 2007; Lundquist et al. 1999). In the root pores, biofilm-forming bacteria may have endured lower moisture more successfully (Hueso et al. 2012; Vu et al. 2009). However, soil moisture may not strongly affect the soil C stock or its turnover (Aira et al. 2009; Guenet et al. 2012).

Earthworm activities, such as mucus secretion, selective ingestion of plant litter and microbial-rich aggregates, create very distinct habitats (Aira et al. 2009; Lal and Akinremi 1983; Sampedro and Whalen 2007; Stromberger et al. 2012; Tiunov and Dobrovolskaya 2002). Earthworms import fresh labile C into their burrows, which had the highest amount of microbial biomass with a clear predominance of Gram-negative bacteria (Fig. 3). Gram-negatives are thought to be decomposers of easily available organics (Bird et al. 2011; Griffiths et al. 1998; Gunina et al. 2014; Paterson et al. 2007; Treonis et al. 2004). Obviously, the C quality, represented by the $\delta^{13}C$ value, was linked to the abundances of Gram-negative and Gram-positive bacteria. In the course of SOM decomposition, $\delta^{13}C$ increases as the lighter ^{12}C gets preferentially lost (Werth and Kuzyakov 2010), leading to higher abundances of Gram-positives – a pattern also discernible in the RDA plot (Fig. 4). The earthworms' mucus secretion, selective grazing on and selective survival of microorganisms in the presence of gut enzymes increase activities of microbes specialised on earthworm faeces. Sampedro et al. (2006) have shown that the prokaryote population in the earthworm gut was mainly Gram-negative. This is in line with the Gram-negative dominance in the earthworm pores (Fig. 3), as well as our analysis of fresh earthworm casts, which contained predominantly PLFAs representing Gram-negatives (Online Resource 3). Moreover, the resulting environmental conditions in the drilosphere, i.e. higher moisture due to mucus secretion, aggregation and more neutral pH in casts (Brown 1995; Parkin and Berry 1999; Tiunov and Scheu 1999), may also shape the community composition and activity. At higher soil moisture, higher growth rates may be sustained due to a greater diffusion of the limiting C resource (Zhou et al. 2002). While the pH effect on the ∑ PLFA content is often not significant (Rousk et al. 2010), small pH changes likely influence the communities and the abundances of single PLFAs (Bååth and Anderson 2003). Individual groups like fungi might cope better with lower pH (Sleutel et al. 2012), while at more neutral pH growth of bacteria might be promoted. However, we did not assume the pH to change throughout these pores as the earthworms were active in both soil depths and the pH of the bulk soil increased only weakly from 45-75 to 75-105 cm (Vetterlein et al. 2013). Earthworms affect the texture of their burrow wall compared to the bulk soil (Lal and Akinremi 1983), but this effect is likely more pronounced in sandy soils (Zhang and Schrader 1993). The important role of the texture for microbial activity (Bach et al. 2010; Sleutel et al. 2012) may not play a large role in affecting the microbial community in our field site because of the low sand content of about 3.8 %.

After two years of bare fallow and therefore absence of C inputs, the microbial abundance in the root pores was still 8 times higher compared to bulk soil, with a trend towards increased bacterial biomass and significantly increased abundances of Gram-positives 1 and actinobacteria with depth. This may be explained by less decomposed root material in 75–105 cm compared to 45-75 cm, which is supported by an increase in the C content and C/N ratio from 45-75 cm to 75–105 cm (Table 1). The slow and continuous decomposition of roots may have led to the continuous release of bioavailable C over two years (Fontaine et al. 2003; Kuzyakov 2010; Kuzyakov and Blagodatskaya 2015), resulting in increased bacterial PLFAs with depth in both pore types that contained roots. Thus, positive effects of biopores on microbial nutrient cycling and consequently plant nutrition are expected for at least two years. These results are in good agreement with Sanaullah et al. (2016), who incubated root detritus and bulk subsoil for three years. They reported sequential growth of first Gram-negatives and fungi on fresh root detritus, while Gram-positives appeared only much later and were linked to turnover of more processed and native SOM.

Finally, it can be summarised that root pores without fresh C input for 2 years and potentially drier conditions were mainly colonised by general decomposers (Gram-positives, actinobacteria) whereas in earthworm pores featuring recent C inputs, additional moisture and near neutral pH, a higher Gram-negatives abundance was found in 45-75 cm, i.e. degraders of more easily available low molecular weight organic substances. This coincides with the general shift of Gram-negative dominance near the soil surface towards Gram-positive dominance in deeper soil layers as a function of C content, C quality, mean annual temperature and soil moisture (Blume et al. 2002; Franzmann et al. 1998; Kramer and Gleixner 2008; Stromberger et al. 2012).

Fungal abundances

Higher fungal PLFA contributions were found in both earthworm pore types than in root pores in 45-75 cm. This may be connected to a lack of plant residues since fungi are primary decomposers of structural plant material. In the two-year-old root pores, visible cellulose fibres or lignocellulose structures were absent, thus this late decomposition state accounts for the rather low importance of fungi in subsoil root pores (Sanaullah et al. 2016). Regarding earthworm pores, often no increases of fungi relative to bacteria are reported (Devliegher and Verstraete 1997; Stromberger et al. 2012; Tiunov and Scheu 1999).

PLFAs and amino sugar ratios were consistent as both methods returned decreased fungal contribution with depth for almost all treatments (Fig. 3, 6). Consequently, this community shift was present not only in living microflora but had already affected the accumulated microbial necromass. Such a decrease of fungal abundance with depth is common for bulk soils (Fierer et al. 2003; Moll et al. 2015) and mainly explained by a decrease of available C with depth. However, in biopores, where the C content is rather constant throughout the pores because earthworms distribute organic matter vertically (Table 1; Jégou et al. 1998; 2000), this explanation is not valid. Other mechanisms and soil properties which co-regulate the fungal biomass may need to be considered: apart from a change in SOM quality with depth, lower oxygen availability and the promotion of bacterial growth by an increased pH in the bulk soil (6.9 to 7.1) may help explain this pattern in this loess soil.

Comparing the microbial necromass data with the literature, smaller amino sugars to muramic acid ratios have been reported for agricultural soils (Amelung 2001; Engelking et al. 2007; Glaser et al. 2004), indicating that mainly fungal residues make up the microbial necromass in these biopores. The amino sugar ratios GalN : MurAc and GlcN : MurAc were similar among the pore types (Fig. 6a, b), leading to the conclusion that, despite deviating communities, the amount of necromass accumulated during two years of pore wall genesis has not been sufficient yet to achieve a representative imprint of the PLFA pattern on the necromass. The ratio of MurAc: GlcN may be skewed since after the depolymerisation of peptidoglycan a single, yet very strong, ether bond needs to be broken up to convert muramic acid to glucosamine. Such reactions are catalysed by high pH conditions, e.g. found in earthworm guts (Amelung 2001; Millar and Casida 1970; White et al. 1996).

The highest ratios of NLFA: PLFA of 16:1ω5 (value was approximately 6) were found in root pores showing residual storage lipids by former mycorrhization. Lower ratios around 3 were found in pores with earthworm activity (45-75 cm) and thus, 16:1ω5 needs to be interpreted as a Gram-negative marker fatty acid there. We also found PLFA 16:1ω5 in fresh earthworm casts (Online Resource 3) and this further supports the generally high Gram-negative abundance in the earthworm pores (Fig. 3). To sum up, earthworm pores showed highest fungal biomass among treatments, while the ratio of fungal: bacterial necromass was not different between pores and got smaller with depth.

Implications for C turnover in subsoil biopores

The majority of studies on subsoil microbial communities have focused on bulk soils, where C decreases with depth, the localisation of C inputs and biopores are not accounted for and the fluctuations of the environmental conditions are not as strong as near the surface. When the C content remains constant with depth, changing abiotic factors help explain the microbial community composition (Struecker and Joergensen 2015). As similar C contents with depth occur in the investigated biopores, it also likely that soil physical factors such as water fluctuations control the microbial community composition. The root pores in the deeper subsoil were significantly drier than the earthworm pores and this is one of the likely explanations for the higher abundance of biofilm-forming Gram-positives under such circumstance. However, apart from the C content in the pores, the quality of the C input is likely a key factor governing abundances and activities of microbes (Fierer et al. 2003).

In bulk soil, more stable and less bioavailable compounds are usually found in deeper soil (Rumpel and Kögel-Knabner 2011), leading to stronger specialisation of microbial communities compared to the topsoil. It has been suggested subsoil microbial communities were specialised to their environment and distinct from the topsoil communities (Fierer et al. 2003; Moll et al. 2015). This might not be true in the case of biopores as they feature high oxygen availability (Gliński and Lipiec 1990; Stewart et al. 1999), abundant C sources (Hafner and Kuzyakov 2016) and microbes and C distributed nearly homogeneously throughout the pores (Fig. 2, Table 1). Also, biopores have been likened to topsoil due to repeated fresh C inputs (Don et al. 2008). Compared to the bulk soil, microorganisms in biopores live in the 'land of plenty'. Although absolute C contents are not unusually high, they are three times higher than in bulk soil.

Earthworm pores

Earthworms influence larger soil volumes than the 2 mm around their burrows (Don et al. 2008; Jégou et al. 2000; Tiunov and Scheu 1999). However, horizontal diffusion is not an important process in earthworm pores (Don et al. 2008; Schrader et al. 2007), due to higher bulk densities and higher hydrophobicity than in root pores (Lipiec et al. 2015). This hampers C export from the burrow into the bulk soil, creating distinct burrows of C accumulation. Also, this would explain the not decreasing C contents along the vertical extension of the pores, as C contents and bacterial biomass did not change significantly with depth.

It remains to be determined to which degree C stabilisation occurs in earthworm pores (Kögel-Knabner et al. 2008). Long-term stabilisation depends on physical disconnection, sorption on reactive mineral surfaces (Lee 1985; Schmidt et al. 2011) and absence of labile C sources promoting priming (Kuzyakov 2002). Large C inputs, increased moisture and good oxygen supply (Dziejowski et al. 1997; Gliński and Lipiec 1990; Görres et al. 1997) paired with frequent disturbance by the earthworms destabilise organic matter. The mixing of C input with mineral phases during the gut passage may enhance stabilisation. However, no increased adsorption of C on iron oxides by earthworms was found so far (Don et al. 2008). The C sequestration may be favoured in earthworm-incubated pores with higher fungal abundance compared to native earthworm pores. It was hypothesised, that this may be due to improved aggregate formation by hyphae (Rillig et al. 2015; Six et al. 2006), the decomposability of the melanised necromass (Clemmensen et al. 2015) or higher C use efficiency of fungal-dominated communities (Herrmann et al. 2014; Jastrow et al. 2007). Furthermore, extended hyphal networks may help sequester more C by exporting it to the bulk soil. Don et al. (2008) found no evidence of persistent C enrichment, short mean residence times of 3-8 years of earthworm-imported C and also high turnover rates. This does not necessarily contradict C sequestration. Earthworm pores likely indirectly support C sequestration by stimulation of root growth through e.g. soil structure changes and improved nutrient and water supply in subsoils, which in turn increase belowground biomass and C input (Brown 1995). Depending on pore angle, relief, bulk density and moisture, roots growing in earthworm pores also may re-enter the bulk subsoil after having benefitted from higher nutrient supplies in the pore, effectively increasing root biomass in deep soil layers (Athmann et al. 2013; Hirth et al. 2005). To conclude, repeated priming hampers C sequestration, boosts C turnover in the earthworm pores and earthworm pores support C sequestration through large C accumulation and root growth promotion.

Root pores

To sequester high C amounts in the subsoils, deep rooting plants with abundant belowground biomass appear useful (Kell 2012; Lorenz and Lal 2007). Regarding C sequestration, first, the root pore walls may not be as hydrophobic as the earthworm pores (Lipiec et al. 2015), facilitating soluble C export into the bulk soil, where it can be stabilised on mineral surfaces. Second, lateral roots, root hairs and fungal hyphae are likely to leave the root pores and export C into the bulk soil. In contrast, labile C in the earthworm biopores limits the C stabilisation, since priming provides energy for the simultaneous mineralisation of pre-existing, possibly more complex compounds (Fontaine et al. 2007; Kuzyakov and Blagodatskaya 2015). In the root pores, C input happens only once. As soon as the easily available C is respired, subsoil root C may be stabilised. C stabilisation was already apparent as a large microbial necromass accumulation relative to the bulk soil (75-105 cm; Table 3). For large C sequestration, new root pores are ideally created regularly and pores are cut off from the fresh C supply by e.g. harvesting.

2.3.5 Conclusions

At the heart of discussion on the roles of biopores lies the fundamental issue of promoting C turnover for nutrient supply or promoting C sequestration in unsaturated subsoils. In both cases, microorganisms are key actors and their community composition is one important factor regarding C turnover or microbial necromass production to be stabilised. Microbes in subsoil biopores live in the land of plenty compared to the bulk subsoil due to high C and oxygen supply, resulting in 26-35 times higher PLFA abundances in biopores. Soil depth affected the microbial community composition of the bulk soil much more strongly than of the biopores. The distribution of bacteria and fungi among pore types was an indicator for SOM quality in the pore walls. Decomposers of more complex organic matter (Gram-positives and actinobacteria) had higher abundances in the root pores, whereas the earthworm pores featured fungi and Gram-negatives. Earthworms had strong effects on microbial communities: highest Σ PLFAs and highest amounts of rapidly metabolising Gram-negatives were found for both earthworm pore types and, thus, highest C and nutrient turnover are assumed. Introducing earthworms into decaying root pores influenced the microbial community heavily. The microbial community in these pores was rendered hardly distinguishable from native earthworm pores after six months of earthworm activity.

C turnover is inversely correlated with C sequestration. Therefore, low sequestration per unit of C input is expected in biopores unless C is stabilised in organo-mineral associations, exported to the bulk soil or occluded in aggregates. Earthworm pores support C sequestration through improving root growth in the subsoil. In the root pores, more of the remaining detritus C might be sequestered since no fresh C is repeatedly supplied from the surface. Overall, biopores strongly contribute to C input into subsoils. The functions of C and nutrient turnover, as well as, C sequestration in subsoils depend on the biopore history: earthworm biopores boost C turnover and plant nutrition in the subsoil, whereas root pores may be more responsible for C sequestration because of lacking priming. Biopores contribute to C sequestration directly by 1) large C inputs in the subsoil, 2) mixing with mineral phases for stabilisation, and indirectly 3) by promoting deep root growth, i.e. increasing the total C input into subsoils.

Acknowledgements: This study was supported by the German Research Foundation, grants DFG KU 1184/29-1 and INST 186/1006-1. We would like to thank PD Dr Timo Kautz and the colleagues from Institute of Organic Agriculture of the University of Bonn for establishing and managing the field trial Klein-Altendorf, as well as the Centre for Stable Isotope Research and Analysis, Goettingen, for $\delta^{13}C$ determination.

2.3.6 References

- Aira M, McNamara N, Piearce T, Domínguez J (2009) Microbial communities of Lumbricus terrestris L. middens: structure, activity, and changes through time in relation to earthworm presence. J Soils Sediments 9:54–61
- Amelung W 2001 Methods using amino sugars as markers for microbial residues in soil. In: Lal R, Kimble JM, Follett RF, Stewart BA (eds) Assessment methods for soil carbon; [papers from the International Workshop on "Assessment Methods for Soil C Pools", held at The Ohio State University, Columbus Ohio, in November 1998]. Lewis, Boca Raton, FL, USA, pp 233–272
- Amelung W (2003) Nitrogen biomarkers and their fate in soil. J. Plant Nutr. Soil Sci. 166:677–686
- Andriuzzi WS, Bolger T, Schmidt O (2013) The drilosphere concept. Fine-scale incorporation of surface residue-derived N and C around natural Lumbricus terrestris burrows. Soil Biol Biochem 64:136–138
- Apostel C, Dippold MA, Glaser B, Kuzyakov Y (2013) Biochemical pathways of amino acids in soil: Assessment by position-specific labeling and 13C-PLFA analysis. Soil Biol Biochem 67:31–40
- Athmann M, Kautz T, Pude R, Köpke U (2013) Root growth in biopores—evaluation with in situ endoscopy. Plant Soil 371:179–190
- Bååth E, Anderson T-H (2003) Comparison of soil fungal/bacterial ratios in a pH gradient using physiological and PLFA-based techniques. Soil Biol Biochem 35:955–963. http://www.sciencedirect.com/science/article/pii/S0038071703001548
- Bach EM, Baer SG, Meyer CK, Six J (2010) Soil texture affects soil microbial and structural recovery during grassland restoration. Soil 42:2182–2191
- Bird JA, Herman DJ, Firestone MK (2011) Rhizosphere priming of soil organic matter by bacterial groups in a grassland soil. Special Issue: Knowledge gaps in soil C and N interactions. Soil Biol Biochem 43:718–725
- Bligh EG, Dyer WJ (1959) A rapid method of total lipid extraction and purification. Can. J. Biochem. Physiol. 37:911–917
- Blume E, Bischoff M, Reichert JM, Moorman T, Konopka A, Turco RF (2002) Surface and subsurface microbial biomass, community structure and metabolic activity as a function of soil depth and season. Appl Soil Ecol 20:171–181
- Bouché MB 1975 Action de la faune sur les états de la matière organique dans les écosystèmes. In: Gilbertus K, Reisinger O, Mourey A, Cancela da Fonseca JA (ed) Biodegradation et Humification. Pierron Editeur, Sarreguemines, France, pp 157–168
- Brant JB, Sulzman EW, Myrold DD (2006) Microbial community utilization of added carbon substrates in response to long-term carbon input manipulation. Soil Biol Biochem 38:2219–2232
- Brown GG (1995) How do earthworms affect microfloral and faunal community diversity? Springer. Dordrecht, Netherlands
- Butt KR, Lowe CN (2007) A viable technique for tagging earthworms using visible implant elastomer. Appl Soil Ecol 35:454–457

- Chen M-M, Zhu Y-G, Su Y-H, Chen B-D, Fu B-J, Marschner P (2007) Effects of soil moisture and plant interactions on the soil microbial community structure. Eur J Soil Biol 43:31–38
- Clemmensen KE, Finlay RD, Dahlberg A, Stenlid J, Wardle DA, Lindahl BD (2015) Carbon sequestration is related to mycorrhizal fungal community shifts during long-term succession in boreal forests. New Phytol 205:1525–1536
- Devliegher W, Verstraete W (1997) Microorganisms and soil physico-chemical conditions in the drilosphere of Lumbricus terrestris. Soil Biol Biochem 29:1721–1729
- Don A, Steinberg B, Schöning I, Pritsch K, Joschko M, Gleixner G, Schulze E-D (2008) Organic carbon sequestration in earthworm burrows. Soil Biol Biochem 40:1803–1812
- Dorodnikov M, Fangmeier A, Kuzyakov Y (2007) Thermal stability of soil organic matter pools and their δ13C values after C3–C4 vegetation change. Soil Biol Biochem 39:1173–1180
- Drenovsky RE, Elliott GN, Graham KJ, Scow KM (2004) Comparison of phospholipid fatty acid (PLFA) and total soil fatty acid methyl esters (TSFAME) for characterizing soil microbial communities. Soil Biol Biochem 36:1793–1800
- Dziejowski JE, Rimmer A, Steenhuis TS (1997) Preferential Movement of Oxygen in Soils? Soil Sci Soc Am J 61:1607–1610
- Ehlers W, Köpke U, Hesse F, Böhm W (1983) Penetration resistance and root growth of oats in tilled and untilled loess soil. Soil Till Res 3:261–275
- Engelking B, Flessa H, Joergensen RG (2007) Shifts in amino sugar and ergosterol contents after addition of sucrose and cellulose to soil. Soil Biol Biochem 39:2111–2118
- Fierer N, Schimel JP, Holden PA (2003) Variations in microbial community composition through two soil depth profiles. Soil Biol Biochem 35:167–176
- Fontaine S, Barot S, Barre P, Bdioui N, Mary B, Rumpel C (2007) Stability of organic carbon in deep soil layers controlled by fresh carbon supply. Nature 450:277–280
- Fontaine S, Mariotti A, Abbadie L (2003) The priming effect of organic matter. A question of microbial competition? Soil Biol Biochem 35:837–843
- Franzmann PD, Zappia LR, Patterson BM, Rayner JL, Davis GB (1998) Mineralisation of low concentrations of organic compounds and microbial biomass in surface and vadose zone soils from the Swan Coastal Plain, Western Australia. Aust. J. Soil Res. 36:921–940
- Frostegård Å, Bååth E (1996) The use of phospholipid fatty acid analysis to estimate bacterial and fungal biomass in soil. Biol Fertil Soils 22:59–65
- Frostegård Å, Tunlid A, Bååth E (1991) Microbial biomass measured as total lipid phosphate in soils of different organic content. J Microbiol Meth 14:151–163
- Frostegård Å, Tunlid A, Bååth E (2011) Use and misuse of PLFA measurements in soils. Soil Biol Biochem 43:1621–1625
- Glaser B, Gross S (2005) Compound-specific delta13C analysis of individual amino sugars—a tool to quantify timing and amount of soil microbial residue stabilization. Rapid Commun. Mass Spectrom. 19:1409–1416
- Glaser B, Turrión M-B, Alef K (2004) Amino sugars and muramic acid—biomarkers for soil microbial community structure analysis. Soil Biol Biochem 36:399–407

- Gliński J, Lipiec J (1990) Soil physical conditions and plant roots. CRC Press. Boca Raton, FL, USA
- Görres JH, Savin MC, Amador JA (1997) Dynamics of carbon and nitrogen mineralization, microbial biomass, and nematode abundance within and outside the burrow walls of anecic earthworms (Lumbricus terrestris). Soil Sci 162:666–671
- Graff O (1967) Über die Verlagerung von Nährelementen in den Unterboden durch Regenwurmtätigkeit. Landw. Forsch 20:117–127
- Griffiths BS, Ritz K, Ebblewhite N, Dobson G (1998) Soil microbial community structure: effects of substrate loading rates. Soil Biol Biochem 31:145–153
- Guenet B, Lenhart K, Leloup J, Giusti-Miller S, Pouteau V, Mora P, Nunan N, Abbadie L (2012) The impact of long-term CO2 enrichment and moisture levels on soil microbial community structure and enzyme activities. Geoderma 170:331–336
- Gunina A, Dippold MA, Glaser B, Kuzyakov Y (2014) Fate of low molecular weight organic substances in an arable soil: From microbial uptake to utilisation and stabilisation. Soil Biol Biochem 77:304–313
- Gunina A, Kuzyakov Y (2014) Pathways of litter C by formation of aggregates and SOM density fractions: Implications from 13C natural abundance. Soil Biol Biochem 71:95–104
- Hafner S, Kuzyakov Y (2016) Carbon input and partitioning in subsoil by chicory and alfalfa. Plant Soil 406:29–42
- Hammer Ø, Harper D, Ryan P (2001) PAST. Palaeontol Electron 4:9
- Han E, Kautz T, Perkons U, Uteau D, Peth S, Huang N, Horn R, Köpke U (2015) Root growth dynamics inside and outside of soil biopores as affected by crop sequence determined with the profile wall method. Biol Fertil Soils 51:847–856
- Harwood JL, Russell NJ (1984) Lipids in Plants and Microbes. Springer. Dordrecht, Netherlands
- Herrmann AM, Coucheney E, Nunan N (2014) Isothermal microcalorimetry provides new insight into terrestrial carbon cycling. Environ Sci Technol 48:4344–4352
- Heuer H, Krsek M, Baker P, Smalla K, Wellington EM (1997) Analysis of actinomycete communities by specific amplification of genes encoding 16S rRNA and gel-electrophoretic separation in denaturing gradients. Appl. Environ. Microbiol. 63:3233–3241
- Hirth JR, McKenzie BM, Tisdall JM (2005) Ability of seedling roots of Lolium perenne L. to penetrate soil from artificial biopores is modified by soil bulk density, biopore angle and biopore relief. Plant Soil 272:327–336
- Hoang DTT, Pausch J, Razavi BS, Kuzyakova I, Banfield CC, Kuzyakov Y (2016) Hotspots of microbial activity induced by earthworm burrows, old root channels, and their combination in subsoil. Biol Fertil Soils 52:1105–1119
- Hueso S, García C, Hernández T (2012) Severe drought conditions modify the microbial community structure, size and activity in amended and unamended soils. Soil Biol Biochem 50:167–173
- IUSS Working Group WRB (2008) World reference base for soil resources 2006. Ein Rahmen für internationale Klassifikation, Korrelation und Kommunikation. BGR. Hannover

- Jastrow J, Amonette J, Bailey V (2007) Mechanisms controlling soil carbon turnover and their potential application for enhancing carbon sequestration. Climatic Change 80:5–23
- Jégou D, Cluzeau D, Balesdent J, Tréhen P (1998) Effects of four ecological categories of earthworms on carbon transfer in soil. Appl Soil Ecol 9:249–255
- Jégou D, Cluzeau D, Hallaire V, Balesdent J, Tréhen P (2000) Burrowing activity of the earthworms Lumbricus terrestris and Aporrectodea giardi and consequences on C transfers in soil. Eur J Soil Biol 36:27–34
- Jégou D, Schrader S, Diestel H, Cluzeau D (2001) Morphological, physical and biochemical characteristics of burrow walls formed by earthworms. Appl Soil Ecol 17:165–174
- Kautz T (2015) Research on subsoil biopores and their functions in organically managed soils: A review. Renew. Agric. Food Syst. 30:318–327
- Kautz T, Amelung W, Ewert F, Gaiser T, Horn R, Jahn R, Javaux M, Kemna A, Kuzyakov Y, Munch J-C, Pätzold S, Peth S, Scherer HW, Schloter M, Schneider H, Vanderborght J, Vetterlein D, Walter A, Wiesenberg GL, Köpke U (2013) Nutrient acquisition from arable subsoils in temperate climates: A review. Soil Biol Biochem 57:1003–1022
- Kell DB (2012) Large-scale sequestration of atmospheric carbon via plant roots in natural and agricultural ecosystems: why and how. Phil Trans R Soc B 367:1589–1597
- Kögel-Knabner I, Guggenberger G, Kleber M, Kandeler E, Kalbitz K, Scheu S, Eusterhues K, Leinweber P (2008) Organo-mineral associations in temperate soils. Integrating biology, mineralogy, and organic matter chemistry. J. Plant Nutr. Soil Sci. 171:61–82
- Kramer C, Gleixner G (2008) Soil organic matter in soil depth profiles. Distinct carbon preferences of microbial groups during carbon transformation. Soil Biol Biochem 40:425–433
- Kuhlmann H, Baumgärtel G (1991) Potential importance of the subsoil for the P and Mg nutrition of wheat. Plant Soil 137:259–266
- Kuzyakov Y (2002) Review: Factors affecting rhizosphere priming effects. J. Plant Nutr. Soil Sci. 165:382–396
- Kuzyakov Y (2010) Priming effects: Interactions between living and dead organic matter. Soil Biol Biochem 42:1363–1371
- Kuzyakov Y, Blagodatskaya E (2015) Microbial hotspots and hot moments in soil: Concept & review. Soil Biol Biochem 83:184–199
- Lal R, Akinremi OO (1983) Physical properties of earthworm casts and surface soil as influenced my management. Soil Sci 135:114–122
- Lauer F, Kösters R, Du Preez CC, Amelung W (2011) Microbial residues as indicators of soil restoration in South African secondary pastures. Soil Biol Biochem 43:787–794
- Lee KE (1985) Earthworms. Their ecology and relationships with soils and land use. Academic Press. Sydney, Orlando
- Lipiec J, Brzezińska M, Turski M, Szarlip P, Frąc M (2015) Wettability and biogeochemical properties of the drilosphere and casts of endogeic earthworms in pear orchard. Soil Till Res 145:55–61

- Lorenz K, Lal R 2007 The Depth Distribution of Soil Organic Carbon in Relation to Land Use and Management and the Potential of Carbon Sequestration in Subsoil Horizons. In: Sparks DL (ed) Advances in agronomy. Academic Press, San Diego, Calif, London, pp 35–66
- Lozán JL, Kausch H (1998) Angewandte Statistik für Naturwissenschaftler. Parey Buchverlag. Singhofen, Germany
- Lundquist E, Scow K, Jackson L, Uesugi S, Johnson C (1999) Rapid response of soil microbial communities from conventional, low input, and organic farming systems to a wet/dry cycle. Soil Biol Biochem 31:1661–1675
- McCarthy AJ, Williams ST (1992) Actinomycetes as agents of biodegradation in the environment—a review. Gene 115:189–192
- Millar WN, Casida LE (1970) Evidence for muramic acid in soil. Can. J. Microbiol. 16:299–304
- Miltner A, Bombach P, Schmidt-Brücken B, Kästner M (2012) SOM genesis: microbial biomass as a significant source. Biogeochemistry 111:41–55
- Moll J, Goldmann K, Kramer S, Hempel S, Kandeler E, Marhan S, Ruess L, Krüger D, Buscot F (2015) Resource Type and Availability Regulate Fungal Communities Along Arable Soil Profiles. Microb Ecol 70:390–399
- Nakamoto T (2000) The Distribution of Wheat and Maize Roots as Influenced by Biopores in a Subsoil of the Kanto Loam Type. Plant Prod. Sci. 3:140–144
- Nannipieri P, Ascher J, Ceccherini MT, Landi L, Pietramellara G, Renella G (2003) Microbial diversity and soil functions. Eur J Soil Science 54:655–670
- Olsson PA (1999) Signature fatty acids provide tools for determination of the distribution and interactions of mycorrhizal fungi in soil. FEMS Microbiol. Ecol. 29:303–310
- Parkin TB, Berry EC (1999) Microbial nitrogen transformations in earthworm burrows. Soil Biol Biochem 31:1765–1771
- Parsons JW 1981 Chemistry and distribution of amino sugars in soils and soil organisms. In: Paul EA, Ladd JN (eds) Soil Biochemistry, New York, NY, USA, pp 197–227
- Paterson E, Gebbing T, Abel C, Sim A, Telfer G (2007) Rhizodeposition shapes rhizosphere microbial community structure in organic soil. New Phytol 173:600–610
- Perkons U, Kautz T, Uteau D, Peth S, Geier V, Thomas K, Lütke Holz K, Athmann M, Pude R, Köpke U (2014) Root-length densities of various annual crops following crops with contrasting root systems. Soil Till Res 137:50–57
- Ponge J-F (2015) The soil as an ecosystem. Biol Fertil Soils 51:645–648
- Rillig MC, Aguilar-Trigueros CA, Bergmann J, Verbruggen E, Veresoglou SD, Lehmann A (2015) Plant root and mycorrhizal fungal traits for understanding soil aggregation. New Phytol 205:1385–1388
- Rousk J, Brookes PC, Bååth E (2010) The microbial PLFA composition as affected by pH in an arable soil. Soil Biol Biochem 42:516–520
- Rumpel C, Kögel-Knabner I (2011) Deep soil organic matter—a key but poorly understood component of terrestrial C cycle. Plant Soil 338:143–158

- Salome C, Nunan N, Pouteau V, Lerch TZ, Chenu C (2010) Carbon dynamics in topsoil and in subsoil may be controlled by different regulatory mechanisms. Glob Change Biol 16:416–426
- Sampedro L, Jeannotte R, Whalen JK (2006) Trophic transfer of fatty acids from gut microbiota to the earthworm Lumbricus terrestris L. Soil Biol Biochem 38:2188–2198
- Sampedro L, Whalen JK (2007) Changes in the fatty acid profiles through the digestive tract of the earthworm Lumbricus terrestris L. Appl Soil Ecol 35:226–236
- Sanaullah M, Chabbi A, Leifeld J, Bardoux G, Billou D, Rumpel C (2011) Decomposition and stabilization of root litter in top-and subsoil horizons: what is the difference? Plant Soil 338:127–141
- Sanaullah M, Chabbi A, Maron P-A, Baumann K, Tardy V, Blagodatskaya E, Kuzyakov Y, Rumpel C (2016) How do microbial communities in top-and subsoil respond to root litter addition under field conditions? Soil Biol Biochem 103:28–38
- Schmidt MWI, Torn MS, Abiven S, Dittmar T, Guggenberger G, Janssens IA, Kleber M, Kögel-Knabner I, Lehmann J, Manning DAC, Nannipieri P, Rasse DP, Weiner S, Trumbore SE (2011) Persistence of soil organic matter as an ecosystem property. Nature 478:49–56
- Schrader S, Rogasik H, Onasch I, Jégou D (2007) Assessment of soil structural differentiation around earthworm burrows by means of X-ray computed tomography and scanning electron microscopy. Geoderma 137:378–387
- Six J, Frey SD, Thiet RK, Batten KM (2006) Bacterial and Fungal Contributions to Carbon Sequestration in Agroecosystems. Soil Sci Soc Am J 70:555–568
- Sleutel S, Bouckaert L, Buchan D, van Loo D, Cornelis WM, Sanga HG (2012) Manipulation of the soil pore and microbial community structure in soil mesocosm incubation studies. Soil Biol Biochem 45:40–48
- Stewart JB, Moran CJ, Wood JT (1999) Macropore sheath: quantification of plant root and soil macropore association. Plant Soil 211:59–67
- Stromberger ME, Keith AM, Schmidt O (2012) Distinct microbial and faunal communities and translocated carbon in Lumbricus terrestris drilospheres. Soil Biol Biochem 46:155–162
- Struecker J, Joergensen RG (2015) Microorganisms and their substrate utilization patterns in topsoil and subsoil layers of two silt loams, differing in soil organic C accumulation due to colluvial processes. Soil Biol Biochem 91:310–317
- Tiunov AV, Dobrovolskaya TG (2002) Fungal and bacterial communities in Lumbricus terrestris burrow walls. A laboratory experiment. Pedobiologia 46:595–605
- Tiunov AV, Scheu S (1999) Microbial respiration, biomass, biovolume and nutrient status in burrow walls of Lumbricus terrestris. Soil Biol Biochem 31:2039–2048
- Treonis AM, Ostle NJ, Stott AW, Primrose R, Grayston SJ, Ineson P (2004) Identification of groups of metabolically-active rhizosphere microorganisms by stable isotope probing of PLFAs. Soil Biol Biochem 36:533–537
- Uksa M, Fischer D, Welzl G, Kautz T, Köpke U, Schloter M (2014) Community structure of prokaryotes and their functional potential in subsoils is more affected by spatial heterogeneity than by temporal variations. Soil Biol Biochem 75:197–201

- van Groenigen JW, Lubbers IM, Vos HMJ, Brown GG, Deyn GB de, van Groenigen KJ (2014) Earthworms increase plant production: a meta-analysis. Scientific reports 4:6365
- Vetterlein D, Kühn T, Kaiser K, Jahn R (2013) Illite transformation and potassium release upon changes in composition of the rhizophere soil solution. Plant Soil 371:267–279
- Volkmar KM (1996) Effects of biopores on the growth and N-uptake of wheat at three levels of soil moisture. Can. J. Soil. Sci. 76:453–458
- von Luetzow M, Kögel-Knabner I, Ekschmitt K, Matzner E, Guggenberger G, Marschner B, Flessa H (2006) Stabilization of organic matter in temperate soils. Mechanisms and their relevance under different soil conditions - a review. Eur J Soil Sci 57:426–445
- Vu B, Chen M, Crawford RJ, Ivanova EP (2009) Bacterial Extracellular Polysaccharides Involved in Biofilm Formation. Molecules 14:2535–2554. http://www.mdpi.com/1420-3049/14/7/2535/pdf
- Waldrop M, Balser T, Firestone M (2000) Linking microbial community composition to function in a tropical soil. Soil Biol Biochem 32:1837–1846
- Werth M, Kuzyakov Y (2010) 13C fractionation at the root–microorganisms–soil interface: A review and outlook for partitioning studies. Soil Biol Biochem 42:1372–1384
- White GF, Russell NJ, Tidswell EC (1996) Bacterial scission of ether bonds. Microbiol Rev 60:216–232
- Zelles L (1997) Phospholipid fatty acid profiles in selected members of soil microbial communities. Experimental and Theoretical Approaches in Environmental Chemistry. Chemosphere 35:275–294
- Zelles L (1999) Fatty acid patterns of phospholipids and lipopolysaccharides in the characterisation of microbial communities in soil: a review. Biol Fertil Soils 29:111–129
- Zhang H, Schrader S (1993) Earthworm effects on selected physical and chemical properties of soil aggregates. Biol Fertil Soils 15:229–234
- Zhang X, Amelung W (1996) Gas chromatographic determination of muramic acid, glucosamine, mannosamine, and galactosamine in soils. Soil Biol Biochem 28:1201–1206
- Zhou J, Xia B, Treves DS, Wu L-Y, Marsh TL, O’Neill RV, Palumbo AV, Tiedje JM (2002) Spatial and Resource Factors Influencing High Microbial Diversity in Soil. Appl. Environ. Microbiol. 68:326–334

2.3.7 Supplementary Material

Table S1 Full PLFA dataset: Given are PLFA amounts in µg per g dry soil for each pore type and bulk soil for two soil depths

20:0	20:1w 9c	20:4w 6c	cy19:0	10Me1 8:0	18:0	18:1w 7c	18:1w 9c	18:3w 6,9,1	18:2w 6,9	17:0	cy17:0	a17:0	i17:0	10Me1 6:0	16:0	16:1w 5c	16:1w 7c	a16:0	i16:0	15:0	a15:0	i15:0	14:0	14:1w 5c	a14:0	i14:0		[µg g^{-1} soil]
0.000	0.022	0.007	1.155	0.390	0.605	2.431	1.161	0.000	0.380	0.068	0.795	0.000	0.548	0.460	2.404	1.232	1.901	0.000	0.536	0.014	1.020	1.425	0.127	0.000	0.000	0.424	PL1	**Root pores 45 - 75 cm**
0.000	0.000	0.000	1.204	0.421	0.594	2.033	0.908	0.000	0.295	0.053	0.650	0.000	0.551	0.601	2.134	0.883	1.605	0.000	0.546	0.000	0.997	1.361	0.062	0.000	0.000	0.557	PL5	
0.000	0.000	0.040	1.058	0.404	0.496	1.992	0.897	0.000	0.300	0.053	0.671	0.000	0.512	0.432	2.130	0.982	1.628	0.000	0.476	0.000	0.923	1.259	0.071	0.000	0.000	0.350	PL9	
0.000	0.000	0.000	1.318	0.560	0.703	2.613	1.165	0.000	0.284	0.037	0.875	0.000	0.652	0.599	2.663	1.238	2.030	0.000	0.738	0.002	1.235	1.762	0.153	0.000	0.000	0.738	PL13	
0.000	0.063	0.177	1.222	0.684	1.232	5.604	2.272	0.000	1.507	0.214	1.221	0.154	0.850	0.269	4.772	3.186	5.006	0.000	1.322	0.085	1.781	2.327	0.476	0.000	0.000	1.267	PL2	**EW-incubated pores 45 - 75 cm**
0.000	0.167	0.253	1.111	0.662	1.239	5.291	2.072	0.000	1.922	0.231	1.166	0.340	0.758	0.348	4.678	2.704	5.093	0.000	1.512	0.136	2.206	2.175	0.483	0.000	0.000	1.450	PL6	
0.000	0.033	0.105	0.823	0.399	0.995	3.959	1.484	0.000	0.899	0.165	0.848	0.099	0.625	0.229	3.855	2.562	4.000	0.000	1.012	0.075	1.454	1.839	0.460	0.000	0.000	1.227	PL10	
0.000	0.069	0.123	1.037	0.702	1.148	4.962	2.038	0.000	1.221	0.209	1.132	0.209	0.854	0.342	4.870	2.852	4.806	0.000	1.503	0.120	2.115	2.536	0.654	0.000	0.000	1.712	PL14	
0.000	0.000	0.061	1.105	0.375	1.039	4.398	1.871	0.000	0.994	0.097	1.495	0.050	0.710	0.301	4.094	3.111	4.339	0.000	1.193	0.000	1.758	2.224	0.344	0.000	0.000	1.554	PL3	**Native earthworm pores 45 - 75 cm**
0.000	0.000	0.000	1.000	0.171	1.609	4.941	0.701	0.000	0.954	0.078	1.397	0.000	0.597	0.000	5.095	2.861	4.409	0.000	1.091	0.000	1.766	2.018	0.053	0.000	0.000	1.546	PL7	
0.000	0.040	0.126	1.671	0.650	1.416	5.795	2.338	0.000	1.052	0.160	2.070	0.167	1.067	0.593	5.675	4.507	5.603	0.000	1.945	0.000	2.652	3.195	0.498	0.000	0.000	2.025	PL11	
0.000	0.000	0.008	1.641	0.450	2.957	5.952	1.966	0.000	1.419	0.154	1.858	0.054	0.937	0.410	6.047	3.728	5.117	0.000	1.641	0.000	2.327	2.823	0.298	0.000	0.000	2.013	PL15	
0.000	0.000	0.000	0.000	0.000	0.111	0.075	0.000	0.000	0.000	0.000	0.000	0.000	0.040	0.000	0.342	0.012	0.126	0.000	0.000	0.000	0.024	0.104	0.000	0.000	0.000	0.065	PL4	**Bulk soil 45 - 75 cm**
0.000	0.000	0.000	0.030	0.000	0.112	0.050	0.000	0.000	0.000	0.000	0.000	0.000	0.081	0.000	0.331	0.000	0.056	0.000	0.082	0.000	0.048	0.193	0.000	0.000	0.000	0.180	PL8	
0.000	0.000	0.000	0.123	0.000	0.118	0.178	0.000	0.000	0.000	0.000	0.083	0.000	0.139	0.049	0.443	0.033	0.173	0.000	0.127	0.000	0.166	0.393	0.000	0.000	0.000	0.194	PL16	
0.000	0.002	0.035	1.432	0.311	0.802	3.247	1.062	0.000	0.373	0.060	1.520	0.000	0.717	0.552	3.220	1.627	2.565	0.000	0.641	0.000	1.479	1.932	0.027	0.000	0.000	0.517	PL17	**Root pores 75 - 105 cm**
0.000	0.062	0.013	2.424	0.545	1.251	4.600	1.641	0.000	0.504	0.103	2.085	0.071	1.082	0.791	4.419	2.225	3.429	0.000	1.098	0.000	1.928	2.577	0.087	0.000	0.000	1.206	PL21	
0.000	0.000	0.019	1.151	0.290	0.729	2.390	0.474	0.000	0.136	0.087	1.106	0.036	0.594	0.502	2.193	1.115	1.812	0.000	0.564	0.000	1.137	1.510	0.034	0.000	0.000	0.524	PL25	
0.000	0.014	0.005	1.639	0.362	0.783	3.073	0.847	0.000	0.163	0.041	1.407	0.000	0.760	0.665	2.995	1.418	2.328	0.000	0.727	0.000	1.478	2.018	0.000	0.000	0.000	0.684	PL29	
0.000	0.058	0.103	0.963	0.273	1.166	4.077	1.527	0.000	0.640	0.125	1.290	0.059	0.660	0.250	3.853	2.377	3.712	0.000	1.071	0.000	1.459	1.927	0.290	0.000	0.000	1.100	PL18	**EW-incubated pores 75 -**
0.000	0.057	0.172	1.128	0.401	1.169	5.134	1.775	0.000	0.729	0.138	1.573	0.144	0.764	0.232	4.242	2.753	4.815	0.000	1.202	0.000	1.802	2.227	0.243	0.000	0.000	1.378	PL22	
0.000	0.078	0.222	1.589	0.503	1.532	6.429	2.353	0.000	0.955	0.130	1.842	0.061	1.076	0.470	5.494	4.053	6.242	0.000	1.646	0.000	2.459	3.372	0.369	0.000	0.000	1.981	PL30	
0.000	0.000	0.040	0.898	0.191	1.829	3.753	1.127	0.000	0.580	0.069	1.106	0.000	0.555	0.142	3.539	2.312	3.119	0.000	0.730	0.000	1.136	1.565	0.109	0.000	0.000	0.855	PL19	**Native earthworm pores 75 - 105 cm**
0.000	0.075	0.097	0.930	0.366	1.180	4.150	1.788	0.000	1.119	0.116	1.397	0.117	0.743	0.334	4.154	3.131	4.504	0.000	1.274	0.000	1.865	2.296	0.307	0.000	0.000	1.434	PL23	
0.000	0.000	0.000	1.399	0.417	1.318	4.918	1.221	0.000	0.355	0.074	1.689	0.000	0.896	0.443	5.060	3.277	4.623	0.000	1.212	0.000	2.065	2.747	0.181	0.000	0.000	1.895	PL27	
0.000	0.000	0.007	0.678	0.069	1.085	3.060	0.569	0.000	0.182	0.028	0.784	0.000	0.411	0.049	2.696	1.712	2.320	0.000	0.462	0.000	0.828	1.109	0.000	0.000	0.000	0.803	PL31	
0.000	0.000	0.000	0.075	0.000	0.057	0.000	0.000	0.000	0.000	0.000	0.000	0.000	0.000	0.000	0.105	0.000	0.000	0.000	0.000	0.000	0.000	0.000	0.000	0.000	0.000	0.023	PL20	**Bulk soil 75 -105 cm**
0.000	0.000	0.000	0.000	0.000	0.166	0.003	0.000	0.000	0.000	0.000	0.000	0.000	0.037	0.000	0.260	0.000	0.019	0.000	0.007	0.000	0.028	0.097	0.000	0.000	0.000	0.146	PL24	
0.000	0.000	0.000	0.000	0.000	0.267	0.000	0.000	0.000	0.000	0.000	0.000	0.000	0.024	0.000	0.287	0.000	0.015	0.000	0.000	0.000	0.000	0.077	0.000	0.000	0.000	0.123	PL28	
0.000	0.000	0.000	0.000	0.000	0.162	0.000	0.000	0.000	0.000	0.000	0.018	0.000	0.029	0.000	0.263	0.000	0.019	0.000	0.000	0.000	0.003	0.098	0.000	0.000	0.000	0.127	PL32	

Table S2 Full amino sugar dataset: Given are PLFA amounts in µg per g dry soil for each pore type and bulk soil for two soil depths

[µg g^{-1} dry soil]	Sample #	Glucosamin	Mannosamin	Muramic acid	Galactosamin
Root pores 45 - 75 cm	1	577	21	3	282
	5	162	19	16	142
	9	573	15	7	250
	13	1595	36	24	643
EW-incubated pores 45 - 75 cm	2	802	15	17	374
	6	122	6	22	167
	10	618	30	6	264
	14	768	26	21	281
Native earthworm pores 45 - 75 cm	3	559	22	7	224
	7	1729	25	26	854
	11	1831	0	43	879
	15	1114	30	13	373
Bulk soil 45 - 75 cm	4	582	0	9	176
	8	239	3	14	131
	12	472	5	10	226
	16	882	3	20	280
Root pores 75 -105 cm	17	674	17	13	293
	21	1511	60	36	736
	25	2037	0	106	1078
	29	2176	50	21	998
EW-incubated pores 75 -105 cm	18	1041	28	14	487
	22	46	14	21	147
	26	865	10	24	470
	30	1124	13	32	472
Native earthworm pores 75 -105 cm	19	704	17	15	378
	23	1171	0	30	525
	27	1468	47	0	686
	31	1577	21	32	830
Bulk soil 75 -105 cm	20	541	0	18	138
	24	487	1	13	183
	28	731	0	22	257
	32	665	0	36	259

Table S3 PLFA amounts of fresh earthworm casts, given in µg per g dry material

[µg g^{-1} soil]	Fresh earthworm casts
i14:0	
a14:0	
14:1w5c	
14:0	
i15:0	0.96474491
a15:0	1.13214915
15:0	
i16:0	
a16:0	
16:1w7c	0.20932059
16:1w5c	0.06819256
16:0	0.37147805
10Me16:0	
i17:0	
a17:0	
cy17:0	
17:0	
18:2w6,9	
18:3w6,9,1	
18:1w9c	0.98936008
18:1w7c	0.5499325
18:0	
10Me18:0	
cy19:0	
20:4w6c	
20:1w9c	
20:0	

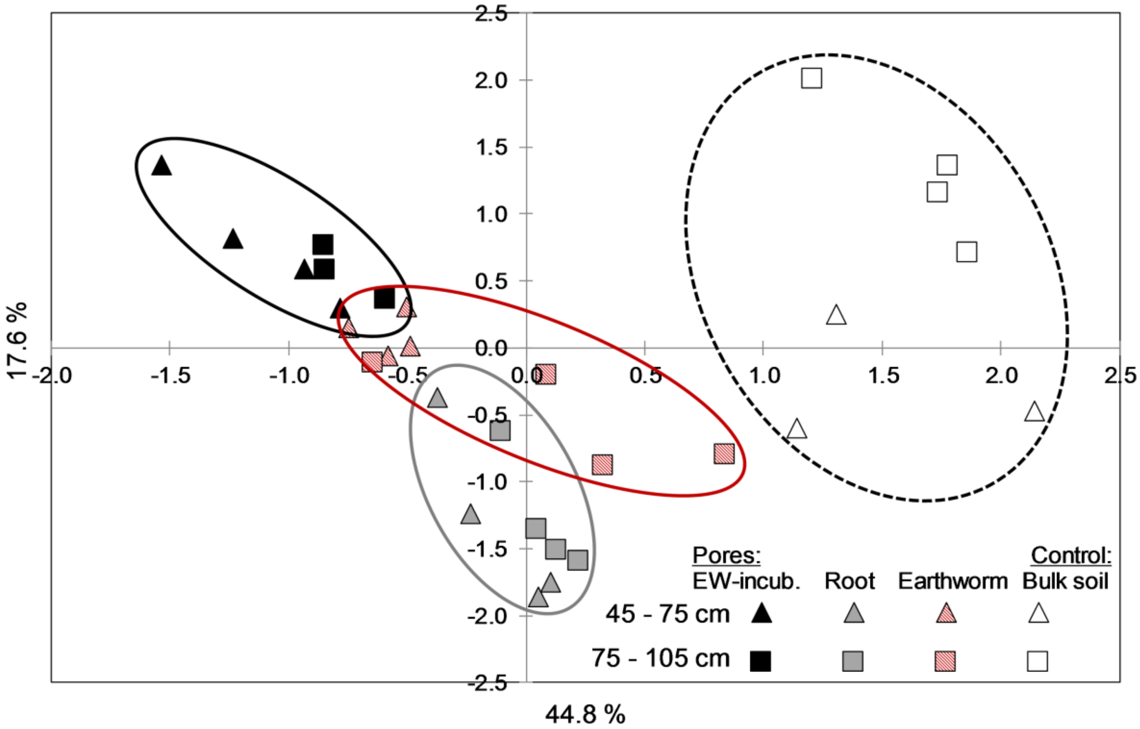

Fig S4 Principal component analysis of the PLFA dataset, without rotation.

2.4 Study 4: Six months of *L. terrestris* L. activity in root-formed biopores increases nutrient availability, microbial biomass and enzyme activity

Authors and affiliations

Miriam Athmann [a,b,*],Timo Kautz [a,b], Callum Banfield [c], Sara Bauke [d], Duyen T.T. Hoang [c], Marcel Lüsebrink [a,b], Johanna Pausch [c], Wulf Amelung [d], Yakov Kuzyakov [c], Ulrich Köpke [a,b]

[a] Institute of Organic Agriculture, University of Bonn, Katzenburgweg 3, 53115 Bonn, Germany

[b] Campus Klein-Altendorf, Klein-Altendorf 2, 53359 Rheinbach, Germany

[c] Georg-August-University Goettingen, Dept. of Soil Science of Temperate Ecosystems, Buesgenweg 2, 37077 Goettingen, Germany

[d] Institute for Crop Science and Resource Conservation (INRES) – Soil Science and Soil Ecology, University of Bonn, Nussallee 13, 53115 Bonn, Germany

[*] corresponding author

• E-mail address:

mathmann@uni-bonn.de

• Telephone number:

++49-228-735616

• Fax number:

++49-228-735617

Keywords [4-6]: Earthworm burrows, plant available P, phospholipid biomarkers, enzyme activity

Abstract

In arable fields, biopores are primarily formed by taproots, but may also be bored by earthworms. Irrespective of the pore origin, repeated use by anecic earthworms yields a wall coating that is rich in carbon, nutrients and microorganisms. *However, this effect is halted by routine tillage, and* it remains unclear how quickly earthworms are able to alter biopore properties in subsoil. We conducted an earthworm incubation field experiment in arable soil to test the capacity of *Lumbricus terrestri*s to i. increase total nutrient contents including plant available P, ii. alter the microbial community and iii. increase enzyme activities in biopore walls over one vegetation period. Firstly, biopores that contained chicory roots were identified on a plot scale (4.2 x 1.5 m). After two years under fallow, roots were decomposed. We then inserted individual earthworms at 45 cm depth into a subset of these pores, afterwards refilling with topsoil. After six months, earthworms were removed and soil was opened at 45 - 75 cm and 75 - 105 cm soil depth layers. The inner pore wall (1 mm) of individual root biopores (‘RBP’) or root biopores modified by earthworms (‘EBP’) as well as the bulk soil were sampled in 6 depth intervals of 10 cm each and analyzed for total C, N, S content, plant available P, microbial biomass, phospholipid fatty acids (PLFA) and enzyme activity. Biochemical properties of bulk soil, RBP and EBP clearly differed after one vegetation period as indicated by principal component analysis. PLFA markers of fungi and protozoa were detected only in biopores. Compared with the bulk soil, total C, N, S were enriched in RBP by a factor of 2.0-3.1, plant available P by a factor of 8-10, and microbial biomass by a factor of 12-36. In EBP, all of these parameters were as in RBP or elevated even further (C, N, S: factor 1.0-1.4, plant available P: factor 1.3-1.5, microbial biomass: factor 1.5-2.0, PLFA markers of fungi: factor 2.6-4.4, PLFA markers of protozoa: factor 9.2-14.2). PLFA markers indicative of the ratio of Gram-positive to Gram-negative bacteria (G+ : G-) were 5-10 fold lower in RBP than in bulk soil, the microbial metabolic quotient ($q\text{CO}_2$) was 0.4-0.6 times as high. In EBP, these parameters were further reduced (ratio G+: G-: factor 0.7, $q\text{CO}_2$: factor 0.7-0.8). RBP were particularly characterized by high contents of 10-methyl branched fatty acid indicators of actinobacteria.

Activities of enzymes involved in the C-cycle (xylanase, cellobiohydrolase, ß-glucosidase) and N-cycle (chitinase, chitotriosidase, leucine aminopeptidase) were also elevated in RBP as compared to the bulk soil (factor 1.1-3.6) and further increased in EBP (factor 1.2-3.7). *All these effects were more pronounced in* the *45–75 cm soil layer. We conclude that, in only six months,* L. terrestris in arable fields modified ordinarily nutrient-rich biopores into ‘super-hotspots’ of microbial biomass, enzyme activity and nutrient availabilities. Hence, even short-term promotion of earthworm populations by agricultural management practices

can increase microbial biomass and enzyme activity in biopores and its coupling to nutrient mobilization in the subsoil.

2.4.1 Introduction

Tubular shaped, continuous vertical biopores in arable fields are typically created either by taprooted crops or, to a minor degree, by anecic earthworms (Kautz et al., 2014). These biopores have diameters of up to 12 mm (Edwards and Bohlen, 1996), can be several meters deep, and can persist for decades in the subsoil beneath the plow layer (Hagedorn and Bundt, 2002; Shipitalo et al., 2004). Crop roots have been reported to preferentially follow such pores especially in compacted soils (Logsdon and Linden, 1992; Passioura, 1991), allowing them to reach deeper soil horizons more rapidly, thereby facilitating water uptake during dry spells (Gaiser et al., 2012). Likewise, anecic earthworms repeatedly utilize biopores, covering the pore walls with material rich in organic matter and nutrients, particularly N and P. Thus, they have been characterized as hotspots of microbial activity (Kuzyakov and Blagodatskaya, 2015) and a potential source of nutrients in the subsoil (Kautz et al., 2013). Moreover, earthworm burrows markedly contribute to water infiltration (Edwards et al., 1988; Ehlers, 1975), which can be advantageous for draining heavy rainfalls.

In general, biopore generating earthworms can be promoted by reduced tillage intensity (Ehlers et al. 1983; Kuntz et al., 2013; Pelosi et al., 2014), because tillage operations remove their surface food supply and destroy the top portion of permanent burrows (Kladivko, 2001). Fodder crops such as grass clover also have beneficial effects on earthworm populations, especially when cultivated as perennials (Mäder et al., 2002; Riley et al., 2008). Recently, occasionally reduced tillage (ORT) was shown to also result in increased earthworm abundances (Moos et al., 2016). However, the positive effects of perennial fodder cropping or ORT are temporary, as increases in earthworm populations following ca. two vegetation periods of soil dissipate with the onset of tillage.

Anecic earthworms such as *Lumbricus terrestris* reach maturity after approximately one year under field conditions (Satchell, 1967). In the early growth stages, they are known to largely behave like endogeics (Lowe and Butt, 2005), i.e. they predominantly stay beneath the soil surface. As such, the time for *L. terrestris* to generate biopores and influence pore properties in the subsoil during cultivation of perennial crops or ORT may be on the scale of only a few months. Kautz et al. (2014) have shown that the number of anecic earthworms increased during cultivation of perennial fodder crops, but the worms hardly contributed to the formation of new biopores in the subsoil, primarily as a consequence of re-colonization of established pores. However, in another study X-ray computed tomography in combination with *in situ* endoscopy revealed considerable effects of short-term earthworm incubation in microcosms on physical pore properties such as pore diameter distribution, pore connectivity, and accessible pore surface area (Pagenkemper et al., 2015). The extent to which earthworms are able to alter biochemical properties and thus pore quality in the short-term remains uncertain. Graff (1967) distinguished ‘young’ burrows from ‘old’ burrows by the color of the pore wall and demonstrated that the former exhibited higher nutrient contents. Similarly, Athmann et al. (2014) found that only biopores showing visible signs of earthworm passage were significantly elevated in C and N contents in comparison to the bulk soil. For grassland subsoils, Don et al. (2008) reported that pores inhabited by earthworms exhibited higher nutrient contents and enzyme activities than abandoned earthworm burrows, but no such data are available for short-term effects in arable fields. In this study, we conducted an earthworm incubation field experiment in arable soil to test the capacity of *L. terrestris* to i. increase total nutrient contents including plant available P, ii. alter the microbial community and iii. increase enzyme activities in biopore walls over one vegetation period.

2.4.2 Material and Methods

2.4.2.1 Site conditions and experimental design

The field trial was performed at ‘Campus Klein Altendorf’ experimental station in Rheinbach, Germany (50°37’N, 6°59’E) with a mean annual temperature of 9.4°C and total annual precipitation of 603 mm. The soil is a Haplic Luvisol derived from loess with a clay content of 18 % in the Ap and 29-32 % in the Bt horizon. A detailed description of soil properties at the experimental site is given by Vetterlein et al. (2013).

The experiment had a completely randomized block design with four replications that had the following treatments: i. bulk soil, ii. root channels after two and a half years of decay (i.e., root biopores ‘RBP’) and iii. root channels after two years of decay followed by earthworm incubation for six months (i.e., earthworm modified biopores, ‘EBP‘). It is important to note that the age and origin of these pores was not known. It is likely that most were older biopores that had been visited by both roots and earthworms before chicory cultivation, while a smaller portion of biopores were newly generated by chicory taproots.

In detail, the treatments were established as follows: Four 6 x 10 m replicate field plots of a larger randomized field experiment with arable crops were selected for this study. Chicory ‘Puna’ (*Cichorium intybus* L.) was sown in spring 2009 with a sowing density of 385 seeds m^{-2} (5 kg ha^{-1}) and cultivated continuously for 3 years. On January 30th 2012, the trial was plowed to 30 cm depth. On September 10th 2012, the topsoil was removed down to 45 cm depth in subplots with surface areas of 4.2 x 1.5 m in each of the replicate field plots and stored adjacent to the study area. A depth of 45 cm was chosen to be sure to also remove the plow pan. The horizontal area in 45 cm depth was carefully planed and biopores were cleared from loose and smeared soil particles using a vacuum cleaner. The prepared surface was covered with transparent films and the locations of large biopores (diameter > 5 mm) containing roots were mapped. No visible signs of earthworm activity were detected in these root containing biopores. Afterwards, the topsoil was put back and the plots were left under fallow conditions for 19 months to allow for root decomposition and to remove all food sources, thereby discouraging earthworms native to the site from colonizing these biopores.

In April 2014, half of the subplots (2.1 x 1.5 m) were re-opened, and the topsoil was stored next to the experimental area as before. Again, a horizontal area in 45 cm depth was prepared for identification of biopores. In each field replicate, 25 biopores were identified that had previously contained roots, but were now found to be empty. Each selected pore was incubated with one dew worm (*L. terrestris*). The worms were adults obtained from Canadian wild harvesting (Superwurm e.K., Düren, Germany), and were kept for four weeks at 4-6°C in buckets with nutrient rich soil and horse manure. Prior to incubation all worms were kept on filter tissues for 3 days to ensure complete defecation. Then they were labeled with visual implant elastomers (Butt and Lowe, 2007). Wooden sticks (diameter 8 mm, length 45 cm) were inserted into all incubated pores before the subplots were refilled with topsoil. Finally, removal of the wooden sticks created a connection between incubated pores and the soil surface. For the next six months all subplots were covered with mulching material from a grass clover field. Weeds that occasionally emerged were manually removed from the experimental area. After the incubation period the topsoil was removed from all subplots and incubated earthworms were removed via the octet method (Thielemann, 1986).

2.4.2.2 Sampling

In October 2014, an excavator was used to create a trench along the long side of the subplots as a base for collecting samples from the bulk soil and from pore walls of RBP and EBP. For RBP, no visible signs of earthworm activity were detected before or during sampling. EBP were only taken into account if an earthworm with a clearly recognizable implant elastomer was found after the incubation period. The recovery rate of labeled earthworms was 39% (39 of 100 pores), with 6-13 pores sampled in each plot. Within a layer of 10 cm (45 - 55 cm depth) single biopores were opened and approximately 1 mm of the inner wall material was sampled with microspatulas. The procedure was repeated for 6 depth intervals down to a maximum depth of 105 cm. Bulk soil was also collected from each treatment and depth layer with a spatula, keeping a distance to biopores of at least 5 cm. Samples from 45 - 75 cm and 75 - 105 cm depth layers were merged to gain sufficient material for all analyses.

Due to the large volume of work, several persons were required to collect all of the samples. We were aware that a change in the sampling personnel might influence the results due to individual differences in the amount of material taken from the pore wall. To minimize such effects, the sampling personnel was trained prior to the field work and each field replicate was sampled by one person only.

2.4.2.3 Plant nutrients

Total C, N and S contents of pore wall and bulk soil samples were analyzed by dry combustion with an elemental analyzer. Soil pH was around 6.5 so we considered total C as soil organic content (C_{org}).

Calcium-acetate-lactate soluble P (CAL-P_i) was extracted according to Schüller (1969). Specific P pools were determined following the sequential extraction procedure of Hedley et al. (1982) as modified by Tiessen und Moir (1993); however, residual P was extracted by digestion in aqua regia. Concentrations of inorganic P (P_i) in each of the extracts were determined with a spectrophotometer by the molybdenum blue method (Murphy und Riley, 1962). Total P concentration in the extracts was determined by inductively coupled plasma optical-emission spectroscopy. Concentrations of organic P (P_o) were calculated as the difference of inorganic to total P. We classified P pools according to Negassa and Leinweber (2009), distinguishing highly available P (resin and $NaHCO_3$ extracts), moderately available P (NaOH extracts) and stable P (HCl_{dil}, HCl_{conc} and residual P in aqua regia) for interpreting our findings, but restrict to mentioning the chemical extractions as nomenclature.

2.4.2.4 Basal respiration, microbial biomass carbon (C_{mic}) and microbial metabolic quotient (qCO_2)

A fresh subsample (1 g oven-dry soil equivalent) was adjusted to 50% of the water holding capacity (WHC) and gravimetrically controlled. After two days preincubation at room temperature to avoid side effects of sieving (Blagodatskaya et al., 2011), samples were incubated at 20 °C (Creamer et al., 2014) in 12 ml septum-capped vials. Six other vials without soil were prepared as controls to correct for atmospheric carbon dioxide.

The basal respiration was measured at time 0 (t_0, i.e., right after adding the soil to the vials and flushing the vials with ambient air), then at 24 hour intervals for three additional time points (t_1, t_2, t_3). Thereafter, 100 µl of a glucose solution (60 mg mL^{-1}) were amended to all the vials to determine the soil microbial biomass (µg C_{mic} g^{-1} soil dry mass) by the substrate induced respiration (SIR) method (Anderson and Domsch, 1978; Lin and

Brookes, 1999; West and Sparling, 1986). The WHC reached 70% after aliquot amendment. Immediately after glucose addition, we used a manifold combined with a pump to standardize air inside vials with ambient air. All vials were then incubated for 2h at 20 ^{0}C (Lin and Brookes, 1999). The measurements of basal respiration and substrate induced respiration were undertaken directly via gas chromatography. The CO_2 evolution (ppm) was calculated by subtracting the CO_2 concentrations of the blanks from those of the sample.

The basal respiration (µg C g^{-1} h^{-1}) was calculated by subtracting CO_2 concentrations in soil vials measured at t_1, t_2 and t_3 from CO_2 concentrations in blank vials and the initial CO_2 evolution of soil vials at t_0 (Creamer et al., 2014). Using the Ideal Gas Equation, CO_2 respiration was converted from ppm to µg C g^{-1} h^{-1} in accordance with headspace volume of the sealed flask containing the soil sample, incubation temperature and air pressure (Orchard and Cook 1983). The SIR was applied to calculate microbial biomass C (µg C g $soil^{-1}$) based on the equation by Anderson and Domsch (1978)

$$x = 40.4y + 0.37 \qquad (1)$$

where y is the maximum initial rate of respiration (CO_2 evolution 2 h after adding glucose). Similarly, the microbial metabolic quotient (qCO_2) was calculated by dividing initial respiration (BR) by C_{mic} and expressed as µg CO_2-C mg^{-1} C_{mic} h^{-1} (Anderson and Domsch, 1990).

2.4.2.5 Phospholipid fatty acids (PLFA)

Phospholipids were extracted based on the protocol of Frostegård et al. (1991) with the modifications described by Apostel et al. (2013) using phosphatidylcholine-dinonadecanoic acid and tridecanoic acid methyl ester as internal standards (IS 1 and IS 2, respectively). Samples were measured on a coupled gas chromatography mass spectrometry (GC-MS) system employing a 45 m DB5-MS column (0.25 mm I.D., 0.25 µm film thickness). Stock solutions containing external standards of 27 fatty acids and IS 1, with total fatty acid contents of 1, 4.5, 9, 18 and 24 mg, were derivatised together with the samples. The detailed measurement procedure is described in supplement 1. Individual groups of microorganisms were determined based on previously published PLFA biomarker data (Zhang et al., 2015). Specifically, 18:2ω6,9 was used as a marker for fungal biomass (Frostegård and Bååth, 1996); 10Me16:0 and 10Me18:0 were used as markers for actinobacteria; a15:0, i15:0, i17:0, a17:0 were used as markers for Gram-positive bacteria, and 16:1ω5c, 16:1ω7c, 18:1ω7c, Cy17:0 were used as markers for Gram-negative bacteria. In addition, 20:4ω6 was used as a marker for protozoa (Fierer et al., 2003).

2.4.2.6 Enzyme activities

Enzymes were assayed according to the modified methodology of Razavi et al. (2015) for three out of four field replicates. Half a gram of fresh soil (dry weight equivalent) was dispersed in 50 mL sterilized water of which 50 µL soil suspension was pipetted to a 96-well microplate. Subsequently, 50 µL of buffer [MES $C_6H_{13}NO_4SNa_{0.5}$. (pH: 6.5) buffer for 4-methylumbelliferone (MUF) substrate and TRIZMA $C_4H_{11}NO_3$•HCl, $C_4H_{11}NO$ (pH: 7) buffer for 7-amino-4-methylcoumarin (AMC) was added. We measured activities of 3 enzymes regarding the C-cycle: 1) β-glucosidase (**EC** 3.2.1.21) measured with MUF-β-D-glucopyranoside (MUF-G), 2) cellobiohydrolase (**EC** 3.2.1.91) measured with MUF-β-D-cellobioside (MUF-C), and 3) xylanase (**EC** 3.2. 1.8) measured with MUF-β-D-xylopyranoside (MUF-X); and 3 enzymes regarding the N-cycle: 1) chitotriosidase (**EC** 3.2.1.14) measured with 4-methylumbelliferyl-β–DN, N′,N″-triacetylchitotrioside (MUF-Tr), 2) chitinase (**EC** 3.2.1.14) measured with MUF-N-acetyl-β-D-glucosaminide (MUF-N); 3) leucine-aminopeptidase (**EC** 3.4.11.1) measured with L-Leucine-7-amido-4-methylcoumarin hydrochloride (AMC-L).

The reaction solution was buffered at pH 6.5 whereas the optimal pH is 5.5 for xylanase (Schinner and von Mersi, 1990), 6.0 for cellobiohydrolase (Hong et al., 2003), 5.2 for chitotriosidase (Hollak et al., 1994), 5.5 for chitinase (Parham and Deng, 2000), 6.0 for β-Glucosidase (Eivazi and Tabatabai, 1988), and 7.5 for leucine aminopeptidase (Niemi and Vepsäläinen, 2005). For these assays that were not run at optimal pH, the results cannot be compared to other studies where the optimal buffered pH was used. Also, in these cases, the activities would be expected to be reduced compared to if it had been done at optimal pH. Thus, differences between treatments may have been underestimated.

The microplate was incubated with 100 µL/well of fluorescent substrate solution at the desired concentration range: 0, 10, 20, 30, 40, 50, 100, 200 nmol g^{-1} dry weight in a 96-well microplate. The concentration that resulted in saturation of fluorogenic substrate was determined based on preliminary experiments for which one field replicate was used. The assay of each enzyme at each substrate concentration was replicated three times in each plate, and each plate included a standard curve of the product (4-methylumbelliferone, MUF) or (7-amino-4-methylcoumarin, AMC), substrate controls (for each substrate concentration), and homogenate controls. Enzymatic activity (nmol product released h^{-1} g^{-1} dry soil) was calculated from the MUF or AMC standard curve following Razavi et al. (2015). However, we did not run a control for autohydrolysis. We assumed autohydrolysis of the two substrates MUF and AMC to be ignorable because according to Rakels et al. (1993) substrate hydrolysis occurs for 0.5 % of the total amount of substrate in 1 h and is thus negligible. The calibration solutions were prepared using soil suspension (50µL) and MUF to obtain a series of concentrations 0–1.2 mM (Razavi et al., 2015). The time from substrate addition to the fluorescence measurement (30, 60 and 120 min.) was the same for all enzymes and samples. Linear increase of fluorescence over time during the assay was checked and data obtained after 2 h used for further calculation (Razavi et al., 2015). The fluorescence was measured using a Multilabel Counter at an excitation wavelength of 355 nm and an emission wavelength of 460 nm. In order to calculate V_{max}, a calibration curve was prepared by adding MUF or AMC instead of substrates to the same amount of soil solution and buffers (MES or TRIZMA, respectively) following Freeman et al. (1995) and Razavi et al. (2015). Enzyme activities were calculated as released MUF or AMC in nmol g-1 h-1 (Marx et al., 2005). V_{max} values were determined by nonlinear curve fitting using the software OriginPro 8.5 (OriginLab, Massachusetts, USA).

2.4.2.7 Statistical analyses

Shapiro-Wilk tests were used to confirm normal distribution of the datasets. Means were compared by one-way ANOVA followed by Tukey-tests. For enzyme activities, only three field repetitions were considered, for all other parameters all four field repetitions were included in the analysis. For the 45–75 cm soil depth interval principal component analysis (PCA) was used for further data evaluation. All parameters analyzed were subjected to PCA, including individual PLFAs. Only components with Eigenvalues > 1 were considered. Principal components were not rotated. All calculations were performed using IBM SPSS version 22.

2.4.3 Results

2.4.3.1 Nutrient contents

In walls of pores with or without earthworm incubation total contents of C, N, P, S were generally higher than in the bulk soil (Tab. 1). This effect was particularly pronounced for C, N and S with at least two-fold increased contents in pore walls relative to the bulk soil in both depths (45–75 cm and 75–105 cm). Moreover, short-term earthworm incubation in EBP resulted in higher C contents than in RBP in the 45–75 cm soil depth layer.

Hedley fractionation of phosphorus revealed markedly higher contents of resin P_i, $NaHCO_3$ P_i, $NaHCO_3$ P_o, NaOH P_i, NaOH P_o, and HCL_{dil} P_i in pore walls than in the bulk soil, and the same was also observed for CAL-P_i. Furthermore, in EBP CAL-P_i and resin P_i were significantly enriched as compared to RBP in the 45–75 cm soil depth layer, and $NaHCO_3$ P_o in both soil depths. In the bulk soil, increased soil depth resulted in lower contents of total N and S as well as NaOH P_o, while total P and HCl_{conc} P_i increased with depth. In RBP generally no effect of depth on nutrient contents was observed, but in EBP contents of total N and NaOH P_o and HCl_{conc} P_o were higher at 45–75 cm than at 75–105 cm.

Table 1 Total nutrient contents and P fractions in bulk soil and the walls of different pore types. Different uppercase and lowercase letters indicate significant differences between depth levels and soil compartments respectively (one way ANOVA with Tukey-HSD, $p < 0.05$).

Soil depth	45–75 cm			75–105 cm		
Treatment	EBP[a]	RBP[b]	Bulk soil	EBP[a]	RBP[b]	Bulk soil
C (mg g^{-1})	11.6 a	8.10 b	4.10 c	10.7 a	9.30 a	3.50 b
N (mg g^{-1})	1.60 a A	1.40 a	0.70 b A	1.30 a B	1.30 a	0.60 b B
S (mg g^{-1})	0.15 a	0.14 a	0.07 b A	0.10 a	0.11 a	0.03 b B
P (mg kg^{-1})	917 a	800 a	454 b B	825 a	797 a	580 b A
CAL-P_i (mg kg^{-1})	242 a	163 b	15.8 c	194 a	153 a	19.8 b
Resin P_i (mg kg^{-1})	74.3 a	40.4 b	16.0 c	55.3 a	34.5 ab	14.8 b
$NaHCO_3$ P_i (mg kg^{-1})	35.1 a	33.1 a	15.9 b	27.9	31.8	18.9
$NaHCO_3$ P_o (mg kg^{-1})	23.9 a	7.19 b	n.d.	19.6 a	9.21 b	n.d.
$NaHCO_3$ P_t (mg kg−1)	59.0 a	40.3 b	15.9 c	47.5 a	41.0 a	18.9 b
NaOH P_i (mg kg^{-1})	72.5 a	68.1 a	48.8 b	69.0	66.9	49.9
NaOH P_o (mg kg^{-1})	31.7 a A	24.7 ab	16.8 b A	20.4 a B	20.5 a	10.1 b B
NaOH P_t (mg kg^{-1})	104 a	92.7 a	65.6 v	65.6 b	87.4	59.9
HCldil Pi (mg kg^{-1})	194.4 a	207 a	135 b	214	231	240
HClconc Pi (mg kg^{-1})	171	186	144 B	187	159	166 A
HClconc Po (mg kg^{-1})	40.6 A	30.2	35.9	10.7 b B	53.2 a	33.3 ab
HClconc Pt (mg kg^{-1})	211 ab	216 a	180 b	198	213	199
Residual P_t (mg kg^{-1})	31.5 ab	40.7 a	25.6 b	28.1	38.1	27.8

P_i: inorganic phosphorus, P_o: organic phosphorus, P_t: total phosphorus.

[a] EBP: Earthworm-modified biopores.

[b] RBP: Root biopores.

2.4.3.2 Microbiological properties

Microbial biomass (C_{mic}) related to soil organic carbon was low in bulk soil regardless of soil depth (Fig. 1). In both biopore types, but especially in EBP, C_{mic} was considerably elevated, with the highest value in EBP at 45–75 cm soil depth. The microbial metabolic quotient (qCO_2) related to the microbial biomass was very high in bulk soil, especially in the 75–105 cm soil depth layer (Fig. 1), and decreased in both biopore types.

Similarly, to C_{mic}, the total PLFA content (Fig. 2a) was much higher in both biopore types than in the bulk soil, increasing by a factor of 12-54 depending on biopore type and soil depth. Total PLFA was further increased by short-term earthworm incubation (factor 1.5-2.0 as compared to RBP; this difference was significant in the 45–75 cm soil depth layer). The ratio of Gram positive : Gram negative bacteria as determined with PLFA biomarkers (Fig. 2b) was much higher in bulk soil than in both biopore types (factor 3.4-16.3). In the bulk soil there was a significant effect of soil depth, with a much higher ratio in 75–105 cm soil depth. Biomarkers for fungi and protozoa (Fig. 2c) were not found in bulk soil, and both parameters were significantly increased by short-term earthworm incubation as compared to RBP (factor 2.6-4.4 for fungi and 9.2-14.2 for protozoa). Biomarkers for actinobacteria (Fig. 2d) in bulk soil were present only at trace levels and only in the upper soil layer (45–75 cm). In the 45–75 cm soil depth layer there were almost equal amounts of actinobacteria in both biopore types, while at 75–105 cm, biomarkers for actinobacteria were about 1.8 times higher in RBP as compared to EBP. This increase was not significant.

Activities of enzymes related to the C-cycle (cellobiohydrolase, ß-glucosidase and xylanase) and of enzymes related to the N-cycle (chitinase, chitotriosidase, leucine aminopeptidase) were increased in EBP and partially also in RBP as compared to the bulk soil (Tab. 2). These effects were more pronounced in the 45–75 cm soil depth layer. While there was only one effect of soil depth in the bulk soil and depth effects in RBP were inconsistent, all enzyme activities except for chitinase were higher in the upper depth layer (45–75 cm) of EBP (Tab. 2).

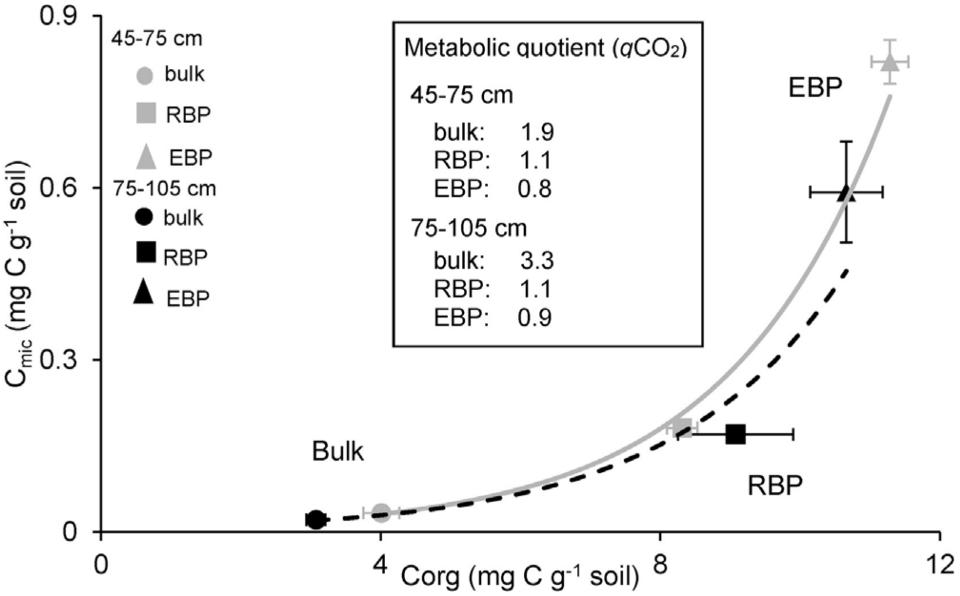

Fig. 1 *Microbial biomass (C mic) related to organic carbon content and microbial metabolic quotient (qCO 2). Error bars indicate standard deviation. RPB: root biopores, EBP: earthworm-modified biopores. C mic is significantly higher in EBP than in RBP and bulk soil in both soil depth horizons and, only in EBP, significantly higher at 45–75 cm (ANOVA with Tukey-HSD, $p < 0.05$). qCO 2 is significantly lower in EBP and RBP as compared to the bulk soil and, only in bulk soil, significantly lower at 45–75 cm.*

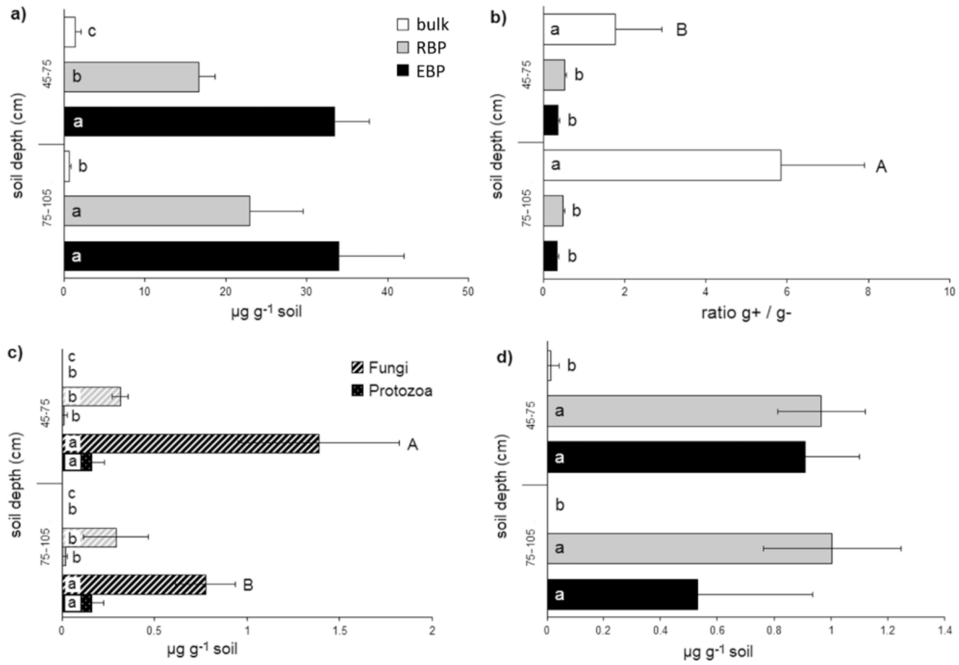

Fig. 2 *a) Microbial biomass (total PLFA), b) ratio of biomarkers for gram-positive and gram-negative bacteria (a15:0, i15:0, i17:0, a17:0 and 16:1 ω 5c, 16:1ω7c, 18:1ω7c, Cy17:0), c) biomarkers for fungi (18:2ω6,9) and protozoa (20:4ω6) and d) biomarkers for actinobacteria (10Me16, 10Me18). Different uppercase and lowercase letters indicate significant differences between depth levels and soil compartments (ANOVA with Tukey-HSD, $p < 0.05$). Error bars indicate standard deviation. RPB: root biopores, EBP: earthworm-modified biopores.*

Table 2 *Enzyme activities (Vmax) in bulk soil and the walls of different pore types. Different uppercase and lowercase letters indicate significant differences between depth levels and soil compartments, respectively (one way ANOVA with Tukey-HSD, $p < 0.05$).*

Soil depth	45–75 cm			75–105 cm		
Treatment	EBP[a]	RBP[b]	Bulk soil	EBP[a]	RBP[b]	Bulk soil
V_{max} Cellobiohydrolase (nmol g^{-1} MUF h^{-1})	89.0 a A	31.7 b B	16.1 c	70.7 a B	43.3 b A	12.1 c
V_{max} ß-Glucosidase (nmol g^{-1} MUF h^{-1})	1169 a A	511.1 b A	234.5 c	347.8 a B	295.3 ab B	256.8 b
V_{max} Xylanase (nmol g^{-1} MUF h^{-1})	66.6 a A	32.0 b	23.7 b	38.0 a B	27.1 b	23.1 b
V_{max} Chitotriosidase (nmol g^{-1} MUF h^{-1})	22.5 a A	7.58 b	6.11 b	15.4 a B	6.48 b	5.99 b
V_{max} Chitinase (nmol g^{-1} MUF h^{-1})	68.6 a	24.4 b	10.4 b	45.5 a	30.4 ab	13.3 b
V_{max} Leucine amino-peptidase (nmol g^{-1} AMC h^{-1})	540 a A	147 b	48.9 c B	354 a B	142 b	89.1 b A

[a] EBP: Earthworm-modified biopores.

[b] RBP: Root biopores.

2.4.3.3 Principal component analysis

Bulk soil, RBP and EBP were clearly distinguished by PC 1, explaining 68.3 % of total variance (Fig. 3a). Additionally, RBP were separated from bulk soil and EBP by PC 2, which explained 14.6 % of total variance. PC 1 loads high on C, N, CAL-P_i, microbial biomass, biomarkers for fungi and protozoa and enzyme activities such as xylanase and chitinase (Fig. 3b). Negative loadings were recorded for iso-branched fatty acids. PC 2 loadings were particularly high for 10-methyl branched fatty acids.

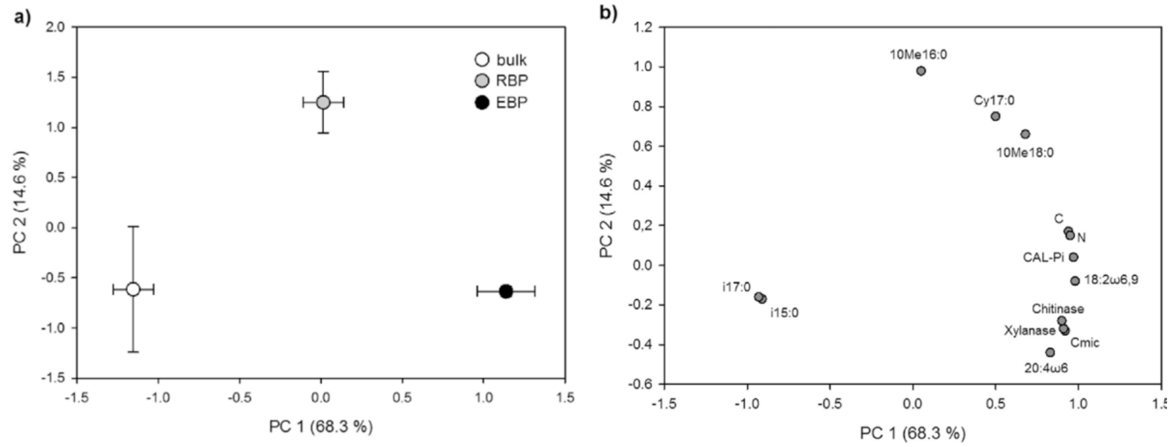

Fig. 3 *a) Principal-component scores for bulk soil (open circles), root biopores (gray circles) and earthworm-modified biopores (black circles) in 45–75 cm soil depth and b) selected factor loadings of the first two principal components extracted from the dataset.*

2.4.4 Discussion

2.4.4.1 General properties of biopore walls

The increased C and N contents in pore walls vs bulk soil observed in our study are consistent with previous laboratory and field studies (e.g. Stromberger et al., 2012; Amador et al., 2003; Pankhurst et al., 2002; Tiunov and Scheu, 1999). These characteristics of biopores are obviously a result of organic material inputs by earthworms and plant roots. Accordingly, pore walls were previously found to be enriched in P, in particular in resin-P_i, $NaHCO_3$-P_i, NaOH-P_i and NaOH-P_o compared with the bulk soil (Barej et al., 2014). Also, increased microbial biomass (Stromberger et al., 2012; Tiunov et al., 2001; Tiunov and Scheu, 1999), bacterial counts (Parkin and Berry, 1999), PLFA contents (Pankhurst et al., 2002) and enzyme activities (Hoang et al., 2016; Jégou et al., 2001; Stehouwer et al., 1993; Uksa et al., 2015) in pore walls have repeatedly been reported.

2.4.4.2 Properties of root biopores

We differentiated between pores filled with roots prior to the experiment (RBP) and pores incubated with *L. terrestris* for one vegetation period (EBP). Despite RBP not being visited by earthworms for at least two years, their properties clearly differed from the bulk soil, with higher nutrient contents, microbial biomass and enzyme activity. In particular, this pore type was characterized by increased contents of the 10-methyl branched fatty acid biomarkers of actinobacteria (Fig. 2 and 3).

Actinobacteria are involved in late stages of plant residue degradation (Bernard et al., 2007; Goodfellow and Williams, 1983) and are adapted to survive at slower growth rates when resources are limited or consist of more complex organic matter (Bastian et al., 2009). Relative enrichment of these biomarkers in RBP supports the assumption that the resident microbes primarily respire old and recalcitrant plant residues.

2.4.4.3 Properties of earthworm-modified biopores

Short-term earthworm incubation resulted in import of carbon, increased enzyme activity and changes in the microbial community. *L. terrestris* removes plant residues from the soil surface and deposits organic matter on the burrow wall (Lavelle, 1988; Stromberger et al., 2012). Intake of primary organic matter into soil generally results in higher activity of enzymes related to the decomposition of polysaccharides from plant tissues (Bandick and Dick, 1999; Debosz et al., 1999; Kautz et al., 2004). Xylanase is mainly bound to particulate organic matter (Kandeler et al., 1999a; Kandeler et al., 1999b) which is likely to be enriched in the drilosphere. Hence, it is plausible that presence of *L. terrestris* increases the activity of such enzymes in the burrow wall, as also reported by Don et al. (2008). Additionally, the composition of the microbial community in pore walls was evidently altered by the presence of *L. terrestris*: actinobacteria were reduced, as indicated by the relatively lower abundance of 10-methyl branched fatty acids, while fungal and protozoan fatty acids (i.e., 18:2ω6,9 and 20:4ω6, respectively) were relatively enriched in comparison with RBP. Both fungi and protozoa are assumed to form a substantial part of the earthworm diet (Curry and Schmidt, 2007; Edwards and Fletcher, 1988) and were previously determined to be enriched in burrow walls of *L. terrestris* (Tiunov et al., 2001). Moreover, 20:4ω6 was also found to be increased in drilosphere vs bulk soil samples (Stromberger et al., 2012). Thus, *L. terrestris* acts as an ecosystem engineer (Jones et al. 1994) by defecating and importing plant residues into the pore wall, thus creating a distinct habitat for microorganisms which in turn provide a suitable food source. The increased content of a PLFA-biomarker for fungi as a result of earthworm incubation is in line with higher activity of chitotriosidase and chitinase, possibly indicating a decomposition of chitin from fungal cell walls. These results indicate that fungal hyphae and spores may be transported downwards through biopores by earthworm activity. However, Tiunov and Scheu (1999) found a lower ratio of fungal:bacterial biomass in drilosphere samples than in the bulk soil, while Stromberger et al. (2012) reported no difference in this ratio in bulk soil and drilosphere as revealed by PLFA analysis. As explained by Stromberger et al. (2012), the reason for these contradictory results may be the complex equilibrium of fungi, bacteria, and fungivorous and bacterivorous fauna in drilosphere and bulk soil. This equilibrium is affected by earthworms via dispersal and activation, predation, habitat destruction, competition for organic matter, and production of fungicides and bactericides (Brown et al., 2004). Further research is required to determine the conditions under which earthworm activity promotes fungal or bacterial growth.

Apart from the diet, changes in PLFA contents in the burrow wall can also be related to processes in the digestive tract of *L. terrestris*. Sampedro and Whalen (2007) reported that the fatty acid pattern markedly changed in the gut of *L. terrestris* with enrichments of 16:1ω5 and 20:4ω6 in the gut content. These PLFA were also enriched in the walls of EBP.

Increased enzyme activity can also promote the mobilization of nutrients. The enrichment of total P and particularly of labile P forms in RBP vs. the bulk soil was similar to the results of Barej et al. (2014), who sampled biopores with a smaller lower diameter limit (> 2 mm) at the same site. This is plausible as smaller biopores are visited by earthworms less often than larger pores. Further significant enrichments of labile P as a result of earthworm activity suggest that walls of recently inhabited burrows can be hotspots of P acquisition by plants. This notion is supported by the finding of Kuczak et al. (2006) that earthworm casts are enriched in total P with higher proportions of P mainly in forms that are more readily extracted (resin, $NaHCO_3$, NaOH and HCl_{dil}). Moreover, Vos et al. (2014) noted that in a pot experiment the presence of *L. terrestris* increased plant growth and P uptake, but it remained questionable if this result could be applied to native, structured soils. Our results support the link between *L. terrestris* activity and P uptake by plants, as the shared burrows of *L. terrestris* and plant roots in natural conditions were significantly loaded with plant available P after earthworm incubation for a period of just six months.

2.4.4.4 Effects of soil depth

Microbial activity and availability of plant nutrients such as N and P have generally been reported to decline with soil depth (e.g., Fierer et al., 2003; Lynch und Brown; 2001). In the bulk soil from our field trial, significant decreases in the 75–105 cm depth layer were merely found for total N, total S and NaOH P_o, and significant increases were observed in the microbial metabolic quotient and the ratio of Gram positive : Gram negative bacteria. Interestingly, these depth effects were not observed in RBP, showing that these pores feature rather stable conditions throughout the soil profile and provide an attractive environment for plant roots even in greater soil depths. The effect of short-term incubation of *L. terrestris* on nutrient contents and microbial biomass was more pronounced at 45–75 than at 75–105 cm soil depth, resulting in many significant differences between both depth levels. Little is known about the *in situ* patterns of vertical movement of *L. terrestris*. One older study (Joyner and Harmon, 1961) indicates that earthworms tend to oscillate in rather stable day-and-night cycles between the soil surface around midnight and about 60 cm soil depth around noon. These observations coincide with our field experiment, where earthworm activity was obviously greater in the upper subsoil, although a clear impact on burrow properties was also detected in the deeper soil layers.

2.4.5 Conclusions

Subsoil biopores inhabited by roots for at least two years were enriched in microbial biomass and enzyme activity as well as N and plant available P compared to surrounding bulk soil. These hotspots turned into ‘super-hotspots’ with further inputs of C and nutrients, higher microbial and enzyme activities and altered microbial community composition as a consequence of colonization by *Lumbricus terrestris* – even during only one vegetation period. Both biopore properties and microbial performance in biopores are thus highly dynamic – and prone to effects of even short-term management practices that influence earthworm activity.

Acknowledgements

This study was supported by the German Research Foundation (Deutsche Forschungsgemeinschaft) within the framework of the research consortium DFG PAK 888. We thank the staff of the Institute of Organic Agriculture in Bonn for assistance with the field work.

2.4.6 References

- Amador, J.A., Görres, J.H., Savin, M.C., 2003. Carbon and Nitrogen Dynamics in *Lumbricus terrestris* (L.) Burrow Soil: Relationship to Plant Residues and Macropores. Soil Sci. Soc. Am. J. 67, 1755-1762.
- Anderson, J.P.E., Domsch, K.H., 1978. A physiological method for the quantitative measurement of microbial biomass in soils. Soil Biol. Biochem. 3, 215-221.
- Anderson, T.H., Domsch, K.H., 1990. Application of eco-physiological quotients ($q\mathrm{CO}_2$ and qD) on microbial biomasses from soils of different cropping histories. Soil Biol. Biochem. 22, 251-255.
- Apostel, C., Dippold, M., Glaser, B., Kuzyakov, Y., 2013. Biochemical pathways of amino acids in soil: Assessment by position-specific labeling and ^{13}C-PLFA analysis. Soil Biol. Biochem. 67, 31-40.
- Athmann, M., Huang, N., Kautz, T., Köpke, U., 2014. Biopore characterization with *in situ* endoscopy: Influence of earthworms on carbon and nitrogen contents. Proceedings of the 4th ISOFAR Scientific Conference, 13-15 Oct. 2014, Istanbul, Turkey: 415-418.
- Bandick, A.K., Dick, R.P., 1999. Field management effects on soil enzyme activities. Soil Biol. Biochem. 31, 1471-1479.
- Barej, J., Pätzold, S., Perkons, U., Amelung, W., 2014. Phosphorus fractions in bulk subsoil and its biopore systems. Eur. J. Soil Sci. 65, 553-561.
- Bastian, F., Bouziri, L., Nicolardot, B., Ranjard, L., 2009. Impact of wheat straw decomposition on successional patterns of soil microbial community structure. Soil Biol. Biochem. 41, 262-275.
- Bernard, L., Mougel, C., Maron, P.-A., Nowak, V., Lévêque, J., Henault, C., el Zahar Haichar, F. , Berge, O., Marol, C., Balesdent, J., Gibiat, F., Lemanceau, P., Ranjard, L., 2007. Dynamics and identification of soil microbial populations actively assimilating carbon from ^{13}C-labelled wheat residue as estimated by DNA- and RNA-SIP techniques. Environ. Microbiol. 9, 752-764.
- Blagodatskaya, E., Yuyukina, T., Blagodatsky, S., Kuzyakov, Y., 2011. Three-source partitioning of microbial biomass and of CO_2 efflux from soil to evaluate mechanisms of priming effects. Soil Biol. Biochem. 43, 778-786.
- Brown, G.G., Edwards, C.A., Brussaard, L., 2004. How earthworms affect plant growth: burrowing into the mechanisms. In: Edwards, C.A. (Ed.), Earthworm Ecology, second ed. CRC Press, Boca Raton, pp. 13–49.
- Butt, K.R., Lowe, C.N., 2007. A viable technique for tagging earthworms using visible implant elastomer. Appl. Soil Ecol. 35, 454-457.
- Creamer, R.E, Schulte R.P.O., Stone D., Gal A., Krogh P.H., Papa G.L., Murray P.J., Pérès G., Foerster B., Rutgers M., Sousa J.P., Winding A., 2014. Measuring basal soil respiration across Europe: Do incubation temperature and incubation period matter. Ecol. indic. 36, 409-418.
- Curry, J.P., Schmidt, O., 2007. The feeding ecology of earthworms – A review. Pedobiologia 50, 463-477.
- Debosz, K., Rasmussen, P.H., Pedersen, A.R., 1999. Temporal variations in microbial biomass C and cellulolytic enzyme activity in arable soils: effects of organic matter input. Appl. Soil Ecol. 13, 209-218.

- Don, A., Steinberg, B., Schöning, I., Pritsch, K., Joschko, M., Gleixner, G., Schulze, E.-D., 2008. Organic carbon sequestration in earthworm burrows. Soil Biol. Biochem. 40, 1803-1812.
- Edwards, C.A., Bohlen, P.J., 1996. Biology and ecology of earthworms. Third ed. Chapman and Hall, London.
- Edwards, C.A., Fletcher, K.E., 1988. Interactions between earthworms and microorganisms in organic-matter breakdown. Agric. Ecosyst. Environ. 24, 235-247.
- Edwards, W.M., Shipitalo, M.I., Norton, L.D., 1988. Contribution of macroporosity to infiltration into a continuous corn no-tilled watershed: Implications for contaminant movement. J. Contam. Hydrol. 3, 193-205.
- Ehlers, W., 1975. Observations on earthworm channels and infiltration on tilled and untilled loess soil. Soil Sci. 119, 242-249.
- Ehlers, W., Köpke, U., Hesse, F., Böhm, W., 1983. Penetration resistance and root growth of oats in tilled and untilled loess soil. Soil Till. Res. 3, 261-275.
- Eivazi, F., Tabatabai. M.A., 1988. Glucosidases and galactosidases in soils. Soil Biol. Biochem. 20, 601-606.
- Fierer, N., Schimel, J.P., Holden, P.A., 2003. Variations in microbial community composition through two soil depth profiles. Soil Biol. Biochem. 35, 167-176.
- Freeman, C., Liska, G., Ostle, N.J., Jones, S.E., Lock, M.A., 1995. The use of fluorogenic substrates for measuring enzyme activity in peatlands. Plant Soil 175: 147-152.
- Frostegård, Å., Bååth, E., 1996. The use of phospholipid fatty acid analysis to estimate bacterial and fungal biomass in soil. Biol. Fertil. Soils 22, 59-65.
- Frostegård, Å., Tunlid, A., Bååth, E., 1991. Microbial biomass measured as total lipid phosphate in soils of different organic content. J. Microbiol. Methods 14, 151-163.
- Gaiser, T., Perkons, U., Küpper, P.M., Puschmann, D.U., Peth, S., Kautz, T., Pfeifer, J., Ewert, F., Horn, R., Köpke, U., 2012. Evidence of improved water uptake from subsoil by spring wheat following lucerne in a temperate humid climate. Field Crops Res. 126, 56-62.
- Goodfellow, M., Williams, S. T., 1983. Ecology of actinomycetes. Ann. Rev. Microbiol. 37, 189-216.
- Graff, O., 1967. Über die Verlagerung von Nährelementen in den Unterboden durch Regenwurmtätigkeit. Landwirtschaftliche Forschung 20, 117-127.
- Hagedorn, F., Bundt, M., 2002. The age of preferential flow paths. Geoderma 108, 119-132.
- Hedley, M.J., Stewart, J., Chauhan, B., 1982. Changes in inorganic and organic soil phosphorus fractions induced by cultivation practices and by laboratory incubations. Soil Sci. Soc. Am. J. 46, 970-976.
- Hoang, D.T.T., Razavi, B.S., Kuzyakov, Y., Blagodatskaya, E., 2016. Earthworm burrows: Kinetics and spatial distribution of enzymes of C-, N- and P-cycles. Soil Biol. Biochem. 99, 94-103.
- Hollak, C.E., van Weely, S., van Oers, M.H., Aerts, J.M., 1994. Marked elevation of plasma chitotriosidase activity. A novel hallmark of Gaucher disease. J. Clin. Invest. 93, 1288-1292.

- Hong, J., Tamaki, H., Yamamoto, K., Kumagai, H., 2003. Cloning of a gene encoding thermostable cellobiohydrolase from *Thermoascus aurantiacus* and its expression in yeast. Appl. Microbiol. Biotechnol. 63, 42-50.
- Jégou, D., Schrader, S., Diestel, H., Cluzeau, D., 2001. Morphological, physical and biochemical characteristics of burrow walls formed by earthworms. Appl. Soil Ecol. 17, 165-174.
- Jones, C.G., Lawton, J.H., Shachak, M., 1994. Organisms as ecosystem engineers. Oikos 69, 373-386.
- Joyner, J.W., Harmon, N.P., 1961. Burrows and oscillative behavior therein of *Lumbricus terrestris*. Proc. Indiana Acad. Sci. 71, 378-384.
- Kandeler, E., Stemmer, M., Klimanek, E.-M., 1999a. Response of soil microbial biomass, urease and xylanase within particle size fractions to long-term soil management. Soil Biol. Biochem. 31, 261-273.
- Kandeler, E., Tscherko, D., Spiegel, H., 1999b. Long-term monitoring of microbial biomass, N mineralisation and enzyme activities of a Chernozem under different tillage management. Biol. Fertil. Soils 28, 343-351.
- Kautz, T., Amelung, W., Ewert, F., Gaiser, T., Horn, R., Jahn, R., Javaux, M., Kemna, A., Kuzyakov, Y., Munch, J.-C., Pätzold, S., Peth, S., Scherer, H.W., Schloter, M., Schneider, H., Vanderborght, J., Vetterlein, D., Walter, A., Wiesenberg, G.L.B., Köpke, U., 2013. Nutrient acquisition from arable subsoils in temperate climates: A review. Soil Biol. Biochem.57, 1003-1022.
- Kautz, T., Lüsebrink, M., Pätzold, S., Vetterlein, D., Pude, R., Athmann, M., Küpper, P.M., Perkons, U., Köpke, U., 2014. Contribution of anecic earthworms to biopore formation during cultivation of perennial ley crops. Pedobiologia 57, 47-52.
- Kautz, T., Wirth, S., Ellmer, F., 2004. Microbial activity in a sandy arable soil is governed by the fertilization regime. Eur. J. Soil Biol. 40, 87-94.
- Kladivko, E.J., 2001. Tillage systems and soil ecology. Soil Till. Res. 61, 61-76.
- Kuczak, C.N., Fernandes, E.C.M., Lehmann, J, Rondon, M.A., Luizao, F.J., 2006. Inorganic and organic phosphorus pools in earthworm casts (Glossoscolecidae) and a Brazilian rainforest Oxisol. Soil Biol. Biochem.38, 553-560.
- Kuntz, M., Berner, A., Gattinger, A., Scholberg, J.M., Mäder, P., Pfiffner, L., 2013. Influence of reduced tillage on earthworm and microbial communities under organic arable farming. Pedobiologia 56, 251-260.
- Kuzyakov, Y., Blagodatskaya, E., 2015. Microbial hotspots and hot moments in soil: Concept & review. Soil Biol. Biochem. 83, 184-199.
- Lavelle, P., 1988. Earthworm activities and the soil system. Biology and Fertility of Soils 6, 237-251.
- Lin, Q., Brookes P.C, 1999. An evaluation of the substrate-induced respiration method. Soil Biol. Biochem. 31 (14), 1969-1983.
- Logsdon, S.D., Linden, D.R., 1992. Interactions of earthworms with soil physical conditions influencing plant growth. Soil Sci. 154, 330–337.
- Lowe, C.N., Butt, K.R., 2005. Culture techniques for soil dwelling earthworms: A review. Pedobiologia 49, 401-413.
- Lynch, J.P., Brown, K.M., 2001. Topsoil foraging – an architectural adaptation of plants to low phosphorus availability. Plant Soil 237, 225-237.

- Mäder, P., Fliessbach, A., Dubois, D., Gunst, L., Fried, P., Niggli, U., 2002. Soil fertility and biodiversity in organic farming. Science 296, 1694-1697.
- Marx, M.-C., Kandeler, E., Wood, M., Wermbter, N., Jarvis, S.C., 2005. Exploring the enzymatic landscape: distribution and kinetics of hydrolytic enzymes in soil particle-size fractions. Soil Biol. Biochem. 37, 35-48.
- Moos, J.H., Schrader, S., Paulsen, H.M., Rahmann, G., 2016. Occasional reduced tillage in organic farming can promote earthworm performance and resource efficiency. Appl. Soil Ecol. 103, 22-30.
- Murphy, J., Riley, J.P., 1962. A modified single solution method for the determination of phosphate in natural waters. Anal. chim. acta 27, 31-36.
- Negassa, W., Leinweber, P., 2009. How does the Hedley sequential phosphorus fractionation reflect impacts of land use and management on soil phosphorus: A review. J. Plant Nutr. Soil Sci. 172, 305-325.
- Niemi, R.M., Vepsäläinen, M., 2005. Stability of the fluorogenic enzyme substrates and pH optima of enzyme activities in different Finnish soils. J. Microbiol. Meth. 60, 195-205.
- Orchard, V.A., Cook, F.J., 1983. Relationship between soil respiration and soil moisture. Soil Biol. Biochem. 15, 447-453.
- Pagenkemper, S.K., Athmann, M., Uteau, D., Kautz, T., Peth, S., Horn, R., 2015. The effect of earthworm activity on soil bioporosity – Investigated with X-ray computed tomography and endoscopy. Soil Till. Res. 146, 79-88.
- Pankhurst, C.E., Pierret, A., Hawke, B.G., Kirby, J.M., 2002. Microbiological and chemical properties of soil associated with macropores at different depths in a red-duplex soil in NSW Australia. Plant Soil 238, 11-20.
- Parkin, T.B., Berry, E.C., 1999. Microbial nitrogen transformations in earthworm burrows. Soil Biol. Biochem. 31, 1765-1771.
- Passioura, J., 1991. Soil structure and plant growth. Aust. J. Soil Res. 29, 717-728.
- Pelosi, C., Pey, B., Hedde, M., Caro, G., Capowiez, Y., Guernion, M., Peigné, J., Piron, D., Bertrand, M., Cluzeau, D., 2014. Reducing tillage in cultivated fields increases earthworm functional diversity. Appl. Soil Ecol. 83, 79-87.
- Parham, J.A., Deng, S.P., 2000. Detection, quantification and characterization of β-glucosaminidase activity in soil. Soil Biol. Biochem. 32, 1183-1190.
- Rakels, J.L.L., Romein, B., Straathof, A.J.J., Heijnen, J.J., 1993. Kinetic analysis of enzymatic chiral resolution by progress curve evaluation. Biotechno. Bioeng. 43, 411-422.
- Razavi, B.S., Blagodatskaya, E., Kuzyakov, Y., 2015. Nonlinear temperature sensitivity of enzyme kinetics explains canceling effect – a case study on loamy haplic Luvisol. Front. Microbiol. 6, 1126.
- Riley, H., Pommeresche, R., Eltun, R., Hansen, S., Korsaeth, A., 2008. Soil structure, organic matter and earthworm activity in a comparison of cropping systems with contrasting tillage, rotations, fertilizer levels and manure use. Agriculture, Ecosystems & Environment 124, 275-284.
- Sampedro, L., Whalen, J.K., 2007. Changes in the fatty acid profiles through the digestive tract of the earthworm *Lumbricus terrestris* L. Appl. Soil Ecol. 35, 226-236.

- Satchell, J.E., 1967. Lumbricidae. In: Burges, A., Raw, F. (Eds.), Soil Biology, Academic Press, New York, pp. 259–322.
- Schinner, F., von Mersi, W., 1990. Xylanase-, CM-cellulase-and invertase activity in soil: an improved method. Soil Biol. Biochem. 22, 511-515.
- Schüller, H., 1969. Die CAL-Methode, eine neue Methode zur Bestimmung des pflanzenverfügbaren Phosphates in Böden. Zeitschrift für Pflanzenernährung und Bodenkunde 123, 48-63.
- Shipitalo, M.J., Nuutinen, V., Butt, K.R., 2004. Interaction of earthworm burrows and cracks in a clayey, subsurface-drained soil. Appl. Soil Ecol. 26, 209-217.
- Stehouwer, R.C., Dick, W.A., Traina, S.J., 1993. Characteristics of earthworm burrow lining affecting atrazine sorption. J. Environ. Qual. 22, 181-185.
- Stromberger, M.E., Keith, A.M., Schmidt, O., 2012. Distinct microbial and faunal communities and translocated carbon in *Lumbricus terrestris* drilospheres. Soil Biol. Biochem. 46, 155-162.
- Thielemann, U., 1986. The octet-method for sampling earthworm populations. Pedobiologia 29, 296-302.
- Tiessen, H., Moir, J., 1993. Characterization of available P by sequential extraction. In: Carter, M.R. (Ed.), Soil sampling and methods of analysis, Lewis Publishers, Boca Raton, pp. 75-86.
- Tiunov, A.V., Bonkowski, M., Alphei, J., Scheu, S., 2001. Microflora, Protozoa and Nematoda in *Lumbricus terrestris* burrow walls: a laboratory experiment. Pedobiologia 45, 46-60.
- Tiunov, A.V., Scheu, S., 1999. Microbial respiration, biomass, biovolume and nutrient status in burrow walls of *Lumbricus terrestris* L. (Lumbricidae). Soil Biol. Biochem. 31, 2039-2048.
- Uksa, M., Schloter, M., Kautz, T., Athmann, M., Köpke, U., Fischer, D., 2015. Spatial variability of hydrolytic and oxidative potential enzyme activities in different subsoil compartments. Biol. Fertil. Soils 51, 517-521.
- Vetterlein, D., Kühn, T., Kaiser, K., Jahn, R., 2013. Illite transformation and potassium release upon changes in composition of the rhizophere soil solution. Plant Soil 371, 267-279.
- Vos, H.M., Ros, M.B., Koopmans, G.F., van Groenigen, J.W., 2014. Do earthworms affect phosphorus availability to grass? A pot experiment. Soil Biol. Biochem. 79, 34-42.
- West, A.W, Sparling, G.P, 1986. Modification to the substrate-induced respiration method to permit measurement of microbial biomass in soils of differing water contents. J. Microbiol. Methods 5, 177-189.
- Zhang, Q., Zhou, W., Liang, G., Sun, J., Wang, X., He, P., 2015. Distribution of soil nutrients, extracellular enzyme activities and microbial communities across particle-size fractions in a long-term fertilizer experiment. Appl. Soil Ecol. 94, 59-71.

2.4.7 Supplementary Material

Supplement 1: Detailed description of PLFA quantification

15 µl of IS 2 was added prior to measurement. The relation between the integrated peak area of each fatty acid methyl ester (FAME) and the peak area of the IS 2 was calculated. Calibration curves were determined by a linear regression from the external standard substances at five different concentrations. Losses during sample preparation were corrected for by applying the recovery rate of the IS 1 to the quantifications of each FAME. The GC parameters were as follows: Injection was splitless, the inlet temperature was set to 270 °C and the detector temperature to 280 °C. Column head pressure was kept constant at 0.79 bar. The initial oven temperature was 80 °C, held for 1.5 min, then increased at 10 °C min^{-1} to 167 °C and further at 0.7 °C min^{-1} to 196 °C, and finally at 10 °C min^{-1} to 300 °C and held for 8 min.

Supplement 2: PLFAs in bulk soil and the walls of different pore types ± standard deviation. Highest values are not shaded, lowest values are shaded dark grey.

Soil depth (cm)	45-75 cm			75-105 cm		
Treatment^1	EBP †	RBP ‡	bulk	EBP †	RBP ‡	bulk
PLFAtotal (µg g^{-1} soil)	33.51 ± 4.26	16.65 ± 2.08	1.43 ± 0.7	33.97 ± 8.10	23.02 ± 6.6	0.63 ± 0.25
a15:0 (µg g^{-1} soil)	1.89 ± 0.34	1.04 ± 0.13	0.08 ± 0.08	1.91 ± 0.51	1.51 ± 0.32	0.01 ± 0.01
i15:0 (µg g^{-1} soil)	2.22 ± 0.29	1.45 ± 0.22	0.23 ± 0.15	2.51 ± 0.76	2.01 ± 0.44	0.07 ± 0.05
i17:0 (µg g^{-1} soil)	0.77 ± 0.11	0.57 ± 0.06	0.09 ± 0.05	0.83 ± 0.22	0.79 ± 0.21	0.02 ± 0.02
a17:0 (µg g^{-1} soil)	0.2 ± 0.10	0. ± 0.	0. ± 0.	0.09 ± 0.05	0.04 ± 0.04	0. ± 0.
16:1ω5c (µg g^{-1} soil)	2.83 ± 0.27	1.08 ± 0.18	0.02 ± 0.02	3.06 ± 0.88	1.6 ± 0.47	0. ± 0.
16:1ω7c (µg g^{-1} soil)	4.73 ± 0.50	1.79 ± 0.21	0.12 ± 0.06	4.92 ± 1.27	2.53 ± 0.67	0.01 ± 0.01
18:1ω7c (µg g^{-1} soil)	4.95 ± 0.71	2.27 ± 0.30	0.1 ± 0.07	5.21 ± 1.18	3.33 ± 0.93	0. ± 0.
Cy17:0 (µg g^{-1} soil)	1.09 ± 0.17	0.75 ± 0.11	0.03 ± 0.05	1.57 ± 0.28	1.53 ± 0.41	0. ± 0.
10Me16:0 (µg g^{-1} soil)	0.3 ± 0.06	0.52 ± 0.09	0.02 ± 0.03	0.32 ± 0.13	0.63 ± 0.13	0. ± 0.
10Me18:0 (µg g^{-1} soil)	0.61 ± 0.14	0.44 ± 0.08	0. ± 0.	0.39 ± 0.12	0.38 ± 0.12	0. ± 0.
18:2ω6,9 (µg g^{-1} soil)	1.39 ± 0.43	0.31 ± 0.04	0. ± 0.	0.77 ± 0.16	0.29 ± 0.18	0. ± 0.
20:4ω6 (µg g^{-1} soil)	0.16 ± 0.07	0.01 ± 0.02	0. ± 0.	0.17 ± 0.06	0.02 ± 0.01	0. ± 0.

† EBP: Earthworm-modified biopores, ‡ RBP: Root biopores.

Supplement 3: Factor by which PLFA contents are increased by root biopores as compared to the bulk soil and by earthworm-modified biopores as compared to root biopores and to the bulk soil.

Effect of	Bulk → RBP ††	RBP †† → EBP †	Bulk → EBP †	Bulk → RBP ††	RBP †† → EBP †	Bulk → EBP †
$\text{PLFA}_{\text{total}}$ (µg g^{-1} soil)	11.7	2.0	23.5	36.3	1.5	53.5
a15:0 (µg g^{-1} soil)	13.1	1.8	23.7	190.3	1.3	241.0
i15:0 (µg g^{-1} soil)	6.3	1.5	9.6	29.5	1.2	36.8
i17:0 (µg g^{-1} soil)	6.5	1.4	8.9	34.6	1.1	36.6
a17:0 (µg g^{-1} soil)	0.0	n.d.	n.d.	n.d.	2.5	n.d.
16:1ω5c (µg g^{-1} soil)	71.8	2.6	187.3	n.d.	1.9	n.d.
16:1ω7c (µg g^{-1} soil)	15.1	2.6	40.0	191.0	1.9	371.2
18:1ω7c (µg g^{-1} soil)	22.4	2.2	49.0	4304.2	1.6	6743.3
Cy17:0 (µg g^{-1} soil)	27.0	1.5	39.4	332.9	1.0	341.4
10Me16:0 (µg g^{-1} soil)	32.2	0.6	18.3	n.d.	0.5	n.d.
10Me18:0 (µg g^{-1} soil)	n.d.	1.4	n.d.	n.d.	1.0	n.d.
18:2ω6,9 (µg g^{-1} soil)	n.d.	4.4	n.d.	n.d.	2.6	n.d.
20:4ω6 (µg g^{-1} soil)	n.d.	14.2	n.d.	n.d.	9.2	n.d.

† EBP: Earthworm-modified biopores, ‡ RBP: Root biopores.

2.5 Study 5: Labelling plants in the Chernobyl way: A new ^{137}Cs and ^{14}C foliar application approach to investigate rhizodeposition and biopore reuse

Authors and affiliations

Callum C. Banfield[1]; Mohsen Zarebanadkouki[2]; Bernd Kopka[3], Yakov Kuzyakov[1,4]

[1]Georg-August-University of Goettingen, Institute for Soil Science of Temperate Ecosystems, Buesgenweg 2, 37077 Goettingen, Germany.

[2]Georg-August-University of Goettingen, Division of Soil Hydrology, Buesgenweg 2, 37077 Goettingen, Germany.

[3]Georg-August-University of Goettingen, Laboratory for Radioisotopes, Faculty of Forest Sciences and Forest Ecology, Buesgenweg 2, 37077 Goettingen, Germany.

[4]Georg-August-University of Goettingen, Department of Agricultural Soil Science, Buesgenweg 2, 37077 Goettingen, Germany.

Corresponding author: callumba@gmail.com

Telephone: +49 1578 4527077

Fax: +49 551 3933310

Conflicts of interest: The authors declare no conflicts of interest.

Numbers of text pages: 14; **Number of figures**: 12; **Number of tables**: 1

Keywords: Crop rotation; Detritusphere; Foliar application; Leaf feeding; Radionuclides; Root channel; Root system

Abstract

Background and Aims: Biopores as microbial hotspots provide additional nutrients to crops – but only if their roots grow within the biopores. Such reuse has never been quantified as pre-crop-specific biopores were hardly differentiated from the multitude of pre-existing biopores. Quantification requires e.g. radionuclide labelling of pre-crops (^{137}Cs, to label their biopores) and main crops (^{14}C, to detect new roots). Preliminary testing was performed on simulated biopore reuse: both nuclides given to the same plant were excreted into the same rhizosphere.

Methods: *Cichorium intybus (cv.* Puna) and *Medicago sativa* (cv. Planet) were each sequentially labelled via the leaves with ^{137}Cs and $^{14}CO_2$. β-signals were visualised by imaging of horizontal soil cuts - with and without shielding off the weaker ^{14}C.

Results: Both species allocated 7.1-9.4% of the ^{137}Cs and 21-63% of the ^{14}C below ground. The first image gave both activities; while the second gave only ^{137}Cs. Subtracting the second from the first image gave the ^{14}C distribution, resulting in successful separation of the signals. Thus, separate spatial representations of the roots were obtained. Main root locations by ^{137}Cs and ^{14}C showed a very high spatial overlap coefficient (> 0.95).

Conclusions: Biopore reuse quantification likely becomes feasible with this sequential labelling and shielding approach.

2.5.1 Introduction

The root system and its surrounding soil, known as the rhizosphere (Hiltner 1904), are recognised as a key interface of carbon (C) cycling. Roots induce strong chemical, biological and physical changes in soil, e.g. by exudation of easily available carbon sources, i.e. rhizodeposition. As the exuded C sources boost microorganisms, the rhizosphere is deemed a microbial hot spot (Jones et al. 2009; Kuzyakov and Blagodatskaya 2015; Paterson 2003). After their death, roots leave behind voids, so-called biopores (Kautz et al. 2013), through which subsequently grown crop roots grow faster into the subsoil and reach additional resources. One of the presumably largest benefits for subsequent crops is the biochemical environment created by root decay and rhizodeposition. In the field, even two years after root death and decomposition, C contents in root biopores, also known as the detritusphere, were still 2.5 times higher than in bulk soil, leading to up to 5.5 times higher microbial biomass and concomitantly increased enzyme activities (Hoang et al. 2016). This likely causes faster C turnover and simultaneously nutrient mobilisation from soil organic matter and solid phases. Biopores appear particularly interesting for promoting plant growth in low-input systems such as organic agriculture. It was reported that crops growing in previously established biopores may benefit from nutrients and from the reduced mechanical resistance (Athmann et al. 2013; Ehlers et al. 1983; Yunusa and Newton 2003). If biopores are indeed largely beneficial, their relevance depends on if they are reused in a crop rotation or not. Reuse of biopores could be promoted by management practices such as no-till and crop rotations with tap-rooted pre-crops, which create large-sized biopores (Kautz et al. 2013). On the contrary, it is also possible that depending on soil conditions or other not well-understood factors, this may not always be the case: roots may end up trapped within biopores, which may have had their walls compacted due to root expansion or earthworm burrowing (Hirth et al. 2005). Biopores may be lined with hydrophobic root-derived substances hampering water and nutrient uptake (Carminati 2013). What is more, in some biopores the root-soil contact may be limited (White and Kirkegaard 2010). Such points underline that we are far from a full understanding of biopore dynamics and their controlling factors.

Regardless of the positive or negative effects, biopores are re-used by subsequent crops (White and Kirkegaard 2010): barley modified its root size distribution depending on the pre-crops' root system (Han et al. 2016). Up to now, there has been only scarce quantitative information on the reuse of biopores by subsequently grown crops. This is due to the challenging and often impossible determination of roots growing in specific biopores among countless other biopores of varying age and genesis (Athmann et al. 2013; Han et al. 2015). Therefore, a tool is needed to separate and to quantify biopores and active roots.

For this purpose, we propose radionuclide labelling of pre-crops with radiocaesium (^{137}Cs), labelling main crops with $^{14}CO_2$ and visualisation of each. ^{137}Cs was released into the atmosphere by nuclear weapon tests until 1953 and by nuclear power plant accidents, e.g. in Chernobyl, Ukraine (UNSCEAR 2011). ^{137}Cs has been used as a long-term soil erosion proxy all around the globe due to its half-life of ~ 30 years and its strong binding to soil particles, especially clay (Cremers et al. 1988; Schuller et al. 2002; Walling and He 1999). The Chernobyl fallout including ^{137}Cs has also been used to assess the age of preferential flow paths in soil (Hagedorn and Bundt 2002). This makes ^{137}Cs an excellent candidate for the biopore labelling. Its chemical behaviour is also similar to potassium, which means ^{137}Cs may be used to simulate solute dynamics once released by the roots.

The inspiration for our concept was the path of the ^{137}Cs fallout caused by the Chernobyl nuclear disaster through the plant leaves to the roots and into the rhizosphere, where ^{137}Cs strongly binds to the soil matrix. Our approach imitates this by labelling crops through the leaves with $^{137}CsCl$ to create ^{137}Cs-labelled roots. The roots may be left to decompose to form ^{137}Cs-labelled biopores before the next crop. The second labelling with ^{14}C is thought to be performed on the new crops. Assimilated $^{14}CO_2$ will be exuded as ^{14}C-photosynthates into the rhizosphere of some of the previously created ^{137}Cs-biopores. Both radionuclides' β^- decay can be visualised by phosphor imaging of soil cross sections, but the main challenge lies in separating the ^{137}Cs and ^{14}C signals, which are spatially overlapping in some biopores in the case of reuse. The separation of activities should be possible because during the ^{137}Cs decay 95% of the energy is released as β^- radiation with an energy of 514 keV, whereas the maximum energy of the ^{14}C β^- decay is 156 keV (Nucleonica GmbH 2014). Therefore, the two β^- radiations can be separated by shielding off the weaker ^{14}C β^- radiation while allowing the higher energy ^{137}Cs radiation to pass through (Amato and Lizio 2009).

This up-to-now theoretical concept requires at least 1.5 years to test, so we simulated the biopore reuse in a pot experiment to test its feasibility (Fig. 1). The same plants of either fibrous (alfalfa) or tap-rooted (chicory) root systems were labelled first with ^{137}Cs through leaf feeding and after a few days with ^{14}C in $^{14}CO_2$ atmosphere, instead of waiting for root decomposition and growth of new plants. As both radionuclides are excreted into the same locations, this would be the simulation of a reused biopore, i.e. the spatial overlap of both radionuclides in a specific root channel. wo sequential imagings of soil cross sections with and without shielding and image processing will separate the β^- signals (Fig. 1). Thus, two-dimensional representations of the root systems will be acquired, which can be quantified, and the feasibility of visualising biopore reuse will be apparent.

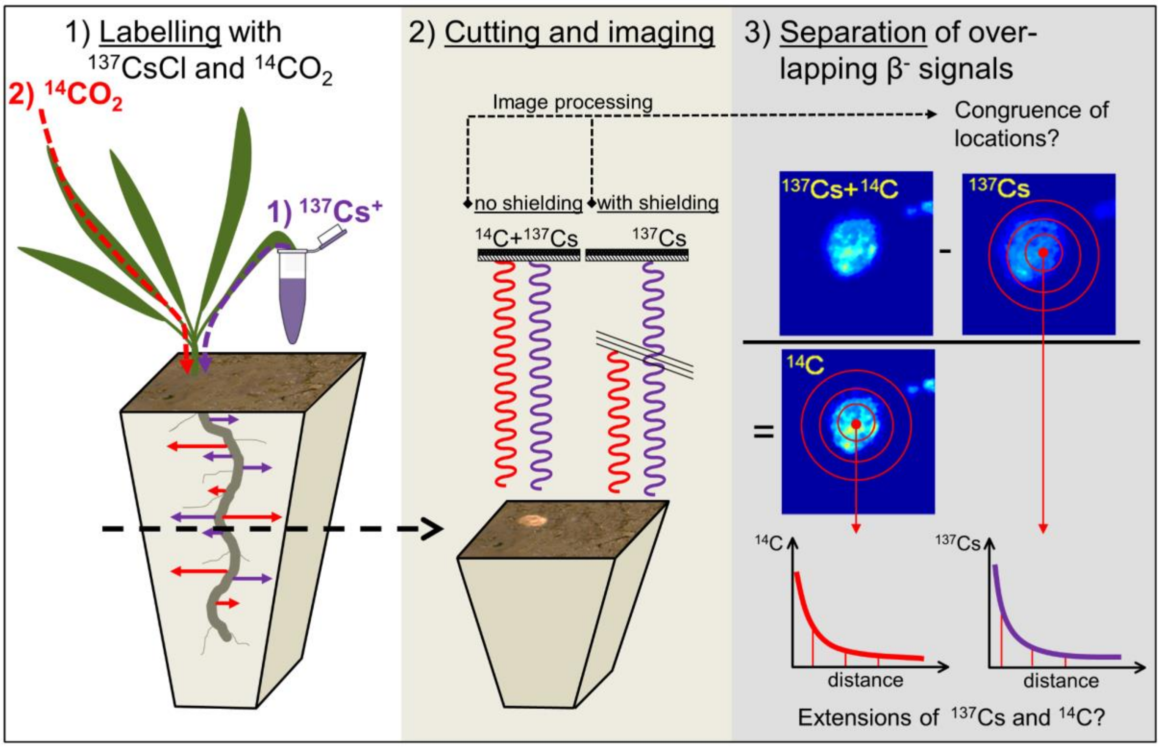
1) Labelling with ^{137}CsCl and ^{14}CO$_2$
2) ^{14}CO$_2$
1) ^{137}Cs$^+$
2) Cutting and imaging
Image processing
no shielding
with shielding
^{14}C+^{137}Cs
^{137}Cs
3) Separation of over-lapping β$^-$ signals
Congruence of locations?
^{137}Cs+^{14}C
^{137}Cs
-
^{14}C
=
^{14}C
^{137}Cs
distance
distance
Extensions of ^{137}Cs and ^{14}C?

Fig. 1 *Concept of the experiment: 1) Labelling the same plants with first ^{137}Cs and then with ^{14}C, 2) imaging with and without shielding and 3) subtracting the signals and image processing.*

2.5.2 Material and methods

2.5.2.1 Soil and plant preparation

Five specimens of chicory (*Cichorium intybus* L. cv. Puna) and five specimens of alfalfa (*Medicago sativa* L. cv. Planet) were grown for 200 days in pots of 15.5 cm height and 5 cm diameter. These species were chosen, as they feature different root system architectures and both species have been widely used in our research group, i.e. their features and peculiarities are well known. The soil was taken from a long-term field experiment site of the Department of Soil Science of Temperate Ecosystems of the Georg-August University of Goettingen in Hohenpoelz (Bavaria), Germany. This loamy Luvisol was chosen as its properties are well known through previous studies (Dippold and Kuzyakov 2016; Gunina et al. 2014). Selected soil properties are given in Online Resource 6. The soil was dried at 40 °C, disaggregated by passing through a 2 mm sieve and then mixed with 25 % fine sand to reduce shrinking and swelling.

The seeds were germinated on wet filter paper for two days. One seedling was planted in each pot at the depth of 0.5 cm. Plants were kept in controlled conditions, i.e. at a temperature of 22 °C, humidity of 50-60% and constant light intensity of ~ 200 µmol m^{-2} s^{-1}. During the growth period, weak fertilisation was carried out twice (N$_{org}$, P$_{org}$, K) and plants were watered every other day.

2.5.2.2 Dual labelling experiment

When plants were 200 days old, the labelling experiment started. The ^{137}Cs labelling solution was prepared as follows: 18.5 MBq of ^{137}CsCl dissolved in 0.1 M HCl were obtained from POLATOM (Otwock, Poland) through Hartmann Analytic (Brunswick, Germany). About 50 Bq µl^{-1} were added to aqueous solutions of unlabelled ^{133}CsCl (0.5 *mM*) (Sigma-Aldrich Chemie GmbH, Munich, Germany) in 5 ml Eppendorf vials (Eppendorf AG, Hamburg, Germany).

For the ^{137}Cs labelling, two chicory leaves of each plant were cut with a razor blade at their widest part and immediately immersed in a 5 ml vial containing 2500 µl of the ^{137}Cs solution (Online Resource 1), whereas 2 - 3 alfalfa stems were cut with a razor blade and immersed in a 1 ml vial filled with 500 µl ^{137}Cs solution. Both solutions contained the same ^{137}Cs activity concentration of 50 Bq µl^{-1}. It was chosen as previous tests carried out with younger plants at 25 Bq µl^{-1} resulted in satisfying images. Eppendorf vials were put into 20 ml scintillation vials for stability and these in turn fixed by clamps attached to a lab stand (Online Resource 1). Transparent tape was used to secure the plant parts onto the vials and to limit evaporation. To monitor evaporation, one vial was filled with a defined volume of ^{133}CsCl solution and left next to the plants. There were considerable differences in the volumes of solution taken up by the plants. As the alfalfa vials were empty after 24 hours, 250 µl of distilled water was added to enable uptake of residual activity possibly remaining in the vials. Chicory leaves took up less solution so that after 2 days the immersed leaves were taken out of the vial, patted dry and two different leaves were cut and immersed for another 24 hours. Remaining ^{137}Cs activity in the vials was measured by the gamma counter HiDex Automatic Gamma counter (550-750 keV, 3“ NaI detector, count time 10 min, count efficiency 17.5%; HiDex Oy, Turku, Finland). In this case, the γ radiation from the ^{137}Cs decay chain is used instead of the direct ^{137}Cs β^- emission. The remaining activities in the vials were related to the initial activities to calculate the uptake of the ^{137}Cs tracer.

$$Eff_{137Cs} = \frac{(A_{initial} - A_{vial})}{A_{initial}} * 100\% \qquad \text{(Eq. 1)}$$

with:
Eff_{137Cs}, the uptake efficiency of the ^{137}Cs tracer from the vial [%]
A_{vial}, the ^{137}Cs activity of the vial and its remaining volume [Bq]
$A_{initial}$, the total ^{137}Cs activity of the vial and the tracer solution prior to labelling [Bq]

To show the potential of the approach, the same plants were labelled also with $^{14}CO_2$ instead of waiting for root decomposition and growth of new plants (Fig. 1). $^{14}CO_2$ labelling was performed in an airtight and transparent plastic chamber under a plant growth lamp. 5 MBq of $Na_2{}^{14}CO_3$ (Hartmann Analytic, Brunswick, Germany) were dissolved by phosphoric acid (Sigma-Aldrich, Chemie GmbH, Munich, Germany) and the formed $^{14}CO_2$ was pumped into the chamber by a peristaltic pump and cycled for 36 h. A 120-mm fan supported the even distribution of the $^{14}CO_2$ inside the chamber. Four days after the ^{14}C labelling, the soil cores were cut horizontally at depth of 5 cm below the soil surface with a sharp utility knife. Prior to this, the plastic pot was cut open with a cut-off wheel tool (Dremel 4000 series, Dremel Corp. Racine, WI, U.S.A.).

2.5.2.3 ^{137}Cs and ^{14}C imaging

The cut soil surfaces were placed on a phosphor imaging plate (BAS-MS 2040; 20 by 40 cm; Fujifilm Europe GmbH, Düsseldorf, Germany). A 12 µm Hostaphan® film (Mitsubishi Polyester Film GmbH, Wiesbaden, Germany) was placed between the samples and the imaging plate to protect it from the labelled soil during the first imaging. This first image showed the activities of ^{137}Cs and ^{14}C, while the second imaging showed only the ^{137}Cs activity. For the second imaging, six additional plastic films (polypropylene, 40 µm thickness, density 0.95 g cm^{-3}, MDF-Verpackungen GmbH, Bergisch Gladbach, Germany) were used to shield off the ^{14}C radiation. Full shielding was checked by 1 µl drops of activities of 125 Bq of ^{137}Cs and ^{14}C put next to the soil cuts. Exposure was three hours for both images. The imaging system FLA 5100 (Fujifilm Europe GmbH, Düsseldorf, Germany) was used to read the images with a resolution of 100 µm. The same procedure was carried out once for each plant species for the dried and flattened leaves and stems.

2.5.2.4 Determination of exposure and shielding

The number of plastic films required for shielding off the ^{14}C β^- radiation was worked out separately. On a sheet of coated paper (DescProtect, LLG Labware GmbH, Meckenheim, Germany) 1 µl drops of dissolved $^{137}CsCl$ and ^{14}C-glucose were added at increasing activities ranging from 1 to 125 Bq. Additionally, the remaining β^- radiation of ^{137}Cs, as well as, the optimal exposure time for the imaging were determined.

2.5.2.5 Image processing

The emitted β^- radiation from the decay of ^{137}Cs and ^{14}C was stored in 16-bit digital images. The imaging plates store the signal as the quantum level (i.e. the logarithmic pixel-wise greyscale data) for each pixel. These were then converted to standardised PSL (**p**hoto-**s**timulated **l**uminescence) units, which is an arbitrary unit describing the absorbed and corrected energy on the imaging plate. For the conversion, we followed the protocol given in the technical documentation of the image format (Fuji Photo Film Co. Ltd. 2003):

$$PSL = \frac{P^2}{100} . \frac{4000}{S} 10^{L.\frac{QL}{G} - 0.5} \qquad \text{(Eq. 2)}$$

with:
P, the pixel size (P=100 µm),
QL, the pixel-wise grey value (quantum level) initially stored in 16-bit images,
S, the sensitivity factor (S=1000)
L, the latitude (L=5) and
G, related to the image format and equals to 65535 for 16-bit images.

Image processing was performed in MATLAB 2015 (The MathWorks GmbH, Ismaning, Germany). As the first step, the converted images were normalised to get a similar background based on a blank area in the images. There were two sets of images for each plant: one capturing the decay of both ^{137}Cs and ^{14}C, and the other one showing the decay of only ^{137}Cs after shielding off the ^{14}C. Each set of images was taken separately and, therefore, were not overlapping pixel by pixel. To quantitatively separate the contribution of ^{137}Cs and ^{14}C, overlapping both sets of images enabled subtraction of the two images, i.e. the second from the first image. The two images were aligned by defining one image the reference and applying geometric transformations to the other image. For this purpose, an intensity-based image registration was used. Since the second imaging also reduced the intensity of the ^{137}Cs signal, this was corrected by calculating the attenuation from defined ^{137}Cs activities put next to the soil samples. Photos of soil cross sections were taken prior to imaging. These photos were aligned with the images obtained by imaging. Thanks to the big contrast between the roots and the soil in these photos, the roots were easily segmented from the soil through a threshold method. We focussed on the main root of each plant. A Euclidean distance map was applied to the segmented root to calculate the root radius. This distance map was used to categorise pixels around the roots according to their lateral distance from the rhizodermis, i.e. the outermost primary cell layer of the root tissue. The pixel-wise PSL values were then converted to activities (full details see next section). To calculate the radial profiles of the nuclide-specific activities as a function of the distance from the rhizodermis, mean activities were determined at given distances from the rhizodermis (Zarebanadkouki et al. 2016) - assuming radial symmetry around the roots. Summing up the increments of activities at each distance gave the total activity excreted by the root (Eq. 3).

$$A_{tot} = \sum_{i=1}^{i=n} \left(\pi r_i^2 - \pi r_{i-1}^2\right) \times A_i \qquad \text{(Eq. 3)}$$

with:
A_{tot}, the total activity of each nuclide excreted by the root [Bq]
r_i, the distance of a pixel *i* from the rhizodermis [mm] with r_0, the root radius
A_i, the mean activity of each nuclide in the distance r_i from the rhizodermis [Bq mm^{-2}]

Since different initial activities were applied to the plant species and the root diameter was different among species, we normalised the total excreted activities accordingly (Eq. 4).

$$A_{tot,norm} = \frac{A_{tot}}{A_{rcvd} \times 2\pi r_0} \qquad \text{(Eq. 4)}$$

with:
$A_{tot,norm}$, the normalised total activity of each nuclide [Bq Bq mm^{-1}]
A_{tot}, the total activity of each nuclide excreted by the root [Bq]
A_{rcvd}, the total activity of a nuclide recovered in a pot and shoot
r_0, the root radius

2.5.2.6 Quantification of the images

The pixel-wise PSL values were converted to ^{137}Cs and ^{14}C activities by a regression describing the relation between PSL values and the activities of ^{137}Cs and ^{14}C standards. The regression function was obtained by imaging known activities of ^{137}Cs and ^{14}C. For this, 0.5 g of the soil from the plant experiment were adjusted to 25% soil moisture (gravimetric) by dropwise addition of 150 µl of dissolved ^{14}C-glucose and ^{137}Cs activities ranging from 20 to 325 Bq µl^{-1}. The soil was mixed to achieve a uniform mixture and transferred to a 96-well microtiter plate (U-shaped well with a diameter of 6.94 mm and a depth of 11.65 mm; Brandplates®, Brand GmbH + Co KG Wertheim, Germany). A smooth soil surface was prepared on the level of the rim of each cup. Aliquots of ^{14}C-glucose were dissolved in Rotiszint® eco plus scintillation cocktail (Carl Roth GmbH + Co. KG, Karlsruhe, Germany) and activities were determined by the liquid scintillation counter Tricarb™ B3180 TR/SL (PerkinElmer Inc., Waltham, MA, U.S.A.). Activities of ^{137}Cs were measured on the HiDex Automatic Gamma counter. The images were normalised to the background and emitted energies were converted to PSL values. The ^{137}Cs and ^{14}C activities and their PSL values were normalised to the applied areas and a linear function was fitted to the PSL values.

2.5.2.7 Spatial overlap of ^{137}Cs and ^{14}C hot spots

The quantified and ready images of ^{137}Cs and ^{14}C were taken and the spatial overlap (r) of the main activities was estimated by the spatial overlap coefficient (Eq. 5) (Bolte and Cordelières 2006; Manders et al. 1993). This was performed by means of the JACoP plugin (Cordelières and Bolte 2009) in Fiji (Schindelin et al. 2012; Schindelin et al. 2015) using manually set thresholds.

$$r = \frac{\sum_i A_i \times B_i}{\sqrt{\sum_i (A_i)^2 \times \sum_i (B_i)^2}} \qquad \text{(Eq. 5)}$$

with:
A, the intensities of a pixel of channel A,
B, the intensities of the corresponding pixel of channel B

2.5.2.8 Determination of ^{137}Cs and ^{14}C bulk activities

At the end of the experiment, all soil was collected, plants were cut above ground and the dry weight of soil and shoots were determined after drying at 75 °C for 120 h. Visible, larger roots were pre-ground separately in a ball mill (PM 100; Retsch, Haan, Germany) for at least 15 min prior to adding the soil and milling for another 15 min. Five replicates of ~ 1 g of soil and roots were taken and ^{137}Cs γ activity was measured. The same samples were incinerated at 500 °C and the resulting $^{14}CO_2$ was trapped in Oxysolve C-400 scintillation cocktail (Zinsser Analytic GmbH, Frankfurt, Germany) prior to the scintillation measurement.

The belowground tracer allocation was expressed as the belowground activity relative to the total recovered activity (shown for ^{137}Cs in Eq. 6a). The aboveground allocation was calculated as the aboveground activity relative to the total activity recovered (shown for ^{14}C in Eq. 6b).

$$^{137}Cs_{belowground} = \frac{\sum_{i=1}^{n} \frac{^{137}Cs_{belowground,i}}{(^{137}Cs_{aboveground,i} + \, ^{137}Cs_{belowground,i})}}{n} * 100\% \qquad \text{(Eq. 6a)}$$

with:
$^{137}Cs_{belowground,}$ the mean belowground ^{137}Cs allocation of a plant species [%]
$^{137}Cs_{belowground,i}$, the total belowground ^{137}Cs activity of a replicate *i*, i.e. soil and roots [kBq]
$^{137}Cs_{aboveground,i}$, the ^{137}Cs activity in the shoot of a replicate *i* [kBq]
n, the number of replicates

$$^{14}C_{aboveground} = \frac{\sum_{i=1}^{n} \frac{^{14}C_{aboveground,i}}{(^{14}C_{aboveground,i} + \, ^{14}C_{belowground,i})}}{n} * 100\% \qquad \text{(Eq. 6b)}$$

with:
$^{14}C_{belowground}$, the mean aboveground ^{14}C allocation of a species [%]
$^{14}C_{belowground,i}$, the total belowground ^{14}C activity recovered in a replicate *i*, i.e. roots and soil [kBq]
$^{14}C_{aboveground,i}$, the aboveground ^{14}C activity recovered in a replicate *i* [kBq]
n, the number of replicates

2.5.3 Results

2.5.3.1 Labelling with ^{137}Cs and ^{14}C

^{137}Cs transported within the leaves of both plant species was detectable 6 hours after labelling had started using a Geiger-Müller counter with a small probe. Presence of ^{137}Cs in the roots, i.e. at the bottom of pots, was detectable two days after labelling. Imaging confirmed that strongly increased ^{137}Cs activities were allocated to the more distal parts within four days in the case of both plant species, e.g. in young leaves and leaf bases of chicory (Online Resources 2 and 3). ^{137}Cs uptake was 98.0 ± 0.8% for chicory and 99.8 ± 0.1% for alfalfa (Table 1). Root allocation of ^{137}Cs did not strongly depend on the plant species: chicory allocated 9.4 ± 1.5% and alfalfa allocated 7.1 ± 1.6% of the tracer below ground (Table 1). Even after four days, more than 90% of the ^{137}Cs was still in the shoot, which is also discernible in the imaging of the shoot (Online Resources 2 and 3).

Imaging revealed that the ^{14}C β^- radiation was completely shielded to the background level when using six layers of 40 µm polypropylene film and one layer of 12 µm Hostaphan® film (Online resource 7). Shielding attenuated the ^{137}Cs radiation by 35.8 ± 1.5%.

Table 1 *^{137}Cs and ^{14}C budget. Shown are means of five replicates ± standard errors of the mean*

	^{137}Cs uptake [%]	^{137}Cs aboveground [%] of recovery	^{137}Cs belowground [%] of recovery	^{14}C aboveground [%] of recovery	^{14}C belowground [%] of recovery
Chicory	98.0 ± 0.8%	90.6 ± 1.5%	9.4 ± 1.5%	37.4 ± 4.5%	62.6 ± 4.5%
Alfalfa	99.8 ± 0.1%	92.9 ± 1.6%	7.1 ± 1.6%	79.4 ± 6.0%	20.6 ± 6.0%

The ^{137}Cs and ^{14}C labelling technique and its feasibility will be first illustrated exemplarily for two replicates per species. Detailed images of all pots are given as Online Resources 4 and 5. The example images of both species are shown in Fig. 2, in which the intensities correspond to the quantum level, i.e. the logarithmic pixel-wise greyscale data. Both plants, roots and their rhizosphere showed strongly increased activities of ^{137}Cs and ^{14}C and therefore, their spatial distribution can be easily distinguished. Pixel-wise subtraction of ^{137}Cs images from the images of total ^{137}Cs and ^{14}C activity gave the ^{14}C

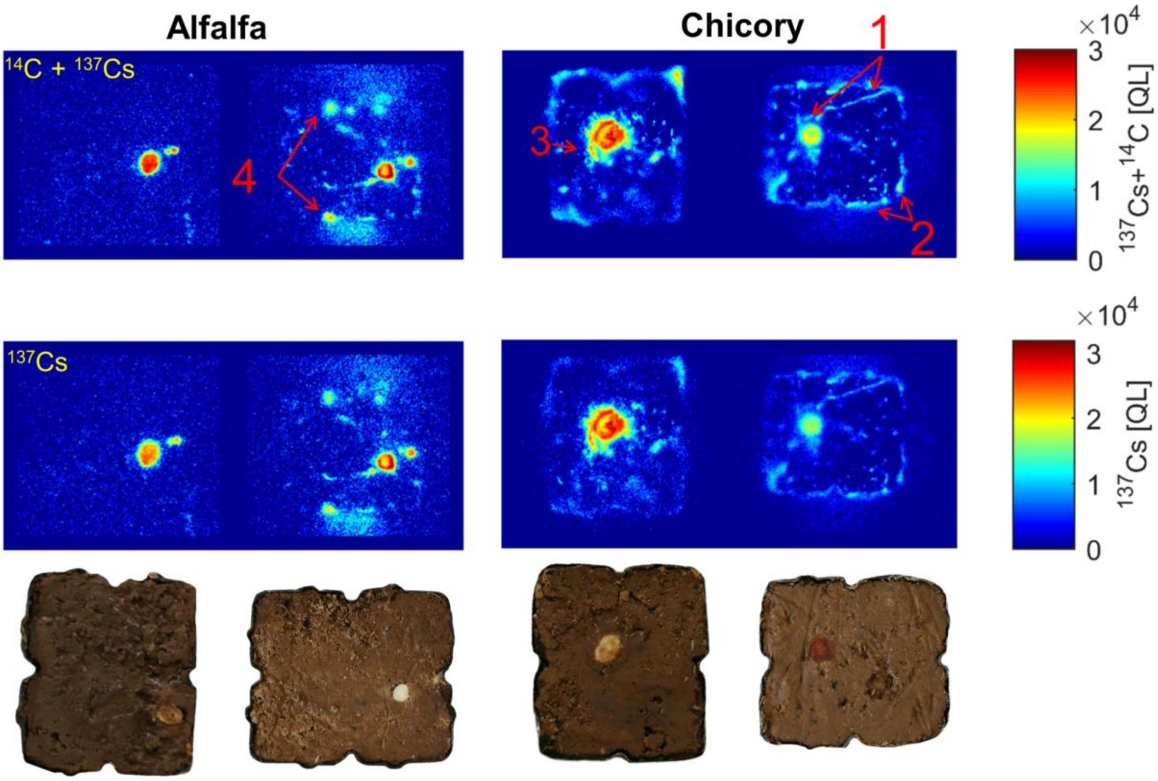

Fig. 2 *Imaging of ^{137}Cs and ^{14}C (top) and ^{137}Cs only (middle) activities in the soil at a depth of 5 cm for alfalfa (left) and chicory (right). Below the imagings are rotated photos of the respective soil cuts. The images presented quantum level data (QL, i.e. the pixel-wise grey values stored in 16-bit images) which was initially captured during imaging. The red colour corresponds to the higher activities. Note that here two plants are given as examples and all plants are given as supplementary information (Online Resources 4 and 5). Numeric identifiers and red arrows relate to 1) lateral root emerging from the single tap root of chicory, 2) a large number of fine roots growing in the gap between the soil and the container, 3) sloughed off rhizodermis, and 4) smaller secondary roots as opposed to chicory's taproot.*

contribution (Fig. 3). Here, subtracting the ^{137}Cs image from the total image worked remarkably well and resulted in two separate datasets of ^{137}Cs and ^{14}C, which was the main aim of this experiment. Both radionuclide distributions gave good representations of the roots (Fig. 2, top and below, Online Resources 4 and 5), including the prominent main roots and laterals (chicory), as well as secondary roots (alfalfa). Congruence of the main root locations by both radionuclide distributions was very high as determined by the overlap coefficient with 96.0 ± 1.1% for chicory and 95.3% ± 0.9% for alfalfa

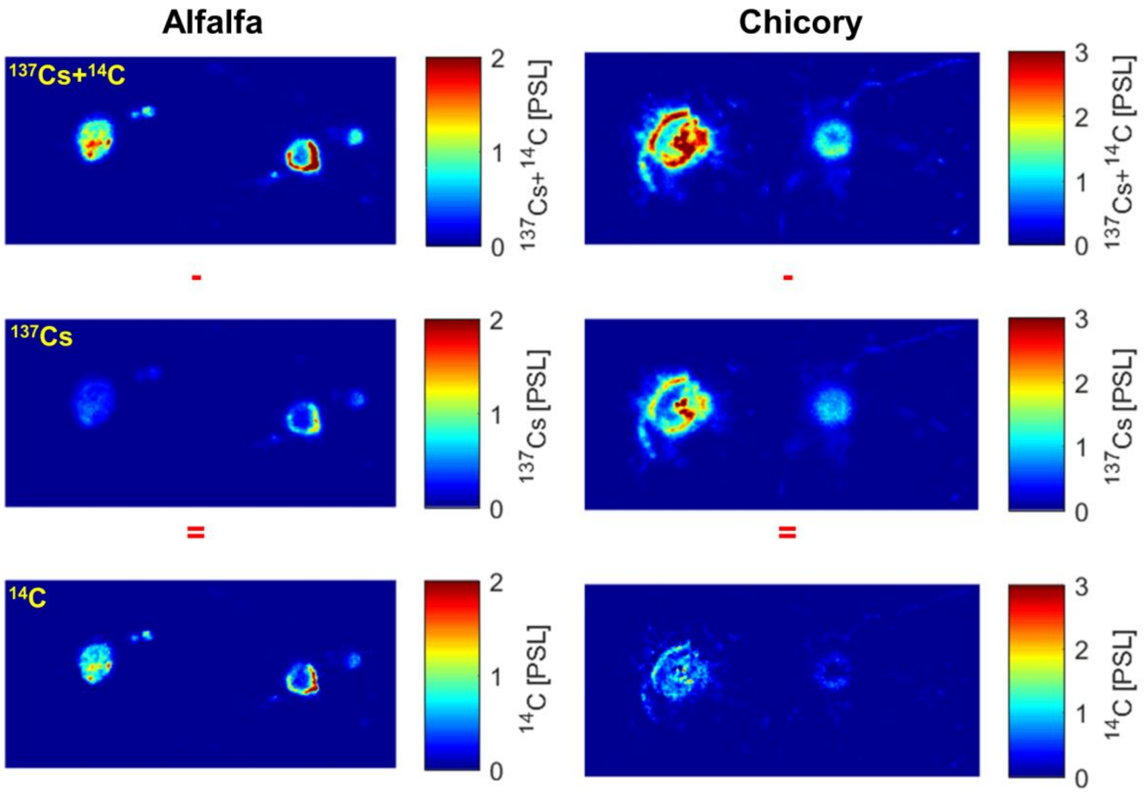

Fig. 3 *Procedure of image processing after conversion to PSL units and successful subtraction of ^{137}Cs activity (middle) of total activity (top) to yield the pure ^{14}C activity (bottom), shown for two examples of the largest, i.e. main roots, to which a colour map was applied.*

.

2.5.3.2 Quantification of the intensities

The two separated radionuclide visualisations were quantified by a regression function, which described the linear relation between PSL value and the activities of each radionuclide ($R^2 > 0.98$, Fig. 4). For further quantifications, we focussed on the main root of each plant. Radial distributions of ^{137}Cs and ^{14}C activities as a function of distance from the rhizodermis are given in Fig. 5. For both plants, the activities were higher near the rhizodermis and decreased towards the bulk soil. In general, the ^{137}Cs activity at the rhizodermis was about 4-5 times higher than the activity of ^{14}C. The radial extension of ^{137}Cs was also larger in both plants than the ^{14}C (e.g. alfalfa, ca. 0.25 cm vs. 0.15 cm). The rhizosphere extensions of ^{137}Cs and ^{14}C were about 40% smaller in the case of alfalfa compared to chicory. The two plant species initially received different total activities and their roots had different diameters. Therefore, Fig. 6 shows activities normalised to the total recovered activities and root perimeter: chicory excreted ~ 23 times more ^{14}C and 15 times more ^{137}Cs than alfalfa. Both species gave more ^{137}Cs than ^{14}C into the rhizosphere at 5 cm depth. So, the excretion of nuclides depended on the plant species and the type of nuclide.

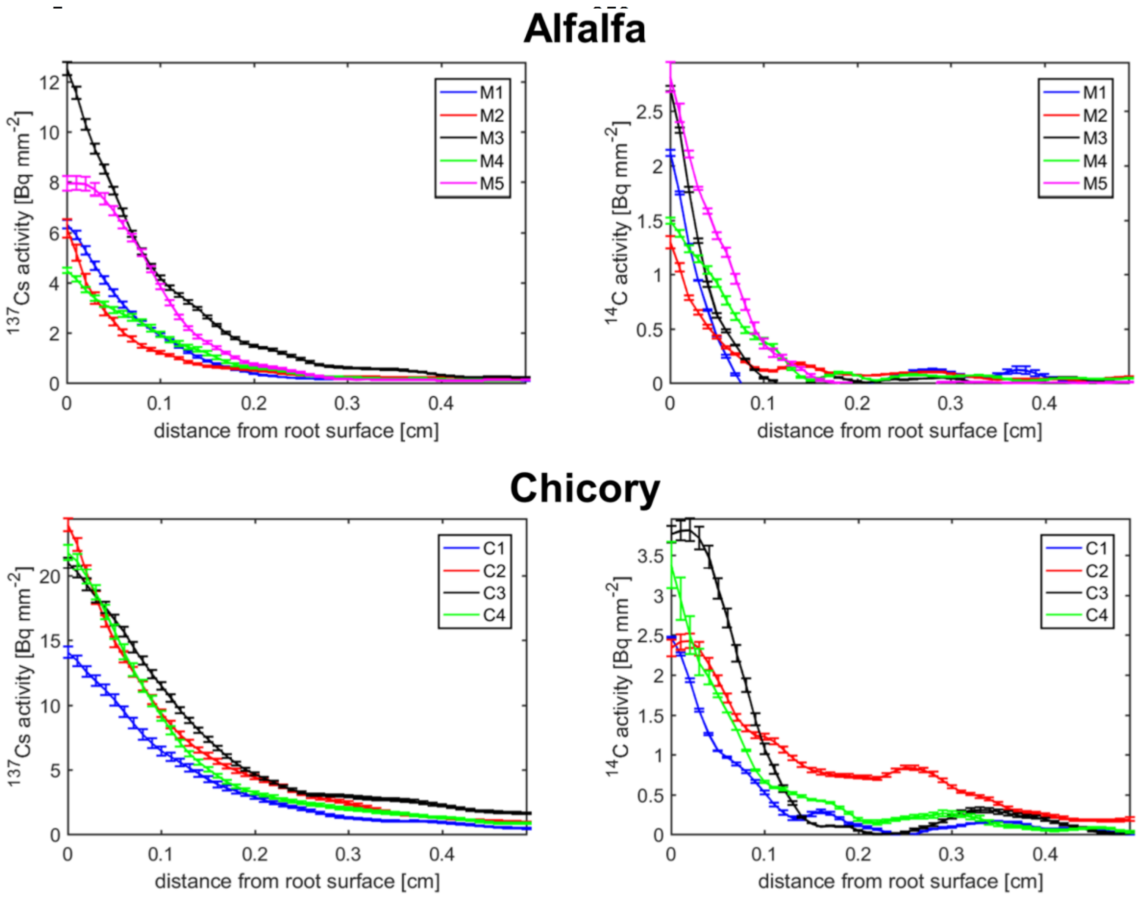

Fig. 5 *Radial profiles of ^{137}Cs (left) and ^{14}C (right) activities as a function of distance from the rhizodermis for five alfalfa replicates (top) and four chicory replicates (bottom). Data averaged in radial direction around (360 °) the largest root of each plant. Error bars show the variance of the activities (as standard errors) in the respective distance from the rhizodermis.*

2.5.4 Discussion

2.5.4.1 The double labelling approach

We presented a proof-of-concept, which should enable the visualisation and quantification of the reuse of biopores (Fig. 1). Our approach simulates the path of the Chernobyl ^{137}Cs fallout from the leaves into the roots by labelling crops through the leaves with ^{137}CsCl to create ^{137}Cs-labelled root biopores. The roots of the subsequently grown crop could then be differentiated by $^{14}CO_2$ labelling to create ^{14}C-labelled roots. The feasibility of our concept was shown in an experiment, in which the same plants were labelled by both tracers. This simulates the situation of a re-used root channel, i.e. both radionuclides spatially overlapping in the same root channel.

Applying ^{137}Cs and ^{14}C to plants was easy, fast and straightforward. Labelling plants with $^{14}CO_2$ and ^{14}C-photosynthate release into the soil is well established (Pausch and Kuzyakov 2011). There were earlier hints that the labelling with ^{137}Cs might be feasible: ^{137}Cs from seedlings incubated in ^{137}CsCl solution was released from their roots into the ^{137}Cs-free soil (Bystrzejewska-Piotrowska and Urban 2004). Of the total ^{137}Cs activity, 7.1-9.4% was allocated below ground within four days (Table 1). At least four reasons explain why the ^{137}Cs labelling worked remarkably well: I) the absence of uptake-regulating barriers in cut leaves and stems as compared to roots (e.g. Casparian strip in the root endodermis), II) the comparatively high mobility of caesium in plants (Online Resources 1 and 2; Bystrzejewska-Piotrowska and Urban 2004), III) its similarity to K and, therefore, possibly selective uptake, and IV) the translocation of it to the roots through the phloem (Buysse et al. 1995; Zhu and Smolders 2000). It may be speculated that the ^{137}Cs uptake follows the uptake mechanisms of other cations, i.e. uptake through the cut surface or stomata, or cuticular penetration (Fernández and Eichert 2009; Stock and

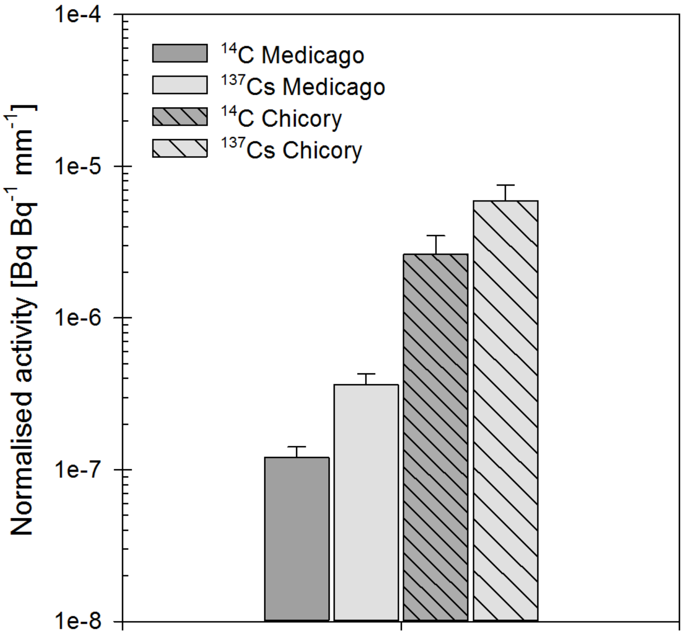

Fig. 6 *Total ^{137}Cs and ^{14}C activities in the rhizosphere of alfalfa and chicory obtained from Eq. 4, normalised by total activities taken up by each plant and the root perimeter. The data are averaged among replicates and error bars show standard errors.*

Holloway 1993). The contributions of the three mechanisms for the two species cannot be estimated from our data. However, we found evidence of selective uptake of ^{137}Cs by chicory. Almost all ^{137}Cs activity was taken up from the tracer solution (Table 1). Yet, there was still solution present at the end of the experiment in the chicory vials, which contained ^{137}Cs activities lower than the ^{137}Cs activity expected in the remaining volume. Hence, we assume selective uptake of Cs compared to water, most probably since Cs is a K analogue.

The belowground allocation induced very strong signals in the soil - far above the detection limit and the background luminescence of the imaging plate. Herein, we focused on the main roots, which turn into biopores desirable in organic agriculture (Kautz et al. 2013), but finer roots were also labelled. The main challenge was to prove that both nuclides are individually detectable. This required separation of ^{137}Cs and ^{14}C β^- radiation signals, which was achieved by shielding during the two-step imaging procedure (Fig. 3, Online Resource 7). It was shown that the root release of radionuclides could be used to visualise roots, their locations and features such as laterals or secondary roots - irrespective of the species (Fig. 2). After labelling, the ^{137}Cs distribution in the rhizosphere represents the Cs^+ and K^+ excretion from the roots from the start of the labelling to imaging. Also, it gives the size distribution of the roots and later biopores in a soil cut. ^{14}C-photosynthates in the rhizosphere are representative of the root exudation of low molecular organic substances. Like ^{137}Cs, the ^{14}C activity distribution gives the size, extension and locations of the roots (Fig. 3). Consequently, the size distribution and count data of roots and biopores of both fibrous and tap-rooted plants could be determined and compared in situ. The descriptive statistics are needed as a foundation for future research.

Our experiment has shown, that both radionuclides were allocated below ground, gave satisfying representations of the roots and the strong signals were successfully separated from each other through shielding during imaging (Fig. 3). The low mobility of ^{137}Cs in soil and its long half-life of about 30 years are well-established properties and should lead to stable labelling of biopores (Cremers et al. 1988; Walling and Quine 1995). Also, the rhizodeposition of ^{14}C-photosynthates is frequently and successfully applied. With these prerequisites met, biopore reuse quantification comes within reach.

2.5.4.2 Implications for biopore reuse

The reuse of pre-crop biopores in crop rotations by subsequently grown main crops is obvious (Elkins 1985; Han et al. 2016), but has not been quantified yet due to a lack of methods. Although not specifically tested herein, our approach should be feasible for biopore studies. Even under the assumption, that only low ^{137}Cs activities were excreted by the roots within four days, the signal was already strong enough for imaging (Fig. 2). The exact ^{137}Cs activities excreted are only of secondary importance in this regard. As long as ^{137}Cs is translocated into the roots prior to root death, it will be released into the developing root channel upon cell death and during root decomposition. Hypothetically and according to our concept, after the main crop phase in a crop rotation, unused biopores would feature only ^{137}Cs, while reused biopores would show a spatial overlap of ^{137}Cs and ^{14}C activities. Finally, roots growing in bulk soil would be only labelled with ^{14}C and not with ^{137}Cs. In principle, earthworm biopores could also be labelled by feeding earthworms ^{137}Cs- or ^{14}C-labelled litter, which would enable more earthworm-related research opportunities. ^{14}C and bomb-fallout ^{137}Cs were already shown to be possible tools to determine the age of individual burrows, bioturbation and organic matter turnover (Cheshire and Griffiths 1989; Hasegawa et al. 2013; VandenBygaart et al. 1998).

We presented one approach to quantify the ^{137}Cs and ^{14}C signals to later quantify biopore reuse from the imagings: the overlap coefficient (Bolte and Cordelières 2006; Manders et al. 1993). Since both labellings were performed on the same plants without waiting for root decomposition after the pre-crop phase, all ^{137}Cs-labelled roots were also labelled with ^{14}C (Fig. 3). This is discernible from the high overlap coefficient of > 0.95.

2.5.4.3 Further applications

This dual labelling approach could be particularly useful to localise and visualise further processes on different scales: on the smaller rhizosphere scale, estimating the rhizosphere extension for organic and inorganic substances, and on a larger scale, the root system architecture.

Extension of photosynthates and solutes' diffusion in the rhizosphere: the rhizosphere boundary

As the highest ^{137}Cs and ^{14}C activities were located around the main roots, i.e. the tap roots and largest fibrous roots, these were considered the main regions of interest (Fig. 2). Radial distributions of ^{137}Cs and ^{14}C starting from the rhizodermis into the bulk soil are shown in Fig. 5. The distance of the rhizodermis to the point where the activity was for the first time down to 5% of the activity of the root centre was defined the rhizosphere extension. This definition is rather arbitrary since it only serves the purpose of showing the feasibility of the approach also in the narrow rhizosphere: heterogeneous rhizodeposition patterns in varying soil depths can be determined easily.

The radionuclide localisation and activity distribution explain I) the pattern of the gradients and II) the amount of tracer excreted by the root. Radionuclide-specific rhizosphere extensions were expected according to size and charge of the excreted compounds (Fig. 5). ^{137}Cs^{+} strongly binds to iron oxides and clays (Giannakopoulou et al. 2007; Riise et al. 1990) and is not taken up by microorganisms in large amounts like C, e.g. as an energy source. This results in a ^{137}Cs rhizosphere extension which is monotonically decreasing. The ^{137}Cs distribution represents the microbially non-decomposable release of K. On the contrary, ^{14}C-labelled photosynthates are taken up very fast and efficiently by microorganisms (Fischer et al. 2010), respired, used for biofilm formation or stabilised as necromass (Miltner et al. 2012). The locations of such processes are clearly visible in Fig. 5 as the distribution of ^{14}C increases and decreases within the rhizosphere. The radial distribution of ^{14}C was similar to the distribution of enzyme activities in the rhizosphere (Razavi et al. 2016). Apart from these lateral patterns, exudation along the roots could be studied by cutting the soil cores either horizontally at different depths, by cutting it vertically or by using rhizotrons (Razavi et al. 2016).

Separating and quantifying radionuclides in the rhizosphere on a resolution of 100 µm was accomplished (Fig. 3). Enhancing the resolution to 25 µm is possible and will capture finer details and more exact rhizosphere extensions. Utilising the ^{14}C activity as a proxy for organic compounds in the rhizosphere will help elucidate C dynamics in root-induced hot spots (Pausch and Kuzyakov 2011). ^{137}Cs as an analogue for the nutrient potassium could be a new tool not just for biopore reuse but also a proxy for solute excretion from roots. To our knowledge, there is no tool available yet to quantitatively visualise the rhizosphere dynamics of both root exudates and solutes in situ. We, therefore, propose this radionuclide imaging/shielding approach, which should in principle also work with ^{40}K, ^{90}Sr (as an analogue for Ca), ^{36}Cl, ^{35}S or ^{33}P. Changing the radionuclides would also enable to study other processes or elements, e.g. behaviour of anions in the rhizosphere.

Root system architecture

Albeit the biopore reuse was our prime interest, the approach may also be useful to study the root system architecture. Herein, the soil core was cut once in 5 cm depth. By increasing the number of cuts, one may be able to get a 3D approximation of the root system. Additionally, extra vertical cuts could be helpful for modelling. Repeated pulses of ^{14}C and ^{137}Cs ensure that the roots are homogenously labelled. Compared to computer tomography, this approach may be less accurate and needs destructive sampling, but it is certainly more affordable.

2.5.4.4 Methodological recommendations

It is recommended to label the first crop with ^{137}Cs and the subsequent crop with ^{14}C due to the rapid microbial C tracer turnover in the rhizosphere and fast losses as $^{14}CO_2$ compared to ^{137}Cs. If biopore reuse of further crops appears interesting, a third crop could be labelled with radionuclides having maximum β^- decay energies not too close to 156 or

514 keV, such as ^{40}K (1.31 MeV) or ^{36}Cl (0.71 MeV). In case extremely high activities are used, an overglow effect may occur, i.e. very high activities paired with long exposure times may cause not proportional luminescence on the imaging plates. We have not found this to impact the image quality in our setup. If this effect occurs, two measures could help to maintain a high localising resolution: I) keeping the distance between the soil and imaging plate as small as possible and II) 3D collimators or anti-scatter grids cutting off scattered radiation.

High CsCl concentrations in plants may inhibit photosynthesis and may cause contractile roots in young plants (Bystrzejewska-Piotrowska et al. 2004). Even though the actual ^{137}Cs tracer concentrations are orders of magnitude too low to cause such effects, we recommend high activities of the ^{137}Cs tracer and lowest concentrations of a $^{133}CsCl$ medium. Mature plants are expected to be less affected by salinity as compared to young plants (Hasegawa et al. 2015). Leaves of our 200 day-old plants did not show any colour changes at CsCl concentration of 0.5 *mM*. Chicory leaves were left in the ^{137}Cs solution for up to 48 h without visible damage. In a different pre-test (not shown), damages were observed after > 48 h, but this may vary for different species or growth stages. We, therefore, recommend pre-tests with the desired plant species and unlabelled solutions. The unlabelled CsCl medium is also required to handle the ^{137}Cs, as its actual concentration would be too small to handle: the slightest contamination with clay or iron oxides in a tracer solution without ^{133}Cs would bind a large part of the ^{137}Cs.

For the leaf-feeding, cutting the leaves under water and adding a surfactant such as Silwet® Gold (Spiess-Urania, Hamburg, Germany) to the CsCl solution may further reduce the risk of unsuccessful labellings caused by embolies. If performed in the field, the leaf feeding procedure may be carried out like in the laboratory, i.e. cutting the leaves and immersing them in a solution of tracer and surfactant. Repeated ^{137}Cs pulse labelling at different growth stages is expected to label the root pores more homogenously throughout soil depths.

$^{14}CO_2$ pulse labelling is regularly performed and specific issues were reviewed extensively elsewhere (Kuzyakov and Domanski 2000; Meharg 1994). Due to rapid C turnover in soil and rhizosphere, the imaging procedure should be carried out as soon as possible after the second, i.e. ^{14}C labelling, to receive the strongest ^{14}C signals. In the field, the $^{14}CO_2$ labelling can be performed in a portable plastic chamber similar to our laboratory setup (Hafner and Kuzyakov 2016). In the field and unlike in this experiment, roots will not be as concentrated as in our pots, but rather be more dispersed. One countermeasure could be to use larger imaging plates (i.e. maximum 35 x 43 cm with our manufacturer). Also, the signals may be weaker because of a higher root mass and, therefore, possibly lower ^{137}Cs activity per rhizodermis. To maintain a high image quality, two measures are recommended: I) repeated pulse labelling of both nuclides (cf. above) and II) longer exposure.

For easier cutting of the soil cores, we adjusted the water content to 45-50% of the water holding capacity. Freezing the soil cores could also be a suitable approach to avoid the redistribution of soil particles during the cutting (Kuzyakov et al. 2003). However, care should be taken not to cause excessive stress on the surrounding soil. Regarding occupational health and safety, during the cutting and handling of the soil and solutions in the lab, we strongly recommend to always follow common radiation protection rules to keep radiation exposure as low as reasonably achievable. Incorporation of ^{137}Cs-contaminated soil dust could be minimised by wearing face masks and performing dust-producing tasks in a fume hood.

Some issues are conceivable and may need consideration when scaling this proof-of-concept up to a crop rotation – since this was not yet tested. The largest difference between this experiment and a crop rotation would be the duration of root decomposition and with this comes a range of issues regarding the feasibility of the approach. First, ^{137}Cs release upon root cell death needs to be shown. In soils with a high biotic activity, the signals might be disturbed in the long run: even though ^{137}Cs should not diffuse away from mineral surfaces, soil particles may be pushed away by earthworms or roots. For instance, secondary thickening or growth of thicker main crop roots may be expected to weakly impact the positions of ^{137}Cs signals by slightly pushing soil particles away from their former position. Even if the main crops pushed ^{137}Cs-labelled soil away, e.g. in the case of a fibrous pre-crop and a tap rooted main crop, spatial overlap of ^{137}Cs and ^{14}C would still be expected. In the opposite case, i.e. the main crop features small roots compared to the biopore diameter, the main crop ^{14}C signal may be small. In this case, multiple pulse or continuous labelling is recommended. It remains to be determined if these effects are relevant for the time frame of root decomposition in a crop rotation.

2.5.5 Conclusions

A new dual labelling approach with foliar application of ^{137}Cs and ^{14}C and selective shielding during the imaging of soil cuts was successfully tested: more than 99% of the ^{137}Cs tracer was taken up irrespective of the plant species and of this 7.1-9.4% were allocated below ground within four days. β^- radiation around the roots proved both ^{137}Cs and ^{14}C were released into the rhizosphere, effectively creating roots labelled with both ^{137}Cs and ^{14}C. Shielding successfully separated the two signals. Albeit not specifically tested herein, if the two tracers are applied to separate, subsequent crops in a crop rotation, the ultimate goal of biopore reuse quantification appears feasible: the long half-life of ^{137}Cs, its relatively high energy β^- radiation and very low mobility in soil should enable stable and long-term labelling of rhizosphere soil and, after decomposition, root biopores. Labelling main crops with ^{14}C would enable quantification of the reuse of root biopores and would help estimate their importance over longer periods and on larger scales – possibly under field conditions. We conclude that ^{137}Cs can be a useful proxy of biopore reuse and possibly for the extent of solute dynamics in the rhizosphere and root system architecture studies.

Acknowledgements

This study was supported by the German Research Foundation (KU 1184/29-1). We would like to thank Gabriele Lehmann and Rainer Schulz of the Laboratory for Radioisotopes (LARI) of the University of Goettingen for their advice, support and measurements.

2.5.6 References

- Amato E, Lizio D (2009) Plastic materials as a radiation shield for β − sources. A comparative study through Monte Carlo calculation. Journal of Radiological Protection 29:239–250.
- Athmann M, Kautz T, Pude R, Köpke U (2013) Root growth in biopores—evaluation with in situ endoscopy. Plant and Soil 371:179–190.
- Bolte S, Cordelières FP (2006) A guided tour into subcellular colocalization analysis in light microscopy. Journal of Microscopy 224:213–232.
- Buysse J, Van den Brande, Karen, Merckx R (1995) The Distribution of Radiocesium and Potassium in Spinach Plants Grown at Different Shoot Temperatures. Journal of Plant Physiology 146:263–267.
- Bystrzejewska-Piotrowska G, Jeruzalski M, Urban PL (2004) Uptake and distribution of caesium and its influence on the physiological processes in croton plants (Codiaeum variegatum). Nukleonika 49:35–38.
- Bystrzejewska-Piotrowska G, Urban PL (2004) Accumulation and translocation of cesium-137 in onion plants (Allium cepa). Environmental and Experimental Botany 51:3–7.
- Carminati A (2013) Rhizosphere wettability decreases with root age: a problem or a strategy to increase water uptake of young roots? Frontiers in Plant Science:298.
- Cheshire MV, Griffiths BS (1989) The influence of earthworms and cranefly larvae on the decomposition of uniformly 14C labelled plant material in soil. Journal of Soil Science 40:117–124.
- Cordelières FP, Bolte S (2009) JACoP v2.0: improving the user experience with co-localization studies, 2nd ImageJ User and Developer Conference.
- Cremers A, Elsen A, Preter PD, Maes A (1988) Quantitative analysis of radiocaesium retention in soils. Nature 335:247–249.
- Dippold MA, Kuzyakov Y (2016) Direct incorporation of fatty acids into microbial phospholipids in soils: Position-specific labeling tells the story. Geochimica et Cosmochimica Acta 174:211–221.
- Ehlers W, Köpke U, Hesse F, Böhm W (1983) Penetration resistance and root growth of oats in tilled and untilled loess soil. Soil and Tillage Research 3:261–275.
- Elkins CB (1985) Plant roots as tillage tools.Journal of Terramechanics 22:177-178.
- Fernández V, Eichert T (2009) Uptake of Hydrophilic Solutes Through Plant Leaves. Current State of Knowledge and Perspectives of Foliar Fertilization. Critical Reviews in Plant Sciences 28:36–68.
- Fischer H, Ingwersen J, Kuzyakov Y (2010) Microbial uptake of low-molecular-weight organic substances out-competes sorption in soil. European Journal of Soil Science 61:504–513.
- Giannakopoulou F, Haidouti C, Chronopoulou A, Gasparatos D (2007) Sorption behavior of cesium on various soils under different pH levels. Journal of hazardous materials 149:553–556.
- Gunina A, Dippold MA, Glaser B, Kuzyakov Y (2014) Fate of low molecular weight organic substances in an arable soil: From microbial uptake to utilisation and stabilisation. Soil Biology and Biochemistry 77:304–313.

- Hafner S, Kuzyakov Y (2016) Carbon input and partitioning in subsoil by chicory and alfalfa. Plant and Soil 406:29–42.
- Hagedorn F, Bundt M (2002) The age of preferential flow paths. Geoderma 108:119–132.
- Han E, Kautz T, Köpke U (2016) Precrop root system determines root diameter of subsequent crop. Biology and Fertility of Soils 52:113–118.
- Han E, Kautz T, Perkons U, Uteau D, Peth S, Huang N, Horn R, Köpke U (2015) Root growth dynamics inside and outside of soil biopores as affected by crop sequence determined with the profile wall method. Biology and Fertility of Soils 51:847–856.
- Hasegawa H, Tsukada H, Kawabata H, Takaku Y, Hisamatsu S (2015) Foliar uptake and translocation of stable Cs and I in radish plants. Journal of Radioanalytical and Nuclear Chemistry 303:1409–1412.
- Hasegawa M, Ito MT, Kaneko S, Kiyono Y, Ikeda S, Makino S (2013) Radiocesium concentrations in epigeic earthworms at various distances from the Fukushima Nuclear Power Plant 6 months after the 2011 accident. Journal of environmental radioactivity 126:8–13.
- Hiltner L (1904) Über neuere Erfahrungen und Probleme auf dem Gebiete der Bodenbakteriologie unter besonderer Berücksichtigung der Gründüngung und Brache. Arbeiten der Deutschen Landwirtschaftlichen Gesellschaft 98:59–78.
- Hirth JR, McKenzie BM, Tisdall JM (2005) Ability of seedling roots of Lolium perenne L. to penetrate soil from artificial biopores is modified by soil bulk density, biopore angle and biopore relief. Plant and Soil 272:327–336.
- Hoang DTT, Pausch J, Razavi BS, Kuzyakova I, Banfield CC, Kuzyakov Y (2016) Hotspots of microbial activity induced by earthworm burrows, old root channels, and their combination in subsoil. Biology and Fertility of Soils 52:1105–1119.
- Jones DL, Nguyen C, Finlay RD (2009) Carbon flow in the rhizosphere: carbon trading at the soil–root interface. Plant and Soil 321:5–33.
- Kautz T, Amelung W, Ewert F, Gaiser T, Horn R, Jahn R, Javaux M, Kemna A, Kuzyakov Y, Munch J-C, Pätzold S, Peth S, Scherer HW, Schloter M, Schneider H, Vanderborght J, Vetterlein D, Walter A, Wiesenberg GL, Köpke U (2013) Nutrient acquisition from arable subsoils in temperate climates: A review. Soil Biology and Biochemistry 57:1003–1022.
- Kuzyakov Y, Blagodatskaya E (2015) Microbial hotspots and hot moments in soil: Concept & review. Soil Biology and Biochemistry 83:184–199.
- Kuzyakov Y, Domanski G (2000) Carbon input by plants into the soil. Review. Journal of Plant Nutrition and Soil Science 163:421–431.
- Kuzyakov Y, Raskatov A, Kaupenjohann M (2003) Turnover and distribution of root exudates of Zea mays. Plant and Soil 254:317–327.
- Manders EM, Verbeek FJ, Aten JA (1993) Measurement of co-localization of objects in dual-colour confocal images. Journal of Microscopy 169:375–382.
- Meharg AA (1994) A critical review of labelling techniques used to quantify rhizosphere carbon-flow. Plant and Soil 166:55–62.
- Miltner A, Bombach P, Schmidt-Brücken B, Kästner M (2012) SOM genesis: microbial biomass as a significant source. Biogeochemistry 111:41–55.

- Nucleonica GmbH (2014) Nucleonica Nuclear Science Portal (www.nucleonica.com), Karlsruhe, Germany.
- Paterson E (2003) Importance of rhizodeposition in the coupling of plant and microbial productivity. European Journal of Soil Science 54:741–750.
- Pausch J, Kuzyakov Y (2011) Photoassimilate allocation and dynamics of hotspots in roots visualized by 14C phosphor imaging. Journal of Plant Nutrition and Soil Science 174:12–19.
- Razavi BS, Zarebanadkouki M, Blagodatskaya E, Kuzyakov Y (2016) Rhizosphere shape of lentil and maize. Spatial distribution of enzyme activities. Soil Biology and Biochemistry 96:229–237.
- Riise G, Bjørnstad HE, Lien HN, Oughton DH, Salbu B (1990) A study on radionuclide association with soil components using a sequential extraction procedure. Journal of Radioanalytical and Nuclear Chemistry Articles142:531–538.
- Schindelin J, Arganda-Carreras I, Frise E, Kaynig V, Longair M, Pietzsch T, Preibisch S, Rueden C, Saalfeld S, Schmid B, Tinevez J-Y, White DJ, Hartenstein V, Eliceiri K, Tomancak P, Cardona A (2012) Fiji: an open-source platform for biological-image analysis. Nature methods 9:676–682.
- Schindelin J, Rueden CT, Hiner MC, Eliceiri KW (2015) The ImageJ ecosystem: An open platform for biomedical image analysis. Molecular reproduction and development 82:518–529.
- Schuller P, Voigt G, Handl J, Ellies A, Oliva L (2002) Global weapons' fallout 137 Cs in soils and transfer to vegetation in south–central Chile. Journal of environmental radioactivity 62:181–193.
- Stock D, Holloway PJ (1993) Possible mechanisms for surfactant-induced foliar uptake of agrochemicals. Pesticide Science 38:165–177.
- UNSCEAR (2011) Sources and effects of ionizing radiation. UNSCEAR 2008 report to the General Assembly, with scientific annexes : Volume II: Effects, Annex. D. United Nations, New York.
- VandenBygaart AJ, Protz R, Tomlin AD, Miller JJ (1998) 137 Cs as an indicator of earthworm activity in soils. Applied Soil Ecology 9:167–173.
- Walling DE, He Q (1999) Improved models for estimating soil erosion rates from cesium-137 measurements. Journal of Environmental Quality 28:611–622.
- Walling DE, Quine T (1995) Use of fallout radionuclide measurements in soil erosion investigations. In: IAEA (ed), Nuclear techniques in soil plant studies for sustainable agriculture and environmental preservation. Proceedings of an International Symposium on Nuclear and Related Techniques in Soil Plant Studies on Sustainable Agriculture and Environmental Preservation jointly org. by the IAEA and the FAO and held in Vienna, 17 - 21 October 1994. Vienna, pp 597–619.
- White RG, Kirkegaard JA (2010) The distribution and abundance of wheat roots in a dense, structured subsoil—implications for water uptake. Plant, Cell & Environment 33:133–148.
- Yunusa IAM, Newton PJ (2003) Plants for amelioration of subsoil constraints and hydrological control. The primer-plant concept. Plant and Soil 257:261–281.
- Zarebanadkouki M, Ahmed MA, Carminati A (2016) Hydraulic conductivity of the root-soil interface of lupin in sandy soil after drying and rewetting. Plant and Soil 398:267–280.

- Zhu YG, Smolders E (2000) Plant uptake of radiocaesium: a review of mechanisms, regulation and application. Journal of experimental botany 51:1635–1645.

2.5.7 Supplementary Material

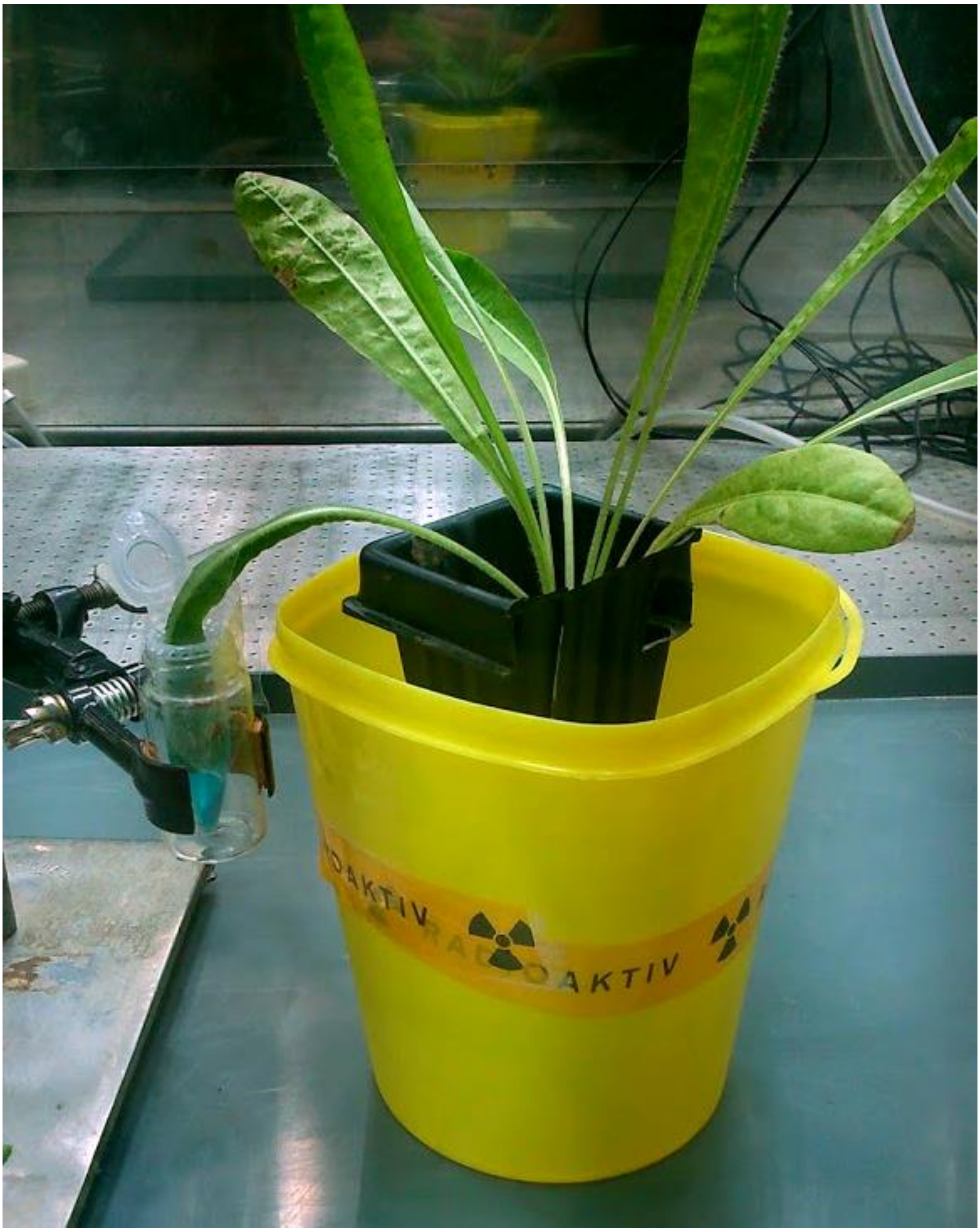

ESM 1 Leaf feeding of *Cichorium intybus* with ^{137}CsCl solution in action.

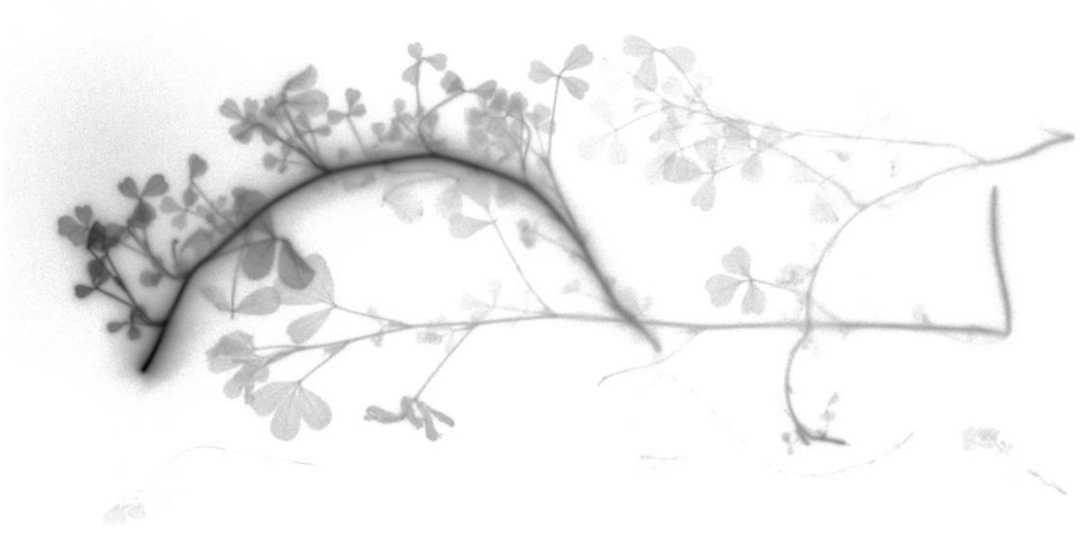

ESM 2 Imaging of one *Medicago sativa* shoot, exposure was 3 hours with 6 layers of polypropylene to shield off ^{14}C, showing the mobility of ^{137}Cs.

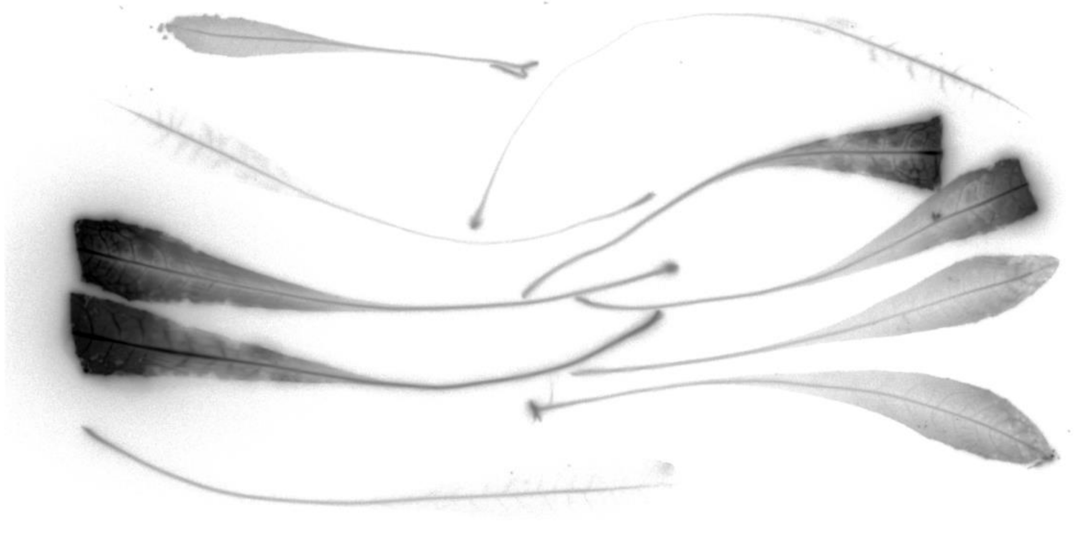

ESM 3 Imaging of one *Cichorium intybus* shoot, exposure was 3 hours with 6 layers of polypropylene to shield off ^{14}C, showing the mobility of ^{137}Cs.

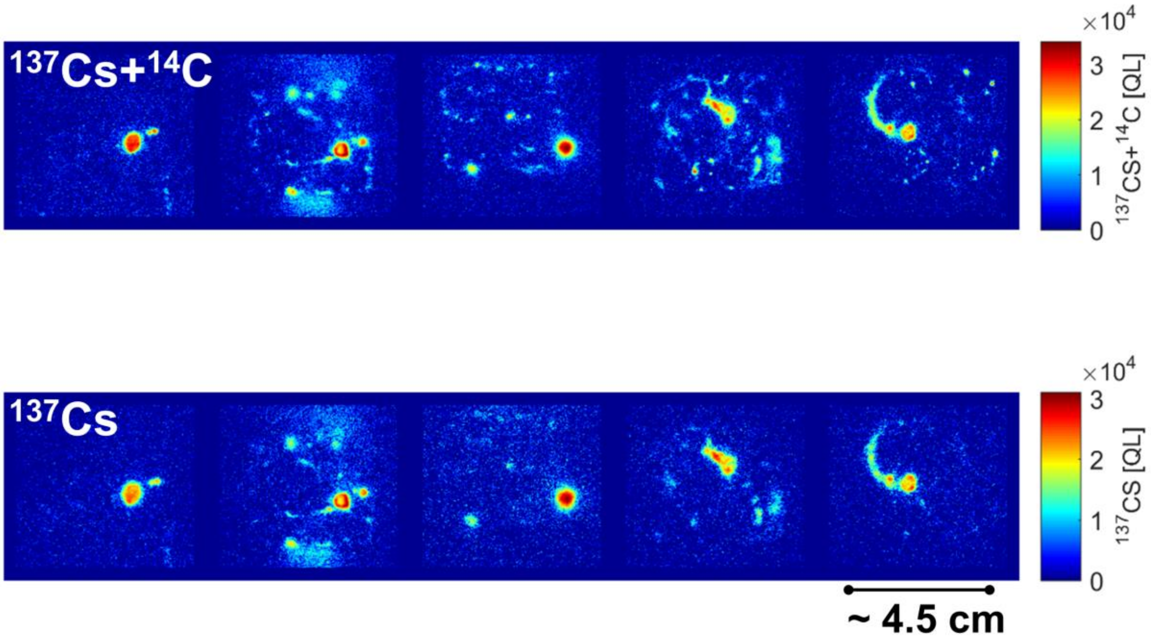
137Cs+14C
×10^4
3
2
1
0
137CS+14C [QL]
137Cs
×10^4
3
2
1
0
137CS [QL]
~ 4.5 cm

ESM 4 All replicates of the imaging of *Medicago sativa*. Top: Quantum level (QL) data of ^{137}Cs and ^{14}C activities; below: QL data for the ^{137}Cs activity only.

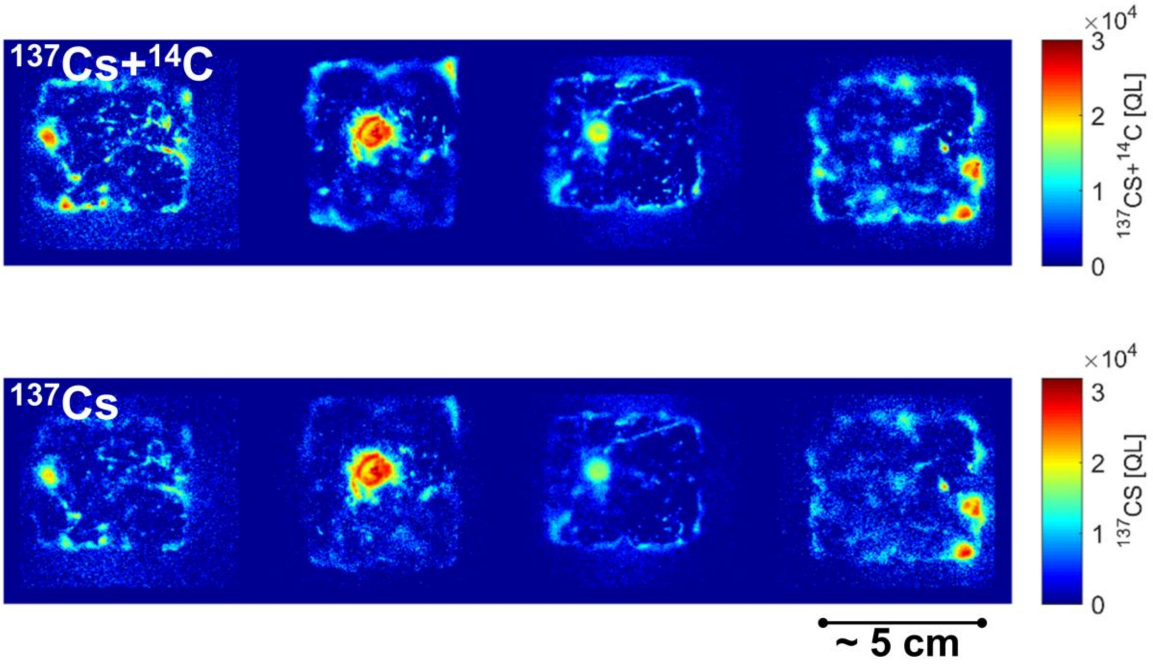
137Cs+14C
×10^4
3
2
1
0
137CS+14C [QL]
137Cs
×10^4
3
2
1
0
137CS [QL]
~ 5 cm

ESM 5 All replicates of the imaging of *Cichorium intybus.* Top: Quantum level (QL) data of ^{137}Cs and ^{14}C activities; below: QL data for the ^{137}Cs activity only.

ESM 6 Physico-chemical properties of the Ap horizon of the Haplic Luvisol. Data compiled from Dippold and Kuzyakov (2016) and Gunina et al. (2014)

Soil parameter	
Sand content	36 ± 5%
Silt content	8 ± 5%
Clay content	56 ± 5%
pH KCl	4.88 ± 0.12
pH H_2O	6.49 ± 0.11
Total organic Carbon	1.77 ± 0.07%
Total nitrogen	0.19 ± 0.01%
Cation exchange capacity	13.6 $cmol_c$ kg^{-1} soil
Microbial biomass C	42.5 ± 1.1 µmol C g^{-1} soil
Microbial C/N ratio	9.9 ± 0.3

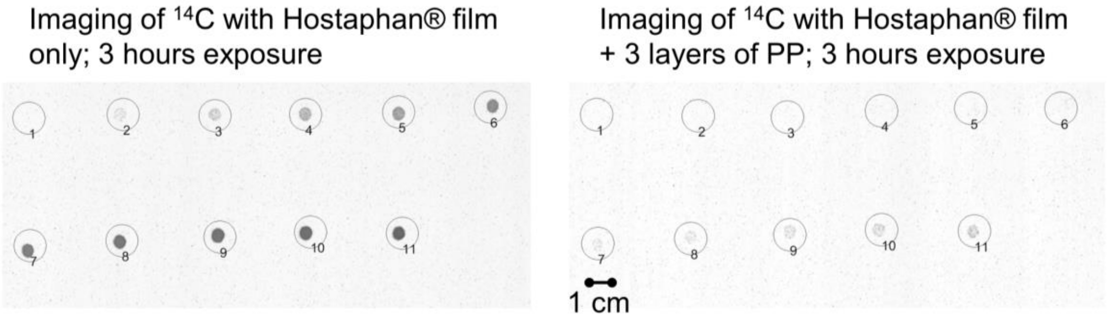
Imaging of 14C with Hostaphan® film only; 3 hours exposure
Imaging of 14C with Hostaphan® film + 3 layers of PP; 3 hours exposure
1
2
3
4
5
6
7
8
9
10
11
1 cm

ESM 7 A shielding and exposure pre-test with Hostaphan® film (to protect the imaging plate; left side) and Hostaphan® film plus 3 layers of polypropylene for shielding (right side). Activities increasing from 1 to 125 Bq of ^{14}C-glucose were applied to coated paper. All ^{14}C was shielded off (right side). Please note, the signals in case of higher ^{14}C activities were visually discernible after shielding (right side; identifiers 7-11), but were in fact only marginally above the background value (36 PSL vs 21 PSL of the background). The number of PP films was increased after this test

2.6 Study 6: Subsoil exploitation: The re-use of root biopore hotspots in crop rotations

Authors and affiliations

Callum C. Banfield[1,*], Michaela A. Dippold[1], Johanna Pausch[2], Mohsen Zarebandhouki[3], Bernd Kopka[4], Yakov Kuzyakov[5,6]

[1] University of Goettingen, Biogeochemistry of Agricultural Ecosystems, Buesgenweg 2, 37077 Goettingen, Germany.
[2] University of Bayreuth, Agroecology, Universitätsstrasse 30, 95440 Bayreuth, Germany.
[3] University of Bayreuth, Chair of Soil Physics, Universitätsstrasse 30, 95447 Bayreuth, Germany.
[4] University of Goettingen, Laboratory for Radioisotopes, Faculty of Forest Sciences and Forest Ecology, Buesgenweg 2, 37077 Goettingen, Germany.
[5] University of Goettingen, Department of Agricultural Soil Science, Department of Soil Science of Temperate Ecosystems, Buesgenweg 2, 37077 Goettingen, Germany.
[6] Institute of Physicochemical and Biological Problems in Soil Science, Russian Academy of Sciences, 142290 Pushchino, Russia

Corresponding author: callumba@gmail.com
Telephone: +49 1578 4527077
Fax: +49 551 3933310

Role of the funding source: DFG KU 1184/29-1

Conflicts of interest: The authors declare no conflicts of interest.

Keywords: Radiocesium, biopores, detritusphere, subsoil, re-use, macropores, continuous, imaging, radioactivity

Section	**# of words / Figures / Tables**
Introduction	831
Material and Methods	1306
Results	517
Discussion	1399
Conclusions	366
# of Figures	6
# of Tables	1
# of supporting information	3

Summary

- Root biopores provide nutrients and shortcuts to subsoil resources like water. Succeeding crops potentially benefit if they root within biopores, which was quantified pre-crop-specifically.
- ^{137}Cs + ^{14}C labelling of pre- and main crops, respectively, followed by phosphor imaging of soil cuts with selective shielding enabled quantification of biopores (^{137}Cs), roots (^{14}C), re-use (^{14}C + ^{137}Cs) and estimation of geometric biopore properties.
- Biopore properties of *Cichorium intybus* L. and *Phacelia tanacetifolia* Benth. were similar after 12 weeks cultivation: biopore volume of 0.0027 m^3 m^{-3} and a wall volume of 0.0040 m^3 m^{-3}. Biopore abundance decreased with depth but re-use increased, following bulk soil density. 53–75% of biopores were re-used by wheat irrespective of the pre-crop, i.e. 200% higher than stochastically expected, suggesting positive biopore effects. Biopore re-use was positively correlated with wheat shoot nitrogen contents. A constant proportion of roots (25%) grew in bulk soil, likely to acquire additional resources limited in biopores.
- This method successfully applied imaging to characterise the spatial distribution of biopores, their geometric properties, and re-use in crop rotations. One season of cover cropping with tap-rooted *vs* fibrous crops provided equal opportunities for subsoil exploitation by main crops and were crucial for aboveground wheat biomass production.

2.6.1 Introduction

Agriculture has long neglected subsoils with regard to crops' nutrient acquisition (Kautz *et al.*, 2013a). Agricultural subsoils, i.e. the soil below the ploughed horizon, also contain relevant stocks of nutrients like potassium (Andrist-Rangel *et al.*, 2006), calcium and phosphorus (Schwertmann & Huith, 1975; Barej *et al.*, 2014). Organic agriculture aims at acquiring nutrients from the subsoil (Kautz *et al.*, 2013a), e.g. through growing deep rooting crops. Considering an increasing population at times of global climate change (Godfray *et al.*, 2010; IPCC, 2014), maintaining crop productivity is of pivotal importance. Not just nutrients, but also water resources can become scarce in future. As drought periods may become more frequent in the course of climate change (Pal *et al.*, 2004; Li *et al.*, 2009), subsoil water resources could alleviate drought stress of plants (Lynch & Wojciechowski, 2015). Therefore, strategies or plant traits to make use of subsoil resources could contribute to more sustainable agriculture.

Macropores induced by earthworms or decomposed taproots (biopores) provide opportunities for faster subsoil access (Ehlers *et al.*, 1983; Cresswell & Kirkegaard, 1995) (Stirzaker *et al.*, 1996; Kautz, 2015). Large root biopores with diameters of up to 10 mm may stretch from the soil surface down to three meters, while anecic earthworms may even induce biopores down to four meters depth. Following the principle of least effort, roots use these shortcuts to access subsoil resources. In crop rotations, growing tap-rooted pre-crops could be useful to create 'highways of root growth' (Passioura, 2002). They do not only 'drill' the soil but also accumulate nutrient-rich organic matter (OM) on the inner walls, which induces microbial hotspots of nutrient turnover and release (Kuzyakov & Blagodatskaya, 2015). Roots growing in biopores could consequently acquire additional nutrients from the subsoil biopore walls as well as the bulk subsoil (by leaving the biopores with side roots) to improve crop nutrition and thus yields (Jakobsen & Dexter, 1988; Gaiser *et al.*, 2013).

A higher share of roots exploring the subsoils would also increase the amount of C stored in subsoils. As subsoils are assumed unsaturated in C, they would make an effective and long-term C sink (Kell, 2012). However, any direct benefit of biopores for crops or indirect effect for C sequestration depends on the utilisation of previously created biopores. The quantification of biopore re-use in crop rotations was never achieved, despite the fact that it is often hinted at, e.g. yield improvement studies (Elkins, 1985) or from morphological changes: the root system architecture of barley reacted to the preceding crop's root system (fibrous *vs* tap-rooted,(Nakamoto, 2000; Han *et al.*, 2016). Plants also have developed strategies to exploit the biopore nutrients, e.g. by growing in a spiralling manner in contact with the pore walls (Athmann *et al.*, 2013) or by root hairs (White & Kirkegaard, 2010).

Consequently, roots could benefit twice, i.e. from biopore wall nutrients and from using the biopore as a shortcut into the subsoil.

In agriculture, the links between biopore properties, re-use and their effects are of interest to optimise subsoil exploitation and nutrient cycling. The re-use's relevance depends on the outcome to be optimised, e.g. yields (Kautz *et al.*, 2010), resilience towards drought (Kirkegaard *et al.*, 2007), or, C sequestration in subsoils (Lorenz & Lal, 2007). Higher biopore re-use may not lead to more positive outcomes since effects may be soil, crop or nutrient-specific (Duncan *et al.*, 2018) and may be modulated by same-species successions: maize root growth in maize root channels was low (Rasse & Smucker, 1998). Regarding soil properties, especially in hard-setting soils, clumped wheat roots may end up trapped in biopores (Cresswell & Kirkegaard, 1995), which may deplete the biopore nutrient quickly and limit water uptake.

Commonly, biopore effects are studied after cultivation of biopore-inducing crops for up to three years, followed by main crop cultivation and comparing yields, nutrient uptake and the proportion of roots growing in macropores. Such set-ups have severe shortcomings like mixing other pre-crop effects (e.g. topsoil nutrient mobilisation or pathogen reduction) with the pure biopore effect. We suspect that methodological constraints have hampered biopore re-use quantification so far. It appears too challenging to determine roots growing in specific biopores among countless other pre-existing macropores of varying age and genesis (Athmann *et al.*, 2013; Han *et al.*, 2015). We recently showed the feasibility of a dual radiotracer labelling and selective shielding approach for this scenario (Banfield *et al.*, 2017). This approach was further developed to allow quantification of biopore properties and biopore re-use in real crop rotations. A two-year crop rotation was carried out in the laboratory: Two pre-crops (chicory and phacelia for different root systems) were grown on undisturbed subsoil cores to create root biopores and labelled with ^{137}Cs. After 11 months of decomposition of root residues of pre-crops, wheat was grown for three months and labelled with $^{14}CO_2$. Wheat roots growing in pre-crop root pores were identified by dual (^{137}Cs + ^{14}C) phosphor imaging. Image processing gave fundamental geometric data like size distributions – invaluable for modelling and upscaling of biopores' role in agroecosystems.

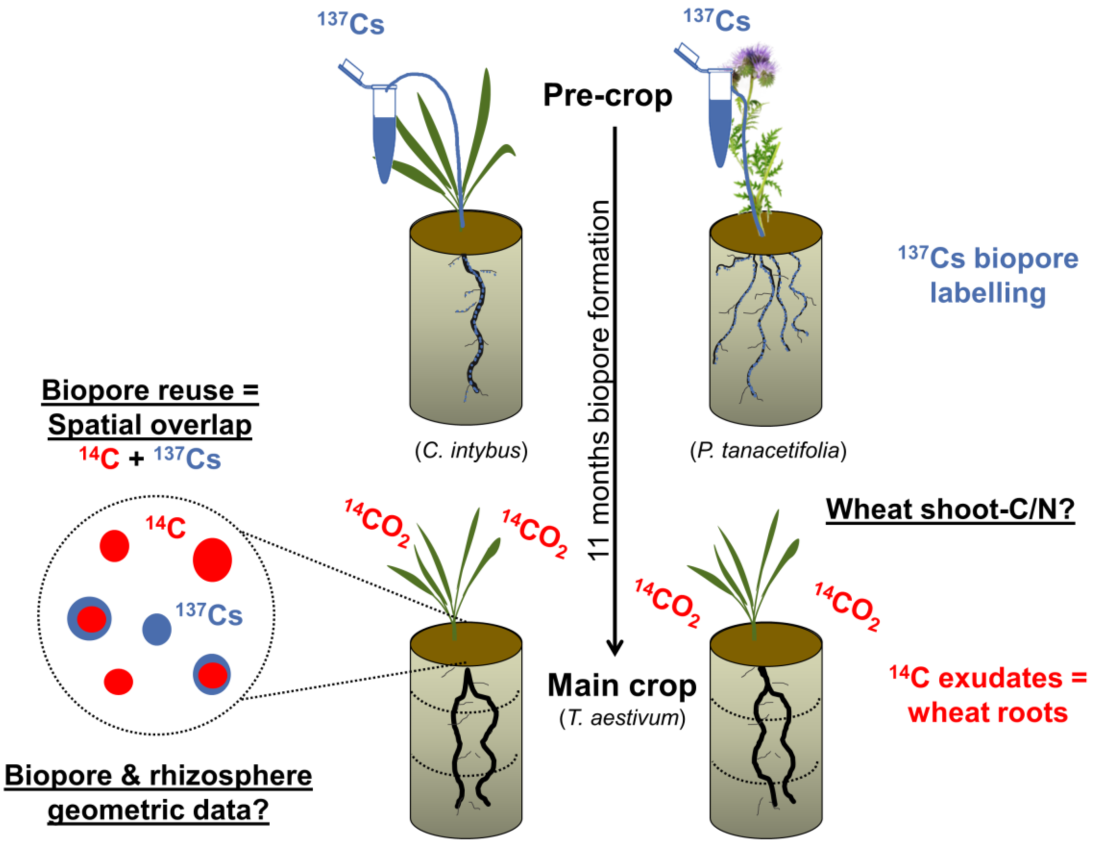
^{137}Cs
^{137}Cs
Pre-crop
11 months biopore formation
^{137}Cs biopore labelling
Biopore reuse = Spatial overlap
^{14}C + ^{137}Cs
(C. intybus)
(P. tanacetifolia)
$^{14}CO_2$
$^{14}CO_2$
Wheat shoot-C/N?
^{14}C
^{137}Cs
$^{14}CO_2$
$^{14}CO_2$
Main crop
(T. aestivum)
^{14}C exudates = wheat roots
Biopore & rhizosphere geometric data?

Fig. 1 *Overview of the experimental design including tracer application during pre-crop and main crop phase, biopore formation and imaging. ^{137}Cs was applied to all pre-crop plants (fibrous Phacelia tanacetifolia Benth. vs tap-rooted Cichorium intybus L., grown for three months) to label above- and belowground biomass and, after root decay, the biopores. After 11 months of biopore formation, T. aestivum L. was grown for three months during which 6 pulses of $^{14}CO_2$ were applied. Spatial overlap of ^{14}C and ^{137}Cs spots was determined on soil cuts in 10, 25 and 50 cm soil depth.*

2.6.2 Material and Methods

2.6.2.1 Origin of the soil cores

Undisturbed subsoil cores were taken from 45–115 cm soil depth of a Haplic Luvisol (Hypereutric, Siltic) from the research station Klein-Altendorf, Germany. The soil properties (Table 1) were previously described by Vetterlein *et al.* (2013). A maritime climate characterises the location near the river Rhine with temperate humid conditions (50°37′9″N 6°59′29″E, 9.6 °C mean annual temperature, 625 mm annual precipitation).

2.6.2.2 Pre-crop phase: Labelling with ^{137}Cs

The soil cores (20 cm diameter each) were stored at 8 °C and were pre-incubated at 20 °C for two weeks before seeding. Twelve soil cores were used for this experiment: on six cores chicory (*Cichorium intybus* L. var Puna; ~ 20 seeds per core) was grown for three months), and on the remaining six phacelia (*Phacelia tanacetifolia* Benth. var Maja KWS; ~ 20 seeds per core). The temperature was kept constant at 20 °C, air humidity was kept constant at

Table 1 *Selected properties of the Haplic Luvisol, after Vetterlein (2013) including soil organic carbon (SOC) and total nitrogen (TN) of bulk soil, and, total organic carbon (TOC) contents ± SE in bulk soil and biopores of the soil core of the experiment. Letters regarding TOC indicate significant differences ($p<0.05$) between biopores and bulk soil for the pre-crops (two-way ANOVA). Asterisks indicate significant differences of one treatment (soil compartment, pre-crop species) between soil depths.*

Depth [cm]	**Horizon (WRB)**	**Reference soil group (WRB)**	**Bulk density [g cm^{-3}]**	**SOC [g kg^{-1}]**	**TN [g kg^{-1}]**	**Soil depth of soil core**	**TOC [%]**			
							Biopores		**Bulk soil**	
							C. intybus	***P. tanacetifolia***	***C. intybus***	***P. tanacetifolia***
0–27	Ap	SiL	1.29	10.0	1.02					
27–41	E/B	SiL	1.32	4.6	0.55					
41–75	Bt1	SiCL	1.42	4.5	0.51	-10 cm (45-55 cm)	0.68 ± 0.04%b	0.55 ± 0.04%c	0.35 ± 0.01%a	0.32 ± 0.00%a
						-25 cm (55-70 cm)	0.58 ± 0.02%b	0.58 ± 0.02%b*	0.31 ± 0.02%a*	0.28 ± 0.02%a
75–87	Bt2	SiCL	1.52	3.9	0.50	-50 cm (70-95 cm)	0.71 ± 0.04%b	0.59 ± 0.03%c*	0.24 ± 0.01%a*	0.21 ± 0.02%a*
87–115	Bt3	SiL	1.52	2.5	0.34	>-50 cm (95-115 cm)	0.72 ± 0.09%a	0.57 ± 0.02%a	0.13 ± 0.02%a*	0.15 ± 0.00%a
115–127	Bw	SiL	1.46	2.6	0.34					
127–140+	C	SiL	1.47	n.d.	> 0					

SOC soil organic carbon, TOC total organic carbon, WRB World Reference Base

50% (relative humidity), and the light intensity kept constant at 200 µmol m^{-2} s^{-1}. The photoperiod was set to 14 hours. The soil surface was covered with gravel to limit soil surface drying by strong evaporation and subsequent cracking. A drip irrigation system watered plants. Mildew infections were treated with azoxystrobin and sulphur.

Each pre-crop plant was labelled with 75 kBq of ^{137}Cs (^{137}CsCl dissolved in 0.1 M HCl, POLATOM, Otwock, Poland; additional carrier: unlabelled 0.5 mM mL^{-1} ^{133}CsCl (Sigma-Aldrich Chemie GmbH, Munich, Germany) by cutting one of its leaf tips off with a sterile razor blade. The leaf tips were immersed for 36 hours in 1.5 mL Eppendorf vials (Eppendorf AG, Hamburg, Germany) containing the aqueous radiotracer solution and Silwet Gold surfactant (Spiess-Urania Chemicals GmbH, Hamburg, Germany). The pre-crop shoots were harvested after three months by cutting them off at the soil surface. Dicamba was applied after the harvest to kill the pre-crops. The soil cores were stored at 5 °C for nine months, followed by two months at 18 °C to simulate spring. The soil moisture was kept constant throughout root rotting.

2.6.2.3 Main crop phase: Labelling with $^{14}CO_2$

On the same soil cores, the main crop wheat (*Triticum aestivum* L. var. KWS Scirocco) was sown at 20 seeds per core and was kept at the same conditions as the pre-crops and harvested after three months (BBCH 77). Main crops were fertilised as recommended by the seed provider, i.e. 120, 80 and 60 kg N, P and K ha^{-1}, respectively.

Six repeated pulses of $^{14}CO_2$ were applied to the main crops. Each time, 3 MBq of $Na_2{}^{14}CO_3$ (Hartmann Analytic, Brunswick, Germany) were added to unlabelled $Na_2{}^{12}CO_3$. Labelled CO_2 was generated from this solution by adding lactic acid (100%, p.a., Carl Roth, Karlsruhe, Germany) within an airtight labelling chamber for 6 h under the conditions mentioned above. About 1000 ppm CO_2 were released in total per pulse.

2.6.2.4 Imaging procedure

After the wheat shoots were harvested, the 20-cm diameter soil cores and 70 cm depth were cut in 10, 25 and 50 cm depth, i.e. into four intact layers of 10, 15, 25 and 20 cm height. The plastic tubing (5 mm strength) was horizontally cut open with a circular saw. A thin, strong wire was used to cut the soil, and the cut surface was immediately cleaned with a 30-cm knife and a soft brush.

The cut surfaces were placed on storage phosphor screens (BAS-MS 2040; 20 by 40 cm; Fujifilm Europe GmbH, Düsseldorf, Germany). A 12 µm Hostaphan® film (Mitsubishi Polyester Film GmbH, Wiesbaden, Germany) was put between the soil surface and the screen to protect the latter from contamination. This first image captured the activities of ^{137}Cs and ^{14}C. For the second imaging, eight plastic films (polypropylene, 40 µm thickness, density 0.95 g cm^{-3}, MDF-Verpackungen GmbH, Bergisch Gladbach, Germany) were put between same soil surface (used for first imaging) and the screen to shield off the ^{14}C radiation (Banfield *et al.*, 2017). Thus, the second imaging captured only the ^{137}Cs decay. Exposure was 20 hours. The imaging system FLA 5100 (Fujifilm Europe GmbH, Düsseldorf, Germany) was used to read the screen with a resolution of 100 µm.

2.6.2.5 Determination of biopore re-use by image processing

The images capturing the emitted β^- radiation from the decay of ^{14}C and / or ^{137}Cs were converted to PSL units, i.e. the captured raw data was log-linearised in AIDA Image Analyzer (Fujifilm Europe GmbH, Düsseldorf, Germany) and were saved as 16-bit images. All further image processing was performed in Fiji 1.51 (Schindelin *et al.*, 2012; Schindelin *et al.*, 2015). First, all data which did not correspond to the imaging plates was discarded. The second imaging with eight plastic films did not only shield off all ^{14}C radiation but also attenuated the stronger ^{137}Cs β^- radiation. The intensities of these images were reverted to the original intensities: a separate calibration of seven ^{137}Cs activities were added to soil, and an identical imaging routine was carried out. The linear relationship between the intensities of the first (one plastic film) and the second image (eight plastic films) was calculated ($r^2 = 0.999$). All intensities of the ^{137}Cs only images were multiplied by the inverse of the slope. Both images were normalised by selecting a region of interest (ROI) with representative, normally distributed noise and calculating the mean background intensity.

All pixelwise intensity data was divided by the mean background intensity to reduce the noise. The corresponding pairs of images were combined into a stack and were registered by the ImageJ implementation of Linear Stack Alignment with SIFT (Scale-invariant feature transform; (Lowe, 2004). For this, the ^{14}C+^{137}Cs image was defined as the source image and ^{137}Cs the target image. If no registration was obtained, the TurboReg/StackReg algorithm was used instead (Rigid Body or Scaled Rotation transformations, (Thévenaz *et al.*, 1998). The registered ^{137}Cs image was subtracted from the ^{14}C+^{137}Cs image using the Image Calculator gave the ^{14}C image.

2.6.2.6 Comparison of ^{137}Cs and ^{14}C hotspots

The separated, registered images of ^{14}C and ^{137}Cs represent the main crop roots and the biopores, respectively. For each image, the spots with the highest activities were considered roots and biopores and were manually saved as regions of interest (ROI) in the ROI manager. Spatial overlap of the ROI of both activities was manually determined, i.e. the count of overlapping ^{14}C and ^{137}Cs spots divided by the count of biopores (^{137}Cs spots). The ROI data was used to calculate basic biopore and geometric properties of the roots and their rhizosphere as well as biopore re-use. We calculated the following parameters: I) volumes, II) biopore wall/rhizosphere volumes (assuming 1 mm extension), III) area fraction of all ^{137}Cs or ^{14}C spots on a cross-section, and, IV) lateral surface per biopore / root, surface area assuming a cylindrical shape (Supporting Information Table S1).

2.6.2.7 Statistics

All data presented in the text, figures and tables are mean values ± standard errors to account for uncertainties. Samples from the three soil depths were assumed to be dependent (paired). Therefore, means of chicory- or phacelia-induced samples were compared to each other separately in each soil depth. Two sample *t*-tests for dependent samples were used to identify significant depth effects in each pre-crop treatment. For all tests, we assumed significance below $\alpha = 0.05$. Biopore size distributions were compared by F statistics, i.e. pairwise tests for significantly different variances. The counts of biopores, roots and re-used biopores (presented in Fig. 6) were compared by Mann Whitney *U*-tests. Associations were analysed by the Spearman correlation coefficient. For the ANOVA, homogeneity of variances was checked by Levene's test. Normality of the residues was checked in Q-Q plots. Post-hoc comparisons were by Tukey's Honest Significant Differences test. If assumptions of the linear ANOVA model were not met, non-parametric ANOVA (Kruskal-Wallis ANOVA) including post-hoc comparisons of mean ranks were used instead. All statistical analyses were performed in STATISTICA 13.3 (TIBCO Software Inc., Palo Alto, CA, U.S.A.).

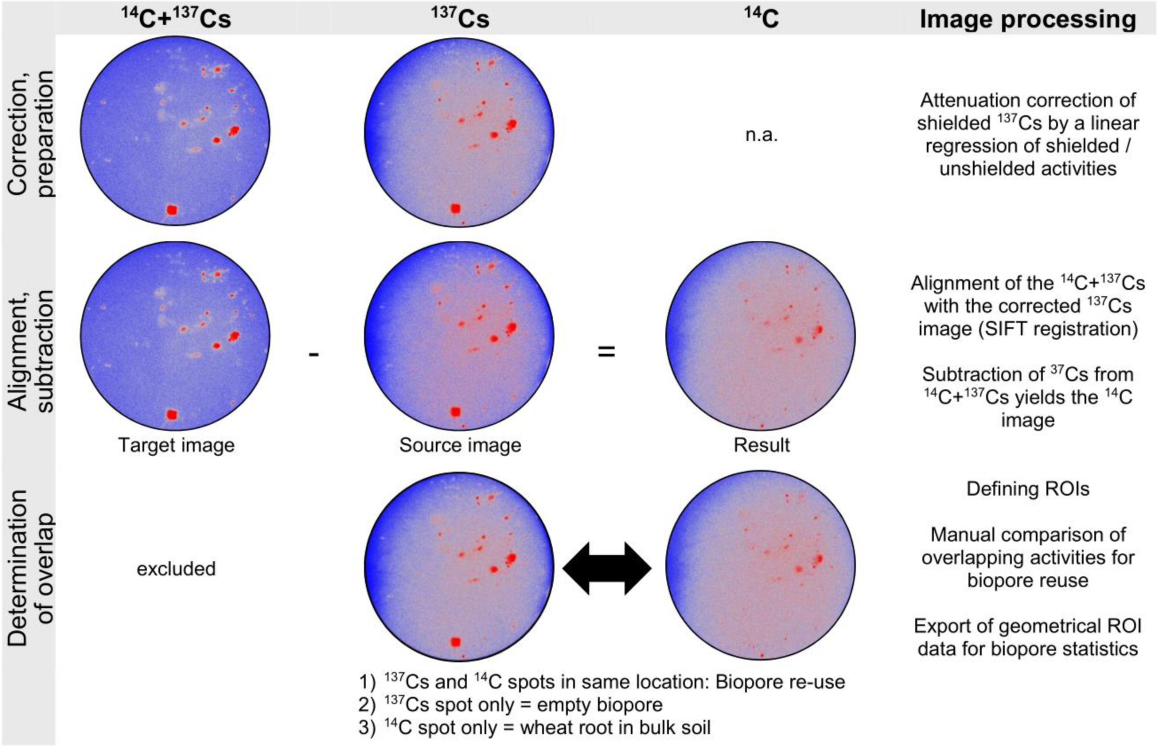
^{14}C+^{137}Cs
^{137}Cs
^{14}C
Image processing
Correction, preparation
n.a.
Attenuation correction of shielded ^{137}Cs by a linear regression of shielded / unshielded activities
Alignment, subtraction
-
=
Target image
Source image
Result
Alignment of the ^{14}C+^{137}Cs with the corrected ^{137}Cs image (SIFT registration)
Subtraction of ^{37}Cs from ^{14}C+^{137}Cs yields the ^{14}C image
Determination of overlap
excluded
Defining ROIs
Manual comparison of overlapping activities for biopore reuse
Export of geometrical ROI data for biopore statistics
1) ^{137}Cs and ^{14}C spots in same location: Biopore re-use
2) ^{137}Cs spot only = empty biopore
3) ^{14}C spot only = wheat root in bulk soil

Fig. 2 *The three-step image processing calculates the spatial representation of ^{14}C by subtracting an attenuation corrected ^{137}Cs-only image from the $^{137}Cs+^{14}C$ image. Shown are the three consecutive steps (from top to bottom) for chicory in 25 cm soil depth (20 cm diameter).*

2.6.3 Results

2.6.3.1 Biopore properties

At the end of the experiment, the total biopore volume (0–50 soil depth; Fig. 3, Supporting Information Table S2) was significantly higher after phacelia as a pre-crop than after chicory. The biopore volumes in the individual soil layers (0–10, 10–25, 25–50 cm) were similar and decreased with depth. Relative to 0–10 cm, the biopore volume was 50% and 70% lower in 10–25 cm and 25–50 cm, respectively. Likewise, the volumes of the biopore walls (assuming a 1 mm extension, (Parkin & Berry, 1999), Fig. 3) decreased with depth. While for chicory it decreased two and four times from 0–10 cm to 10–25 cm and 25–50 cm, respectively, the decrease with depth was lower for phacelia (20% and 40% for the same layers). The lateral surface, describing the inner biopore surface area created per pre-crop plant, was significantly higher after phacelia in the topmost layer. The mean *biopore radius* was independent of pre-crop species or soil depth (≈ 0.15 cm, Fig. 3). Related to the mean radius, the *biopore cut surface* was between 1.3 and 1.6% of the total area (Fig. 3) and sharply decreased with depth to nearly zero - irrespective of the pre-crop species. The size class distribution (Fig. 4) revealed that the experimental setup created mostly larger biopores. In the case of chicory, the distribution changed from 10 cm to 25 cm depth.

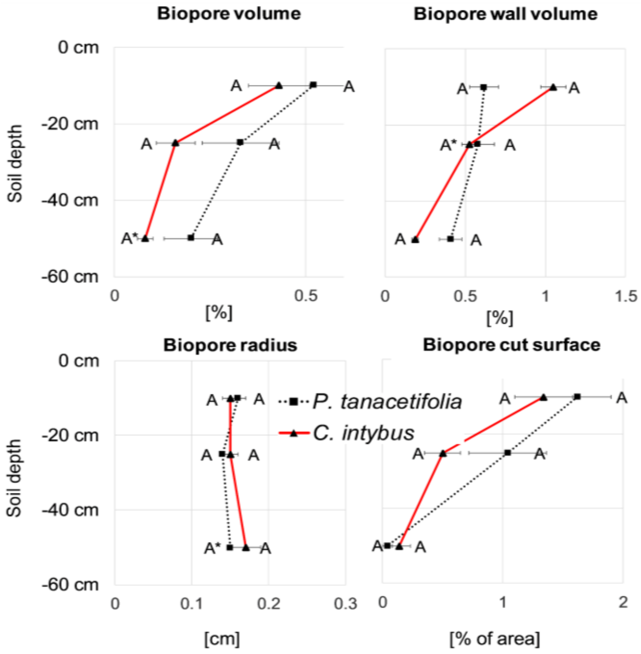

Fig. 3 Physical biopore properties (means ± SE) volume, wall volume, radius and cut surface) of biopores induced by Phacelia tanacetifolia Benth. (dotted lines, squares) and Cichorium intybus L. (red, solid lines, triangles) from 0–50 cm depth. Letters indicate significant differences on α 0.05 (two sample t-test for one soil depth), while asterisks indicate significant differences for one pre-crop between two soil depths (denoted in lower depth).

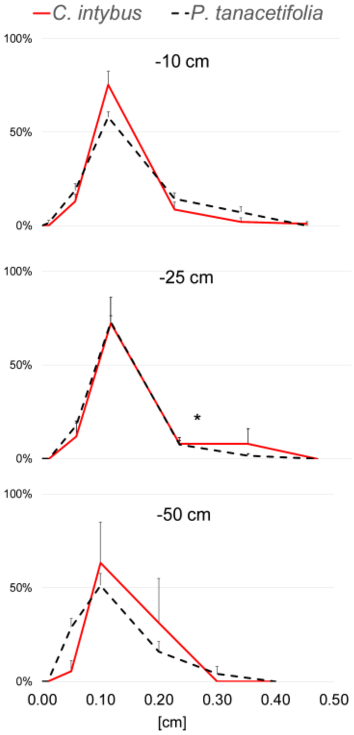

Fig. 4 Biopore size distributions [%] in 10 cm (top), 25 cm (middle) and 50 cm (below) soil depth created by Phacelia tanacetifolia Benth. (black lines) or Cichorium intybus L. (red lines). Given are means ± SE. Significantly different variances between chicory and phacelia are denoted with asterisks (F statistics).

2.6.3.2 Rhizosphere parameters

The total rhizosphere volume of wheat (0–50 cm) did not correspond to the pre-crop species: it was smaller than the total biopore volume (Fig. 5, Supporting Information Table S3) and decreased with depth ($p<0.05$ for chicory). The rhizosphere volume (assuming a 1 mm extension around a detectable root signal) was similar among soil depths and pre-crops. The lateral surface of the rhizosphere was also not dependent on the pre-crop species and decreased significantly with depth. The mean radius of wheat rhizosphere was not affected by soil depth or pre-crop. The proportion of wheat roots growing in bulk soil did not change with depth (Fig. 6).

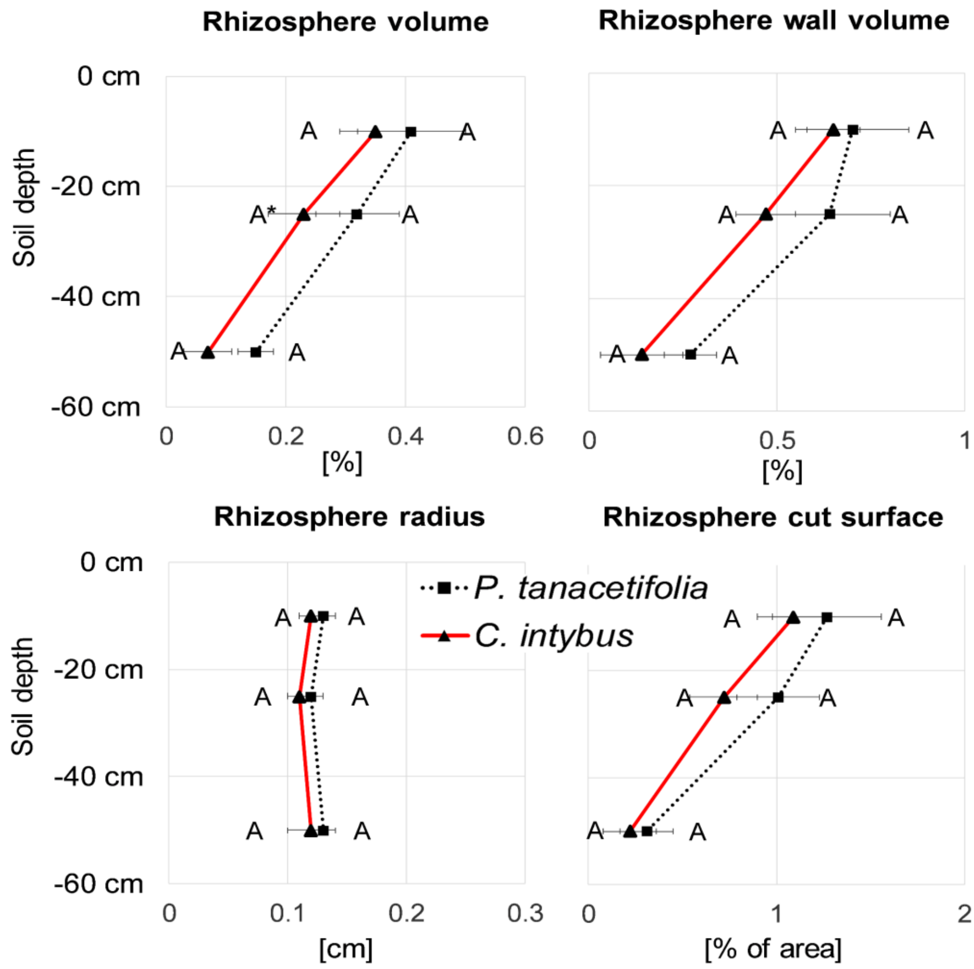

Fig. 5 *Physical rhizosphere properties (means ± SE) volume, wall volume, radius and cut surface) of biopores induced by Phacelia tanacetifolia Benth. (dotted lines, squares) and Cichorium intybus L. (red lines, triangles) from 0–50 cm depth. Letters indicate significant differences on α 0.05 (two sample t-test for one soil depth), while asterisks indicate significant differences for one pre-crop between two soil depths (denoted in lower depth).*

2.6.3.3 Biopore re-use

Figure 6 illustrates biopores abundances and re-use depending on soil depths using count data and frequencies: pre-crop biopores of phacelia and chicory decreased with depth 50% and 75%, respectively (far left). The count of wheat roots growing in bulk soil was constant (centre left) with depth, while the wheat roots in biopores decreased (centre right). The number of biopores also decreased, and the biopore re-use was constant with depth (phacelia) or increased from 0–10 cm to 10–25 cm, and then remained constant (chicory). In the topmost layer (0-10 cm) about 64% and 58% of chicory and phacelia biopores were re-used by wheat, respectively (Fig. 6, Supporting Information Table S2), while in 10-50 cm around 75% of chicory biopores were re-used.

Biopore reuse was significantly positively correlated with the TN content of the wheat shoots: in 10, 25 and 50 cm depth, the Spearman correlation coefficients were 0.61, 0.71 and 0.65, respectively. Consequently, the highest correlation between TN contents and reuse was for the 10-25 cm soil depth.

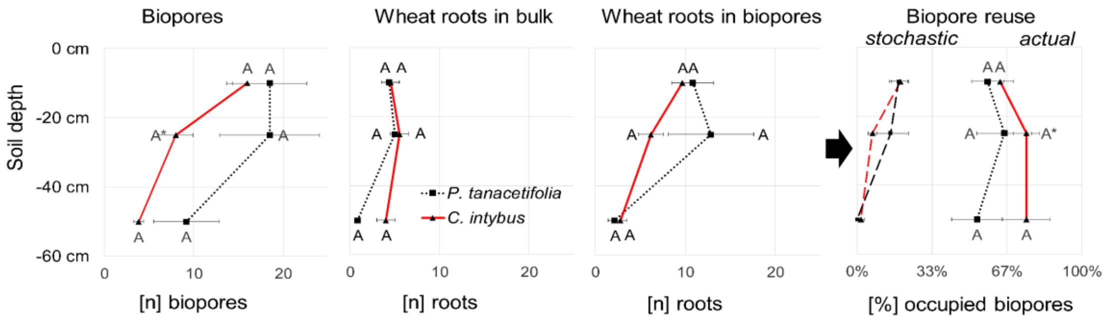

Fig. 6 *Distributions of biopores and wheat roots depending on soil depth and pre-crop species (Phacelia tanacetifolia Benth., dotted lines; Cichorium intybus L., red, solid lines). Given are means ± SE of counts of biopores (left), counts of wheat roots outside biopores (centre left), wheat roots in biopores (centre right) and biopore re-use (%, right). Letters indicate significant differences between crops in one soil depth. Asterisks denote significant differences ($p < 0.05$) of a soil layer and the layer above.*

2.6.4 Discussion

2.6.4.1 Biopore properties

The **count of biopores** (Fig. 6, Supporting Information Table S2) decreased with depth, and most parameters decreased concomitantly. One cropping season was not sufficient to cause differences in biopore abundance or geometry between the pre-crops. With depth, the biopore count was decreasing. Since the biopore re-use increased (Fig. 6), biopores become more relevant in deeper soil. Thus, the number of biopores was suggested as a major determinant for root growth in the subsoil (Wang *et al.*, 1986). The **biopore radius** (Fig. 3) may be a meaningful approximation for the likelihood of biopore re-use as larger biopores are seemingly more often re-used (Volkmar, 1996; Han *et al.*, 2015). It is unclear if this is merely a matter of probability or higher wall density (‘trapping’). Smaller biopores are much more frequent than larger biopores (Wuest, 2001) and may force more root-pore wall contact and higher nutrient uptake (Stirzaker *et al.*, 1996). Larger biopores may therefore not be necessarily better for nutrient supply, but they could be more long-term stable (Hagedorn & Bundt, 2002). Compared to methods like endoscopy (Athmann *et al.*, 2013), the method presented visualises biopores smaller than 1 mm.

The **biopore size distribution** (Fig. 4) remained relatively constant with depth for both pre-crop species. Large biopores get less frequent with depth (Athmann *et al.*, 2013) but biopore diameters stay rather constant with depth (Passioura, 2002), confirming our data (Fig. 3). Possibly, the effect on the radius was weak as only the top 50 cm were studied. The **biopore volume** (Fig. 3) describes 50–80% of the soil macroporosity (Pagenkemper *et al.*, 2013; Zhang *et al.*, 2018). The volume was in good agreement with Gaiser *et al.* (2013) who have determined a biopore volume of 0.44–0.62% from 300–660 roots m^{-2} in the field. In our experiment, 0.19–0.35% biopore volume was determined from 520–620 younger roots m^{-2} (Fig. 3, Supporting Information Table S2). Thus, our lab data reflects real soil conditions. The larger the biopore volume, the more likely is a deep penetration into the subsoil. Maximum root density was simulated to occur at 2% biopore volume (Gaiser *et al.*, 2013). Consequently, an eight times higher biopore volume (0.25%; Fig. 3) may be required to ensure optimal rooting of wheat. The biopore **wall volume** is an approximation for the physical size of the OM pool from which nutrients can be mobilised. The small volumes (0.2–0.9%) and high TN contents (+70% relative to the bulk soil, Table 1) illustrate the concentration of nutrients, potentially attractive for roots. The biopore wall volume is possibly underestimated as we did not account for tortuosity or surface roughness. In the case of tap-rooted crops, the tortuosity is not expected to contribute strongly (Hirth *et al.*, 2005).

The limited effects of pre-crop species on biopore (Fig. 3, Supporting Information Table S2) or rhizosphere parameters (Fig. 5, Supporting Information Table S3) fade with the duration of cover cropping (Han *et al.*, 2017). Nearly identical rhizosphere parameters suggest that neither pre-crop had a positive or negative influence on the root system of wheat. However, this does not allow any conclusion on physiological responses. If one cover cropping season is included in a crop rotation, the choice of pre-crop may not matter for physical biopore properties. When pre-crops are cultivated perennially, tap-rooted crops likely induce larger biopores than fibrous crops.

2.6.4.2 Biopore re-use

From the biopore properties limited can be inferred on the relevance of biopores. Biopores can only be *potentially* relevant if subsequent crops re-use them. Root growth in macropores is positively correlated with the count and mean diameter of pores (Wang *et al.*, 1986), i.e. re-use should be higher after tap-rooted chicory than after fibrous phacelia. This was not confirmed after one season as biopore size distributions, and re-use did not differ between species (Figs. 3, 4). The pure chance of a wheat root to grow into an existing biopore in a given soil depth was between 0.1–1.5% (Fig. 3, (Perkons *et al.*, 2014)). Considering the wheat root counts, the theoretical biopore re-use in 10 cm depth was 19 ± 4% for chicory and phacelia (Fig. 6). However, biopores were re-used to a much larger extent (53–75%; Fig. 6). Root growth in macropores was previously estimated between 25–47% (Nakamoto, 2000; Athmann *et al.*, 2013; Han *et al.*, 2017), i.e. 50% lower than in our study, which considers both large and small biopores. The reasons may be that I) this results from a closed soil column, which may force roots into biopores (albeit the plant density was not higher than in the field) or, II) during the field sampling, fine roots may get lost or have died before sampling and counting visible roots strongly underestimates re-use, or, III) without labelling, it is hardly possible to determine the re-use of small biopores. Nevertheless, our method may underestimate *total* biopore re-use, as some pre-existing biopores may have been re-used by wheat, but not by a pre-crop and were not ^{137}Cs labelled. Pre-crop-specific biopore re-use is not affected, which is an important issue as the re-use of same-species biopores may be lower than different-species biopores (Rasse & Smucker, 1998).

Biopore re-use increased with depth (Fig. 6) and bulk density (from 1.42 to 1.52 g cm^{-3}, Table 1), which was previously postulated (Ehlers, 1975; Kautz *et al.*, 2013b; Dresemann *et al.*, 2018). The increase of bulk density did not reduce the proportion of wheat roots in bulk soil (Fig. 6). The bulk density is only one factor driving roots into biopores. Alternatively, roots may have been searching for available nutrients in biopores since the TN and TOC contents decrease with depth in bulk soil (Table 1). This finding was supported by the positive significant association of biopore re-use and TN contents of wheat – which was independent of soil depth. Biopore re-use was far above the stochastically estimated value; it is likely not random (Rasse & Smucker, 1998). Crops have developed traits to acquire biopore wall nutrients, e.g. increasing contact with the biopore wall by growing in a spiralling manner or by root hairs (Athmann *et al.*, 2013). Furthermore, roots tips may sense OM decomposition by glutamate sensors (Edwards & Lofty, 1980; Filleur *et al.*, 2005). As in the subsoil the strongest OM turnover occurs in biopores (Kuzyakov & Blagodatskaya, 2015), it is plausible that roots grow towards biopores. This fact could explain the high biopore re-use and the increase with depth. However, not under all circumstances are biopores more advantageous than bulk soil, e.g. high wall strength biopores lock up roots in hard-setting soils (White & Kirkegaard, 2010).

2.6.4.3 Plant properties influence biopore re-use

The root system of the main crop governs the spatial accessibility of nutrients in the biopore. The delicate roots of wheat can easily exploit the biopores of both phacelia and chicory. Smaller roots may use biopores more frequently (Nakamoto, 2000) as they suffer from stronger mechanical limitations in bulk soil. In contrast, a tap-rooted main crop might not have accessed the one-season biopores as easily as fibrous crops.

Most wheat roots were found to be rooting in biopores in 50 cm soil depth (Fig. 6; (Ehlers *et al.*, 1983; White & Kirkegaard, 2010). Crops may vary in their likelihood to grow in biopores: e.g. it was already shown that wheat prefers macropores compared to maize

(Nakamoto, 2000). Wheat roots tend to clump together when growing in biopores (White & Kirkegaard, 2010), which was confirmed in this study. Larger ^{14}C spots could not always be differentiated to single roots. It is not clear if clumping affects yields (White & Kirkegaard, 2010).

Even if wheat biopore re-use was considerable (Fig. 6), the proportion of roots outside biopores was constant from 0–50 cm depth. Not all resources are sufficiently available in biopores, so that a part of roots needs to grow in bulk soil – even though 25–40% of pre-crop biopores were unused (Fig. 6). It may be speculated that this was due to low water availability in biopores due to hydrophobic pore walls (Czarnes *et al.*, 2000) or because roots branch to occupy more volume. If biopore re-use was detrimental, roots would not preferentially grow in biopores. Also, the physiological activity of roots would decrease drastically. The ^{14}C signals were not obviously lower in biopores than in bulk soil. Consequently, the C exudation activity, i.e. physiological activity related to exudation, was not altered between roots in biopores and those in bulk soil.

2.6.5 Conclusions

Dual isotope labelling (^{137}Cs + ^{14}C) enables localisation of biopores, determination of their properties, and specific biopore re-use in crop rotations — without disturbing the soil and root systems. Crops benefit from biopores — as shortcuts to subsoil resources — since biopores were occupied three times more often than expected (20-25%): most wheat roots (65%) were growing inside biopores. However, a constant proportion of roots was growing in bulk soil – possibly to obtain resources which are scarce in biopores. After one season of cover cropping, neither biopore re-use nor their physical properties depended on the root characteristics of the pre-crops. The choice of species for cover cropping may only matter for more extended pre-cropping periods. Biopores became less frequent with depth, but their re-use increased with depth (up to 75% of biopores were occupied with wheat roots) suggesting a higher relevance of biopores especially in the subsoil. Preferential root growth and unaffected physiological activity (^{14}C exudation) in biopores clearly confirms their benefits for plants especially in the subsoil. Second, higher biopore re-use was closely correlated with higher wheat shoot biomass production. If biopores increase the availability of a limiting factor for crop production, e.g. water or nutrients from subsoil, then not only pre-crop management but also optimisation of main crops towards an improved root biopore use is a further direction for plant breeding. Since 25–45% of biopores were not occupied by roots, a considerable potential is expected. If roots met a larger part of their demands from biopores, the need for an extensive root system is reduced. A lower belowground C investment is beneficial for aboveground productivity but detrimental to the total C input into the subsoil.

Biopores may have various functions depending on their diameter and wall strength. While larger, stable biopores lead roots to subsoil resources, smaller biopores may provide more nutrients and therefore may effectively increase total C deposition close to the subsoil mineral phases. Consequently, the choice of pre-crop could depend on the desired advantageous aspect and agricultural management targets (tap-rooted perennials: more drought resilience vs. fibrous roots: C sequestration). After three months of cultivation, both pre-crops of varying root system provided equal opportunities for subsoil exploration and nutrient uptake by wheat.

Acknowledgements

We thankfully acknowledge the support by the German Research Foundation for funding this project (KU 1184/29) in the framework of DFG PAK 888. The contribution of YK was supported by the Russian Science Foundation (project No. 18-14-00362). We also appreciate the support by Fabian Stiewe, and Gabriele Lehmann of the Laboratory for Radioisotopes of the University of Goettingen.

2.6.6 References

- **Andrist-Rangel, Y, Simonsson, M, Andersson, S, Öborn, I, Hillier, S. 2006.** Mineralogical budgeting of potassium in soil. A basis for understanding standard measures of reserve potassium. *Journal of Plant Nutrition and Soil Science* **169**: 605–615.
- **Athmann, M, Kautz, T, Pude, R, Köpke, U. 2013.** Root growth in biopores—evaluation with in situ endoscopy. *Plant and Soil* **371**: 179–190.
- **Banfield, CC, Zarebanadkouki, M, Kopka, B, Kuzyakov, Y. 2017.** Labelling plants in the Chernobyl way. A new 137Cs and 14C foliar application approach to investigate rhizodeposition and biopore reuse. *Plant and Soil* **29**: 239.
- **Barej, JAM, Pätzold, S, Perkons, U, Amelung, W. 2014.** Phosphorus fractions in bulk subsoil and its biopore systems. *European Journal of Soil Science* **65**: 553–561.
- **Cresswell, HP, Kirkegaard, JA. 1995.** Subsoil amelioration by plant-roots - the process and the evidence. *Australian Journal of Soil Research* **33**: 221.
- **Czarnes, S, Hallett, PD, Bengough, AG, Young, IM. 2000.** Root- and microbial-derived mucilages affect soil structure and water transport. *European Journal of Soil Science* **51**: 435–443.
- **Dresemann, T, Athmann, M, Heringer, L, Kautz, T. 2018.** Effects of Continuous Vertical Soil Pores on Root and Shoot Growth of Winter Wheat: A Microcosm Study. *Agricultural Sciences* **09**: 750–764.
- **Duncan, EG, O'Sullivan, CA, Roper, MM, Palta, J, Whisson, K, Peoples, MB. 2018.** Yield and nitrogen use efficiency of wheat increased with root length and biomass due to nitrogen, phosphorus, and potassium interactions. *Journal of Plant Nutrition and Soil Science* **181**: 364–373.
- **Edwards, CA, Lofty, JR. 1980.** Effects of Earthworm Inoculation Upon the Root Growth of Direct Drilled Cereals. *The Journal of Applied Ecology* **17**: 533.
- **Ehlers, W. 1975.** Observations on earthworm channels and infiltration on tilled and untilled loess soil. *Soil Science* **119**: 242–249.
- **Ehlers, W, Köpke, U, Hesse, F, Böhm, W. 1983.** Penetration resistance and root growth of oats in tilled and untilled loess soil. *Soil and Tillage Research* **3**: 261–275.
- **Elkins, CB. 1985.** Plant roots as tillage tools. *Journal of Terramechanics* **22**: 177–178.
- **Filleur, S, Walch-Liu, P, Gan, Y, Forde, BG. 2005.** Nitrate and glutamate sensing by plant roots. *Biochemical Society transactions* **33**: 283–286.
- **Gaiser, T, Perkons, U, Küpper, PM, Kautz, T, Uteau-Puschmann, D, Ewert, F, Enders, A, Krauss, G. 2013.** Modeling biopore effects on root growth and biomass production on soils with pronounced sub-soil clay accumulation. *Ecological Modelling* **256**: 6–15.
- **Godfray, HCJ, Beddington, JR, Crute, IR, Haddad, L, Lawrence, D, Muir, JF, Pretty, J, Robinson, S, Thomas, SM, Toulmin, C. 2010.** Food Security: The Challenge of Feeding 9 Billion People. *Science* **327**: 812–818. http://science.sciencemag.org/content/sci/327/5967/812.full.pdf.
- **Hagedorn, F, Bundt, M. 2002.** The age of preferential flow paths. *Geoderma* **108**: 119–132.

- **Han, E, Kautz, T, Huang, N, Köpke, U. 2017.** Dynamics of plant nutrient uptake as affected by biopore-associated root growth in arable subsoil. *Plant and Soil* **415**: 145–160.
- **Han, E, Kautz, T, Köpke, U. 2016.** Precrop root system determines root diameter of subsequent crop. *Biology and Fertility of Soils* **52**: 113–118. http://link.springer.com/article/10.1007/s00374-015-1049-5/fulltext.html.
- **Han, E, Kautz, T, Perkons, U, Uteau, D, Peth, S, Huang, N, Horn, R, Köpke, U. 2015.** Root growth dynamics inside and outside of soil biopores as affected by crop sequence determined with the profile wall method. *Biology and Fertility of Soils* **51**: 847–856.
- **Hirth, JR, McKenzie, BM, Tisdall, JM. 2005.** Ability of seedling roots of Lolium perenne L. to penetrate soil from artificial biopores is modified by soil bulk density, biopore angle and biopore relief. *Plant and Soil* **272**: 327–336.
- **IPCC. 2014.** Climate change 2014: synthesis report. Contribution of Working Groups I, II and III to the fifth assessment report of the Intergovernmental Panel on Climate Change. Geneva, Switzerland: IPCC.
- **Jakobsen, BE, Dexter, AR. 1988.** Influence of biopores on root growth, water uptake and grain yield of wheat (Triticum aestivum) based on predictions from a computer model. *Biology and Fertility of Soils* **6**: 315–321.
- **Kautz, T. 2015.** Research on subsoil biopores and their functions in organically managed soils: A review. *Renewable Agriculture and Food Systems* **30**: 318–327.
- **Kautz, T, Amelung, W, Ewert, F, Gaiser, T, Horn, R, Jahn, R, Javaux, M, Kemna, A, Kuzyakov, Y, Munch, J-C, Pätzold, S, Peth, S, Scherer, HW, Schloter, M, Schneider, H, Vanderborght, J, Vetterlein, D, Walter, A, Wiesenberg, GLB, Köpke, U. 2013a.** Nutrient acquisition from arable subsoils in temperate climates: A review. *Soil Biology and Biochemistry* **57**: 1003–1022.
- **Kautz, T, Perkons, U, Athmann, M, Pude, R, Köpke, U. 2013b.** Barley roots are not constrained to large-sized biopores in the subsoil of a deep Haplic Luvisol. *Biology and Fertility of Soils* **49**: 959–963. http://dx.doi.org/10.1007/s00374-013-0783-9.
- **Kautz, T, Stumm, C, Kösters, R, Köpke, U. 2010.** Effects of perennial fodder crops on soil structure in agricultural headlands. *Journal of Plant Nutrition and Soil Science* **173**: 490–501.
- **Kell, DB. 2012.** Large-scale sequestration of atmospheric carbon via plant roots in natural and agricultural ecosystems: why and how. *Phil Trans R Soc B* **367**: 1589–1597.
- **Kirkegaard, JA, Lilley, JM, Howe, GN, Graham, JM. 2007.** Impact of subsoil water use on wheat yield. *Australian Journal of Agricultural Research* **58**: 303.
- **Kuzyakov, Y, Blagodatskaya, E. 2015.** Microbial hotspots and hot moments in soil: Concept & review. *Soil Biology and Biochemistry* **83**: 184–199.
- **Li, Y, Ye, W, Wang, M, Yan, X. 2009.** Climate change and drought: a risk assessment of crop-yield impacts. *Climate research* **39**: 31–46.
- **Lorenz, K, Lal, R. 2007.** The Depth Distribution of Soil Organic Carbon in Relation to Land Use and Management and the Potential of Carbon Sequestration in Subsoil Horizons. In: Sparks, DL, ed. Advances in agronomy. San Diego, Calif, London: Academic Press, 35–66.

- **Lowe, DG. 2004.** Distinctive image features from scale-invariant keypoints. *International Journal of Computer Vision* **60**: 91–110.
- **Lynch, JP, Wojciechowski, T. 2015.** Opportunities and challenges in the subsoil: pathways to deeper rooted crops. *Journal of experimental botany* **66**: 2199–2210.
- **Nakamoto, T. 2000.** The Distribution of Wheat and Maize Roots as Influenced by Biopores in a Subsoil of the Kanto Loam Type. *Plant Production Science* **3**: 140–144.
- **Pagenkemper, SK, Peth, S, Puschmann, DU, Horn, R. 2013.** Effects of root-induced biopores on pore space architecture investigated with industrial X-Ray computed tomography. In: Anderson, SH, Hopmans, JW, eds. Soil-Water-Root Processes: Advances in Tomography and Imaging. SSSA Special Publication 56: The Soil Science Society of America, Inc, 69–96.
- **Pal, JS, Giorgi, F, Bi, X. 2004.** Consistency of recent European summer precipitation trends and extremes with future regional climate projections. *Geophysical Research Letters* **31**. http://onlinelibrary.wiley.com/doi/10.1029/2004GL019836/full.
- **Parkin, TB, Berry, EC. 1999.** Microbial nitrogen transformations in earthworm burrows. *Soil Biology and Biochemistry* **31**: 1765–1771.
- **Passioura, JB. 2002.** Soil conditions and plant growth. *Plant, Cell & Environment* **25**: 311–318.
- **Perkons, U, Kautz, T, Uteau, D, Peth, S, Geier, V, Thomas, K, Lütke Holz, K, Athmann, M, Pude, R, Köpke, U. 2014.** Root-length densities of various annual crops following crops with contrasting root systems. *Soil and Tillage Research* **137**: 50–57.
- **Rasse, DP, Smucker, AJM. 1998.** Root recolonization of previous root channels in corn and alfalfa rotations. *Plant and soil* **204**: 203–212. https://doi.org/10.1023/A:1004343122448.
- **Schindelin, J, Arganda-Carreras, I, Frise, E, Kaynig, V, Longair, M, Pietzsch, T, Preibisch, S, Rueden, C, Saalfeld, S, Schmid, B, Tinevez, J-Y, White, DJ, Hartenstein, V, Eliceiri, K, Tomancak, P, Cardona, A. 2012.** Fiji: an open-source platform for biological-image analysis. *Nature methods* **9**: 676–682.
- **Schindelin, J, Rueden, CT, Hiner, MC, Eliceiri, KW. 2015.** The ImageJ ecosystem: An open platform for biomedical image analysis. *Molecular reproduction and development* **82**: 518–529.
- **Schwertmann, U, Huith, M. 1975.** Erosionsbedingte Stoffverteilung in zwei hopfengenutzten Kleinlandschaften der Hallertau (Bayern). *Zeitschrift für Pflanzenernährung und Bodenkunde* **138**: 397–405.
- **Stirzaker, RJ, Passioura, JB, Wilms, Y. 1996.** Soil structure and plant growth: Impact of bulk density and biopores. *Plant and Soil* **185**: 151–162.
- **Thévenaz, P, Ruttimann, UE, Unser, M. 1998.** A pyramid approach to subpixel registration based on intensity. *IEEE transactions on image processing : a publication of the IEEE Signal Processing Society* **7**: 27–41.
- **Vetterlein, D, Kühn, T, Kaiser, K, Jahn, R. 2013.** Illite transformation and potassium release upon changes in composition of the rhizophere soil solution. *Plant and Soil* **371**: 267–279.
- **Volkmar, KM. 1996.** Effects of biopores on the growth and N-uptake of wheat at three levels of soil moisture. *Canadian Journal of Soil Science* **76**: 453–458.

- **Wang, J, Hesketh, JD, Woolley, JT. 1986.** Preexisting channels and soybean rooting patterns. *Soil Science* **141**: 432–437.
- **White, RG, Kirkegaard, JA. 2010.** The distribution and abundance of wheat roots in a dense, structured subsoil—implications for water uptake. *Plant, Cell & Environment* **33**: 133–148.
- **Zhang, Z, Liu, K, Zhou, H, Lin, H, Li, D, Peng, X. 2018.** Three dimensional characteristics of biopores and non-biopores in the subsoil respond differently to land use and fertilization. *Plant and soil* **428**: 453–467.

2.6.7 Supplementary Material

Table S1 Overview of the calculated biopore and rhizosphere properties including equations.

Wheat root / biopore volume (V) [cm³]: Σ of cylindric volumes with base areas $(r^2\pi)_i$ and multiplied by height (h) of soil layer	$$V = \sum_{i=1}^{n}(r^2\pi\, h)_i$$
Volume [cm³] of biopore wall / rhizosphere (V_{wall}): radius of base area enlarged by 0.1 cm: ${(r+0.1)_i}^2\pi$ minus base area $(r^2\pi)_i$ multiplied by height (h) of soil layer	$$V_{Wall} = \sum_{i=1}^{n}\left(\left((r+0.1)^2 - r^2\right)\pi\, h\right)_i$$
Lateral surface (A) of biopores / roots assuming cylindrical shapes: circumference of pore ($2r\,\pi$) multiplied by height (h) of soil layer, normalised by number of pre-crops per soil core	$$A = \frac{\sum_{i=1}^{n}(2r\,\pi\, h)_i}{n\,(crops)_i}$$
Area fraction [%] describing the cut surface area of all biopores / roots on a 20-cm cross section (${r_{ttl}}^2\pi$)	$$A_{Cut\,surface} = \frac{\sum_{i=1}^{n}(r^2\pi)_i}{({r_{ttl}}^2\pi)}$$
Biopore reuse (BPR) [%] describing the count of overlapping ^{14}C and ^{137}Cs spots divided by the count of biopores created (^{137}Cs spots)	$$BPR = \frac{n\left(^{14}C + {}^{137}Cs\right)}{n\left(^{137}Cs\right)}$$
Wheat roots growing in bulk soil expressed as the count of ^{14}C spots (wheat roots) minus wheat roots in biopores (overlap) divided by the count of wheat plants	$$W_{BS} = \frac{n\left(^{14}C\right) - n\left(^{14}C + {}^{137}Cs\right)}{n(wheat)}$$

Table S2 Full quantitative data on the physical biopore properties in different soil depths after the pre-crops *Cichorium intybus* or *Phacelia tanacetifolia*.

	Soil depth	***C. intybus***	***P. tanacetifolia***
Biopore volume [%]	0-10 cm	0.4 ± 0.1%a	0.5 ± 0.1%a
	10-25 cm	0.2 ± 0.0%a	0.4 ± 0.1%a
	25-50 cm	0.1 ± 0.0%a*	0.2 ± 0.1%a
	Ø	0.19 ± 0.03%b	0.35 ± 0.06%a
Biopore wall volume [%]	0-10 cm	0.91% ± 0.23%a	0.71% ± 0.12%a
	10-25 cm	0.43% ± 0.13%a*	0.58% ± 0.15%a
	25-50 cm	0.19% ± 0.04%a	0.41% ± 0.13%a
	Ø	0.35% ± 0.09%a	0.46% ± 0.11%a
Biopore lateral surface per plant [cm^2]	0-10 cm	8.6 ± 1.2b	14.4 ± 2.4a
	10-25 cm	3.8 ± 0.8a*	11.9 ± 3.0a
	25-50 cm	2.0 ± 0.5a	6.8 ± 2.1a
Biopore radius [cm]	-10 cm	0.15 ± 0.01a	0.16 ± 0.01a
	-25 cm	0.15 ± 0.01a	0.14 ± 0.00a
	-50 cm	0.17 ± 0.02a	0.15 ± 0.00a*
	Ø	0.16 ± 0.01a	0.15 ± 0.01a
Biopore cut surface [% of total cut surface]	-10 cm	1.3% ± 0.2%a	1.6% ± 0.3%a
	-25 cm	0.5% ± 0.1%a*	1.0% ± 0.3%a
	-50 cm	0.1% ± 0.1%a	0.0% ± 0.0%a
Biopore reuse [%]	-10 cm	63.6% ± 5.9%a	58.1% ± 7.3%a
	-25 cm	75.3% ± 5.8%a*	65.5% ± 12.3%a
	-50 cm	75.3% ± 10.4%a	53.3% ± 11.2%a
Theoretical biopore reuse [%]	-10 cm	19.4 ± 3.9%	18.6 ± 4.0%
	-25 cm	6.9 ± 2.0%	14.9 ± 7.9%
	-50 cm	1.7 ± 1.6%	0.1 ± 0.1%

Table S3 Full quantitative data on the physical rhizosphere properties of *Triticum aestivum* in different soil depths after the pre-crops *Cichorium intybus* or *Phacelia tanacetifolia*.

	Soil depth	**After *C. intybus***	**After *P. tanacetifolia***
Rhizosphere volume [%]	0-10 cm	0.35 ± 0.06%a	0.41 ± 0.09%a
	10-25 cm	0.23 ± 0.06%a*	0.32 ± 0.07%a
	25-50 cm	0.07 ± 0.04%a*	0.15 ± 0.03%a
	Ø	0.17 ± 0.04%a	0.25 ± 0.05%a
Rhizosphere wall volume [%]	0-10 cm	0.65 ± 0.07%a	0.70 ± 0.15%a
	10-25 cm	0.47 ± 0.08%a	0.64 ± 0.16%a
	25-50 cm	0.14 ± 0.11%a	0.27 ± 0.07%a
	Ø	0.34 ± 0.08%a	0.47 ± 0.09%a
Rhizosphere surface [cm^2 $plant^{-1}$]	0-10 cm	8.60 ± 1.28a	9.44 ± 2.26a
	10-25 cm	6.17 ± 1.29a*	7.66 ± 1.99a
	25-50 cm	1.82 ± 1.33a*	3.32 ± 0.00a*
Rhizosphere radius [cm]	0-10 cm	0.12 ± 0.01a	0.13 ± 0.01a
	10-25 cm	0.11 ± 0.01a	0.12 ± 0.01a
	25-50 cm	0.12 ± 0.02a	0.13 ± 0.00a
Roots in bulk soil [%]	0-10 cm	25.5% ± 5.9%a	21.8% ± 7.2%a
	10-25 cm	31.4% ± 3.6%a	29.6% ± 17.1%a
	25-50 cm	23.4% ± 12.5%a	4.4% ± 2.3%a

2.7 Study 7: The fate of pre-crop nitrogen: Biopores as hotspots for interannual nitrogen transfer in crop rotations?

Authors and affiliations

Callum C. Banfield[1], Magdalena Holzapfel[1], Michaela A. Dippold[1], Johanna Pausch[2], Yakov Kuzyakov[3]

[1] University of Goettingen, Biogeochemistry of Agricultural Ecosystems, Buesgenweg 2, 37077 Goettingen, Germany.

[2] University of Bayreuth, Agroecology, Universitaetsstrasse 30, 95440 Bayreuth, Germany

[3] University of Goettingen, Department of Agricultural Soil Science, Buesgenweg 2, 37077 Goettingen, Germany.

Corresponding author: callumba@gmail.com

Telephone: +49 1578 4527077

Fax: +49 551 3933310

Role of the funding source: DFG KU 1184/29-1

Conflicts of interest: The authors declare no conflicts of interest.

Keywords: ^{15}N labelling, root biopores, detritusphere, hotspots, subsoil, Nutrient cycling, interannual N transfer

Abstract

In crop rotations, plants likely benefit from rooting within biopores — but it is not clear to which extent crops take up nutrients localised in biopores of preceding crops. We tested if there is an interannual nutrient transfer from pre-crops to wheat by applying ^{15}N to the leaves of the pre-crops Cichorium intybus L. and Phacelia tanacetifolia Benth. to label their biopores vs ^{15}N fertiliser application. After eleven months of root biopore development, ^{15}N mobilisation was determined in the shoots of the succeeding crop Triticum aestivum L.

^{15}N supplied during the pre-crop phase was mobilised by wheat after one year of soil rest. Leaf feeding did not exclusively label the biopores with ^{15}N but was dispersed homogeneously in biopores and bulk soil. Pre-crop ^{15}N was 3–5 times more available after fertiliser application (~11% recovery) than after leaf feeding (~3% recovery) — irrespective of pre-crop species — suggesting that the plant-derived organic N of both pre-crops was equally available to wheat. Lower biopore re-use was correlated with lower TN contents, but re-use was not correlated with ^{15}N. Consequently, wheat preferentially mobilised older SON and likely other nutrients (K, P), which boosted its dry matter.

Even though the availability of last-year pre-crop N is rather small in biopores, the most substantial part of the pre-crop-N remained in soil and may be available in future — posing a slow-release fertilisation add-on. The direct relevance of biopores for plant nutrition is likely much higher when topsoils become nutrient-depleted and for less mobile nutrients such as potassium and phosphorus.

2.7.1 Introduction

In times of climate change and a growing global population, sustainable and resource-efficient agriculture is needed to maintain food production (Cordell and White, 2011; Godfray et al., 2010; Schmidhuber and Tubiello, 2007). Organic agriculture addresses this issue by aiming at closing nutrient cycles, e.g. through crop rotations and exploiting the subsoils, i.e. the soil below the ploughed horizon in agricultural lands. So far, nutrient acquisition from the subsoil has received little attention. Total nutrient stocks are considerable in the subsoil, but their concentrations are low. Therefore, subsoils do not appear especially attractive for plant nutrition on a first glance (Kautz et al., 2013; Rumpel et al., 2012). Roots mobilise nutrients from the mineral phases in the subsoil, e.g. through exudation of enzymes and acids, or by boosting the root-associated microflora through exuding organic C (Jones et al., 2009). Boosted microbial turnover increases in turn nutrient release from both soil organic matter (OM) and weathering of mineral phases. Deep-reaching roots concentrate nutrients accumulated from various sources within them (Riedell et al., 2009). When roots grow into the subsoil and die, they leave behind nutrients not only from the topsoil but also those mobilised in the subsoil (Kautz et al., 2013). Upon death, the root OM with the concentrated nutrients turns into microbial hotspots (detritusphere; (Kuzyakov and Blagodatskaya, 2015; Mathers et al., 1975). Microbial turnover releases and cycles nutrients in the pore walls (Passioura, 2002; Volkmar, 1996). On top of the microbial cycling, the former root becomes an accessible macropore, a biopore (McCallum et al., 2004). Biopores are preferential pathways of root growth into the dense subsoil according to the principle of least resistance (Athmann et al., 2013; McCallum et al., 2004). Subsequent crops benefit from the physically accessible and biochemically available biopore nutrients (Gaiser et al., 2013) but this does not automatically mean that biopores contribute to plant nutrition. Plants appear to have developed strategies to acquire root detritus-derived nutrients by growing in contact with the inner pore walls, e.g. by root hairs or by a spiralling growth (Athmann et al., 2013). Yield improvements in crop rotations were previously linked to biopore densities (Gaiser et al., 2013; Kautz et al., 2010; Riedell et al., 2009), but never linked to actual physical biopore re-use and remobilisation of detritus-N. It remains unclear if biopores are beneficial for the plant nutrition and under which conditions. This is the case for wheat, which under dry conditions was estimated to get 10% of its N demand from former root residues (Evans et al., 2001). Nitrogen is strongly enriched in biopores and enzyme activities related to N turnover are increased relative to the bulk soil (Athmann et al., 2017; Hoang et al., 2016). We hypothesise that the use of accessible biopore nutrients, i.e. pre-crop nutrient ‘carry over' in biopores to the next crop ('interannual nutrient transfer'), significantly contributes to the plant nutrition.

We tested the interannual nutrient transfer hypothesis for N in a crop rotation. Subsoil columns were planted either with tap-rooted chicory (*Cichorium intybus* L.) or fibrous phacelia (*Phacelia tanacetifolia* Benth.) as the pre-crop, which were labelled once with ^{15}N-NO_3^- through the leaves (to label the biopores) or onto the soil surface (to mimic fertiliser application). After eleven months of root decay, the uptake of pre-crop N was determined from ^{15}N in wheat shoots (*Triticum aestivum* L.), which was grown for three months.

2.7.2 Material and Methods

2.7.2.1 Experimental setup

Undisturbed soil columns of 20 cm diameter and 70 cm length were taken from 45–115 cm soil depth of a Haplic Luvisol (Hypereutric, Siltic) located at the agricultural research station Klein-Altendorf near Bonn, Germany. The soil properties (Table 1) were previously reported by Vetterlein et al. (2013). The C and N contents of the layer 45–70 cm were 0.32 ± 0.05% and 0.05 ± 0.00%, respectively. Likewise, for the layer 70–115 cm, the corresponding values were 0.18 ± 0.01% and 0.04 ± 0.00%. It was assumed that pre-existing biopores were equally distributed among all soil columns (Gaiser et al., 2013; Han et al., 2015a). The location (50°37′9″N 6°59′29″E) is characterised by a maritime climate with temperate humid conditions (9.6 °C mean annual temperature, 625 mm annual precipitation). After sampling, the soil columns were stored at 8 °C and were pre-incubated at 20 °C for two weeks until the beginning of the experiment. Twelve soil columns were used for this experiment (Fig. 1): on six columns chicory was grown for three months (*Cichorium intybus* L. var. Puna; 20 seeds per column) and on the other six columns *Phacelia tanacetifolia* Benth. (var. Maja KWS; 20 seeds per column) was grown. The temperature in the growth chamber was kept at 20 °C, air humidity was kept at 50% (relative humidity), and the light intensity kept at 200 µmol m^{-2} s^{-1} for 14 hours a day. The columns were watered regularly with a redundant drip irrigation system. Mildew infections were treated with azoxystrobin and sulphur. The pre-crops were cut after three months, and Dicamba was applied to the stems to kill the plants. The soil columns were stored at 5 °C for nine months, followed by two months at 18 °C. The soil moisture was kept constant during the fallow. *Triticum aestivum* L. var. KWS Scirocco was sown at ~ 20 seeds per column; plants were kept at the same conditions as before and harvested after three months at BBCH 77 (Meier, 1997). Main crops were fertilised as recommended, i.e. 120, 80 and 60 kg N, P and K ha^{-1}, respectively.

Table 1 Selected properties of the Haplic Luvisol at Klein-Altendorf, modified after Vetterlein (2013) including TN contents in bulk soil and biopores of the soil core of the experiment (own data).

Depth [cm]	**Horizon (WRB)**	**Reference soil group (WRB)**	**Bulk density [g cm^{-}**	**SOC [g kg^{-1}]**	**N_{tot} [g kg^{-1}]**		**TN [%]**			
							Biopores		**Bulk soil**	
							C. intybus	***P. tanacetifolia***	***C. intybus***	***P. tanacetifolia***
0–27	Ap	SiL	1.29	10.0	1.02					
27–41	E/B	SiL	1.32	4.6	0.55					
41–75	Bt1	SiCL	1.42	4.5	0.51	-10 cm (45-55 cm)	0.08 ± 0.01%b	0.07 ± 0.00%b	0.06 ± 0.00%a	0.05 ± 0.00%a*
						-25 cm (55-70 cm)	0.08 ± 0.00%b	0.08 ± 0.00%b	0.05 ± 0.00%a*	0.05 ± 0.00%a*
75–87	Bt2	SiCL	1.52	3.9	0.50	-50 cm (70-95 cm)	0.08 ± 0.00%b	0.08 ± 0.00%b	0.05 ± 0.00%a*	0.05 ± 0.00%a*
87–115	Bt3	SiL	1.52	2.5	0.34	>-50 cm (95-115 cm)	0.07 ± 0.00%c*	0.07 ± 0.00%c*	0.03 ± 0.00%a*	0.04 ± 0.00%a*
115–127	Bw	SiL	1.46	2.6	0.34					
127–140+	C	SiL	1.47	n.d.	> 0					

2.7.2.2 Labelling with ^{15}N and determination of tracer fate

Half (six) of the soil columns planted with chicory or phacelia were labelled with $K^{15}NO_3$ by leaf feeding. For the leaf feeding, one leaf tip per pre-crop plant was cut with a sterile razor blade. The leaf was immersed for 36 hours in 1.5 ml Eppendorf vials (Eppendorf AG, Hamburg, Germany) containing an aqueous solution of the tracer at 1 mM ml^{-1} and Silwet Gold surfactant (Spiess-Urania Chemicals GmbH, Hamburg, Germany). The other half of the soil columns received the same amount of $K^{15}NO_3$ by pipetting it onto the soil surface to simulate conventional fertiliser application. ^{15}N uptake in wheat shoots and ^{15}N remaining in the pre-crops shoots were determined by cutting the shoots near the soil surface, drying them at 60 °C for four days, determining the total dry mass of the shoots, shredding and mixing the shoots to obtain a representative aliquot, which was ground in a ball mill into a fine powder (MM 200, Retsch GmbH, Haan, Germany). Aliquots were measured by EA-C-IRMS (details below).

After the wheat harvest, soil columns were cut horizontally into four layers in 10 cm, 25 cm and 50 cm depth, i.e. in layers of 10, 15, 25 and 20 cm thickness. Biopores were visually identified, and the soil around them was removed with knives. The biopores were opened on one side, and the inner pore wall coating was taken as a composite sample from the entire layer with micro spoons and dried at 60 °C for four days and ground in a ball mill. Soil (40-50 mg) and plant samples (2 mg) were put in tin capsules (IVA, Meerbusch, Germany) and were incinerated by the FLASH 2000 CHNS/O Element analyser which was coupled by the ConFlo III interface to the Delta V Advantage isotope ratio mass spectrometer (all Thermo Fisher Scientific, Cambridge, U.K.). Contents of total organic carbon (TOC) and total nitrogen (TN), as well as $\delta^{15}N$ values, were determined.

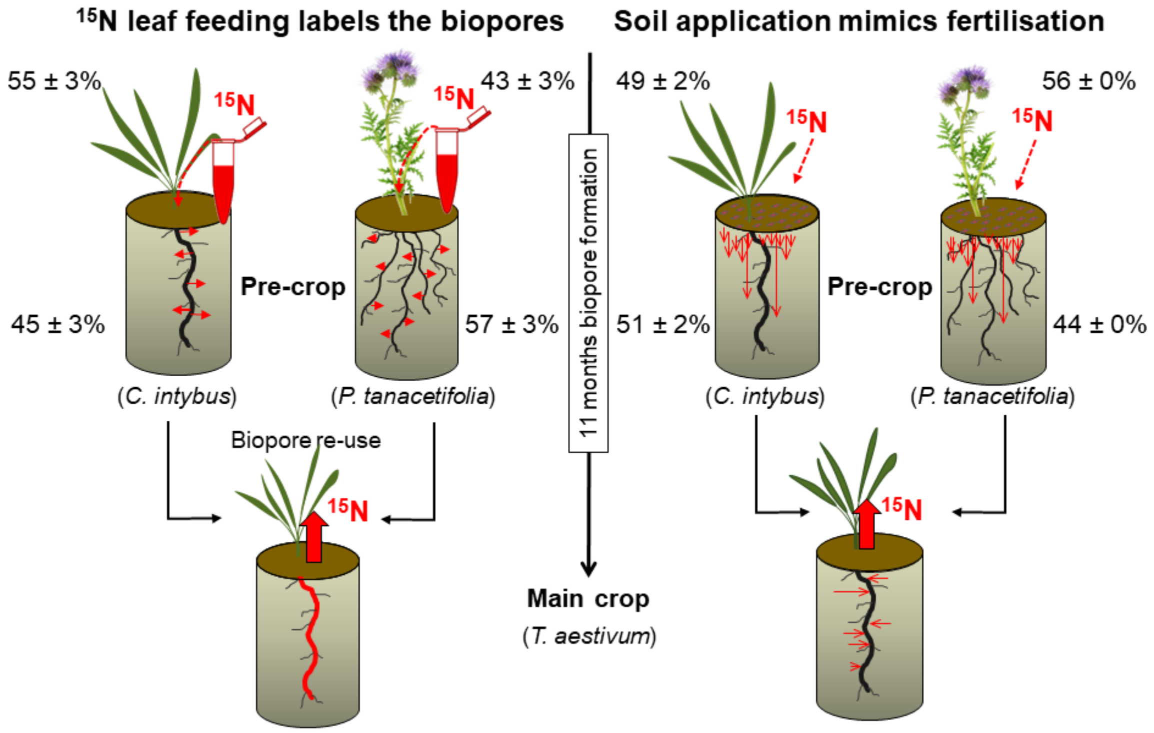
15N leaf feeding labels the biopores
Soil application mimics fertilisation
55 ± 3%
15N
15N
43 ± 3%
45 ± 3%
Pre-crop
57 ± 3%
(C. intybus)
(P. tanacetifolia)
Biopore re-use
15N
49 ± 2%
15N
56 ± 0%
15N
51 ± 2%
Pre-crop
44 ± 0%
(C. intybus)
(P. tanacetifolia)
15N
11 months biopore formation
Main crop
(T. aestivum)

Fig. 1 *A crop rotation experiment: after the pre-crop phase of either a fibrous root system crop (P. tanacetifolia) or tap-rooted chicory (C. intybus; top), the root biomass had one year to decay and enrich biopores with ^{15}N from leaf labelling. $K^{15}NO_3$ was applied either through the leaves (to label the pre-crop root biomass and therefore biopores) or onto the soil surface (to simulate fertiliser application). After the decay, wheat (T. aestivum) was grown (below) and ^{15}N was quantified in the wheat biomass to determine the uptake and remobilisation of ^{15}N from either biopores or bulk soil. The percent data indicates the ^{15}N partitioning between above and belowground allocation of ^{15}N ± SEM.*

2.7.2.3 Calculations and statistics

Total N in a pool (N_{pool}) was partitioned into N derived from the tracer ($N_{tracer\text{-}derived}$) and N originating from the soil (N_{soil_bg}), with ^{15}N atom percent of the unlabelled background soil columns used as the reference value ($atom\%_{soil\_bg}$):

$$N_{tracer-derived} = N_{Pool} \times \frac{(atom\%_{tot} - atom\%_{soil\_bg})}{(atom\%_{tracer} - atom\%_{soil\_bg})} \qquad \text{(Eq. 1)}$$

where $atom\%_{tot}$ and $atom\%_{tracer}$ are the ^{15}N abundances of the measured N and of the added N, respectively. In the case of the fertiliser application mode, all excess ^{15}N in the bulk soil derives from the tracer. The ^{15}N input into the biopore ($N_{biopore}$) is the amount of

^{15}N tracer (N_{tracer}) in the Eppendorf vial minus the ^{15}N which was not taken up (N_{rem}) minus the ^{15}N in the pre-crop shoot at harvest (N_{shoot}).

$$N_{biopore} = N_{tracer} - N_{rem} - N_{shoot} \qquad \text{(Eq. 2)}$$

The results of the mixing model were normalised to the applied tracer amounts (i.e.by leaf feeding or fertiliser application).

2.7.2.4 Statistics

Each dataset was screened for outliers by Nalimov's test, and maximum one outlier per treatment combination and proxy was removed, if more than three data points were available. Data given are mean values ± standard errors to account for uncertainties. Significant differences of means between treatments were tested by two-way analyses of variance (ANOVA; factors: mode of ^{15}N application and pre-crop species) for each depth separately since biopores provide paired samples between soil depths. Homogenous variances were checked for by Levene's test. Normality of the residues was visually checked in Q-Q plots. If the ANOVA model was significant, post-hoc comparisons were analysed by Tukey's Honest Significant Differences test. If assumptions were not met, non-parametric ANOVA (Kruskal-Wallis ANOVA) including post-hoc comparisons of mean ranks were used instead. Pairwise t-tests for dependent samples were used to determine differences between soil depths. All statistical analyses were performed in Statistica 13.3 (TIBCO Software Inc., Tulsa, U.S.A.).

2.7.3 Results

2.7.3.1 ^{15}N budget

49-56% of the ^{15}N applied to either the soil surface or by leaf feeding was recovered in the pre-crop – without any clear trend between the application modes (Fig. 1). The remainder was allocated belowground, of which 5-10% was recovered in the main crop wheat (details below) and 8-18% was recovered in biopores and bulk soil (Fig. 4). Regardless of the application mode, both biopores and bulk soils were statistically equally labelled with ^{15}N (Fig. 4).

2.7.3.2 Carbon and nitrogen contents

The TOC content of the bulk soil decreased steadily from 0 to 60 cm depth by 60% - independent of the pre-crop species (Fig. 2, above, solid lines). At the time of sampling after the main crop phase, the biopore wall material stemming from both pre-crops had higher TOC contents than bulk soil throughout the entire subsoil. On average, the TOC content was 150% higher in biopores than in bulk soil. The difference between biopores and bulk soil increased with soil depth. Chicory increased the biopore TOC content more than phacelia, likely due to its tap roots as compared to the fibrous roots of phacelia. Both

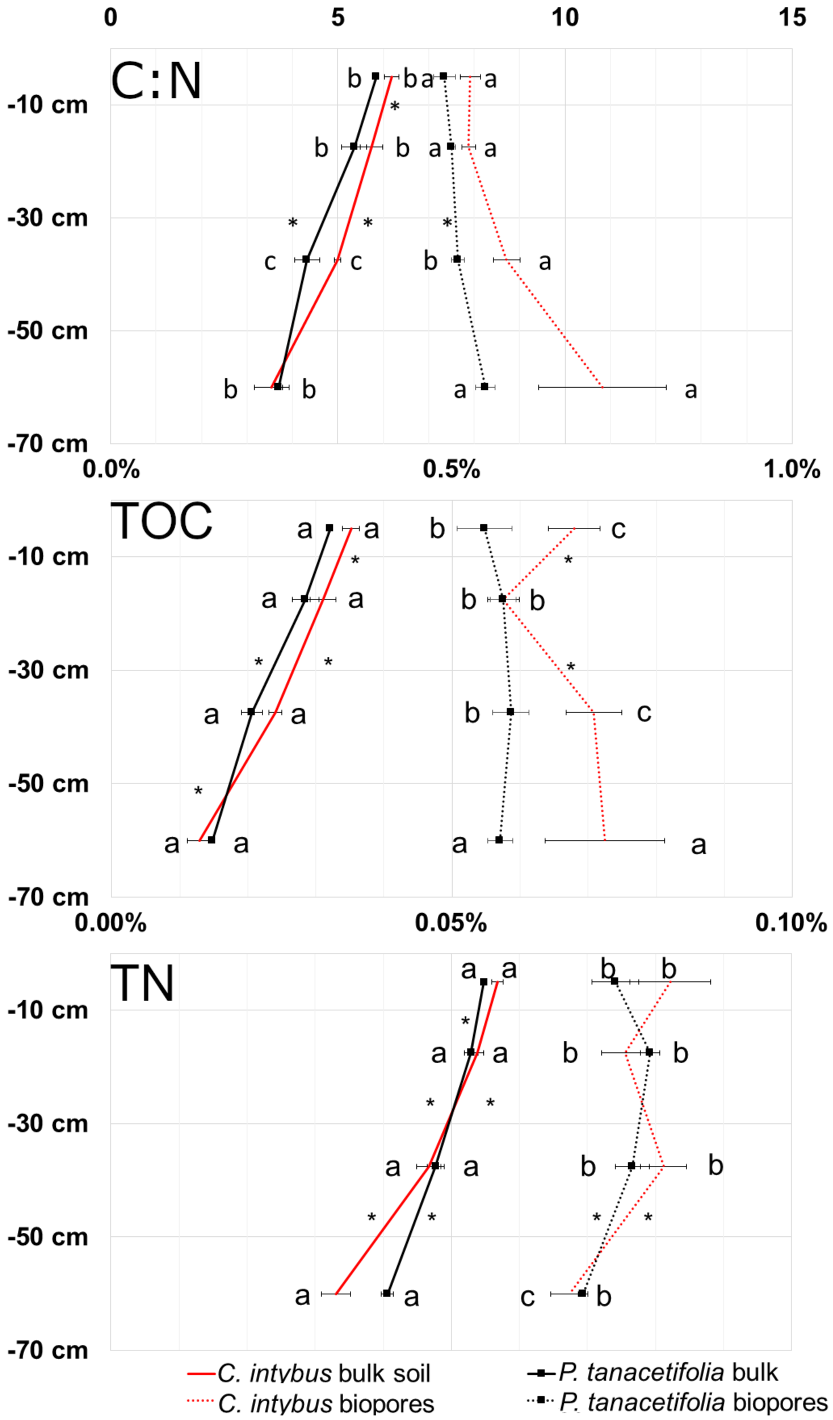

Fig. 2 *C:N ratio (top), TOC (middle) and TN contents (below) ± standard errors from 0–70 cm soil depth at the end of the experiment in biopores (dotted lines) and bulk soil (solid lines for the soil columns planted with either chicory (red) or phacelia (black with cubes as symbols, six replicates each). Letters indicate significant differences in one soil depth on α 0.05 (ANOVA). Asterisks show significant differences between soil depths (two-sample t-test for paired samples).*

pre-crops featured either increasing or constant TOC contents with increasing depth, illustrating the increasing relevance of biopores in the deeper soil.

In the bulk soil, the TN content decreased steadily from 0 cm to 60 cm depth by 30% – like the TOC content irrespective of the pre-crop (Fig. 2, below). Biopores stemming from both pre-crops had 70% higher TN contents relative to bulk soil when averaging over all depths. The TN contents in biopores kept constant from 0 cm to 37.5 cm depth and decreased below - likely because the maximum rooting depth was around 50 cm depth. The mode of application (leaf feeding *vs* fertilisation) did not influence the N contents of either pre-crop or main crops.

The C/N ratio (Fig. 2) decreased steadily in bulk soil irrespective of the pre-crop and was always narrower than in the biopores. In the biopores, there was no difference in the C/N ratio among pre-crops.

The shoot biomass production per wheat plant depended on the pre-crop species and was doubled after phacelia (Fig. 3, black bars). However, the TN content of the shoots was not significantly affected either by the application mode or the pre-crop species (Fig. 3, white bars) – albeit there was a trend towards higher TN contents after chicory. The C contents of the shoot biomasses of the main crop wheat depended on the mode of application or the plant species to which the tracer was applied to (Table S1, Supplementary data).

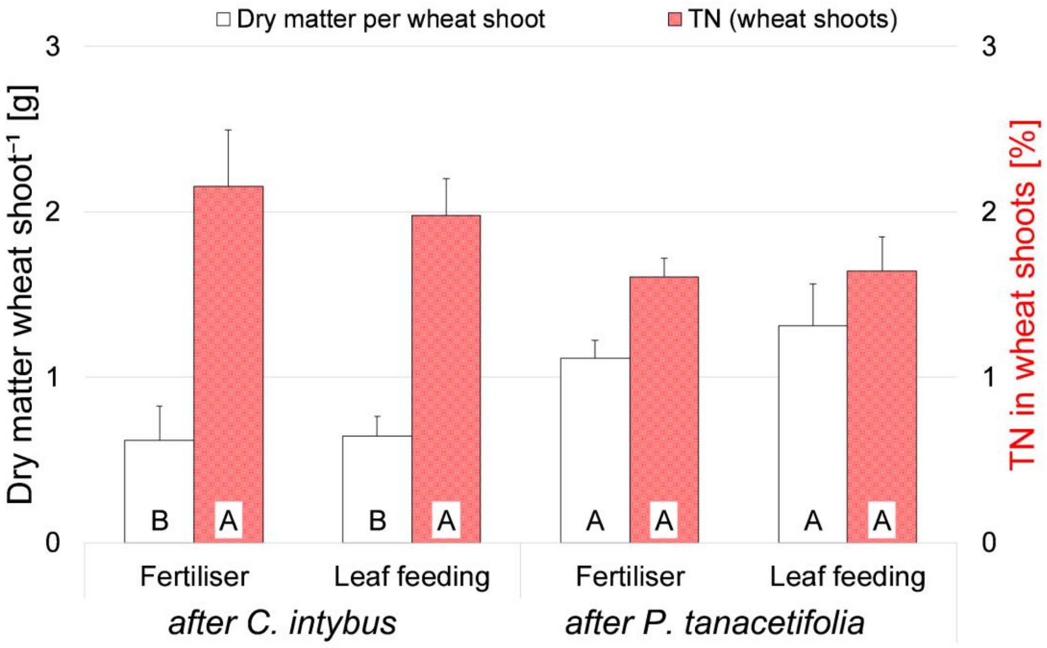

Fig. 3 *Plant productivity (dry mass of wheat shoots, white bars) and TN contents of wheat shoots (red bars); ^{15}N recovery from biopores and bulk soil (relative to applied tracer). Given are means ± standard errors. Letters indicate significant differences between response application modes and pre-crop species (Two-way ANOVA, Tukey's HSD test on α 0.05).*

2.7.3.1 Tracer recovery in wheat shoots

^{15}N applied to either pre-crop was recovered in the shoot biomass of the main crop wheat (Fig. 3, red bars). 3% and 2.6% of the ^{15}N applied to chicory and phacelia were recovered in wheat, respectively. Wheat mobilised 3.4–4.8 times more ^{15}N from the bulk soil than from biopores, i.e. 10.3–12.2% of the fertiliser-^{15}N applied during the pre-crop phase was recovered in wheat shoots. The pre-crop species did not affect the ^{15}N mobilisation.

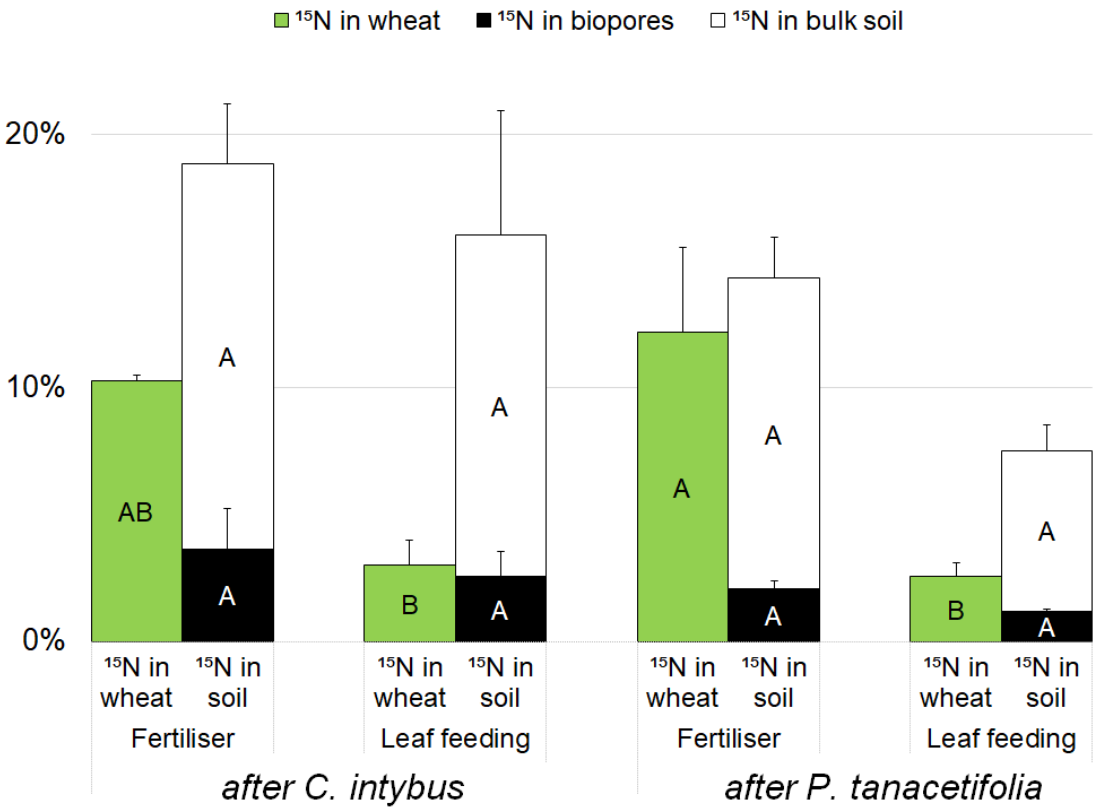

Fig. 4 *Recovery of the pre-crop applied ^{15}N in wheat (main crop; green bars, left), or in soil (black stacked bars: biopores, white stacked bars: bulk soil) – depending on pre-crop species and application mode. Given are means ± standard errors. Letters indicate significant differences between application modes and pre-crop species (Two-way ANOVA, Tukey's HSD test on α 0.05).*

2.7.4 Discussion

2.7.4.1 Pre-crops (but not biopores) enable interannual N transfer to main crops

To assess the relevance of biopores for plant nutrition, prior studies have correlated root growth in macropores with shoot parameters, e.g. yield or N content (Volkmar, 1996). Isotopic tracers can help assess nutrient uptake from biopores, e.g. after cover cropping. The tracer enrichment of biopore walls through pre-crop leaf feeding was shown in principal for ^{137}Cs (Banfield et al., 2017b). However, for ^{15}N, leaf feeding of pre-crops did not exclusively label the biopores (Fig. 4). When a root decays and forms a biopore, the biopore wall is not necessarily strongly enriched in N. The dispersed N distribution is likely due to the high mobility of N-exudates, transport in fungal highways, and exudation from fine roots outside the main biopore (Frey et al., 2000; Mäder et al., 2000). Consequently, nutrients with low mobility such as K (by its tracer $^{137}Cs^{+}$) or P (by $^{33}P\text{-}PO_4^{3-}$) behave differently (Cremers et al., 1988; Hagedorn and Bundt, 2002). Regarding N, the pre-crop effects can be assessed, but not the effect of biopores.

2.7.4.2 The relevance of pre-crop N and its speciation for nutrient uptake

Crops exploit the subsoils for water and nutrients: e.g. wheat may cover 25% of its N demand from the subsoil (Kuhlmann et al., 1989). The nutrient acquisition from the subsoils is expected to increase when topsoils become nutrient-depleted or dry (Dresemann et al., 2018; Gaiser et al., 2012). Nutrients acquired by the pre-crop are partly re-allocated to the subsoil, where they can be mobilised by subsequent crops (Kautz et al., 2013). N cycling in crop rotations is very relevant for plant nutrition: Pre-crop-N was spatially accessible and chemically available as 3–12% of pre-crop-^{15}N was recovered in the subsequently grown wheat (Fig. 4) – independent of the pre-crop species or its N quality (root detritus, exudates). Pre-crop N may either reduce necessary fertiliser applications or can be considered a slow-release add-on to conventional fertilisation because the polymeric structure needs hydrolysis first (Evans et al., 2001).

Neither did the above/belowground partitioning of ^{15}N depend on the application mode (Fig. 1), nor did the partitioning between biopores and bulk soil depend on it (Fig. 4). Consequently, the ^{15}N was similarly spatially distributed in bulk soil and biopores. If tracer-N was spatially similarly distributed but the recovery in wheat was up to five times lower after leaf feeding (Fig. 4), then there must be a (physico-)chemical reason. The speciation of SON may be the decisive factor for the lower mobilisation after leaf feeding. After fertiliser application, the N may have been much more available. It may be speculated that the largest part of ^{15}N released in the leaf feeding treatment was organic N, while in the fertiliser treatment possibly a large part was in the form of mineral N (Filleur et al., 2005) – or in a fast-cycling microbial pool. This theory would agree with Evans et al. (2001) who found that wheat-N is more likely obtained from soil N reserves than from the previous year’s residues.

2.7.4.3 Accessibility of pre-crop N

It is plausible that roots grow towards and within biopores because of I) environmental conditions and II) active regulation. Regarding environmental conditions, dry and nutrient-depleted topsoils and higher bulk density (Table 1) in the deeper soil make rooting in biopores physically more probable and biochemically more attractive (Hirth et al., 2005).

Regarding active regulation, roots sense organic N decomposition by glutamate sensors and, therefore, grow directly towards biopores (Edwards and Lofty, 1980; Filleur et al., 2005). In the subsoil, OM decomposition occurs predominantly in biopores as they strongly accumulate OM and microbial biomass relative to the bulk soil (Banfield et al., 2017a; Hoang et al., 2016; Kuzyakov and Blagodatskaya, 2015). Plants have developed further strategies to acquire nutrients from the biopore walls. These strategies include spiralling root growth and root hairs reaching out to the biopore walls so that up to 85% of roots in large biopores grew in contact with their walls (Athmann et al., 2013). Apparently, roots are attracted to the concentrated nutrients in biopores such as C and N (Fig. 2).

Phacelia increased the dry matter of wheat shoots (Fig. 3) but did not significantly increase its TN contents (Fig. 3). Thus, the phacelia crop rotation influenced wheat biomass, but not shoot-N. This biomass increase was likely because of biopores, as wheat was preferentially rooting in biopores. However, the TN content of wheat was positively correlated with biopore re-use. Thus, lower biopore re-use reduced TN contents in shoots. Consequently, biopores of N nutrition — however, this was not based on the last-year pre-crop ^{15}N but on much older N stored in biopores or on different nutrients (like K or P; (Kuhlmann and Baumgärtel, 1991). Biopores after this experiment had 70% higher N contents than bulk soil, but the C/N ratio was higher (~8 *vs* ~5 in bulk soil; Fig. 2, top) — suggesting a small but relatively more concentrated N pool of a lower availability — apparently moderately available for wheat.

2.7.5 Conclusions

Nitrogen supplied to pre-crops during cover cropping is stored below ground at least for one year and is mobilizable by wheat (interannual N transfer). Despite application of the recommended N fertilisation, wheat mobilised considerable quantities of the pre-crop-^{15}N (>3–12%) – with the most substantial part of ^{15}N remaining for future crops (~87-97%). Wheat took up more N from the bulk soil than from the last year residues but the stored N resources in the subsoil support plant nutrition at least for the medium-term. Even though biopores were not exclusively ^{15}N-labelled, wheat was preferentially rooting in biopores. This rooting increased shoot biomass – but not shoot TN. Biopore benefits are consequently nutrient-specific. In conclusion, biopores obviously present a beneficial microenvironment to roots: Active wheat roots colonised up to 75% of biopores, but stochastically only 20-25% was expected. After one season of cover cropping, the pre-crop species (fibrous *vs* tap-rooted) provided equal opportunities for N mobilisation

Acknowledgements

We highly acknowledge the support of the German Research Foundation (DFG) for funding the projects KU 1184/29-1 within the framework of DFG PAK 888. We would also like to thank the Competence Centre for Stable Isotopes (University of Goettingen) for their support and measurements.

2.7.6 References

- Athmann, M., Kautz, T., Banfield, C., Bauke, S., Hoang, D.T.T., Lüsebrink, M., Pausch, J., Amelung, W., Kuzyakov, Y., Köpke, U., 2017. Six months of L. terrestris L. activity in root-formed biopores increases nutrient availability, microbial biomass and enzyme activity. Applied Soil Ecology 120, 135–142.
- Athmann, M., Kautz, T., Pude, R., Köpke, U., 2013. Root growth in biopores—evaluation with in situ endoscopy. Plant and Soil 371, 179–190.
- Banfield, C.C., Dippold, M.A., Pausch, J., Hoang, D.T.T., Kuzyakov, Y., 2017a. Biopore history determines the microbial community composition in subsoil hotspots. Biology and Fertility of Soils 9, 54.
- Banfield, C.C., Zarebanadkouki, M., Kopka, B., Kuzyakov, Y., 2017b. Labelling plants in the Chernobyl way. A new 137Cs and 14C foliar application approach to investigate rhizodeposition and biopore reuse. Plant and Soil 29, 239.
- Cordell, D., White, S., 2011. Peak Phosphorus: Clarifying the Key Issues of a Vigorous Debate about Long-Term Phosphorus Security. Sustainability 3, 2027–2049.
- Cremers, A., Elsen, A., Preter, P.D., Maes, A., 1988. Quantitative analysis of radiocaesium retention in soils. Nature 335, 247–249.
- Dresemann, T., Athmann, M., Heringer, L., Kautz, T., 2018. Effects of Continuous Vertical Soil Pores on Root and Shoot Growth of Winter Wheat: A Microcosm Study. Agricultural Sciences 09, 750–764.
- Edwards, C.A., Lofty, J.R., 1980. Effects of Earthworm Inoculation Upon the Root Growth of Direct Drilled Cereals. The Journal of Applied Ecology 17, 533.
- Evans, J., McNeill, A.M., Unkovich, M.J., Fettell, N.A., Heenan, D.P., 2001. Australian Journal of Experimental Agriculture 41, 347.
- Filleur, S., Walch-Liu, P., Gan, Y., Forde, B.G., 2005. Nitrate and glutamate sensing by plant roots. Biochemical Society transactions 33, 283–286.
- Frey, S.D., Elliott, E.T., Paustian, K., Peterson, G.A., 2000. Fungal translocation as a mechanism for soil nitrogen inputs to surface residue decomposition in a no-tillage agroecosystem. Soil Biology and Biochemistry 32, 689–698.
- Gaiser, T., Perkons, U., Küpper, P.M., Kautz, T., Uteau-Puschmann, D., Ewert, F., Enders, A., Krauss, G., 2013. Modeling biopore effects on root growth and biomass production on soils with pronounced sub-soil clay accumulation. Ecological Modelling 256, 6–15.
- Gaiser, T., Perkons, U., Küpper, P.M., Puschmann, D.U., Peth, S., Kautz, T., Pfeifer, J., Ewert, F., Horn, R., Köpke, U., 2012. Evidence of improved water uptake from subsoil by spring wheat following lucerne in a temperate humid climate. Field Crops Research 126, 56–62.
- Godfray, H.C.J., Beddington, J.R., Crute, I.R., Haddad, L., Lawrence, D., Muir, J.F., Pretty, J., Robinson, S., Thomas, S.M., Toulmin, C., 2010. Food Security: The Challenge of Feeding 9 Billion People. Science 327, 812–818.
- Hagedorn, F., Bundt, M., 2002. The age of preferential flow paths. Geoderma 108, 119–132.
- Han, E., Kautz, T., Perkons, U., Lüsebrink, M., Pude, R., Köpke, U., 2015a. Quantification of soil biopore density after perennial fodder cropping. Plant and Soil 394, 73–85.

- Han, E., Kautz, T., Perkons, U., Uteau, D., Peth, S., Huang, N., Horn, R., Köpke, U., 2015b. Root growth dynamics inside and outside of soil biopores as affected by crop sequence determined with the profile wall method. Biology and Fertility of Soils 51, 847–856.
- Hirth, J.R., McKenzie, B.M., Tisdall, J.M., 2005. Ability of seedling roots of Lolium perenne L. to penetrate soil from artificial biopores is modified by soil bulk density, biopore angle and biopore relief. Plant and Soil 272, 327–336.
- Hoang, D.T.T., Pausch, J., Razavi, B.S., Kuzyakova, I., Banfield, C.C., Kuzyakov, Y., 2016. Hotspots of microbial activity induced by earthworm burrows, old root channels, and their combination in subsoil. Biology and Fertility of Soils 52, 1105–1119.
- Jones, D.L., Nguyen, C., Finlay, R.D., 2009. Carbon flow in the rhizosphere: carbon trading at the soil–root interface. Plant and Soil 321, 5–33.
- Kautz, T., Amelung, W., Ewert, F., Gaiser, T., Horn, R., Jahn, R., Javaux, M., Kemna, A., Kuzyakov, Y., Munch, J.-C., Pätzold, S., Peth, S., Scherer, H.W., Schloter, M., Schneider, H., Vanderborght, J., Vetterlein, D., Walter, A., Wiesenberg, G.L.B., Köpke, U., 2013. Nutrient acquisition from arable subsoils in temperate climates: A review. Soil Biology and Biochemistry 57, 1003–1022.
- Kautz, T., Stumm, C., Kösters, R., Köpke, U., 2010. Effects of perennial fodder crops on soil structure in agricultural headlands. Journal of Plant Nutrition and Soil Science 173, 490–501.
- Kuhlmann, H., Barraclough, P.B., Weir, A.H., 1989. Utilization of mineral nitrogen in the subsoil by winter wheat. Zeitschrift für Pflanzenernährung und Bodenkunde 152, 291–295.
- Kuhlmann, H., Baumgärtel, G., 1991. Potential importance of the subsoil for the P and Mg nutrition of wheat. Plant and Soil 137, 259–266.
- Kuzyakov, Y., Blagodatskaya, E., 2015. Microbial hotspots and hot moments in soil: Concept & review. Soil Biology and Biochemistry 83, 184–199.
- Mäder, P., Vierheilig, H., Streitwolf-Engel, R., BOLLER, T., Frey, B., Christie, P., WIEMKEN, A., 2000. Transport of 15N from a soil compartment separated by a polytetrafluoroethylene membrane to plant roots via the hyphae of arbuscular mycorrhizal fungi. The New Phytologist 146, 155–161.
- Mathers, A.C., Stewart, B.A., Blair, B., 1975. Nitrate-nitrogen Removal from Soil Profiles by Alfalfa1. Journal of Environmental Quality 4, 403.
- McCallum, M.H., Kirkegaard, J.A., Green, T.W., Cresswell, H.P., Davies, S.L., Angus, J.F., Peoples, M.B., 2004. Improved subsoil macroporosity following perennial pastures. Australian Journal of Experimental Agriculture 44, 299.
- Meier, U. (Ed.), 1997. Growth stages of mono- and dicotyledonous plants. BBCH monograph = Entwicklungsstadien mono- und dikotyler Pflanzen. Blackwell-Wiss.-Verl., Berlin.
- Passioura, J.B., 2002. Soil conditions and plant growth. Plant, Cell & Environment 25, 311–318.
- Riedell, W.E., Pikul, J.L., Jaradat, A.A., Schumacher, T.E., 2009. Crop Rotation and Nitrogen Input Effects on Soil Fertility, Maize Mineral Nutrition, Yield, and Seed Composition. Agronomy Journal 101, 870.
- Rumpel, C., Chabbi, A., Marschner, B., 2012. Carbon Storage and Sequestration in Subsoil Horizons: Knowledge, Gaps and Potentials, in: Lal, R., Lorenz, K., Hüttl,

R.F., Schneider, B.U., Braun, J. von (Eds.), Recarbonization of the Biosphere. Ecosystems and the Global Carbon Cycle. Springer Netherlands, Dordrecht, pp. 445–464.

- Schmidhuber, J., Tubiello, F.N., 2007. Global food security under climate change. Proceedings of the National Academy of Sciences of the United States of America 104, 19703–19708.
- Vetterlein, D., Kühn, T., Kaiser, K., Jahn, R., 2013. Illite transformation and potassium release upon changes in composition of the rhizophere soil solution. Plant and Soil 371, 267–279.
- Volkmar, K.M., 1996. Effects of biopores on the growth and N-uptake of wheat at three levels of soil moisture. Canadian Journal of Soil Science 76, 453–458.

2.7.7 Supplementary Material

Table S1 TN and TOC contents (means of three replicates ± standard errors, %) of the shoots of the pre-crops chicory and phacelia depending on the mode of application (soil application *vs* leaf feeding, i.e. biopore *vs* fertiliser-derived tracer, as well as untreated background samples). Letters indicate significant differences on α 0.05 (Two-way ANOVA).

	TN [%]	**TOC [%]**
Pre-crop phase		
C. intybus fertiliser	1.10 ± 0.03 A	32.56 ± 1.22 a
C. intybus leaf feeding	1.07 ± 0.02 A	35.06 ± 0.48 b
P. tanacetifolia fertiliser	0.85 ± 0.09 B	35.19 ± 0.47 c
P. tanacetifolia leaf feeding	0.79 ± 0.04 B	36.28 ± 0.23 d
C. intybus background	0.83	29.65
P. tanacetifolia background	0.91	36.14

2.8 Additional peer-reviewed publications

- Ahmed MA*, **Banfield CC***, Sanaullah M, Gunina A, Dippold MA (2017) Utilisation of mucilage C by microbial communities under drought. Biol Fertil Soils 67:31 (* equal contributions)

  https://doi.org/10.1007/s00374-017-1237-6

- **Banfield CC**, Braun AC, Barra R, Castillo A, Vogt J (2018) Erosion proxies in an exotic tree plantation question the appropriate land use in Central Chile. CATENA 161:77–84

  https://doi.org/10.1016/j.catena.2017.10.017

- Braun AC, **Banfield CC** (2017) A Process-based model approach to predict future land-use changes and link biodiversity with soil erosion in Chile. In: Hinz S, Braun A, Weinmann M (eds) Object and pattern recognition in remote sensing. Whittles Publ, Dunbeath, pp 283–307

- Hoang DTT, Pausch J, Razavi BS, Kuzyakova I, **Banfield CC**, Kuzyakov Y (2016) Hotspots of microbial activity induced by earthworm burrows, old root channels, and their combination in subsoil. Biol Fertil Soils 52:1105–1119

  https://doi.org/10.1007/s00374-016-1148-y

3 Acknowledgements / Danksagung

Ohne die großartige Unterstützung vieler Kolleginnen und Kollegen, Vorbilder und Freunde wäre diese Dissertation nicht möglich gewesen.

An erster Stelle möchte ich Prof. Dr. Michaela Dippold danken, die mir —zusammen mit Prof. Dr. Yakov Kuzyakov— die Möglichkeit gegeben hat, diese Dissertation und die Forschungsarbeiten erfolgreich abzuschließen. Ihre eigene Faszination weckte in mir die Leidenschaft für die Kombination von Biomarkern, Isotopen und analytischer Instrumentierung, die mich auch in Zukunft antreibt. Ganz besonders möchte ich mich dafür bedanken, dass sie selbst in den stürmischten Zeiten immer für mich da war und so oft ihre eigenen Bedürfnisse hintenangestellt hat. Die letzten Jahre waren eine tolle Zeit der persönlichen Weiterentwicklung. Vielen Dank!

Prof. Dr. Stefan Scheu danke ich für die Betreuung meiner Arbeit, der Übernahme der Korrektur, viele Denkanstöße und flexiblen, unkomplizierten Lösungen. Meinen weiteren Mitgliedern des Promotionskomitees möchte ich danken: Prof. Dr. Johanna Pausch für die sehr produktive, vertrauensvolle und äußerst angenehme Zusammenarbeit und insbesondere Prof. Dr. Yakov Kuzyakov, mit dem mich nicht nur ein unvergessliches Vorstellungsgespräch verbindet, sondern auch endlose, vertrauensvolle und produktive wissenschaftliche Diskussionen von/in Tschernobyl bis in alle Tiefen der multivariaten Statistik.

Für die finanzielle Förderung des Projekts durch die Deutsche Forschungsgemeinschaft (KU 1184/29-1) möchte ich mich bedanken.

Meine besondere Dankbarkeit und Verbundenheit gilt Bernd Kopka vom Labor für Radioisotope dafür, dass er —aus meiner anfänglichen Faszination für Radionuklide aus einer Fragestellung heraus— meine Leidenschaft für Radionuklidanwendungen und Strahlenschutz geweckt hat, die mich sicher noch mein weiteres berufliches Leben begleiten wird: Vielen Dank für dein offenes Ohr und Rückhalt!

Das zweite Laborexperiment war eine große persönliche Herausforderung —auch weil nicht klar war ob es so klappen würde. Bei der Umsetzung konnte ich auf viele helfende Hände und großes Verständnis setzen. Vielen Dank an Karin Schmidt, Susann Enzmann, Magdalena Holzapfel, Torben Frahm, Kyle Mason-Jones, Andreas Breidenbach, Maire Holz, Lydia Köbele, Marius Schmitt, Fabian Stiewe, Bahar Razavi,

Gabriele Lehmann und Marina Horstmann. Herzlichen Dank für eure Hilfe, insbesondere an alle, die mit mir tagelang Bioporen ausgekratzt haben!!

Meinen Koautorinnen und Koautoren danke ich für unzählige Verbesserungsvorschläge und Anregungen, die aus Manuskripten und Ideen erst richtige Papers gemacht haben. Besonders hervorzuheben ist hier Kyle Mason-Jones für seinen beeindruckenden Durchblick und seine Hilfsbereitschaft.

Den Teams vom Labor für Radioisotope (LARI) und des Kompetenzzentrums für Stabile Isotope (KOSI) möchte ich danken für die immer schnelle und professionelle Bearbeitung meiner Proben und Unterstützung bei Fragen.

Den Kolleginnen und Kollegen des Instituts für organischen Landbau an der Universität Bonn danke ich für ihre großartige Arbeit und Unterstützung beim Feldexperiment in Klein-Altendorf.

Prof. Dr. Tillmann Buttschardt möchte ich dafür danken, dass er mich an die Geoökologie heranführte lange bevor meine akademische Laufbahn überhaupt begonnen hatte.

Mit vielen Kolleginnen und Kollegen sind Freundschaften entstanden. Euch danke ich für tolle Ideen und eine unvergessliche Zeit.

An letzter und herauszustellender Stelle sei meiner Familie gedankt für die Unterstützung während meiner Ausbildung — vor allem aber meiner eigenen Familie, die unglaubliche Geduld mir gegenüber hatte, wenn ich mal wieder mit dem Kopf nicht daheim, sondern bei der Arbeit war.

4 Curriculum vitae

Surname:	Banfield
Names:	Callum Colin
Date and place of birth:	27.07.1987 in Karlsruhe, Germany
Nationality:	British and German

05/2015 – 11/2018	PhD studies at the Georg-August-University Göttingen, Germany
Since 09/2014	Employed at Georg-August-University Göttingen, Germany
10/2007 – 08/2013	Karlsruhe Institute of Technology (KIT), Germany Study of Geoecology (Diplom-Geoökologie) Topic of the thesis: “Soil erosion in commercial forest plantation in South-Central Chile – with an outlook on PPP concentrations in top soils.” Thesis was in collaboration with the environmental research centre EULA in Concepcíon, Chile.

5 Declarations / Erklärungen

Hiermit erkläre ich, dass diese Arbeit weder in gleicher noch in ähnlicher Form bereits anderen Prüfungsbehörden vorgelegen hat. Weiter erkläre ich, dass ich mich an keiner anderen Hochschule um einen Doktorgrad beworben habe.

Göttingen, den ....

....
(Unterschrift)

Hiermit erkläre ich eidesstattlich, dass diese Dissertation selbstständig und ohne unerlaubte Hilfe angefertigt wurde.

Göttingen, den ....

....
(Unterschrift)